

A STIMULUS ACTUATED POLYMERIC DEVICE FOR THE PROLONGED THERAPEUTIC MANAGEMENT OF MODERATE TO SEVERE CHRONIC PAIN

TONG-SHENG TSAI

A dissertation submitted to the Faculty of Health Sciences, University of the
Witwatersrand, in fulfilment of the requirements for the degree of Master of Pharmacy



Supervisor:

Professor Viness Pillay
University of the Witwatersrand
Department of Pharmacy and Pharmacology
South Africa

Co-Supervisors:

Doctor Yahya E. Choonara, University of the Witwatersrand,
Department of Pharmacy and Pharmacology, South Africa

Ms Lisa C. du Toit, University of the Witwatersrand,
Department of Pharmacy and Pharmacology, South Africa

Professor Girish Modi, University of the Witwatersrand,
Department of Neuroscience, Division of Neurology, South Africa

Doctor Dinesh Naidoo, University of the Witwatersrand,
Department of Neuroscience, Division of Neurosurgery, South Africa

2011

DECLARATION

I, Tong-Sheng Tsai, declare that this dissertation is my own work. It has been submitted for the degree of Master of Pharmacy in the Faculty of Health Sciences at the University of Witwatersrand, Parktown, Johannesburg, South Africa. It has not been submitted before for any degree or examination at this or any other University.

.....

This.....day of July 2011

RESEARCH PUBLICATIONS ARISING FROM THIS WORK

1. A polyvinyl alcohol-polyaniline based electro-conductive hydrogel for controlled stimuli-actuable release of indomethacin, Tong-Sheng Tsai, Viness Pillay, Yahya E. Choonara, Lisa C. du Toit, Girish Modi, Dinesh Naidoo and Pradeep Kumar, *Polymers*, 3, 150-172, 2011

RESEARCH PRESENTATIONS ARISING FROM THIS WORK

1. Electro-conductive hydrogel for controlled stimuli-responsive liberation of indomethacin, Tong-Sheng Tsai, Viness Pillay, Yahya E. Choonara, Lisa C. du Toit, Girish Modi, Dinesh Naisoo, Pradeep Kumar and Valence M.K. Ndesendo, October 2010, Polymer Science Research Center Auditorium, Mississippi, United States of America

PATENT FILED

A stimuli-actuated implantable drug delivery device, Tong-Sheng Tsai, Viness Pillay, Yahya Essop Choonara, Lisa Claire du Toit, University of Witwatersrand, provisional South African patent application (2010/03746), published July 2010 in the Patent Journal.

SUMMARY

Chronic pain may be defined as pain which persists in a patient for a prolonged period of time. Although this period of time may range from 3-12 months, it is most commonly described as pain which extends beyond the time required for healing. Chronic pain may also be classified into two different categories depending on the cause. The first category is nociceptive, which is chronic pain caused by activation of nociceptors. This may be due to several factors such as trauma or temperature. The second category is neuropathic chronic pain. These are chronic pains which are not necessarily caused by trauma, but more likely due to the malfunction of the nervous system. For this study, our aim is to develop a patient-controlled, externally actuated hydrogel system which is capable of 'ON-OFF' drug release. The model drug which was incorporated into the SAPD was a Non-Steroidal Anti-Inflammatory Drugs (NSAID), and thus our drug release system would be beneficial primarily for nociceptive chronic pain. This subcutaneously implanted SAPD is produced with an electroactive polymer which allows drug release in the presence of electrical stimulation. This would result in direct availability of drug at the site of actuation with reduced side-effects and increased drug bio-availability.

The SAPD was formed by crosslinking polyvinyl alcohol (PVA) with diethyl acetamidomaleate (DAA). The result was a hydrogel which was capable of swelling while remaining insoluble when placed in various solvents. After the hydrogel was synthesized, indomethacin was incorporated as the model drug. Indomethacin exhibited superior Drug Entrapment Efficiency (DEE) ($\pm 70-90\%$) and responsive release in the presence of an electrical stimulus. Finally, polyaniline (PANI) was used as the electroactive polymer in order to enhance the conductivity and allow sufficient release of the drug.

Optimization of the SAPD was undertaken with a 3-factor Box-Behnken Design which measured the rate of erosion, drug release and DEE. The optimized SAPD was synthesized using PVA (0.8g) crosslinked with DAA (0.0689g) and a concentration of $1.3418\%_{w/w}$ PANi. Indomethacin was used and the DEE achieved was $76.32 \pm 10.46\%$ (target 80.5381%). The drug release profile was $1.622\% \pm 0.1857\%$ (target 1.7%) per release cycle and erosion rate was $5.73 \pm 1.26\%$ (target 6.3201%) when actuated with a potential difference of 1V for a duration of 1 minute.

Chemometric modelling performed on the SAPD showed that drug release may be attributed to erosion of the SAPD in the presence of an electrical stimulus. The polymeric strands usually rest as a coiled state within the SAPD. This coiled state may be the reason the hydrogel remained intact in the absence of electrical stimulation. However, external electrical fields may adduct to form a coil rather than an extended chain resulting in the formation of a globular aniline-vinyl complex. This formation thus leads to a weakened form of the hydrogel structure, resulting in breakdown and ultimately erosion. This erosive phenomenon ceased once the electrical stimulation was removed. The end result of this hydrogel erosion is the liberation of the entrapped indomethacin.

In vivo animal studies on the SAPD indicated an 'ON-OFF' drug release profile. The drug release was consistent and drug quantity of $\pm 0.15\text{mg}$ per release cycle in the Sprague-Dawley rat model. The SAPD was implanted subcutaneously under the left flank and an electrical stimulation was triggered with the use of a 2-in-1 galvano/potentiostat in order to ensure the electrical stimulus was constant. The potential difference used was 1V over a period of 1 minute. The rats were assessed for signs of illness or swelling after the implantation procedure to determine the biocompatibility of the SAPD. The rats were monitored for 10 days and weighed daily. Results have shown that the rats did not experience any considerable swelling and the weights of each rat were steady, thus indicating biocompatibility of the SAPD. Histopathological samples indicated mild inflammation around the site of implantation 10 days after implantation. This may have been due to minor surgery at site of implantation. The biocompatibility of the SAPD was generally good and there were no signs of tumour or long term tissue inflammation. Future application of the SAPD may include an external actuation device to be worn as a watch which allows actuation of the SAPD when required by the patient.

ACKNOWLEDGEMENTS

I would like to express my deepest gratitude to those who have contributed towards the completion of this research and made this work possible. It is an honour for me to firstly convey my gratitude towards my parents, Liang-Jen Tsai and Hsu-Li Chuang, for making me the man I am today. My deepest thanks and wishes to you and I will continue to make you proud in every aspects of my life. My further gratitude goes towards my Supervisor, Professor Viness Pillay, for without you; this opportunity would not be possible. May you continue to produce many more graduates with high standards and excellence. My extended thanks go to my Co-Supervisors, Doctor Yahya E. Choonara, Professor Girish Modi, Doctor Dinesh Naidoo and Ms Lisa C. Du Toit, for your help and passion in this work. To my beloved wife Nemalini Naiker, I would like to thank you for never giving up on me and being with me every step of the way. I would also like to thank all my office colleagues Thiresen Govender, Derusha Frank and Tasneem Rajan for the memorable times in the office. My colleagues in the Department, Kovanya Moodley, Yusuf Dawood, Latavia Singh, Deshnee Naidoo, Meng-Meng Sun, Ameenah Wadee, Clare Dott, Shivaan Cooppan, Pradeep Kumar, Priya Bawa, Rubina Shaikh, Steven Mufamadi and Valence Ndesendo, without you guys campus would be a dull and gloomy place. To Caren Billing, thank you very much for your guidance when everything about PGSTAT was still unfamiliar to me. My gratitude also goes towards Bruno Steiner, the technical director at Metrohm South Africa, for your help with regards to the equipment. Further gratitude goes to Doctor Leith Meyer and his staff at the Central Animal Services. Your patience and hospitality really meant a lot to me, especially with regards to the procurements and drawing the blood samples. To the staff members at the Department of Pharmacy and Pharmacology, Sello Ramarumo, Tsebogo Chandu, Busisiwe Damane, Bafana Themba and Kleinbooi Mohlabi for all the help you have offered me throughout the years. I understand the responsibility of having to procure and order all equipment and chemicals not only for myself, but the entire Department, was extremely stressful. Lastly, I would like to thank my sister, Ming-Tseng Tsai, for your support during this study.

DEDICATION

The author would like to dedicate this work to all those who have and are still in pursuit of knowledge, for it is and always will be a part of human nature to pursue knowledge beyond our own.

TABLE OF CONTENTS

CHAPTER 1 INTRODUCTION

1.1	Introduction	1
1.2.	Approach to this study	6
1.3.	Overview of this dissertation	7

CHAPTER 2
DESIGN, ADVANCES AND APPLICATIONS OF ELECTROACTIVE POLYMERIC
SYSTEM AS A RESPONSIVE DRUG DELIVERY STRATEGY

2.1.	Introduction	8
2.2.	The methods for preparation of a responsive electroactive polymer-based hydrogel	12
2.3.	The application of electroactive polymer in the Stimuli-Actuated Polymeric Device as a responsive drug release strategy	13
2.4.	Electroactive polymer as a constituent of a polymeric substance delivery system	15
2.4.1.	Polyaniline as a component of the electroactive polymeric-based drug delivery system	18
2.4.2.	Polypyrrole as a component of the electroactive polymeric-based drug delivery system	19
2.4.3.	Polythiophene as a component of the electroactive polymeric-based drug delivery system	20
2.5.	Electropolymerization as a method of synthesis for the electroactive polymers and factors affecting the polymerization effect	21
2.6.	Doping – A crucial process for the optimization of electroactive polymer conductivity	23
2.7.	Redox reaction as an essential process for the conductivity of electroactive polymer	24
2.7.1.	Techniques for the evaluation of redox reactions in electroactive polymers	26
2.7.1.1.	Linear sweep voltammetry	26
2.7.1.2.	Cyclic voltammetry	27
2.7.1.3.	Impedance spectroscopy	28
2.7.1.4.	Chronoamperometry	29
2.8.	Controlled release of substance from the electroactive polymeric-based hydrogel	29
2.9.	Polyelectrolyte and their uses in biological applications	32
2.10.	Current responsive hydrogel system and future prospective	34
2.11.	Concluding remarks	35

CHAPTER 3

PRE-DESIGN ON THE STIMULUS-ACTUATED POLYMERIC DEVICE: THE FORMULATION OF AN ELECTROACTIVE POLYMER-INCORPORATED HYDROGEL

3.1.	Introduction	37
3.2.	Materials and Methods	39
3.2.1.	Materials	39
3.2.2.	The design of an electroactive polymer -based implantable device	40
3.2.3.	Preparation of the electroactive polymer-based implantable device	41
3.2.4.	Effects of counter-ions on the properties of Stimuli-Actuated Polymeric Device	42
3.2.5.	<i>In vitro</i> drug release study of polypyrrole membrane	42
3.3.	Results and Discussion	43
3.3.1.	The constituents and its roles in the responsive hydrogel	43
3.3.2.	Model drugs incorporated into the Stimuli-Actuated Polymeric Device	44
3.3.2.1.	Indomethacin as a model drug in the Stimuli-Actuated Polymeric Device	44
3.3.2.2.	Calibration curve of indomethacin through serial dilution from a stock solution of Indomethacin	46
3.3.2.3.	Diclofenac sodium as a model drug in the Stimuli-Actuated Polymeric Device	47
3.3.2.4.	Calibration curve of diclofenac sodium through serial dilution from a stock solution of diclofenac sodium	48
3.3.2.5.	Aspirin as a model drug in the Stimuli-Actuated Polymeric Device	49
3.3.2.6.	Calibration curve of aspirin through serial dilution from a stock solution of aspirin	50
3.3.2.7.	Ibuprofen as a model drug in the Stimuli-Actuated Polymeric Device	51
3.3.2.8.	Calibration curve of ibuprofen through serial dilution from a stock solution of ibuprofen	52
3.3.3.	Preparation of the crosslinked polyvinyl alcohol Stimuli-Actuated Polymeric Device with indomethacin as a model drug	52
3.3.3.1.	Composition of the drug-loaded polyvinyl alcohol/polyaniline-based Stimuli-Actuated Polymeric Device	52
3.3.4.	The synthesis of the drug-loaded Stimuli-Actuated Polymeric Device	53
3.3.5.	Gel compression measurement of the Stimuli-Actuated Polymeric Device	54
3.3.6.	Surface morphology of the Stimuli-Actuated Polymeric Device	55
3.3.7.	Setup of the circuit for <i>in vitro</i> assessment of drug release from the Stimuli-Actuated Polymeric Device under the presence of electric current	56
3.3.8.	The drug entrapment efficiency of the Stimuli-Actuated Polymeric Device	57
3.3.9.	The amount of drug release from Stimuli-Actuated Polymeric Device under the influence of electrical current	58

3.3.10.	Chemical structure analysis of the Stimuli-Actuated Polymeric Devices	60
3.3.11.	Proposed release mechanism of the Stimuli-Actuated Polymeric Device	65
3.4.	Concluding remarks	66

CHAPTER 4

CHARACTERIZATION AND PRE-FORMULATION INVESTIGATION OF THE STIMULUS-ACTUATED POLYMERIC DEVICE

4.1.	Introduction	68
4.2.	Materials and Methods	69
4.2.1.	Materials	69
4.2.2.	Determination of the physicochemical and physicommechanical properties of Stimuli-Actuated Polymeric Device	69
4.2.3.	Determination of chemical structures of the Stimuli-Actuated Polymeric Device	69
4.2.4.	Calorimetric analysis of the Stimuli-Actuated Polymeric Device	69
4.2.5.	Determination of <i>in vitro</i> drug release from the Stimuli-Actuated Polymeric Device	70
4.2.6.	Surface structure and texture analysis of Stimuli-Actuated Polymeric Device	70
4.2.7.	Assessment of possible erosion in the Stimuli-Actuated Polymeric Device	70
4.2.8.	Electrical conductivity test of the Stimuli-Actuated Polymeric Device	70
4.3.	Results and Discussion	71
4.3.1.	The use of chloroform for the formulation of a Stimuli-Actuated Polymeric Device and the assessment of drug release profile from chloroform-substituted device	71
4.3.2.	The employment of diclofenac sodium as a model drug in the Stimuli-Actuated Polymeric Device	72
4.4.	The investigation of prospective materials which could be used as an electroactive polymer-incorporated hydrogel for the purpose of electrically-controlled drug release implant	73
4.4.1.	Incorporation of polysodium styrene sulfonate as a polyelectrolyte hydrogel for the purpose of local delivery of diclofenac sodium	73
4.4.2.	The use of methylcellulose as the hydrogel component of the Stimuli-Actuated Polymeric Device	74
4.5.	Assessment of prospective crosslinkers and solvents for the synthesis of the Stimuli-Actuated Polymeric Device	77
4.5.1.	Assessment of crosslinking behaviour between various grades of Eudragit® and polyethylene glycol 4000	77
4.5.2.	The use of different solvents suitable for the dissolution of Eudragit® and its effects on the crosslinking	79
4.5.3.	Assessment of drug entrapment efficiency of a crosslinked polyethylene glycol 4000 and Eudragit® hydrogel system	79
4.5.4.	The stability of the Eudragit® crosslinked system in the presence of water and phosphate buffer solution	80
4.5.5.	The employment of Eudragit® RS100 for the purpose of crosslinking	80
4.5.6.	Crosslinking of Eudragit® RS100 and sodium chloride with indomethacin as model drug for drug entrapment and drug release	82
4.5.7.	The employment of tri-ethyl citrate as a plasticizer	85

4.5.8.	The employment of alternative materials as a component of the Stimuli-Actuated Polymeric Device	86
4.5.9.	The employment of high molecular weight polyvinyl alcohol in a crosslinked system	88
4.5.10.	The employment of polyvinyl alcohol ₈₈₀₀₀ and diethyl acetamidomaleate in a crosslinked system and assessment of its drug release profile	90
4.5.11.	Further assessment of drug release profile of the aspirin-loaded device and ibuprofen-loaded device	92
4.5.12.	Determination of a crosslinker ratio and its effect on the system and its drug release profile	93
4.5.13.	Addition of polyaniline as an electroactive polymer for the purpose of enhancing drug release from the crosslinked system	93
4.5.14.	Assessment of ibuprofen release from the Stimuli-Actuated Polymeric Device in the absence and presence of an electric current	94
4.5.15.	Assessment of diclofenac sodium release from the Stimuli-Actuated Polymeric Device in the Presence and the absence of electric current	95
4.5.16.	Assessment of indomethacin release from the Stimuli-Actuated Polymeric device in the presence and the absence of electric current	96
4.6.	The synthesis of the Stimuli-Actuated Polymeric Device for the assessment of drug entrapment efficiency	98
4.6.1.	The drug entrapment efficiency of the Stimuli-Actuated Polymeric Device	99
4.7	The drug release mechanism of the Stimuli-Actuated Polymeric Device	102
4.7.1.	Fourier Transform Infra-Red spectroscopy of the Stimuli-Actuated Polymeric Device with and without indomethacin	103
4.7.2.	Differential scanning calorimetry of the indomethacin loaded Stimuli-Actuated Polymeric Device	104
4.7.3.	Microscopy of the eroded Stimuli-Actuated Polymeric Device	109
4.7.3.1.	Light microscopy of the eroded Stimuli-Actuated Polymeric Device	109
4.7.3.2.	Electron microscopy of the eroded Stimuli-Actuated Polymeric Device	110
4.7.4.	The effect of polyvinyl alcohol and diethyl acetamidomaleate on the rate of erosion in the Stimuli-Actuated Polymeric Device in the presence of electric current	111
4.8.	Concluding remarks	117

CHAPTER 5
INVESTIGATION OF A DRUG-LOADED HYDROGEL SYSTEM FOR CONTROLLED
RELEASE OF NSAIDs IN TREATMENT OF CHRONIC PAIN

5.1.	Introduction	119
5.2.	Materials and Methods	120
5.2.1.	Materials	120
5.2.2.	Optimization of external and internal factors of the Stimuli-Actuated Polymeric Device	120
5.2.2.1.	The optimization of the constituent ratio in order to achieve rapid drug release upon activation	120
5.2.2.2.	The optimization of the Stimuli-Actuated Polymeric Device with the use of a 3 Factor Box-Behnken Design	123
5.3.	Results and Discussion	127
5.3.1.	The characterization and evaluation of the optimized Stimuli-Actuated Polymeric Device	127
5.3.2.	Cyclic voltammetry of the Stimuli-Actuated Polymeric Device	128
5.3.3.	Conductivity measurement of the Stimuli-Actuated Polymeric Device	129
5.3.4.	Molecular mechanics simulations of the Stimuli-Actuated Polymeric Device	130
5.3.5.	Rheological study of the Stimuli-Actuated Polymeric Device	133
5.3.6.	The comparison of the <i>in vitro</i> drug release profile between the Stimuli-Actuated Polymeric Device and the conventional oral system of indomethacin	138
5.4.	Concluding remarks	139

CHAPTER 6

OPTIMIZATION AND ELUCIDATION OF RELEASE MECHANISM OF THE STIMULUS-ACTUATED POLYMERIC DEVICE

6.1	Introduction	141
6.2.	Materials and Methods	143
6.2.1.	Materials	143
6.2.2.	Animal ethics clearance	143
6.2.3.	<i>In vivo</i> studies to assess the biocompatibility and drug release kinetics from the Stimuli-Actuated Polymeric Device	143
6.2.4.	Method and approach for the <i>in vivo</i> study of the Stimuli-Actuated Polymeric Device	144
6.2.5.	Implantation of the Stimuli-Actuated Polymeric Device into the rat model	146
6.2.6.	Electrical actuation and safety procedures	147
6.2.7.	Drugs and medicinal substances to be used for this animal study	151
6.2.8.	Plasma sampling from the rat model after experimental procedure	152
6.2.9.	Liquid-liquid extraction technique for the separation of drug bound in plasma	152
6.2.10.	Subcutaneous implantation of the device into the rat	155
6.3.	Results and Discussion	158
6.3.1.	High Performance Liquid Chromatography analysis of plasma sample for the presence of indomethacin	158
6.3.2.	Further analysis of blood sample with the use of Ultra Performance Liquid Chromatography	163
6.3.3.	Histopathological sampling of the tissues obtained from the site of implantation	167
6.4.	Concluding remarks	171

CHAPTER 7
***IN VIVO* EVALUATION OF THE STIMULUS-ACTUATED POLYMERIC DEVICE UPON
SUBCUTANEOUS IMPLANTATION INTO A RAT MODEL**

7.1.	Conclusions	172
7.2.	Recommendations	173
7.3.	Future Outlook	173
REFERENCES		175
APPENDICES		200

LIST OF FIGURES

- Figure 2.1:** The structure of a polyelectrolyte hydrogel.
- Figure 2.2:** a) The migration of positively charged drug particles towards the negatively charged anode. b) The forced exudation of the drugs out of the hydrogel system due to contraction of the hydrogel.
- Figure 2.3:** The chemical structure of a block co-polymer and a graft co-polymer.
- Figure 2.4:** The chemical synthesis of polypyrrole.
- Figure 2.5:** Schematic of polymer protonation by conventional protonic acid. Acid counter-ions are not shown.
- Figure 2.6:** A depiction of the mechanism under which the polyaniline undergoes oxidation reaction. The downward arrow represents the oxidation reaction.
- Figure 2.7:** Cyclic voltammetry performed on polypyrrole-para-toluene-sulfonate in 0.2M KCl as supporting electrolyte. The scan rate is 100mV.s^{-1} A/B represents the redox peak associated with cation insertion/expulsion while C/D represents the redox peak associated with anion insertion/expulsion.
- Figure 2.8:** The mechanism by which the duo layered transport system works. When polypyrrole becomes oxidized, it lost an electron and become positively charged, thus repelling drug M which also possessed a positive charge. Similarly, when PVFc becomes oxidized, it becomes positively charged and thus attracts the negatively charged drug.
- Figure 2.9:** The collapsing of the polyelectrolyte hydrogel upon electrical stimulation. These contractions are what caused the water to exude and thus drug release along with the solvent.
- Figure 3.1:** The three oxidation states of polyaniline. Pernigraniline is the fully oxidized state with imine links instead of amine links. Leucoemeraldine is the fully reduced state.
- Figure 3.2:** The setup of the circuit in the stimulus-actuated polymeric device.
- Figure 3.3:** Demonstration of the oxidation and reduction reactions of polypyrrole.
- Figure 3.4:** The *in vitro* test that was conducted on the stimuli-actuated polymeric device in order to assess its drug release.
- Figure 3.5:** The chemical structure of indomethacin.
- Figure 3.6:** The calibration curve for the drug indomethacin in pH7.4 PBS at 25°C.
- Figure 3.7:** The effect of sodium salt on diclofenac.
- Figure 3.8:** The calibration curve for the drug diclofenac sodium in pH7.4 PBS at 25°C.

- Figure 3.9:** The chemical structures of aspirin and salicylate when compared to each other. Aspirin may be synthesized by esterification of the phenolic hydroxyl group of the salicylic acid.
- Figure 3.10:** The calibration curve for the drug aspirin in pH7.4 PBS at 25°C.
- Figure 3.11:** The chemical structure of ibuprofen.
- Figure 3.12:** The calibration curve for the drug ibuprofen in pH7.4 PBS at 25°C.
- Figure 3.13:** The surface morphology of Device 1-4 under 40X magnification, which showed a non-porous surface morphology.
- Figure 3.14:** The setup of the circuit where drug release profile of the SAPD was conducted.
- Figure 3.15:** FTIR spectrum of Indomethacin.
- Figure 3.16:** FTIR spectrum of polyvinyl alcohol.
- Figure 3.17:** FTIR spectrum of Eudragit®.
- Figure 3.18:** FTIR spectrum of polyaniline.
- Figure 3.19:** FTIR spectrum of Device1.
- Figure 3.20:** FTIR spectrum of Device 2.
- Figure 3.21:** FTIR spectrum of Device 3.
- Figure 3.22:** FTIR spectrum of Device 4.
- Figure 3.23:** The possible mechanism for movement of the drug indomethacin out of the hydrogel.
- Figure 4.1:** The dipole movements of dichloromethane and chloroform. In the case dichloromethane, the dipole on both sides cancels each other out, while chloroform exhibits weak dipole movement from the third chlorine atom.
- Figure 4.2:** Chemical structure of methylcellulose. When dissolved in solvents, the OH group loses the hydrogen and allows chemical interactions.
- Figure 4.3:** The various salts that were used in this experiment and the ions that they dissociate into when dissolved in water.
- Figure 4.4:** The linear relationship between the amount of glycerine used and the drug leakage from the stimuli-actuated polymeric device.
- Figure 4.5:** The chemical structure of tri-ethyl citrate.
- Figure 4.6:** The crosslinking mechanism of polyvinyl alcohol which may be used for the synthesis of a polyvinyl alcohol crosslinked system. Here, the polyvinyl alcohol chains are crosslinked by a divalent compound A.

- Figure 4.7:** The crosslinking mechanism between polyvinyl alcohol and diethyl acetamidomaleate.
- Figure 4.8:** The setup which was used to determine drug release of the device under electric current.
- Figure 4.9:** The amount of drug release from 35 release cycles.
- Figure 4.10:** The drug release from release cycles 36-70
- Figure 4.11:** The calibration curve of indomethacin dissolved in 1:1 acetone:water solution under a wavelength of 318nm of UV light.
- Figure 4.12:** The calibration curve of diclofenac sodium dissolved in 1:1 acetone:water solution under a wavelength of 320nm of UV light.
- Figure 4.13:** a) The SAPD before exposure to electric current. b) The SAPD after exposure to electric current.
- Figure 4.14:** The erosion of the SAPD after 60 samples was taken.
- Figure 4.15:** The FTIR of the eroded SAPD (blue) and SAPD without the indomethacin (pink)
- Figure 4.16:** The DSC thermogram obtained from indomethacin.
- Figure 4.17:** The DSC thermogram of the stimuli-actuated polymeric device without the indomethacin.
- Figure 4.18:** The DSC thermogram of the stimuli-actuated polymeric device with the indomethacin.
- Figure 4.19:** a) The MDSC thermogram obtained on peak E. b) The MDSC thermogram obtained on peak D.
- Figure 4.20:** Microscopy of the first erosion site under 32X magnification.
- Figure 4.21:** Microscopy of the second erosion site under 32X magnification.
- Figure 4.22:** a) The surface morphology of an uneroded stimuli-actuated polymeric device at 350x magnification. b) The surface morphology of an eroded stimuli-actuated polymeric device at 390x magnification.
- Figure 4.23:** The concentration of PANi when the PVA is a) 0.25g b) 0.5g and c) 1g.
- Figure 4.24:** a) The force required to compress a stimuli-actuated polymeric device with no DAA. b) The force required to compress a stimuli-actuated polymeric device with 0.25g DAA. c) The force required to compress a stimuli-actuated polymeric device with 1g DAA.
- Figure 4.25:** Drug release from the stimuli-actuated polymeric device with DAA.
- Figure 4.26:** Drug release from the stimuli-actuated polymeric device without DAA.

- Figure 4.27:** The proposed mechanism of the drug release from stimuli-actuated polymeric device.
- Figure 5.1:** The fractional drug release profile of the stimuli-actuated polymeric device over a three hour period with 45 seconds of electric current at an hourly interval.
- Figure 5.2:** The fractional drug release from the stimuli-actuated polymeric device when exposed to various potential differences.
- Figure 5.3:** The quantity of drug release achievable when various voltages were applied.
- Figure 5.4:** Optimization plots showing the effects of polyvinyl alcohol (PAA), polyaniline (PA) and DAA on the Drug release profile, DEE and the Erosion of the stimuli-actuated polymeric device.
- Figure 5.5:** The surface area plot depicting the effect of a) DAA b) PANi and c) PVA on the SAPD.
- Figure 5.6:** The drug release profile of the optimized stimuli-actuated polymeric device after 4 release cycles.
- Figure 5.7:** Cyclic voltammetry of the stimuli-actuated polymeric device in PBS.
- Figure 5.8:** Variation in total steric energy as a function of applied external electric field.
- Figure 5.9:** Visualization of geometrical preferences of polyvinyl alcohol-polyaniline molecule after molecular simulation in a solvated system under external electric field. Colour codes- polyaniline (yellow), polyvinyl alcohol (red) and water molecule (blue).
- Figure 5.10:** The possible setup of the rheometers which can be used. Each setup is suitable depending on the characteristic of the material being tested.
- Figure 5.11:** The yield value of the stimuli-actuated polymeric device.
- Figure 5.12:** The lag between the stress-strain which may be used to determine whether the material under analysis exhibits predominantly liquid or solid properties.
- Figure 5.13:** The results obtained by oscillatory frequency sweep showing both the storage modulus and the lost modulus of the stimuli-actuated polymeric device.
- Figure 5.14:** The effects of temperature on the storage and loss modulus of the stimuli-actuated polymeric device.
- Figure 5.15:** The drug release profile of the conventional oral system compared to the stimuli-actuated polymeric device.
- Figure 5.16:** The computer generated simulation of an eight hourly dose of 25mg indomethacin.
- Figure 6.1:** Schematic showing the design of the *in vivo* studies model for each time period.
- Figure 6.2:** Sketch of the rat showing the site of implantation of the stimuli-actuated polymeric device system into the flank- abdominal area.

- Figure 6.3:** The pathway of a conventional electric shock.
- Figure 6.4:** The setup to be used for the actuation of SAPD via electrical stimulation from the PGSTAT.
- Figure 6.5:** The setup of the rat restraint device during the drug release testing.
- Figure 6.6:** The depiction of a liquid-liquid extraction.
- Figure 6.7:** The FTIR spectrum obtained from the sucrose obtained via the liquid-liquid extraction technique is depicted as blue, while the FTIR spectra of pure sucrose are depicted as black.
- Figure 6.8:** The rats were shaved on the left flank after general anaesthesia. Oxygen was given and pulse was monitored at all times.
- Figure 6.9:** The animals were draped and the surface was cleaned with Hibiscrub.
- Figure 6.10:** a) and b) A 1cm incision were made on the left flank of the rat.
- Figure 6.11:** The implantation of the device into a pocket made under the skin of the rat.
- Figure 6.12:** The incision was then closed up by the use of suture.
- Figure 6.13:** Once the implantation was complete the rats were left in a cage where post-operative care was given and the animals have recovered.
- Figure 6.14:** The HPLC chromatography obtained during the study.
- Figure 6.15:** The HPLC chromatography obtained by Dawidowicz and co-workers.
- Figure 6.16:** The chromatogram obtained from the HPLC when heparin was injected as sample.
- Figure 6.17:** The calibration curve of the drug concentration in the mobile phase which may be used for determination of drug concentrations gathered from the rat model.
- Figure 6.18:** a) to f) indicated the blood samples obtained from rats in the test group, g) to l) indicates blood samples obtained from the placebo group.
- Figure 6.19:** a)-f) The chromatogram of the 6 blood samples obtained when indomethacin were administered intravenously into the rats in the comparison group.
- Figure 6.20:** The UPLC chromatography obtained by the rat blood sample in the placebo group.
- Figure 6.21:** The UPLC chromatography obtained by the rat blood sample in the test group.
- Figure 6.22:** The drug release profile of the SID from the in vivo rat model.
- Figure 6.23:** a), b) and c) The histological sample of rat 1 obtained from different areas of the implantation site.

Figure 6.24: a), b) and c) The histological sample of rat 2 obtained from different areas of the implantation site.

Figure 6.25: The histological sample of rat 7.

Figure 6.26: a) and b) The histological sample of rat 9 obtained from two different areas of the implantation site.

LIST OF TABLES

Table 1.1:	Other possible model drugs that could be incorporated into the SAPD.
Table 2.1:	Various mechanisms which cause the actuation of responsive hydrogel.
Table 3.1:	The composition of all four devices synthesized. Indomethacin was loaded in all four devices, while varying grades of Eudragit® and PVA was used in order to assess difference in indomethacin released under the presence of electric current.
Table 3.2:	The force required for compression of each device as measured by the texture analyzer.
Table 3.3:	The UV-absorbance of samples collected from Device 1.
Table 3.4:	The UV-absorbance of samples collected from Device 2.
Table 3.5:	The UV-absorbance of samples collected from Device 3.
Table 3.6:	The UV-absorbance of samples collected from Device 4.
Table 4.1:	The results obtained from drug release assessment of the chloroform-substituted SAPD.
Table 4.2:	The amount of drugs present in the control sample after been immersed for 72 hours.
Table 4.3:	The drug release profile of the diclofenac-substituted implant after several time intervals.
Table 4.4:	The release of diclofenac sodium in the absence of the electrical current.
Table 4.5:	The compositions of the modified Devices 5-7.
Table 4.6:	The reactions of various materials with methylcellulose
Table 4.7:	The reactions of various grades of Eudragit®
Table 4.8:	The quantity yielded by crosslinking with Eudragit® and the respective salts.
Table 4.9:	The drug release of the SAPD gathered at the specified time intervals.
Table 4.10:	The composition of the modified Devices 8-12.
Table 4.11:	The devices with varying amounts of plasticizer and its respective drug leakage.
Table 4.12:	The composition of Devices 13-15.

- Table 4.13:** The percentage of drugs which was present in the 30mL PBS sample. Device 14 and 16 has indicated drug leakage and unsuitable for SAPD.
- Table 4.14:** The results obtained from drug release (%) of the two Devices.
- Table 4.15:** The quantity of drugs released by the system converted to percentage
- Table 4.16:** The quantity of ibuprofen present in the samples extracted during the drug release assessment.
- Table 4.17:** Indomethacin release from the SAPD when exposed to electric current.
- Table 4.17:** The quantity of indomethacin released by the SAPD after 35 samples were taken.
- Table 5.1:** The upper and lower limit levels used for the Box-Behnken Template.
- Table 5.2:** The results obtained from Minitab® for the optimization of the stimuli-actuated polymeric device.
- Table 5.3:** The probability of achieving each of the ideal characteristics when employing the yielded optimal value
- Table 5.4:** The conductivity obtained from the SAPD containing various concentrations of PANi. Six readings were obtained for each concentration and an average was recorded as the result.
- Table 5.5:** Calculated energy parameters (kcal/mol) of the PVA/PANi complex in a solvated system under the influence of electric field.
- Table 6.1:** The amount and species of animals required for this animal study.
- Table 6.2:** The amount of drugs to be used for the animal study.
- Table 6.3:** The difference in the weight of the rats 10 days after the implantation procedure was performed.

LIST OF EQUATIONS

Equation 3.1: The total compression of the SAPD

Equation 4.1: The percentage weight loss of the SAPD

Equation 4.2: The maximum amount of glycerine allowed in the SAPD

Equation 4.3: The calibration curve of indomethacin dissolved in 1:1 acetone:water solution

Equation 4.4: The calibration curve of diclofenac sodium dissolved in 1:1 acetone:water solution

Equation 5.1: Conversion of frequency into cycles per second

Equation 6.1: The conversion of voltage to ampere

Equation 6.2: Conversion of ampere into power

Equation 6.3: The target injection volume for the Ultra Performance Liquid Chromatography

Equation 6.4: The gradient duration of the High Performance Liquid Chromatography

Equation 6.5: The target flow rate of the Ultra Performance Liquid Chromatography

Equation 6.6: Gradient step time of the High Performance Liquid Chromatography

Equation 6.7: Gradient step volume of the High Performance Liquid Chromatography

CHAPTER 1

INTRODUCTION

1.1. Introduction

The management of chronic pain has always proved to be challenging for both clinicians and patients. Pain is caused due to the activation of nociceptors, which conveys signals to the brain and is interpreted as pain (Semenchuk, 2000). This activation may be caused by injury and in most cases, complete pain relief is rare and difficult. The World Health Organisation (WHO) has set up a three-step ladder algorithm as a guide for the treatment of the chronic pain (Barakzoy, 2006). This ladder aimed to treat pain by using a combination of non-opioid analgesics and opioid analgesics which proved to be effective for 80-90% of cases. However, treatment with such analgesics and opioids often resulted in significant side-effects. Patients may feel severe chronic nausea, vomiting, itching, constipation or drowsiness (Raghavan, 2011 and Palos, 2004). In severe cases, patient dependence and addiction may occur, leading to treatment complications.

Conventional treatment of chronic pain included patient-controlled pump administration of oral tablets and drugs which relied on patient compliance and often induces gastric side-effects. Long-term use of Non-Steroidal Anti-Inflammatory Drugs (NSAIDs) may cause gastric ulceration, increased risk of cardiovascular disease, fluid retention and interactions with anti-coagulants (Prasad, 2008). Oral drugs tend to have limited dissolution or be strongly ionized which decreases absorption through the intestine (Pleuvry, 2006). Traditional oral or parenteral drugs may have inadequate therapeutic effects and further metabolism and inactivation of the drug which may result in even lower systemic levels of the drug (Pleuvry, 2006).

To date, research on Electro-Active Polymers (EAPs) have shown that EAPs can be employed for various applications (Palmre, 2011; Sheika, 2004; Pernaut, 2000 and Bar-Cohen, 1999). Researchers have envisaged that EAPs may one day be used as artificial muscle and implanted into patients who have suffered from muscular injuries. Robotic scientists have managed to create robotic arms with grippers by using EAPs. The use of EAP for drug delivery is also currently a novel area of research (Prakash, 2008). In 2000, a company called Creganna (Pty) Ltd. (Marlborough, Massachusetts, USA) designed an EAP-based substance delivery system called Micro-muscle[®] using EAPs which allowed a

substance to be released when the system was exposed to an external electric current. EAPs may be the center of current drug delivery system, however, other possible stimuli can also be considered for the purpose of drug delivery. These include polymers such as poly(lactic acid) (PLA), polyglycolides (PGA) and polylactide-co-glycolides (PLGA) which are biodegradable and biocompatible polymers that can be implanted without the need to be removed once the drug-load is depleted from the device.

The use of a patient-controlled targeted drug delivery device may thus prove to be efficient in the treatment of chronic pain. Targeted delivery would remit drug directly at the site of pain, eliminate the problem of first pass metabolism and systemic circulation which occurred with a conventional oral tablet. This may be achieved by implantation of the device directly at the site of pain. In order to allow the patients' control over the device, the device should be capable of an "On-Off" mechanism via an external stimulus. The external stimulus should result in drug release from the device directly to the target site. Once therapeutic dose was achieved, the external stimulus may be removed and drug release would cease.

Research in the sector of EAP is considered as one of the most popular topics. To date, researches on EAPs have shown that EAPs can be employed for a wide variety of applications (Pernaut, 2000; Bar-Cohen, 1999; Chiba 1999). One of these applications included the use of EAPs as an artificial muscle and implants in patients who have suffered from muscular injuries (Sheika, 2004). Robotic scientists have managed to create robotic arms with grippers by the use of an EAP. EAPs used for drug delivery is, however, currently a less explored area of research (Prakash, 2008).

EAPs have gained increased attention from scientists across various fields, starting as early as the 1970's. The EAP's unique ability to undergo redox reactions upon the activation of an electric current has distinguished itself from other polymers. Recently, researchers have been looking at these polymers for the possible use of substance delivery in humans. A few novel EAPs have fulfilled these criteria, however, there are still possibilities of synthesizing new EAPs in the future.

A polymer is chemical specie with a very high molecular weight and comprised of repeating units of low molecular weight. The units that made up the polymer are called monomers. Polymers were initially discovered in 1909 in the form of resin used in adhesives and paints. Since then, chemists have continued to formulate new polymers. Polymers may be classified

as addition polymers or condensation polymers depending on the reaction that was used to form it (Ebbing, 1996).

Recently, a new method of polymerization has been extensively used for the synthesis of an EAP. This method is known as electropolymerization. Electropolymerization is one of the most powerful tools that can be used for the development of modified electrodes. The end result of an electropolymerized material is usually one that possesses unique properties than that of its monomer (Karyakin, 1998). EAPs are capable of exhibiting diverse electrical properties. The imposition of an electric charge upon a polymer will cause a redistribution of any charge of that polymer, provided that it is mobile enough to respond to the charge. In summary, the response of a polymer to an electric field can be summarized into two parameters, and each parameter can be divided further into two subparameters:

Dielectric properties:

- Dielectric constants which represents polarization
- Tangent of dielectric loss angle which represents the relaxation phenomena.

Bulk conductive properties:

- Dielectric strength, which represents the breakdown phenomena
- Conductivity which represents electrical conduction

In addition to these two fundamental sub-parameters, there were other electrical properties which were sought after. New materials have been developed and other special electrical properties include piezoelectric, pyroelectric, ferroelectric, triboelectric, photovoltaic and photoconducting materials (Ku, 1987).

It is generally accepted that during the oxidation or reduction of an EAP, electrochemical charge is transported through the polymer by an electron hopping mechanism. The rate of reduction or oxidation within a polymer film can be expressed in terms of a diffusion coefficient (D_E). This coefficient described the efficiency of charge percolation through the polymer which can be determined by the use of cyclic voltammetry, chronoamperometry or chronocoulometry (Lyons, 1990). These properties are important as the response time in which the EAPs react toward the stimuli is directly related to these properties.

A few drugs that were considered for incorporation into a proposed EAP included those in the groups of opioids and NSAIDs or selective COX II inhibitors. Table 1.1 provided a list of possible water-soluble opioids which may be used in this drug delivery device.

Table 1.1. Other possible model drugs that could be incorporated into the SAPD.

Opioids which may be incorporated	Therapeutic advantage	Water solubility	Properties
Morphine (Bijur, 2005; Masako, 2003; Podczek, 1996; Hasselström, 1990)	By delivering drug directly to the blood stream, a decreased dosage is required and thus less chance of side-effects	Morphine is soluble in water and is administered as an injection. Therefore, morphine may be incorporated as a water soluble base in an EAP matrix system	pKa 7.8. Side-effects include respiratory depression, itching, mouth dryness and nausea. Mean terminal elimination half life is 4.2 hours. Standard dose is 0.1mg/kg intravenous injection.
Hydromorphone HCl (Golembiewski, 2005; Hong, 2008 and Gupta, 2007)	By delivering drug directly to the blood stream, a decreased dosage is required and thus less chance of side-effects	By incorporating hydromorphone HCl, the water solubility is increased to 1:3 hydromorphone:water solubility. This will also allow it to be incorporated as a water soluble water	pKa 8.1. Side-effects include miosis, constipation, respiratory depression and nausea. Mean termination half life is 2.6 hours. Dosage 0.2-0.4mg initially, then 0.1-0.2mg every 5-10min
Methadone HCl (Han, 2008; Sadosky, 2000 and LoVecchio, 2007)	By delivering drug directly to the blood stream, a decreased dosage is required and thus less chance of side-effects	Methadone, when incorporated with a HCl salt, is freely soluble in water and can thus be incorporated as a water soluble base	pKa 8.7 in water at 20°C. Side-effects include respiratory depression, constipation, miosis, nausea and hypotension. Terminal half life ranges from 8-59 hours. Initial dosing is 2.5mg to 10mg i.v. every 8-12 hourly.
Indomethacin (de Jong, 2008)	NSAIDs may be released directly at the target site to achieve anti-inflammatory effect	Indomethacin is poorly soluble in water and solubility increases under basic pH	pKa 4.5. Side effects include constipation, diarrhoea, dizziness, drowsiness, headache, heartburn, nausea and stomach upset.

Diclofenac sodium (Kearney, 2006; Brater 2002)	NSAIDs may be released directly at the target site to achieve anti-inflammatory effect	Diclofenac alone is poorly soluble in water, but incorporation of a sodium salt increases the water solubility	pKa 4.0. Side effects include increased risk of thrombotic event, myocardial infarction, gastric ulceration and renal toxicity.
--	--	--	---

Therefore, when formulating a stimulus-responsive drug delivery device using an EAP, it was important to bear in mind these unique characteristics in order to obtain optimal and efficient release of drug from the device.

The aim of this study was to develop an SAPD that is capable of controlled drug release upon the application of an external electrical stimulus. This would require the patient to carry an external device that would allow them to actuate the SAPD at the patient's own choosing. This system may eliminate the challenges that were encountered in patients who were taking long-term analgesics, had a risk of dependence, tolerance and were susceptible to significant side-effects due to unnecessarily increased doses over prolonged periods of time. The use of this patient-controlled system would also enable prospective drugs to be used in the future by using the concept developed in this study. Furthermore, the development of this SAPD would improve the application of the EAP in a biocompatible setting.

In order to achieve this goal, the following objectives were outlined:

1. Develop a SAPD that allowed drug release at the desired time and quantity.
2. Characterization of the EAP's physicochemical and physicomachanical properties.
3. To develop a novel drug delivery system by using the EAP as a platform for the SAPD.
4. To develop a device that would be compatible with the intended drug to be used and subcutaneous site of implantation.
5. To perform *in vitro* studies to determine the amount of drugs released when exposed to a stimulus such as electric current.
6. To investigate of other factors which may affect the release of drug and the operating of the system as a whole, such as temperature, pH etc.
7. To perform *in vivo* animal studies in order to assess the established pharmacokinetic parameters of the device in a suitable model such as the Sprague Dawley rat
8. To compile a preliminary histomorphological report using the *in vivo* data obtained from animal studies

1.2. Approach to this study

The aim was to develop a subcutaneous implantable system which could be implanted at the site of the chronic pain. This implantable system would release drug, in response to an external stimulus such as electric current, directly to the target site. The external stimulus of the electric current would have to be generated via an external device. This could reduce the gastric side effects that were caused by chronic use of NSAIDs and reduce the dosage required due to its high protein binding.

This approach relied on the use of a hydrogel or a polyelectrolyte hydrogel, into which, analgesic drugs would be incorporated. The drug may be physically blended into the hydrogel while it was in its liquid state, or it may be dissolved in a solvent. The hydrogel may also be placed into the solvent where the drug would be absorbed. The amount of drug absorbed may be calculated by measuring the difference in drug concentration before and after the incorporation of the hydrogel.

Another approach was to form a hydrogel with an inter-penetrating network (IPN) of EAP, through which electricity would be conducted. Once the electric current was flowing through the hydrogel via the EAP, the drug would move out of the hydrogel through mechanisms such as electrophoresis or repulsion of an anionic drug against the electric current. This phenomenon would stop once the electric current was ceased, thus resulting in termination of drug delivery to the target site.

Once the drug was depleted in the hydrogel, the implant would have to be removed, in the case of a non-biodegradable implant, and replaced with a new implant. The implant was aimed to last for a period of two months while delivering standard analgesic dose of the drug which it contained. Therefore, the use of a more potent anionic drug was preferred for the design of this system.

1.3. Overview of this dissertation

Chapter 1 investigated the background and possible challenges to the current development of the SAPD. Electro-behaviour of the EAPs was examined and possible drugs which may be incorporated were discussed. The understanding of these factors was important as these factors would greatly affect the design of the SAPD.

Chapter 2 provided a comprehensive literature review on current research into the stimuli-actuated polymers and hydrogel systems. This provided us with various approaches taken by other researches and possible challenges which still remained in the field of stimuli-actuated drug release systems.

Chapter 3 was the pre-design and formulation of the SAPD. This chapter highlighted the various designs which were used and the efficacy of such design. In the light of a design not producing satisfactory results, the reason of this result was investigated and further designs were made to improve the results. Light microscopy was used to assess the surface morphology coupled with Fourier Transform Infra-Red in order to assess the chemical compositions of the SAPD.

Chapter 4 described the development of a non-soluble hydrogel based on the results obtained in Chapter 3. The formulation of this hydrogel was followed by incorporation of an EAP and a drug which would then be further assessed. The actuation was achieved by the use of a PGSTAT instrument and drug release was ascertained with the use of an UV/visible spectroscopy.

Chapter 5 focused on the optimization and characterization of the developed SAPD. The design of the SAPD in Chapter 4 was initially optimized with a Box-Behnken Design. Once the SAPD was optimized, external factors such as actuation voltage and storage temperature were optimized. The release mechanism was investigated with the use of chemometric modelling to determine the mechanism of the erosion at a molecular level.

Chapter 6 investigated the *in vivo* drug release profile of the SAPD as well as its biocompatibility. SAPD was implanted for a period of 30 days and actuated periodically. Blood samples were taken and analyzed with both HPLC and UPLC to ascertain the presence of drug in the blood sample. Histological samples were taken at the end of the 30 day period to determine the biocompatibility of the SAPD.

Chapter 7 provided the conclusion, recommendations and future developments for further studies.

CHAPTER 2

DESIGN, ADVANCES AND APPLICATIONS OF ELECTROACTIVE POLYMERIC SYSTEMS AS A RESPONSIVE DRUG DELIVERY STRATEGY

2.1. Introduction

A hydrogel is comprised of a 3-dimensional hydrophilic network structure which is capable of absorbing water and remains insoluble in water due to its crosslinked, entanglement or crystalline structure (Peppas, 2006). By incorporating an EAP into the hydrogel, the EAP not only renders the hydrogel responsive, but offered other advantages as well. In order to overcome this drawback, there were three ways in which the EAPs may be prepared in order to enhance its physical property and its uses. The first technique was physical blending of the EAP with an insulating material. The second technique involved electro-chemical or chemical oxidative polymerization of the EAP into another matrix system, and the third technique involved creation of a composite via co-deposition of the EAP and the insulating polymer (Brahim, 2004). The blending of an EAP into a hydrogel was an example of the second technique. This blending may also render the hydrogel responsive towards electrical stimulation. The responsive behaviour that would be exhibited from the hydrogel may be due to conformational changes. The resultant change may be actuation, catalytic, signalling event, movements or interactions with other species (Ehrick, 2005). A responsive hydrogel may respond to stimuli such as pH, temperature, electric fields, saccharides or even antigens (Miyata, 1999). Table 2.1 demonstrated the various stimuli which have been discovered for the actuation of a responsive-hydrogel.

Table 2.1. Various mechanisms which cause the actuation of responsive hydrogel (Kim, 1996).

Stimulus	Hydrogel	Mechanism
Thermal	Thermal responsive hydrogel such as poly-N-isopropyl-acrylamide.	Change in temperature would cause polymer-polymer and water-polymer interaction. This may lead to swelling and drug release.
Magnetic	Magnetic particle dispersed in alginate microsphere.	When magnetic field was present, a change in porosity may lead to drug release.
Ultra-sound irradiation	Ethylene-vinyl alcohol hydrogel.	Upon ultra-sound irradiation, the temperature of the hydrogel may increase, which could result in drug release.
pH	Acidic or basic hydrogel.	Change in pH may lead to swelling and therefore drug release.
Ionic Strength	Ionic hydrogel.	Change in ionic strength which caused changes in concentration of ions inside the gel. This may lead to change in swelling and thus drug release.
Chemical species	Hydrogel containing electron-accepting groups.	Electron-donating compounds may interact with the hydrogel to form charge/transfer complex. This caused swelling of the hydrogel and possible release of drug.
Enzyme substrate	Hydrogel containing immobilized enzyme.	When substrate was present, the hydrogel undergoes enzymatic changes, which lead to drug release

In order to enhance the response from a responsive hydrogel, one may incorporate acidic or basic groups into the hydrogel. These hydrogels are termed polyelectrolyte or ionized hydrogel. Such hydrogel consisted of three species, namely the solid matrix network, interstitial fluids and ionic species. The depiction of the polyelectrolyte hydrogel is provided in Figure 2.1.

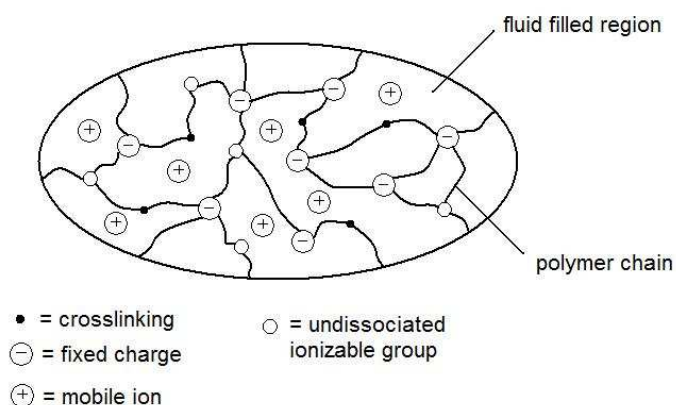


Figure 2.1. The structure of a polyelectrolyte hydrogel (Li, 2007)

Polyelectrolyte hydrogel such as polyacrylic acid, along with sodium or potassium as its salt, is a popular research material (Chansai, 2008; Adnadjevic, 2007; Huang, 2007; Wang, 2006; Li 2005 and Philippova, 1996). Other hydrogel which have been synthesized previously included hyaluronic acid hydrogel sodium salt entrapped hydrogel. It was discovered that when the hydrogel was placed between two electrodes, there was shrinkage in volume at the anode and therefore drug release (Sutani, 2001). Factors which affected drug release from the hydrogel included degree of swelling, crosslinking density and the composition of the monomers used for the synthesis of the polyelectrolyte hydrogel.

This drug release may be due to the ionizable groups of the polyelectrolyte hydrogel, which was responsible for the physical and chemical changes in the hydrogel (Gao, 2003). This phenomenon could be attributed to the charges on the polymer backbone which formed the hydrogel. These charges allowed interactions with the external electric fields or surrounding ionic surfactants. Interactions between polyelectrolyte hydrogel and surrounding ions were particularly interesting in the field of engineering, where it could be used to selectively remove surfactants from water (Zielińska, 1999).

The 2 mechanisms which were responsible for the release of drugs upon electrical stimulation included (Kulkarni, 2009):

- Migration of the drug towards the electrode of opposite charge.
- Hydrogel contraction causing the drug to emit from the hydrogel.

The mechanisms listed above were not exhaustive and other mechanisms may be present. Figure 2.2 depicted these two mechanisms of which the drug migrated outward from the hydrogel.

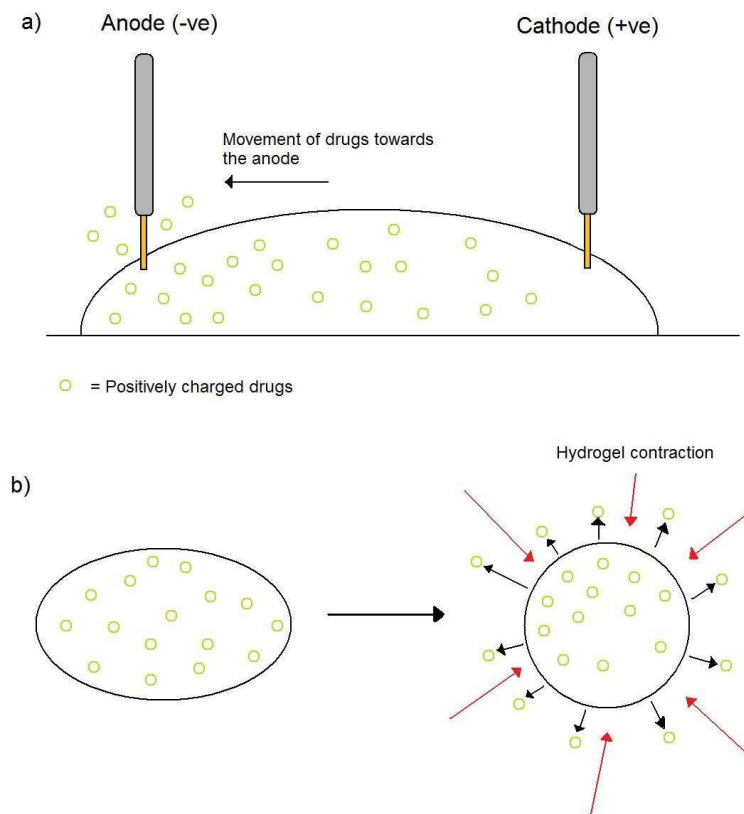


Figure 2.2. a) The migration of positively charged drug particles towards the negatively charged anode. b) The forced exudation of the drugs out of the hydrogel system due to contraction of the hydrogel.

The migration of the drug particle outside the hydrogel may be determined by the porosity and the network structure of the hydrogel, in addition to any fixed charge in the hydrogel, as in the case of polyelectrolyte hydrogel. The forced exudation of the drug out of the hydrogel was caused by the contraction of the hydrogel. This contraction caused a build-up of positive pressure within the hydrogel, which resulted in the exudation of the hydrogel matrix in order to decrease this pressure build-up. Drugs dissolved within the hydrogel matrix may therefore be released via this mechanism. By controlling the rate of this contraction, one may be able to control the amount of drugs that was exuded from the hydrogel. Hydrogel may also be responsive towards electric current, and exhibited contraction when exposed in an electric field. Human muscle is an example of an ionic EAP, and it is therefore not surprising that ionic EAPs have been an extensively researched material for the purpose of artificial muscle. It is important to note that although the EAP and muscle were both responsive towards electric current, human muscle utilizes a sodium potassium pump and calcium pump for the movement of ions in and out of the cell and is generally much more intricate and complex than the ion movements found in a responsive hydrogel. However, the use of an EAP as

artificial muscle is still promising and basic movements from an ionic EAP have been achieved.

2.2. The method of preparation of a responsive electroactive polymer-based hydrogel

The importance of hydrogels in a wide variety of fields meant that it is a very versatile material (Hoffman, 2002). The result was that many varieties of hydrogels have been synthesized using different methods. These varieties of hydrogels are still capable of retaining water within its structure and swell without dissolving, however, the degree of swelling differs according to the degree of crosslinking. Certain hydrogels are capable of absorbing water many hundred times more than its dry weight and are called superabsorbent hydrogels (Francis, 2004). These hydrogels seems like a practical approach for the purpose of environmental cleaning. An increase in crosslinking within a hydrogel would increase the structural integrity, resulting in a decrease in the swelling of the hydrogel. This in turn would decrease the amount of water that the hydrogel can hold (Rokhade, 2007). A hydrogel may be synthesized as a blend, a co-polymer, a graft, an inter-penetrating network (IPN) or a composite and each was structured differently. A blend hydrogel was synthesized by the interaction between two or more reagents. One example would be a hydrogel formed via the esterification of PVA and gelatine (Pawde, 2008). The esterification occurs between the hydroxyl group of the PVA and the carboxyl group of the gelatine, forming a hydrogel. Sometimes, the hydrogel may be the result of two monomers reacting together to form a polymer, or by incorporation of one polymer into another. These hydrogels are termed co-polymer hydrogels. A study done by Henderson and co-workers (2010) has managed to form a hydrogel which consisted of a crosslinked tri-block copolymer network (Henderson *et al.*, 2010). A graft hydrogel would be similar to a copolymer hydrogel, as the polymer which was used to form the hydrogel was a graft co-polymer (Sui, 2010). A graft co-polymer is a type of branched co-polymer with the side chain that was different and separate from the main chain. In the case of the graft co-polymer, the co-polymer formed usually combined the properties of both polymers which formed the co-polymer (Kulkarni, 2009). The difference between the block co-polymer and graft co-polymer may be depicted by Figure 2.3 where A and D represents two different monomers.

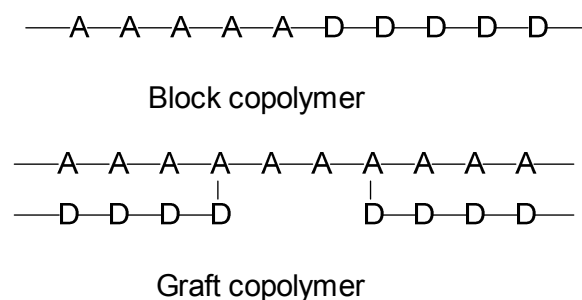


Figure 2.3. The chemical structure of a block co-polymer and a graft co-polymer.

The next hydrogel structure which may be formed was the IPN hydrogel, which was essentially a network within the hydrogel network itself. It may be classified as a class of polymer as it blends in a network fashion, in which at least one component was polymerized in the presence of the other (Prashantha, 2001). EAPs were commonly incorporated into the hydrogel in the form of IPN. This may increase the conductivity of the electrical stimulation into the hydrogel and improve the electro-response of the hydrogel. The IPN hydrogel may be formed by initially creating a solution containing both the raw materials for the hydrogel and the EAP. The initiator and crosslinker would be added into the solution simultaneously. The crosslinking and polymerization can continue for several hours until the hydrogel was formed (Lü, 2010). IPN hydrogels were commonly synthesized with incorporation of an EAP. The last class of hydrogel was the composite hydrogel. A composite hydrogel was formed when a particle has been embedded within the hydrogel network. These particles did not have any direct interactions with the hydrogel. Composite hydrogels can be synthesized as a responsive hydrogel, where the drug was entrapped within the hydrogel. The responsive hydrogel swelled or de-swelled when exposed to various stimuli and resulted in drug release (You, 2010). With all these possible structures, one may be able to synthesize a responsive hydrogel which may suit individual needs in accordance with swellability, structural integrity, response and biocompatibility. In certain cases, a combination of hydrogel types may be formed, such as the incorporation of an IPN in a grafted co-polymer hydrogel. The importance of responsive hydrogels in controlled substance delivery is crucial.

2.3 The application of electroactive polymers in the Stimuli-Actuated Polymeric Device as a responsive drug release strategy

Polymers were initially discovered in 1909 in the form of resin for adhesives and paints. Since then, chemists have continued to formulate new polymers, which lead to the discovery of the EAPs. Polymers may be classified as either addition polymers or condensation polymers, depending on the reaction that was used for its synthesis (Ebbing, 1996). The

polymerization process was important as it may determine the electrical properties of the resultant EAPs. More recently, a new technique of polymerization has emerged, and this was the process of electropolymerization.

Electropolymerization is a useful technique that can be used for the development of a modified EAP. The end result of electropolymerized materials is usually one that possesses unique properties than that of its monomers (Karyakin, 1998). One major drawback which limits the use of electropolymerization in industry is that a small amount of polymers are formed each time since the electropolymerization process occurs only on the surface of the electrodes (Asami, 2005; Ali, 2006; Wang, 2007 and Walter, 2010). Therefore, the mass production of EAP using such methods may prove to be unfeasible.

Electrical properties of a polymer can be extremely diverse. The imposition of an electric charge upon a polymer would cause a redistribution of any charge of that polymer, provided that these charges were mobile enough to respond to the charge. Another subclass of the EAP in the field of drug delivery was that of the conducting polymer. A conducting polymer is a polymer that is capable of carrying electrical charges along its length (Kumar, 1999), while EAPs are polymers which exhibit size or shape changes when exposed to electric current (Dubois, 2006). The changes were usually reversible once the electric current was removed with no permanent change in the volume. One reason why conducting polymer is popular is because they possessed both the conducting property of the metal and the favourable mechanical properties of a non-conducting polymer. Conducting polymers are, however, a sub-category of EAP and a small amount of swelling does occur when electric current is passed along its length.

It is now generally accepted that during the oxidation or reduction of an EAP, electrochemical charge is transported through the polymer by an electron hopping mechanism. The rate of reduction or oxidation within a polymer film can be expressed in terms of the diffusion coefficient (D_E). This coefficient described the efficiency of charge percolation through the polymer and could be determined by the use of cyclic voltammetry or chronoamperometry (Lyons, 1990). The response time of an EAP may also be affected by the type of EAP which it belonged to. Electronic EAP exhibited a rapid response time of milliseconds but required higher voltage in order for actuation to occur, whereas ionic EAP has a slight slower response time, but required much lower voltage for actuation to occur (Bar-Cohen, 2007).

Hydrogels, on the other hand, are crosslinked 3-dimensional system which are capable of swelling and is not soluble in the solvent into which they were placed (Wang, 2010). Hydrogels are themselves, not responsive, but EAPs may be incorporated into the hydrogel in order to render them responsive. Responsive hydrogels are hydrogels which are responsive towards external stimuli (Deng, 2009). Responsive hydrogel is also an area of interest for researchers due to its potential as actuators (De Rossi, 1991), separation device (Park, 1992) and even responsive drug delivery systems (He, 2008 and Bikram, 2007). These gels are capable of swelling and de-swelling when exposed to various stimuli and thus altering the rate of drug release. These responsive hydrogels were termed 'intelligent' hydrogels, and were responsive towards several stimuli, including electrical stimulation (Murdan, 2003). Similar to other responsive hydrogel, swelling or de-swelling may occur when the electro-responsive hydrogel was exposed to electric current, which altered the rate of drug release.

The use of the EAP and responsive hydrogel may be suitable for situations where drug release is preferred in the presence of certain external stimulus to allow the patients control over the drug release from the system. One challenge regarding the use of these 'intelligent' materials was that physical properties such as drug size, charge and solubility have to be taken into account during formulation. Therefore, formulation of a responsive device for multiple drugs or combination therapy may require adaptations of the device in order to achieve an ideal drug release profile for each of the drugs. The use of these responsive materials for drug delivery may improve the compliance with a decrease in side effect profile.

2.4. Electroactive polymers as a constituent of a polymeric substance delivery system

Currently, two of the most promising responsive delivery platforms that have undergone intense research are the responsive hydrogels and EAPs (Kim, 2005 and Bawa, 2009). In order to develop a drug delivery system which ensured an optimal drug release profile, it was important to consider possible drug-hydrogel interactions and drug-EAP interactions. The most common EAPs that was researched included that of PANi (Bidez, 2006), ethylene vinyl acetate, polyethylene (Kamalesh, 2000) and PPy (Wang, 2003). Other materials that could be used include biocompatible EAP such as polylactic acid (PLA), polyglycolic acid (PGA), polylactic-co-glycolic acid (PLGA), ethylene-vinyl acetate (EVA) co-polymer and polyaniline (PANi). EVA is a soft and flexible material that can be moulded. Although ethylene-vinyl acetate co-polymer was not biodegradable, it was also inert in the human body and therefore did not cause any reactions or unwanted effects in the body. PANi is a

conducting polymer with high electrical conductivity. It was readily available, stable and requires simple doping chemistry. It was also characterized by controllable electrical conductivity and has rich redox chemistry. Furthermore, it was a biocompatible substrate and its biocompatibility can be further enhanced by adding side chains such as collagen or gelatin (Huang *et al.*, 2006).

Another possible material that could be used is polypyrrole (PPy). It exhibited high electrical conductivity, stability and rich redox reversibility. However, two drawbacks were the fragility and insolubility (Li, 2007). Polyamide groups that could be considered included those with oligoaniline and ferrocene in the main chain or polymerization of macro-monomer of oligoaniline and *p*-phenylenediamine. This has shown characteristics of reversible electrochemical property with a conductivity of $7.6 \times 10^{-7} \text{Scm}^{-1}$ at room temperature (Chao, 2006). PANi and its derivatives were especially popular because it could be processed into different redox states in addition to a controllable conductivity and stability. Its uses have been extended to the field of dentistry such as thoracic, maxillo-facial surgery and dental implants (Kamalesh, 2000). Uses of PANi in other fields include antistatic applications (Lekpittaya, 2004), gas sensor (Kincal, 1998) and dye removal (Lopes, 2004).

Another popular use of EAPs outside the field of drug delivery was the synthesis of artificial muscle. The polymers could change its size and shape upon actuation with electrical stimulation. Currently, there are other responsive polymers which respond to stimuli such as chemical, pneumatic, optical and magnetic and have already been synthesized. When compared to these responsive polymers, EAPs could be tailor-made into different behaviours when doped with various counter ions. Practitioners in the field of biomimetic science have been able to mimic basic insect and animal movements by the use of EAPs. Previously, EAPs have received little attention due to its poor actuation abilities and short selection of material. This has changed in the past fifteen years as new materials were discovered and synthesized (Bar-Cohen, 2007). Furthermore, the uses of EAPs in the field of drug delivery have been gaining significant attention due to its promising prospective for *in vivo* use. With an increased application for these polymers in human tissue, great concerns have begun to arise as to the biocompatibility of these EAPs. A study was done on ethylene-vinyl acetate co-polymer (EVAc), polyethylene and PANi in its emeraldine, pernigraniline and leucoemeraldine state by implantation of these EAPs into male Sprague-Dawley rats for a period of 19-90 weeks in order to assess for any histological changes in rat tissue. This was due to concerns that prolonged implantation of these EAPs in human tissue may cause increased risk of tumor (Kinoshita, 1995). However, results obtained from the study has

showed that the Sprague-Dawley rat cells did not show any carcinogenic behaviour even after two years of implantation and that these polymers were indeed biocompatible enough to be implanted subcutaneously (Sengothi, 1999).

There are other EAPs groups which also exhibited biocompatibility in humans other than PANi. One such polymer is that of the PPy group. Like PANi, not only was it compatible with human tissue, but it also exhibited controllable physicochemical properties. The synthesis of PPy can either be chemical or electrochemical. Figure 2.4 depicted the chemical polymerization of PPy from the monomer pyrrole.

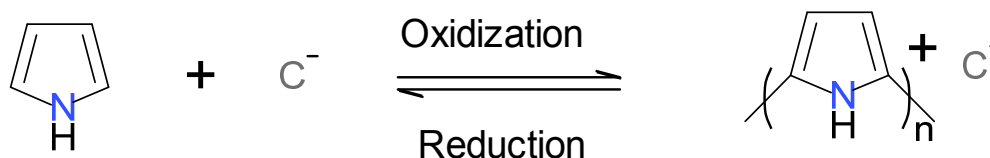


Figure 2.4. The chemical synthesis of polypyrrole.

The polymerization process of most EAPs indeed followed the same concept as the mechanism depicted in Figure 2.4. The polymerization began via the oxidation of the monomer pyrrole. C^- is the counter-ion used in the synthesis of the PPy membrane and was incorporated into the polymer due to its negative charge which compensated for the positive charge on the polymer backbone (Zhao, 1996). Figure 2.4 has demonstrated that it was possible to incorporate various counter-ions during the polymerization process, thus altering the physicochemical properties of the finished product. Although there were a wide variety of counter-ions to choose from, the selection was dramatically reduced when taken into account the conductivity and the mechanical property of the final product. Sometimes, a mixture of counter-ions may be used in order to achieve optimum conductivity and physical property (Zhao, 1998).

The counter-ions, especially the anions, incorporated into the polymer were responsible for the transport mechanism. If enough negative potential was applied, it would force the anion out of the polymer and the reaction undergoes reduction. If a repetitive pulsed potential waveform was applied to the membrane, transportation through the membrane via this mechanism was maintained. The counter-ions may be incorporated into the polymer membrane via the process of electropolymerization. Some suitable counter-ions that may be used include that of sulphonated aromatic groups. However, some counter-ions may inevitably become trapped during the polymerization of the polymer which rendered it immobile in terms of ion transportation (Zhao, 1994).

Once an anion was incorporated into the polymer, it could be expelled and re-incorporated into the polymer again by using an appropriate repetitive pulsed potential waveform. When the polymer doped with the anion was left in a solution with cationic electrolytes, the cations may directly displace the anions incorporated into the polymer. If the surrounding solution contained anionic electrolytes, then the anions that were originally incorporated in the polymer may diffuse outwards and eventually be replaced by the anions in the surrounding solution (Mirmohseni, 1995). In the case where the solution contained both anions and cations, there was generally a combination of both cationic and anionic movements (John, 1993).

In order for this electroactive transport system to be effective, the membrane system must be capable of the following (Zhao, 1996):

- The transport mechanism should have a rapid 'on-off' switching mechanism when necessary.
- Controllable flux and sustainable level of transport.
- Controlled selectivity with regards to the ionic species undergoing transportation.

2.4.1. Polyaniline as a component of the electroactive polymer-based drug delivery system

PANi-derived EAPs have attracted much attention from researchers across various fields due to its high stability in air, moisture, high electrical conductivity and unique redox properties (Moon, 1993), although several challenges still remained when it came to synthesizing PANi for commercial use. The synthesis of PANi required harsh conditions and PANi synthesized usually exhibited poor processability (Samuelson, 1998). Another challenge regarding the use of PANi was the limited solubility in solvents. To date, researchers have combined aniline with other water-soluble monomers during the polymerization to obtain a PANi copolymer which could offer better solubility whilst maintaining the desirable mechanical properties and electrical conductivity of a PANi (Wang, 2003). Several researches have already synthesized water-soluble PANi in order to improve the processability of the PANi (Zhang, 2006; McCarthy, 2002 and Kenji, 2000). This was done either by the process of electropolymerisation or simply polymerizing a water-soluble analogue of the monomer aniline. By using electropolymerisation as the process for developing EAPs such as PANi, we allowed better incorporation of dopant ions into the polymer than that of chemical polymerization. To further enhance the mechanical property of the synthesized polymer, one may also synthesize the polymer as a film by ordinary casting method or via the preparation of composite polymer (Kitani, 1997). Another method would be

synthesizing PANi as a co-polymer along with another water soluble polymer. One disadvantage of electropolymerisation was that the polymers could only be synthesized as a thin film on the electrode and production on a large scale would be unfeasible (Palaniappan, 2006). The fabrication of a large electrode itself was also difficult to achieve (Lindström, 2001). Therefore, for large scale production of electroactive polymer (EAP), the preferred method was still the chemical polymerization. In order for polymerization to occur, the monomers would have to be oxidized first before the polymerization could occur. The traditional oxidant used in the past has been ammonium persulfate (Huang, 2007; Chao, 2006 and Aldissi, 1997). However, because the reaction with such oxidant was exothermic, controlling the temperature under which the polymerization occurred was difficult and due to the temperature fluctuation, polymers with a wide range of molecular weight may occur as a result (Palaniappan, 2006). In recent years, new oxidation reagents such as benzyl peroxide have been used which offers better temperature control for the polymerization method. Despite the temperature fluctuation experienced with these oxidation agents, the problem may be solved by a simple method such as the use of a water bath during the polymerization process as a mean of temperature regulation (Geng, 1998).

2.4.2. Polypyrrole as a component of the electroactive polymer-based drug delivery system

Another popular EAP which underwent intensive research was the PPy-derived EAPs (Sutar, 2007; Ansari, 2006; Kim, 2006 and Chen, 1990). PPy are similar to PANi with regard to chemical structures and both of these EAPs belonged to the same family. Like the PANi, PPy also has three oxidation states, one state being completely unoxidized and the other two states being oxidized to various degrees (Chen, 1989). Similar to the PANi, PPy exhibited high electrical conductivity as a property. The mechanism of conductivity was an area of research, but it is now accepted that both polarons and bipolarons played a crucial part in this mechanism (Brédas, 1984 and Scott, 1983). The dopants used also have a crucial effect on the conductivity of the PPy, such as an increase in sulfonate group in the PPy film decreases the conductivity (Kuwabata, 1988). In addition, the use of monovalent anions instead of a multivalent anion resulted in a decrease in the intensity of crosslinking in the PPy film. Besides electrical conductivity, PPy also exhibited high thermal and environmental stabilities with the ease of synthesis (Lederc, 1999). Similar to the PANi, one drawback with the use of PPy as a drug delivery system was the poor processability of PPy due to its lack of solubility in most solvents (Bae, 2005). Several studies were conducted in order to improve the solubility of PPy. One method was a substitution reaction with an alkyl group at the β -position of the pyrrole ring prior to polymerization. The end result was a PPy-

derived EAP which was soluble in organic solvents under neutral condition (Lee, 1995). Another method was to dissolve the PPy in an organic solvent in the presence of a surfactant, such as sodium dodecyl sulphate (Panero, 1992 and Naoi, 1995). However, the solubility of PPy produced with this method was still poor in polar solvents and water. Various studies have been done in order to improve the water solubility of the PPy. Another method was to synthesize the PPy from modified water-soluble monomers of pyrrole (Hong, 2009). PPy may also be obtained via counterion-processability such as the oxidative polymerization of pyrrole in the presence of poly acrylic acid or poly vinyl pyrrolidone (Lee, 1997). Lastly, the PPy may be synthesized as a self-doped co-polymer, with the co-polymer containing high sulfonic moiety in order to act as a dopant for the PPy (Yin, 2001). By improving the water-solubility of the PPy, the processability improves and allowed the PPy to be incorporated into more applications and technologies. PPy holds a promising future for development in the field of biomimetics, robotics and pharmaceuticals.

2.4.3. Polythiophene as a component of the electroactive polymer-based drug delivery system

Polythiophene (PT) was another EAP which has been developed into a conductive film which exhibited considerable electrical conductivity. This EAP may be differentiated from the other EAP such as PANi or PPy in a way that PT was synthesized from the monomer thiophene, which contained a sulphur heterocyclic structure, as opposed to PANi or PPy which contained imine groups. The mechanism of conductivity was relatively similar to that of the PANi or PPy. Doping a PT would result in bipolaron formation along its backbone. These polarons and bipolarons acted as charge carriers, thus resulting in electrical conduction (Gnanakan, 2009). PT has also been researched for application in other fields such as light-emitting diodes, electrochromic devices, field effect transistors and recording materials (Fichou, 1999; Granstrom, 1999 and Heeger, 2001). The incorporation of PT into these systems was possible due to the interesting optical properties as well as electroactivity possessed by the PT. These optical properties may be modified and may at times be non-linear (Schrof, 1998). By modifying the PT and its optical properties, it may be used successfully in electrochromic devices and light-emitting diodes. The electroluminescence was generally believed to have originated from the recombination of electrons injected into the conduction band and holes within the valence band to form single excitons (Sakurai, 1997). Similar to other EAPs, PT exhibited good environmental stability, thermal stability, processability and mechanical strength with the ease of fabrication (Roncali, 1992; Braun, 1992; Chen, 1993; Andersson, 1995; Chen 1996). PTs may also be modified with alkyl or alkoxy side chains in order to improve its solubility in common organic solvents at room

temperature (Braun, 1991). The advantage a soluble EAP was that moulding would be possible by pouring the polymer solution into an appropriate mould. PTs with an alkyl side chain were soluble in most organic solvents in both doped and undoped form. One drawback to the alkyl substituted PT was that it lacked flexibility due to the rigid backbone that it exhibits (Hotta, 1987). With the application and research of these types of EAPs increasing, it was promising to say that EAPs can one day be used in a broad field of technology with tailor-made requirements to suit individual needs. The processability also means that synthesis and incorporation of these EAPs into future technology should be easier and feasible.

2.5. Electropolymerization as a method of synthesis for the electroactive polymers and factors affecting the polymerization effect

Polymerization is the process whereby the monomers react with each other to form long chains of polymers. Most polymers used today were formed by using chemical methods such as bulk polymerization or solution polymerization. Another method which is less commonly used for the polymerization of EAPs is the process of electropolymerization. During the process of electropolymerization, the monomer was dissolved in a suitable solvent along with the desired anionic doping salt. The monomer was oxidized at the anodic electrode. Due to the oxidation, free cationic radicals of the monomer formed interacted with each other, forming oligomeric products followed by polymeric products (Sadki, 2000). Electropolymerization is an intricate procedure and can be influenced by factors such as:

- Monomer substitution.
- Choice of electrolyte in the solvent.
- Choice of solvent.
- The pH of the solvent and aqueous medium.
- The choice of electrochemical method used for synthesis.

By manipulating some or all of these factors, it was possible to synthesize a novel polymer or a new synthesis method in order to obtain a polymer with the desired properties. By using a monomer which undergoes redox reactions rapidly, it increased the rate of polymerization. Similarly, by substituting a monomer which was a water-soluble analogue of the original monomer, the polymer formed would have higher water solubility. The choice of electrolyte in the solvent directly affected the current intensity, which could affect the amount of polymers formed (Pistoia, 1978). Different solvents have different donor numbers and deprotonation of the cation radical monomer formed would be affected. Furthermore, different solvents also exhibited different dielectric constants, which would affect the chain

propagation during the process of electropolymerization (Yamada, 1995). The solvent should be stable at the oxidation potential of the monomer and provided an ionically conductive medium (Sadki, 2000). The solubility of the monomers in the solvent was also an important factor as monomers which were insoluble in solvent cannot undergo electropolymerization. The pH of the solvent also has a great influence over the solubility of the monomer and the physical properties of the polymers formed, as it may have a chemical reaction with the monomers. Aniline was typically polymerized under acidic condition because the protonation of PANi yields higher conductivity due to the doping effect (Roeder, 2006 and Hatchett, 1999). The methods of electropolymerization used also played a fundamental role in the physicochemical properties of the polymer formed. During electropolymerization, the monomer was dissolved in the solvent along with the anionic doping salt and oxidized at the anode via anodic potential. This oxidation allowed the monomer to react with each other and polymerization occurs. Acetonitrile was considered a good solvent for electropolymerization because it has a large oxidation potential window and allowed good dissociation for a wide variety of electrolytes (Bard, 1980). The anode used for electropolymerization was usually that of an inert material such as platinum, gold or glassy carbon (Shabani-Nooshabadi, 2009 and Kowalski, 2008). If a partially reactive metal was used for the electrode, the electrode may undergo dissolution during anodic polarization and prevented the polymers to be formed on the electrode surface.

Taking all points into consideration, the monomers have to be dissolved in a suitable solvent followed by exposure to the oxidation potential. Polymerization occurred following oxidation and a film of EAP was formed on the electrode. The thickness of the EAP film may be adjusted by the amount of anions present in the solvent. The anion was incorporated into the EAP during polymerization and was essential in maintaining the electroneutrality of the EAP formed. However, because the EAP may only be formed as a film on the electrode, the amount of EAPs formed was determined by the size of the electrode and production on a large scale may be time-consuming and unfeasible. In comparison to electropolymerization, the chemical synthesis of a polymer allowed a more stable yield of an EAP with a more consistent molecular weight. This was due to the exothermic reaction which occurred during the chemical oxidation of the monomer, such as the oxidation of aniline (Cirić-Marjanovic, 2009). This fluctuation in temperature affected the chain length of the EAP formed and in turn the molecular weight. EAPs intended for mass production should be synthesized under well-controlled environmental conditions, as it was possible to produce EAPs with a comparable conductivity than EAPs synthesized via electropolymerization (Rodrigues, 1991).

However, EAPs intended for research may be synthesized via the electropolymerization method.

2.6. Doping – A crucial process for the optimization of electroactive polymer conductivity

Amongst the researches which were conducted on the EAPs, most efforts were directed towards achieving an EAP with desirable conductive, optical and mechanical properties. Doping is the process of introducing a chemical agent which directly interacted with the polymer chain itself. Doping is an important process because it played an important role in the physicomechanical properties of the EAPs formed. An example of the doping process is outlined in Figure 2.5 where the nitrogen atom from the quinoid group of PANi was protonated by a protonic acid (Dimitriev, 2003).

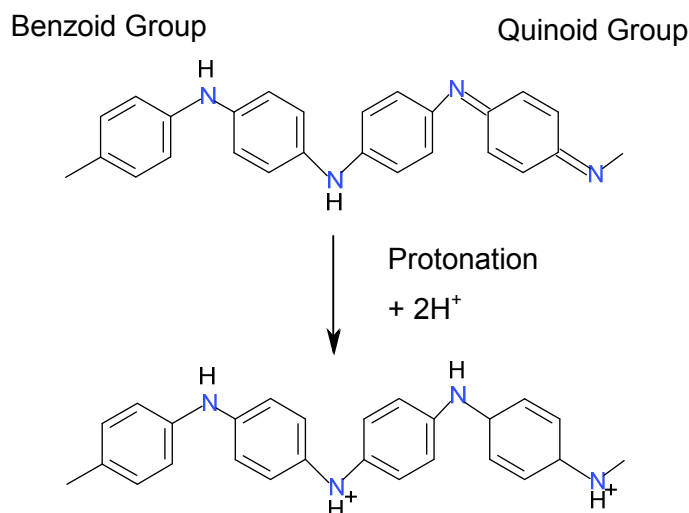


Figure 2.5. Schematic of polymer protonation by conventional protonic acid. Acid counterions are not shown (Adapted from Dimitriev, 2003).

Most doping procedures for an EAP involved combining the EAP in base form, in most cases, preferably with an acid. This was often due to the increased conductivity exhibited in some EAPs when it was protonated. This was thought to be associated with the protonation of imine nitrogen which led to increased polarons (MacCall, 1989 and 1990). Therefore, this theory should apply particularly to EAPs in the PANi and PPy group because both of these EAPs have imine groups present as a part of the polymer backbone. As a result, PANi should be synthesized in an acidic condition, ensuring that the product formed would exhibit good conductivity (Taka, 1994). It was also for this reason that the synthesis of these polymers was deemed harsh and unfavourable. Sometimes, the acid may be mixed with other solutions. Doping agents such as 1:1, acetone:1 M HCl acid has been used as a

dopant for PANi film. The PANi was immersed in the solution for 24 hours in order to allow sufficient time for the doping process and vacuum dried for 48 hours (Mirmohseni, 2003). More recently, new doping agents were discovered and efforts were made to utilize these doping agents in order to produce an EAP with better mechanical, optical and conductive properties.

Newer doping agents such as transition metals have been used as an alternative doping agent as opposed to the conventional protonic acids. With the use of a conventional doping agent, only the dopant change was induced on the polymer. However, when transition metals such as NiCl_2 , EuCl_3 and ZnCl_2 were used, it induced both dopant and morphological changes in the PANi as opposed to the conventional doping agents (Dimitriev, 2003).

When EAPs such as PANi was prepared via emulsion polymerization, it was possible to obtain a conducting salt without the need for a post-doping process step with the acid (Palaniappan, 2005). Sometimes, acid may be added into the emulsion polymerization in order to facilitate additional doping. One example of the emulsion process may be demonstrated by the works done by Kinlen and co-workers (1999). The process was initiated by utilizing a water-soluble organic solvent such as 2-butoxyethanol that facilitates the polymerization of PANi salts of hydrophobic organic acids such as dinonylnaphthalene sulfonic acid (DNNSA) (Kinlen *et al.*, 1999). In addition, acid such as dodecylbenzene-sulfonic acid (DBSA) has emulsifying properties and can be used both as a dopant and an emulsifier (Kim, 2007).

2.7. Redox reaction as an essential process for the conductivity of electroactive polymer

In order for an EAP to be responsive, it must be able to undergo reversible oxidation and reduction processes. EAPs may either be categorized as a redox polymer or a conducting polymer. Redox reactions were important because it provided us with a model to explain how the transport of ions in and out of the EAPs was achieved, and thus controlled movement of these ions from the conductive polymer films. The difference between a redox polymer and a conducting polymer was that redox polymer contained spatially and electronically localized redox sites (Inzelt, 1986). These sites may either be covalently bounded or electro-statically bounded to the polymer. Conducting polymer, on the other hand, contained delocalized electronic states (Bott, 2001). In the case of PANi, the redox centres are the amine groups that were oxidized to imine group. After the oxidation was completed, PANi would become conductive to certain degree. Another example of

conducting polymer would be the PPy, PT and its derivatives (Posada 2004). The redox process generally occurred in the film/solution interface, where the dissolved ion in the solution was able to react with the conducting polymer and was involved in charge balance. The EAPs were synthesized as a film via the process of electropolymerization and were immersed in a solution with various counter-ions dissolved.

Four phenomenons occurred when a polymer undergoes redox switching:

- Conformational changes.
- Entry or exiting of solvent molecule which may change the state of swelling.
- Changes in ion configuration which were bound to the polymer.
- Injection/ejection of ions in order to balance the electroneutrality of the polymer.

Figure 2.6 depicted the mechanism under which the oxidation reaction of 4 monomer unit of PANi occurred.

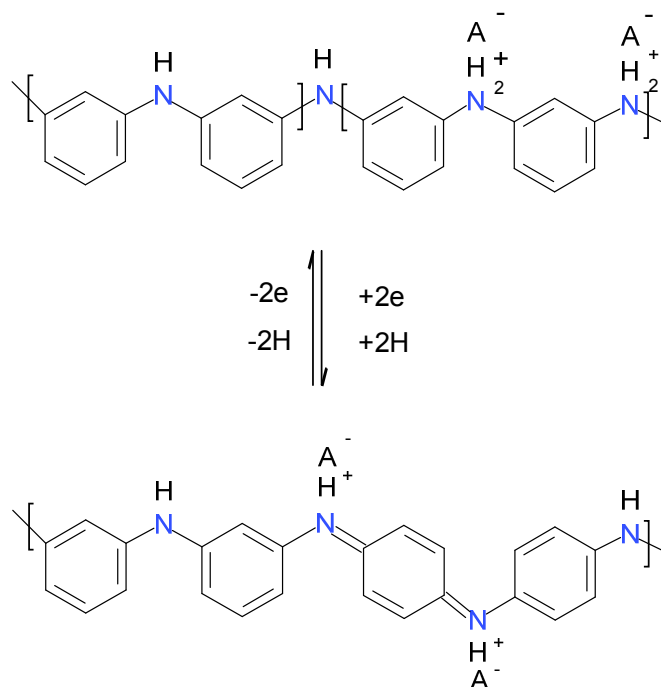


Figure 2.6. A depiction of the mechanism under which the polyaniline undergoes oxidation reaction. The downward arrow represented the oxidation reaction (Posada, 2004).

Currently, several methods which involved substance delivery from an EAP included the incorporation of an electrostatically charged substance into the polymer membrane. The induction of an electric current resulted in the inward and outward movement of the counter-ions for charge balance. An outward movement of the electrostatically charged ions from the polymer membrane therefore resulted in release of the substance. Research has been done on electrostatically charged glutamate (Zinger, 1984) and ATP (Pyo, 1994) in order to achieve controlled release of these two substances. EAPs such as PANi and PPy allowed a

high flux of cations during the oxidized state. Therefore, it was possible to achieve a transport of ions across these polymer membranes when oxidation potential was applied to these conductive membranes.

Another mechanism which may have contributed to the ion transport process exhibited by the EAP was the conformational changes which occur during the redox switching of the EAP. These conformational changes may have resulted in swelling, de-swelling or a change in shape of the EAP, allowing it to act as artificial muscles (Otero, 2004). This moulding effects are called slow-relaxation or memory effect. Several EAPs such as those in the PANi group showed this kind of relaxation effect, while polymers such as poly(o-aminophenol), poly(o-phenylenediamine) or poly(bencidine) did not exhibit this relaxation effect (Moina, 2003). A study by Genoud and co-workers (1985) has been done to explain such behaviour (Genoud *et al.*, 1985). These relaxations may be observed after the EAP has undergone reduction and was independent of the composition and concentration of the surrounding electrolyte. Instead, the electrolytes tend to influence the relaxation time of the EAP (Silk, 1996). There is currently no confirmed model on the mechanism of these relaxations, as EAP relaxation also occurs during oxidation, such as PPy (Otero, 1994). The general model is, however, based on the penetration of counter-ions into the polymer matrix. This relaxation allowed entrapped drug molecules to become liberated provided there was no interaction between the drug, the polymer and the surrounding medium. Therefore, by utilizing this relaxation property of certain EAP, it was possible to achieve controlled release of an entrapped drug.

2.7.1. Techniques for the evaluation of redox reactions in electroactive polymers

The degree of swelling, de-swelling and electroactivity is closely related to the redox capability of the polymer. It is for this reason one should assess the reduction-oxidation of a polymer during electrical stimulation in order to determine the electroactivity of an EAP. Several techniques are available in order to determine the redox capability of a polymer.

2.7.1.1. Linear sweep voltammetry

Linear sweep voltammetry is a method whereby the current of the working electrode is measured against a known range of potentials. Any oxidation or reduction which occurred in the EAP would be registered as a peak or a trough in the voltammogram. Aside from the redox reactions which occur, linear sweep voltammetry may also be used for quantifying purposes, such as the determination of free chloride ions in water or the amount of sulphites present in wine samples (Scampicchio, 2007 and Pathiratne, 2008). Linear sweep

voltammetry was initially used as an assessment tool for the voltammetric response of the EAP (Chambers, 1985). The applications of linear sweep voltammetry in EAP researches nowadays are limited as it is now widely replaced by cyclic voltammetry. This was due to the advantage whereby more data can be obtained from a cyclic voltammetry as compared to a linear sweep voltammetry.

2.7.1.2. Cyclic voltammetry

Cyclic voltammetry is a potentiodynamic electrochemical measurement and is an extension of the linear sweep voltammetry. In linear sweep voltammetry, a known potential is applied across the working electrode and is increased in a linear fashion as time progresses. Cyclic voltammetry extends this technique further by inverting the working electrode potential once the end potential is reached. This allowed the observation of both oxidation and reduction behaviour of the material under analysis, should the sample being analyzed exhibit any reversible redox reaction. The current at the working electrode would be plotted against the applied potential difference to give a cyclic voltammogram trace. During cyclic voltammetry, the potential was increased in a linear fashion. As the potential drew close to the oxidation potential of the analyte, the current would increase and eventually drop when the concentration of the analyte decreased near the electrode due to the oxidation. The potential would be reversed and if the analyte was capable of reversible redox coupling, the oxidized analyte would undergo reduction once the reduction potential was reached. This produced a reduction peak similar to that of the oxidation peak. It is used generally to study the electrochemical properties of an analyte in solution (Nicholson, 1964 and Heinze, 2003), but is also used to assess the redox capability of a material. Figure 2.7 demonstrated an example of cyclic voltammetry done on PPy-para-toluene-sulfonate in 0.2M KCl as supporting electrolyte.

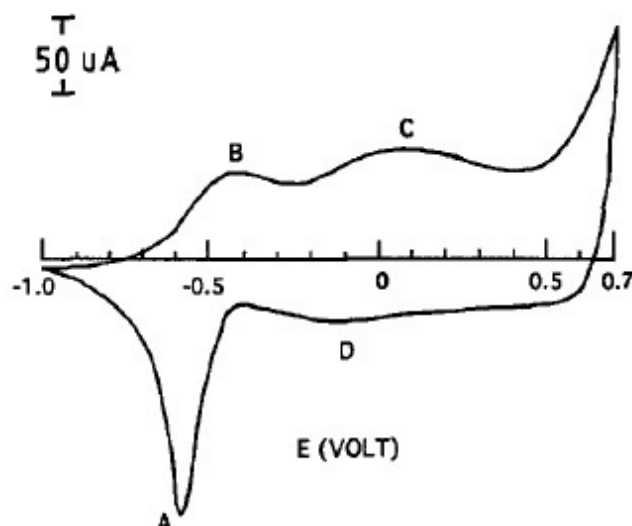


Figure 2.7. Cyclic voltammetry performed on polypyrrole-*para*-toluene-sulfonate in 0.2 M KCl as supporting electrolyte. The scan rate is 100mV.s^{-1} A/B represents the redox peak associated with cation insertion/expulsion while C/D represents the redox peak associated with anion insertion/expulsion (Zhao, 1996).

By using Figure 2.7 as an example, it was possible to demonstrate that PPy-*para*-toluene-sulfonate is capable of undergoing both reduction and oxidation at various potential differences. The oxidation potential and the reduction potential in this case were approximately 0.5V and -0.5V, respectively. Cyclic voltammetry is still one of the most popular techniques used in electrochemical analysis in order to determine an electrochemical property of a substance and is one of the most valuable tools in order to assess the redox reaction of the polymer and its electroactivity.

2.7.1.3. Impedance spectroscopy

Impedance spectroscopy is a versatile tool used to characterize the intrinsic electrical properties of any materials and its interface. The data that one can obtain from the use of an impedance spectroscopy included the conductivity, dielectric coefficient, the static properties of the interface and its dynamic change due to adsorption of charge-transfer phenomenon. The technique itself is non-destructive and has been modified recently in order to assess body composition in those suffering from obesity or being over-weight (Cox-Reijven, 2002, Fortunato, 2005). Another property which could be measured by impedance spectroscopy was the conductivity of an EAP. The impedance of an EAP may be used for conductivity studies, as well as providing us with an understanding of the kinetics and the electrochemical reactions occurring in the EAP (Gabrielli, 2000). Furthermore, it may be used to characterize an EAP such as PANi or PPy in order to confirm a proposed model such as the diffusion of ions in and out of the EAP in a solvent (Musiani, 1990) or counter-ion and electron diffusion at the EAP/solvent interface (Lyons, 1990). Since impedance

spectroscopy could be used to assess the diffusion of electrons and counter-ions, it may be useful for evaluation and confirmation of a redox process of an EAP. Due to its versatility, it may be used in several applications such as corrosion studies, energy storage device, interfacial electrochemistry, biosensors, semiconductors and liquid-liquid interface studies. Some limitations regarding the use of impedance spectroscopy was that data interpretation is usually difficult and it cannot be used as a stand-alone technique.

2.7.1.4. Chronoamperometry

Chronoamperometry is a technique where the potential is maintained for a certain period, then stepped and the current resulting from the faradic process is then recorded. The current is a result of oxidation or reduction which occurs from the analyte. The polymer analyzed was usually coated as a thin film around the electrode, although the presence of a perturbed current in chronoamperometry may deviate the results obtained (Yap, 1987). Chronoamperometry may be employed in cases where elucidation was required for the migration flux of a charged particle in an EAP. This may be done by analyzing the concentration distribution and current-time curves of a polymer film in a constant electric field (Yap, 1983). Conversely, conductive EAPs have been used in chronoamperometry as a sensor for the detection of simple electroactive or non active species, in addition to more complex species (Nguyen, 1999). Chronoamperometry is still important and may be used for elucidation of the kinetics of charged species migration and diffusion.

2.8. Controlled release of substance from the electroactive polymeric-based hydrogel

Over the past few years, pharmaceutical researchers have been looking at developing a drug carrier which could release drug in response to a change in the environment. These changes may be endogenous (e.g. change in blood glucose, change in pH or inflammation) or it may be exogenous i.e. external stimulus was required. These drug carriers were termed 'intelligent' drug carrier because of its ability to release an adequate amount of drug at the correct place and time (Murdan, 2003). The use of this drug delivery system proved to be beneficial for both the patients and the health care providers, due to the improved patient compliance and decreased side effects. Even for researchers in other fields of study, EAP or other intelligent polymers have demonstrated its usefulness and was extensively researched. A study done by Singh *et al* in 2008 has demonstrated that a smart polymer may even have its uses in the field of cell cultivation. Animal studies have always been a controversial issue and it was hoped that with the aid of cell cultivation, it is possible to replace animal studies or reduce the numbers of studies that have to be done on animals

(Singh, 2008). Therefore, it can be seen EAP researches have vast impact on a wide variety of fields.

Controlled release from an EAP-based hydrogel is mainly due to the movement of charged particles in and out of the hydrogel. To date, there have been a few models which tried to explain the mechanism in which drug was released from the electroactive hydrogel. The following 3 models have been proposed by Murdan *et al.* (Murdan, 2003) in relations with drug release from an electroactive hydrogel.

- Forced convection of drug as gel de-swells.
- Drug electrophoresis due to migration of drug toward charged electrodes.
- Drug liberation when an electroactive hydrogel was eroded upon electrical stimulation.

There were, however, certain limitations in which drug released from an EAP-based hydrogel can be exploited. Firstly, only a charged drug may be used in order for electrochemical control of movement of drug in or out of the hydrogel. Secondly, drugs in high volume cannot be easily absorbed or released by the EAP-based hydrogel, and lastly, the ionic exchange between the drug and the surrounding medium slowly diminished the electrochemical control of the drug release from the hydrogel (Lira, 2005).

Controlled release of charged particles has been studied previously, as done by Zinger and co-workers (1984), controlled release of a neurotransmitter from a polymer coated electrode has been successful. The charged particles were covalently bound onto the polymeric backbone and remained on the polymeric electrode until a pulse of electric current was sent through the electrode. The polymer used was PPy attached onto a glassy carbon electrode. PPy was doped with both glutamate as the drug and ferrocyanide in order to enhance the conductivity of the PPy. This has demonstrated that PPy can indeed be used to control the release of anionic drugs (Zinger *et al.*, 1984).

Cationic drug release can also be controlled in a similar manner. Cationic drugs such as protonated dimethyldopamine have been incorporated into a cationic poly(*N*-methylpyrrole)/polyanion composite and released anodically. This study has demonstrated that amines could be bound as its conjugate acid while dopamine, which was a model cationic drug, may be released in a time controlled manner (Zhou, 1989). Biological actives have also been demonstrated for its controlled release capability by using bi-layered polymer, an inner layer which was separated by the outer layer via a separation film. The inner layer exhibited a low redox potential while the outer layer exhibited a high redox potential. This design not only allowed release of charged particles, but also the reuptake of certain

charged particles in the surrounding medium as well. The materials used were PPy and polystyrene sulfonate (PP/PSS) as the inner layer while the outer layer was comprised of either poly (*N*-methyl pyrrole) (PNMP) or poly (vinyl ferrocene) (PVFc) (Pyo, 1995). The schematics of this dual layer transport system may be depicted in Figure 2.8.

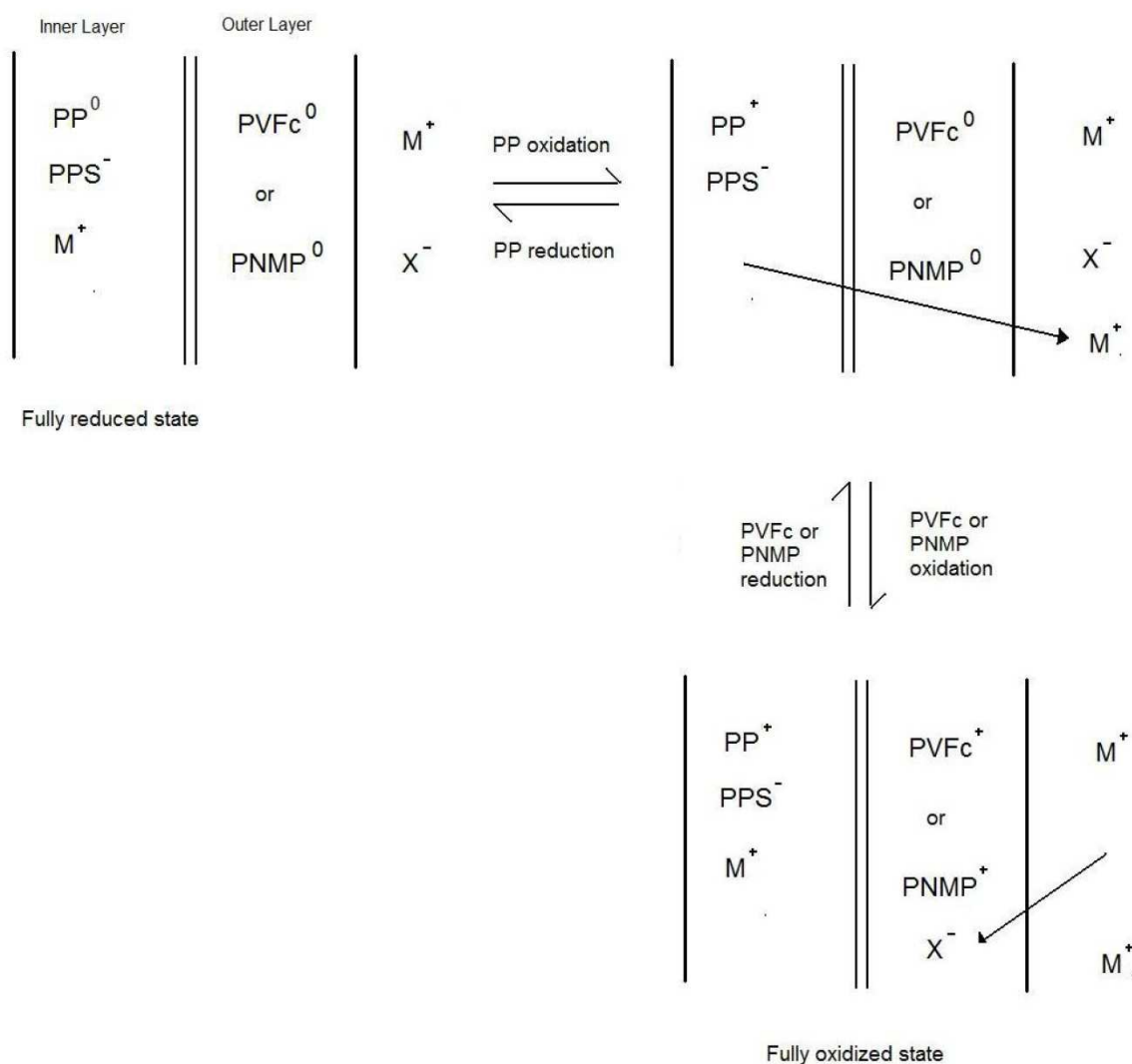


Figure 2.8. The mechanism by which the duo layered transport system works. When polypyrrole becomes oxidized, it lost an electron and become positively charged, thus repelling drug M which also possessed a positive charge. Similarly, when PVFc becomes oxidized, it becomes positively charged and thus attracts the negatively charged drug X (Pyo, 1995).

In order to determine the behaviour of the electroactive hydrogel, it was important that current is applied to the hydrogel appropriately. The hydrogel may be immersed in a conducting medium and either one or both electrodes should be embedded or in contact with the hydrogel or the hydrogel may simply have contact with the electrode without any conducting solutions (Murdan, 2003). It is important to note the different methods used here

would result in different release profiles of the hydrogel and thus the method with an optimized result should be used.

By using similar mechanisms, other researchers have used model drugs such as sulfosalicylic acid in a crosslinked PVA hydrogel. The amount of drugs used is determined by UV visible spectroscopy. It was discovered that drug release may vary in a linear fashion with the square root of time, and moreover, the diffusion coefficient of drug-loaded PVA hydrogel also depended on the electric strength applied (Kanokpom, 2008). Aside from the electrical current and the crosslinking from the hydrogel, another factor which was important for drug release from the hydrogel was the use of polyelectrolyte. These polyelectrolyte may form the main component of the hydrogel which transformed the hydrogel into electrical and pH responsive hydrogels.

2.9. Polyelectrolyte and their uses in biological applications

Polyelectrolyte is defined as water soluble electrically charged polymer. Its shape and movement are governed by a combination of its charge and Brownian motion. As a result, it may coil up or stretch out and may be classified either into polyacid, polybase or polyampholytes. This can be determined according to its ionizable groups, depending whether it was acidic group such as carboxylic, sulfonic or phosphoric groups or basic groups such as amino groups (Katchalsky, 1964). What makes these hydrogels important in the field of stimulus-actuated drug delivery was its structural response induced by a change in pH, temperature and even electrical current (Sorenson, 2009). Structures in our body such as DNAs are polyelectrolyte, and therefore, it was possible to synthesize a biocompatible polyelectrolyte. Biodegradable polyelectrolyte has also been investigated as a pulmonary drug delivery system which may be a desirable route of vaccine delivery (De Koker, 2009).

When polyelectrolytes were incorporated into a hydrogel, these polyelectrolytes could swell and collapse when placed in solution containing different charges or pH (Huang, 2007; Li, 2005 and Budtova, 1994). Besides swelling and collapsing, polyelectrolyte hydrogel was also capable of bending and change in shape. To date, several materials were reported to have been electrically responsive. Some of them including poly(acrylic acid) and poly(vinyl alcohol) co-polymer membranes, sulfonated crosslinked polystyrene gel, acrylamide/acrylic acid co-polymer with PPy/carbon black and chitosan/carboxymethylcellulose hydrogel (Shang, 2008). Other materials which were also being researched includes poly(N-isopropylacrylamide) and its derivatives, poly(methyl methacrylate) and its co-polymers with

methacrylic acid, poly(acrylonitrile), poly(2-acrylamido-2-methyl-1-propanesulfonic acid), poly(propylene phosphate) and poly(N-acryloyl-N'-propylpiperazine) based on a study done by Jabbari and co-workers (Jabbari, 2007). Some of the polyelectrolytes have even exhibited good electrical response over a wide range of pH.

In order to utilize polyelectrolyte hydrogel for the purpose of drug release, it was important to understand its kinesis upon electrical stimulation. The mechanism under which polyelectrolyte hydrogel collapses and/or changes shapes are yet to be elucidated. There are, however, several models which attempted to explain and achieve such mechanism. When a polyelectrolyte hydrogel was connected to an electrical circuit, the hydrogel collapsed as depicted in Figure 2.9.

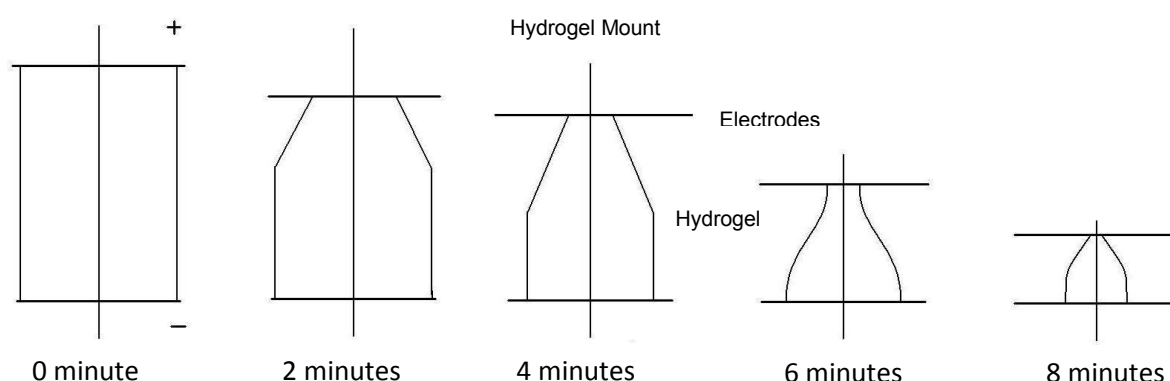


Figure 2.9. The collapsing of the polyelectrolyte hydrogel upon electrical stimulation. These contractions are what caused the water to exude and thus drug release along with the solvent (Budtova, 1995).

Figure 2.9 indicated two areas of contraction. The first one occurred at the area of high gel response at the positive terminal and that may be due to electrochemical process that obeys Faraday's law with a correction coefficient. The second was an area with low response at the negative terminal, and that may be due to the electro-osmosis release of water (Budtova, 1995). The collapse occurring at the anode or cathode was dependent on whether the hydrogel was anodic or cathodic in nature. An anodic hydrogel would collapse predominantly at the anode and vice versa.

Other useful application of environmentally sensitive polyelectrolyte hydrogel included biosensors, DNA hybridizations, micro-surgical tools and miniature bioreactors. Polyelectrolyte hydrogel have shown promising results with regards to electrical stimulus and biocompatibility. PH-Sensitive and temperature-sensitive drug release from this polyelectrolyte has been investigated. A study by Inoue and co-workers (Inoue *et al.*, 1997) has managed to prepare polyelectrolyte hydrogel loaded with drugs and soaked in distilled

water in order to assess drug release when immersed at various different pH. Only cationic or hydrophobic drugs were used in this case and, as predicted, the hydrogel had a different swell rate in different pH and different drug release profiles. Drugs were loaded into the hydrogel by immersing the hydrogel into drug-dissolved solutions. Drug entrapment efficiency was determined by measuring difference in drug concentration before and after the hydrogel immersion.

2.10 Current responsive hydrogel system and future prospective

EAPs and stimulus responsive hydrogels have been a subject of interest for research, not only in the field of drug delivery, but also in various other fields. Although the mechanisms for these electroactive components are yet to be elucidated, various models were made in order to explain the change in behaviour of these electroactive components upon actuation. These models mainly focused on the change of ionic strength and charge which led to repulsion or attraction. Therefore the EAP, hydrogel and model drug all has an impact on each other, and all three components have to be considered prudently in order for the system to operate smoothly as a whole.

Another system which was also under intensive research was the possibility of a biodegradable stimulus-actuated polymer. These polymers would be implanted at target site, and upon actuation, it may degrade and release the drug held within. Once these polymers underwent degradation, it will be metabolized and excreted from the body, due to its biocompatibility. Possible materials included gelatin and dextran (Kurisawa, 1998). There were other biodegradable EAPs which also possessed the potential for controlled release of various substances. Examples of this polymer included multiblock polylactide and aniline pentamer co-polymer used by Huang and co-workers (2008). The biocompatibility of this polymer has been tested on rat models and the broken down metabolites were further tested and proved to be non-toxic (Huang *et al.*, 2008). Another EAP which was synthesized by Guimard and co-workers (2009) was also shown to be biodegradable is the 5,5'''-bis(hydroxymethyl)-3,3'''dimethyl-2,2':5',2'':5'',2'''-quarterthiophene-co-adipic acid polyester (QAPE). This polymer was synthesized by incorporating alternating electroactive quarterthiophene units and biodegradable ester units into one macromolecular framework (Guimard *et al.*, 2009).

EAPs may also be utilized within the nano-scale range (Sohn, 2007), and EAPs have been demonstrated electroactivity even at scales of 100nm (Petu 2007). This is a promising and

interesting prospective for the future of EAP developments. Nanobots or nanobiosensors may one day be injected into a patient and drugs could be released simply by environmental activation, either endogenously or exogenously.

Whichever the case may be, EAP and its family of stimulus actuated polymers have proven to be valuable not only in the field of drug delivery, but also in the field of robotics, biomimetics and space engineering. However, further research is still required so that these polymers may be utilized to its full potential.

2.11. Concluding remarks

The aim of this study was to formulate a drug delivery system which allows patients suffering from chronic pain to obtain a therapeutic dose of drugs at the target site, at the required moment. In order to construct a design for the purpose of electroactive drug delivery, various factors must be taken into account. The crosslinked hydrogel system, the EAP and finally the drugs selected, each one played an important role in affecting the system as a whole. In order to design a system which allowed release of drug, one may attempt to construct a hydrogel system which swells and de-swells under electric current, or one may construct a hydrogel system which undergoes degradation under electric current. One advantage of using NSAIDs as a drug for release directly at the target site was that they exhibit high protein binding when administered orally (Bater, 1988). Therefore, by focusing on target site delivery, only minute quantities of the drug need to be administered to achieve COX II inhibition effect. Another benefit of this system was that it should reduce the GI side effects which are experienced with an oral NSAID. Some products deliver NSAIDs in an enteric coating in order to reduce the GI side effect (Goldstein, 2008; Hawthorne, 1991), but absorption from the GIT still takes time and it does not completely eliminate the ulceration experienced with NSAIDs. The device should be flexible in design and be an appropriate size which is suitable for subcutaneous implantation. Since the human skin is capable of conducting electricity (Williams, 1996), an external device may be used in order to allow electric current to travel through the skin and in turn activating the device implanted below. This system should also eliminate the strong resistance that was experienced by solutes and ions when it was moving across the stratum corneum during cutaneous drug delivery (Karande, 2006). The development of this system should improve patient compliance while reducing side effects which would improve the treatment outcome of patients suffering from chronic pain. As this system was aimed to release NSAIDs directly at the target site, drugs such as opioids which act centrally could not be used. Therefore, in conditions such as

neurological chronic pain where NSAIDs are not the primary drug of treatment, this system may not be effective as the oral opioids or anti-depressants. However, in conditions such as osteoarthritis, back pain or gout, this system may prove to be beneficial.

CHAPTER 3

PRE-FORMULATION STUDIES OF THE STIMULUS-ACTUATED POLYMERIC DEVICE

3.1. Introduction

This pre-design study was conducted by using PANi as an EAP in order to enhance drug release. To date, several EAPs which were capable of redox reactions were under intensive research for several different applications. These EAPs are also termed stimuli-responsive hydrogels, 'intelligent' or 'smart' polymers. An EAP may be defined as a polymer which responds to an electrical stimulation via size or shape changes. These polymers were first discovered over a decade ago and have interested many scientists ever since. Initial displacements of these EAPs were confined to small size or shape changes, but recently EAPs with larger displacements have been discovered (Bar-Cohen, 2002). These polymers can mimic muscle movements and were termed artificial muscles. Scientists in the field of nano-robotics and bio-mimetic have favoured EAPs into their design due to the EAPs' unique ability to respond to an electric current, alongside their low weight, fracture tolerance and pliability (Bar-Cohen, 2007).

More recently, EAPs have been investigated for its use in drug delivery and biosensors (Pernaut 2000). A few EAPs which exhibited promising characters included those of PPy, PANi and PT groups. It was previously thought that PANi was rigid, hard to process and insoluble. Recent discovery of PANi's solubility in a solvent of N-methyl-pyrrolidine have allowed PANi to be processed into a film or fibre, thus improving its physical and mechanical properties. Furthermore, PANi could be doped by using different counter-ions, and this resulted in PANi with varying conductivity (Geng, 1997). Once polymerized, PANi may exist in one of three states: leucoemeraldine, emeraldine or pernigraniline. These states can usually be differentiated by its appearance, as leucoemeraldine has a white/clear colour, emeraldine has a dark green/blue colour and pernigraniline has a blue/violet colour (Huanga, 2006). These three oxidation states may be depicted by Figure 3.1.

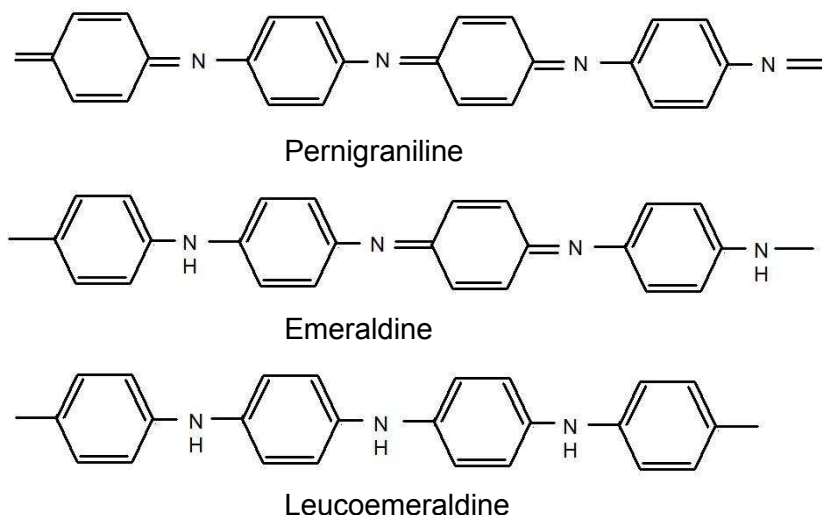


Figure 3.1. The three oxidation states of polyaniline. Pernigraniline is the fully oxidized state with imine links instead of amine links. Leucoemeraldine is the fully reduced state.

Emeraldine state was considered the most useful state of the PANi due to its high stability at room temperature and that upon doping, the emeraldine salt form is electrically conducting. Another important component of the system is the hydrogel. Some hydrogel systems were also ionized and it were termed polyelectrolyte hydrogels, with fixed charges attached onto its polymeric network (Luo, 2007). Within these hydrogels were the mobile ions, which, in some cases, were free to enter and leave the hydrogel upon stimulation and were suspended by fluids which were absorbed by the hydrogel. A hydrogel may be responsive towards temperature (Sun, 1999), pH of the surrounding medium (Zhang, 2007; Mohanan, 2009), enzymes (Thronton, 2006), magnetic and ultra-sound irradiation (Kim, 1996). Another stimulus which is also under investigation is electrical currents in order to achieve structural changes in hydrogels for the purpose of drug delivery (Kulkani, 2009). These structural changes may be bending of the hydrogel towards the anode or cathode, or it may be swelling or de-swelling of certain regions of the hydrogel and several models exists to date to explain the phenomenon. A hydrogel is capable of drug release upon de-swelling and swelling, due to its dynamic mechanism of release. An electro-responsive hydrogel which was attached between an anode and a cathode may exhibit de-swelling either at the anode or the cathode. When the hydrogel de-swelled, it squeezed out any solvents which it contained, and any drug dissolved in the solvent would inevitably be expelled out of the hydrogel along with the solvent, resulting in drug release (Sutani, 2002). When the electric current was ceased, the gel absorbs surrounding solvent and swelled back to its original size. In a different model, a hydrogel in its de-swelled state may form a crosslinked system which held the drug molecule. When the hydrogel was stimulated, the hydrogel swelled up,

leading to increased pore size and free surface area, which resulted in drug diffusion outward (Kim, 1992).

Several other models also existed in order to explain possible release mechanisms of the hydrogel. In the case of electroactive hydrogels, there may be drug electrophoresis due to migration of drug towards charged electrodes or there may be drug liberation when a hydrogel was eroded in the presence of an electrical current (Murdan, 2003).

In this Chapter, the main focus was on the design and application of an indomethacin-loaded crosslinked hydrogel system. Four different devices with varying compositions were built and each was loaded with indomethacin. The four devices were placed under electrical stimulation and the drug release was assessed. In the pre-design study, the four devices were basically comprised of a hydrogel compartment, a crosslinker, an EAP and the drug.

3.2 Materials and Methods

3.2.1 Materials

Polyvinyl alcohol (PVA) 8/88 (Unilab, Krugersdorp, South Africa) was used in order to form the main composition of the hydrogel. The molecular weight as indicated by the manufacturer was approximately 49000g. Another grade of polyvinyl alcohol was used and had a molecular weight of 89000-98000g (99% hydrolysed) (Sigma-Aldrich, Steinheim, Germany). Polyethylene glycol (PEG) 4000 (Unilab, Krugersdorp, South Africa) with molecular weight approximately 3600-4400g was used as a crosslinker with Eudragit®. Two different grades of Eudragit® were used in this study, the first, Eudragit® L100 powder (Methacrylic acid-methyl methacrylate co-polymer 1:1) (Degussa, Darmstadt, Germany) was used. The second was Eudragit® RL100 pellets (Ammonio methacrylate copolymer type A) (Evonik Industries, Darmstadt, Germany). The solvents used were distilled water, Hydrochloric acid (Merck Chemicals (Pty) Ltd., Germiston, South Africa) and Dichloromethane (Merck Chemicals Pty Ltd., Germiston, South Africa) with a purity assay of >99%. Aniline monomer (Sigma-Aldrich, Steinheim, Germany), PANi emeraldine base (Sigma-Aldrich, Steinheim, Germany) with molecular mass approximately 20000g was used as an electroactive agent. PPy (Sigma-Aldrich, Steinheim, Germany) was used as a possible EAP for the SAPD. Finally, the drug used was indomethacin, diclofenac sodium, ibuprofen and aspirin (Sigma-Aldrich, St Louis, MO, USA). All reagents were used as received. Light microscopy performed on the SAPD was the Olympus SZX7 ILLD2-200 (Olympus, Tokyo, Japan). Drug concentration was measured with a UV-visible

Spectroscopy, model Lambda 25 UV/Vis Spectroscopy (Perkin-Elmer, Shelton, CT, USA). Chemical structure analysis was performed with a Fourier Transform Infra-Red (Perkin Elmer, Life & Analytical Science Inc., Shelton, CT, USA)

3.2.2. The design of an electroactive polymer-based implantable system

This study focused on the design of an EAP-based implantable device which would be able to release a desired quantity of drug directly to the target site upon application of an external stimulus for the purpose of chronic pain relief. This device would be engineered as a mono-layered membranous system in which the drug can be loaded and released in a controlled manner. The external stimulus was that of an electric current applied via an external device. The drug-loaded disks may be actuated by applying electrical stimulation. This device would allow the patient to deliver various quantities of drugs by triggering drug release via selecting the adequate external electric current strength as well as the duration. Drug release would cease as a result of removing the external electric current. Therefore by applying either low or high electrical current, we can control the amount of drug released with a single charge. Figure 3.2 provided the setup of the circuit upon which drug release would occur.

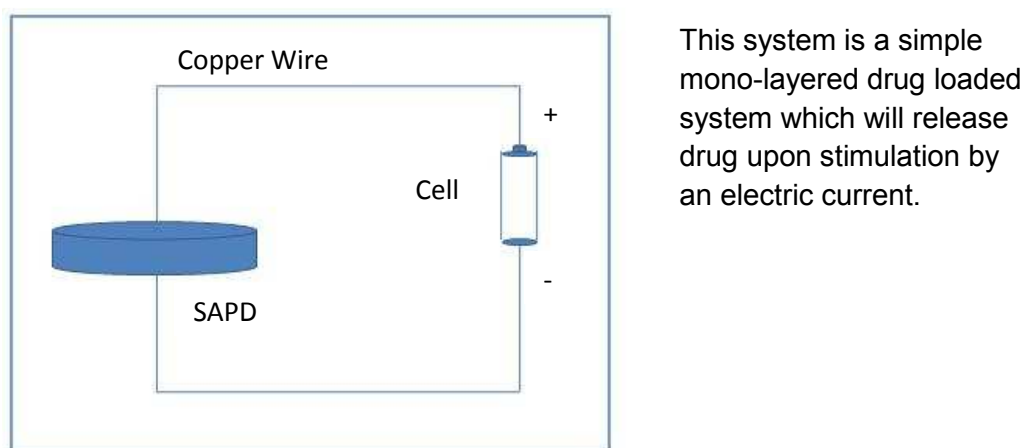


Figure 3.2. The setup of the circuit in the stimuli-actuated polymeric device.

The battery and the circuit would be in the form of a portable device when the SAPD was implanted into the patient. When the circuit was closed, electric current would pass through the device, resulting in a release of drug. The disk-shaped device would allow implantation into the patient due to its flat shape. This device would be implanted subcutaneously. Electrical stimulation applied externally should actuate the device through the skin.

3.2.3. Preparation of the electroactive polymer-based implantable device

The SAPD could be implanted subcutaneously at extremities such as the arm. By implanting the SAPD subcutaneously, it allowed sufficient electric current or stimulus to induce changes in the SAPD. One of the many possible EAPs that may be employed in the design of the SAPD may include the groups of PPy, PANi and EVA as a membrane. This SAPD can be electro-chemically controlled to transport ions across the surface and can be switched on and off when applying potential difference of approximately 1V. Even the rate of transportation across the membrane could be controlled *in situ* by means of potential difference applied. In addition, the use of various counter-ions not only affects the electro-conductivity of the membrane, but also the mechanical and transport activity. This transport mechanism involved incorporation or expulsion of ions as the membrane was continuously oxidised and reduced using a repetitive pulsed potential waveform. This reaction was demonstrated in Figure 3.3.

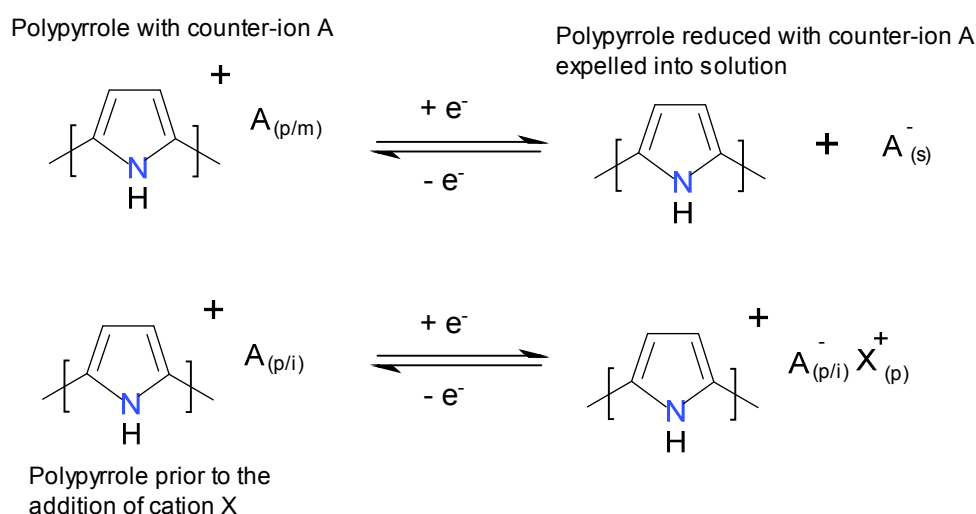


Figure 3.3. Demonstration of the oxidation and reduction reactions of polypyrrole (Zhao, 1998).

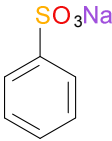
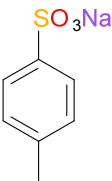
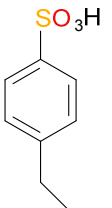
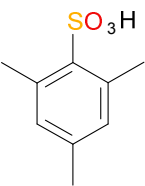
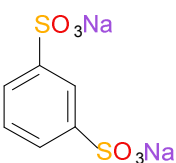
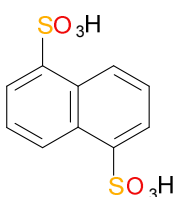
A^- is the counter ion used in the synthesis. X^+ is the cation in the electrolyte solution in which the polymer was either oxidised or reduced. $A_{(p/m)}^-$ was the counter ion that was within the polymer and has sufficient mobility to be expelled into the solution during the reduction. One of the possible designs of the SAPD may comprise PPy which contained a para-toluene sulphate (PTS). The SAPD would be prepared by electro-polymerization from a solution of 0.20M pyrrole and oxidizing agents as initiators. A constant current could be applied for approximately 12 minutes in reagents such as 40% sodium benzene sulfonate and 60% distilled water. A stainless steel plate may be used as a working electrode. By incorporating such reagents into the SAPD, it would allow transportation of an array of sulfonated aromatic

compounds across the membrane. The use of a twin electro-chemical controller continued the oxidation and reduction portions of the potential cycle to different parts of the cell which may make the membrane either an anion or a cation transport system.

3.2.4. Effects of counter-ions on the properties of Stimuli-Actuated Polymeric Device

One advantage of the PPy was that it may be synthesized into a membrane. In addition, the conductivity of the PPy may also be tested. The conductivity of the PPy can be changed by incorporating different counter ions such as benzene sulfonate (BSF), para-toluene sulphonate (PTS), ethylene-benzene sulphonate (EBS), mesitylene sulfonate (MS), benzenedisulfonate (BS) and naphthalene disulphonate (NPS). By incorporating these counter-ions, one could adjust not only the conductivity but also the tensile strength of the PPy membrane. The effects of the aforementioned variety can be seen in Table 3.1.

Table 3.1. Effect of the counterion on the tensile strength and conductivity of the membrane (Zhao, 1994).

	Membranes					
	PP/BSA	PP/PTS	PP/EBS	PP/MS	PP/BS	PP/NPS
						
Tensile Strength	17-23	70-80	60-70	36-47	40-55	40-50
Conductivity (S/cm)	19-20	90-110	90-110	50-70	47-70	50-70

3.2.5. *In vitro* drug release study of polypyrrole membrane

In order to assess the drug release behaviour of the PPy matrix system, a matrix device of drug-loaded PPy should be left in a solution of high electrical conductivity. The solution of choice was NaCl as it is a strong electrolyte. Direct electric current would be passed through the solution while a volt meter was attached to the circuit to measure the current. Samples of the solution would be taken at specific time intervals to test the drug concentration. Generally, a potential difference of 4V or less would be required for the actuation of the EAP (Lin, 2011), so tests may run from as small as a few milli-volts up to 4V. The schematic of the *in vitro* test of drug release of the SAPD may be presented as in Figure 3.4.

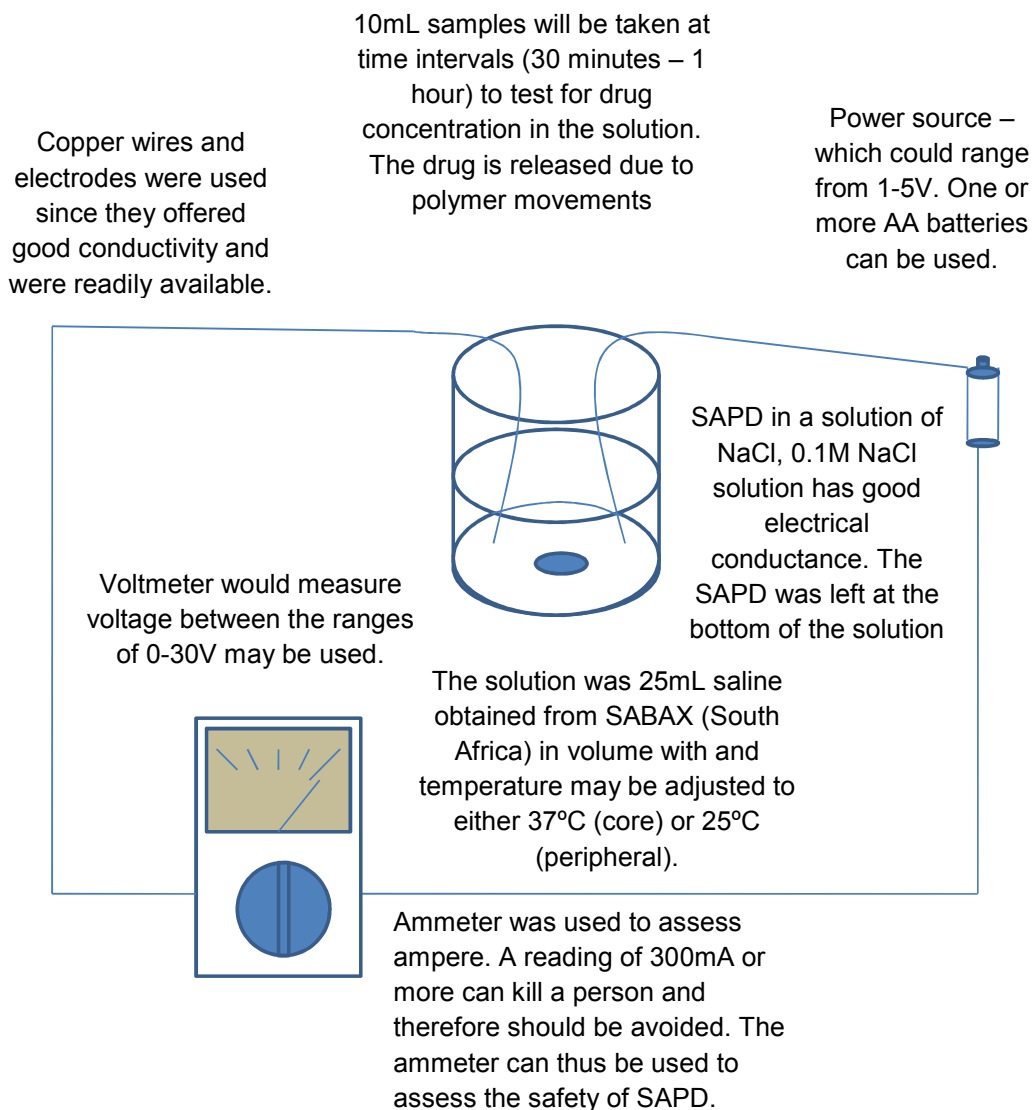


Figure 3.4. The *in vitro* test that was conducted on the stimuli-actuated polymeric device in order to assess its drug release.

The SAPD was developed with a thickness of approximately <1mm. The release of the drugs was determined by High Performance Liquid Chromatography (HPLC) and Ultra-Performance Liquid Chromatography (UPLC). Research has shown that membranes doped with appropriate drugs towards chloride exchange in a 0.1M NaCl solution offered a good result in terms of drug delivery (Kontturi, 1998).

3.3. Results and Discussion

3.3.1. The constituents and its role in the responsive hydrogel

The EAPs used for the purpose of drug delivery included PANi and PPy or its derivatives, which exhibited elastic properties and conductor properties. The electrical conductivity that these polymers possessed was mainly due to the conjugated backbone structure. These conjugated backbone structures contained the free valance electrons which were required

for electrical conduction. This study aimed to achieve drug delivery through the use of the following three groups of materials as the foundation of the device:

- An EAP was incorporated into the device due to its conduction of electrical conductivity into the delivery device. These included PANi or PPy and its derivatives.
- Hydrogel was used as the main component where the drug was held and stored as a matrix. A hydrogel consists of a 3 dimensional network of a crosslinked polymer-based network. In order to enhance the performance of the hydrogel, one may incorporate acidic or basic groups into the hydrogel. These hydrogels are termed polyelectrolyte or ionized hydrogel and consists of three species, namely the solid matrix network, interstitial fluids and ionic species.
- Analgesic drugs which would be used for the purpose of controlled drug release. These drugs may be conventional Non-Steroidal Anti-Inflammatory Drugs (NSAIDs) such as indomethacin, ibuprofen, diclofenac, mefenamic acid or any of the COX II inhibitors, including COX II specific inhibitors such as celecoxib. Although drugs of the opioid class are used for moderate to severe chronic pain, it was less popular due to its abusive properties (Glajchen, 2001; Weinstein, 2000 and Furstenberg, 1998). Long-acting opioid drugs have to be administered daily and do not offer controlled on-site delivery. In addition, the local release of opioids still depends on the action of the drug at the central nervous-system. Local release of opioids therefore offered no benefit for the patient. The use of NSAIDs would be more beneficial as a chronic pain relief in this implantable device.

3.3.2. Model drugs incorporated into the responsive hydrogel system

There were several NSAIDs which were considered for the design of the SAPD. Drugs such as indomethacin, ibuprofen, diclofenac sodium and aspirin were used. These drugs were selected due to the high potency and the ability of the drug to act locally, via inhibition of COX II in the cell membrane, when released directly at the site of pain.

3.3.2.1. Indomethacin as a model drug in the Stimuli-Actuated Polymeric Device

Indomethacin is a potent drug which exhibits analgesic, anti-inflammatory and anti-pyretic properties. It is used for conditions such as acute gout attacks, ankylosing spondylitis, osteoarthritis, rheumatoid arthritis and other musculo-skeletal disorders which resulted in chronic pain. The chemical structure of indomethacin was depicted as in Figure 3.5.

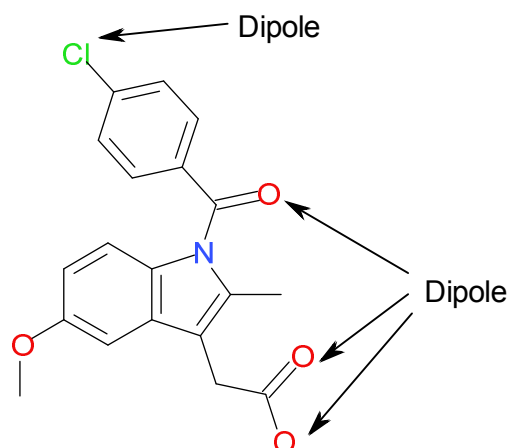


Figure 3.5. The chemical structure of indomethacin.

Indomethacin is practically insoluble in water, mainly due to its minor dipole movement which existed on the oxygen and the chlorine atoms as indicated. The majority of the compound was still composed of long carbon and hydrogen chains, which decreased its water solubility. The solubility did increase when placed in slightly alkali solvents or when the temperature of the solvent is elevated. Indomethacin has a solubility of 1 in 50 in alcohol and 1 in 30 in chloroform (Martindale, 1996). Indomethacin is primarily an anionic drug, and therefore can interact with other cations, such as heavy metal ions. At higher concentrations, indomethacin is capable of self aggregation. Indomethacin dissolves slowly at a pH lower than 8, and is insoluble at an acidic pH. However, when indomethacin is immersed in aqueous mediums of pH 9 or higher, degradation starts to occur. The degradation occurs more rapidly when the pH is 10. Therefore, it is important to dissolve indomethacin in a buffer where the pH is controlled (Fini, 2001). The molecule of indomethacin has an indole moiety linked with *p*-chlorobenzoic acid via an amide bond, and it is this link that is responsible for the degradation of this drug at higher pH. The presence of a bulky hydrophobic head and a polar head makes this molecule a surfactant. Furthermore, this drug has shown electroactive properties and is capable of undergoing reduction under electric current. It is ideal that indomethacin exhibits solubility at pH 7.4, as this renders this drug suitable for release from a subcutaneous implantable device.

Thermal stability of indomethacin has been proven to be good, even at high temperatures. Indomethacin heated under the temperature of 95°C for 15 hours has shown no signs of changes in structure (Lu, 2007). Indomethacin has been dissolved in 100°C of water in order to enhance its solubility which has also shown no signs of degradation when carried out in the laboratory. Therefore, it is quite possible to use indomethacin as a drug for the purpose

of a stimulus actuated polymer device provided that the electric current used for the stimulation is low.

Indomethacin is readily absorbed by the gastro-intestinal tract (GIT) and a peak plasma concentration is reached after 2 hours. Protein binding of indomethacin is 99% and it is found in synovial fluid, the central nervous system (CNS) and the placenta. Since indomethacin exhibits such a high protein binding, it is a desirable drug to be delivered locally to the target site, as only a low dose is required to achieve therapeutic effect. The half life of indomethacin may range from 2.6 hours to 11.2 hours in adults and is metabolized by liver into its glucuronide conjugate and is excreted predominantly in the urine (Martindale, 1996).

3.3.2.2. Calibration curve of indomethacin through serial dilution from a stock solution of indomethacin

In order to determine the amount of indomethacin present in any given sample, a calibration curve of indomethacin was plotted by the use of an UV-visible spectroscopy. This curve plotted a graph of concentration versus absorbance which enabled us to work out the amount of drug present according to the readings obtained from the UV-visible spectroscopy. In order for the absorbance to be measured, the indomethacin was mixed with the PBS until fully dissolved. The UV wavelength used for this spectroscopy was 318nm (Kamal, 2008 and Anoopkumar-Dukie, 2003). The initial plot for the calibration curve had a concentration of 0.0625mg/mL, which was then diluted in the ratio 4:1 of drug solution: PBS. This calibration curve was depicted as Figure 3.6

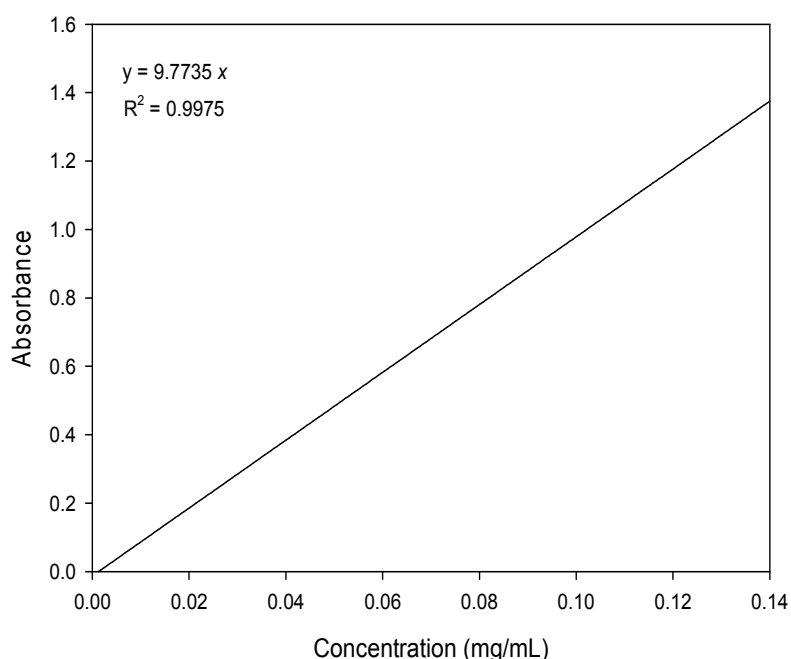


Figure 3.6. The calibration curve for the drug indomethacin in pH7.4 PBS at 25°C.

3.3.2.3. Diclofenac sodium as a model drug in the Stimuli-Actuated Polymeric Device

Diclofenac sodium is another drug which falls under the class of NSAIDs, which was the sodium salt of the drug diclofenac. The reason for incorporating the sodium salt is to increase the water solubility of diclofenac. Diclofenac on its own was sparingly soluble, whereas diclofenac sodium is freely soluble in water. Another common salt which is used with diclofenac is potassium salt. Both salt are combined with the drug and are protonated once they are in the gastric acid, with the only difference being the potassium salt offers higher water solubility for diclofenac as compared to the sodium salt. The chemical structures of diclofenac sodium and the effect that sodium salt has on water solubility are shown as in Figure 3.7.

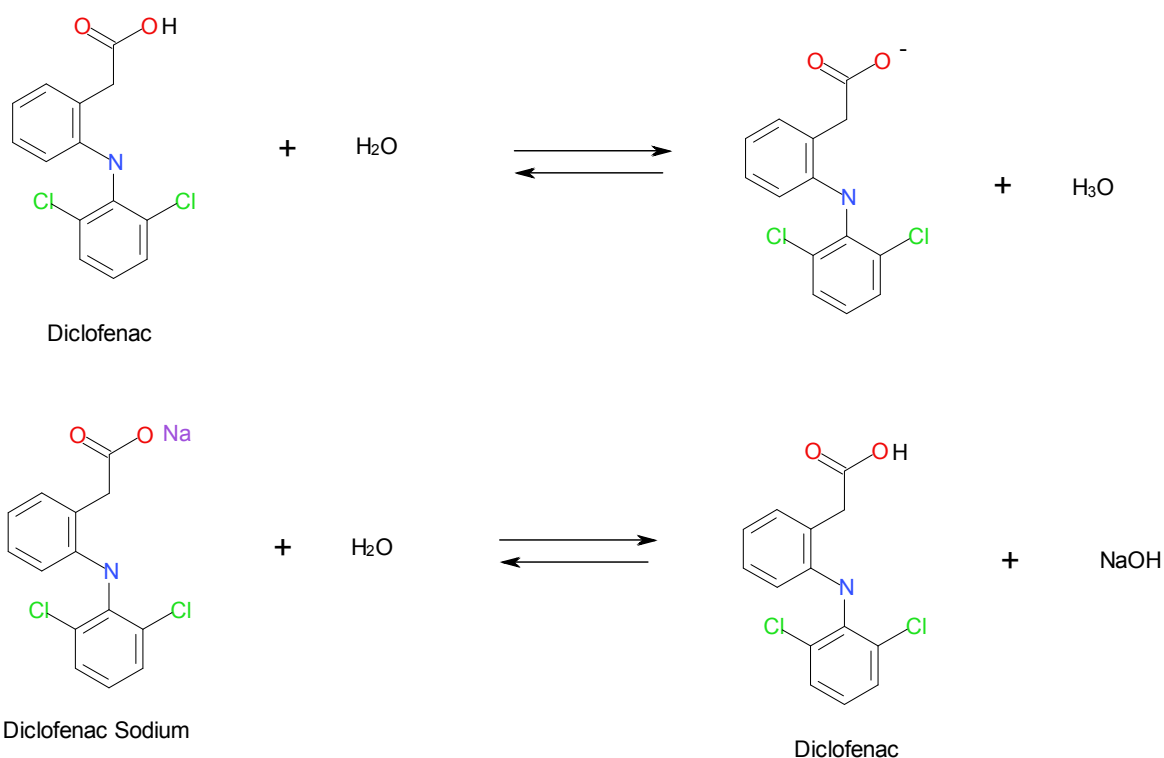


Figure 3.7. The effect of sodium salt on diclofenac.

In the case of unsalted diclofenac, the dissociation of the diclofenac forms H_3O^+ ions in the surrounding medium, thus resulting in an acidic surrounding solution. On the other hand, the sodium salt forms $NaOH$ which results in alkaline solution. Diclofenac is insoluble in an acidic pH (1-3) but soluble in basic pH (5-8) (Manjunatha, 2007). Therefore, the diclofenac with the sodium salt would be more soluble in water as compared to the unsalted diclofenac.

Diclofenac was rapidly absorbed from the GIT, but 50% of the dosage form is subject to first-pass metabolism. Like indomethacin, diclofenac is more than 99% protein bound at therapeutic dose, which indicates that a low dose is required at the target site in order to achieve therapeutic dose. Diclofenac has a terminal half life of 1-2 hours, which indicates a fast acting drug with fast excretion. It is excreted mainly through urine and a minor portion through the bile. Conditions which are indicated for diclofenac sodium includes musculo-skeletal and joint disorder such rheumatoid arthritis, osteoarthritis and ankylosing spondylitis. Other conditions include bursitis, tendonitis, sprains, strains and other chronic pain condition.

3.3.2.4. Calibration curve of diclofenac sodium through serial dilution from a stock solution of diclofenac sodium

In order to plot a calibration curve of diclofenac sodium, the diclofenac sodium was initially dissolved in PBS. An initial concentration of 0.05mg/mL was used because it has a

favourable absorbance of 1,131. Then it was diluted in a 4:1 drug solution: PBS and the absorbance were recorded after every dilution. For this calibration curve, a wavelength of 276nm was used (Aurora-Prado, 2002). The calibration curve was then plotted and depicted as in Figure 3.8.

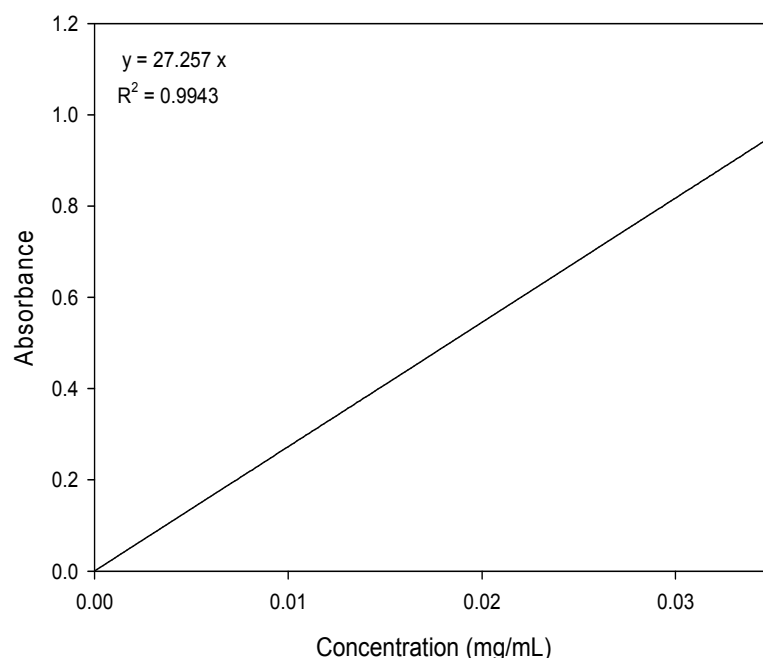


Figure 3.8. The calibration curve for the drug diclofenac sodium in pH7.4 PBS at 25°C.

3.3.2.5. Aspirin as a model drug in the Stimuli-Actuated Polymeric Device

Aspirin is a salicylate drug which contains anti-pyretic, anti-inflammatory and analgesic properties. In low doses, it also has an anti-coagulant effect and can be used for prevention of heart attacks, strokes and blood clot formation for patients with a high risk for emboli (Manson, 1990). The main side effect of aspirin is gastro-intestinal ulcers, tinnitus and blood thinning. When used in children under the age of 16, there is a possible risk of causing Reye's syndrome (Macdonald, 2002). The structure of aspirin is demonstrated in Figure 3.9, along with the salicylate group for comparison.

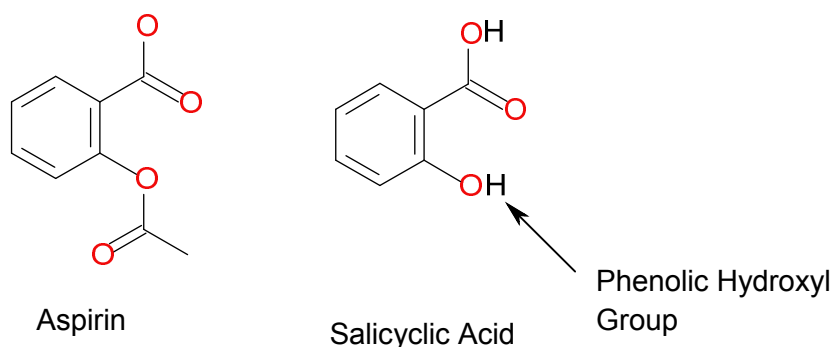


Figure 3.9. The chemical structures of aspirin and salicylate when compared to each other. Aspirin may be synthesized by esterification of the phenolic hydroxyl group of the salicylic acid.

Aspirin is a weak acid and ionizes slightly after it is ingested. A reason why aspirin should be used as a medication for this implant is due to its acidic nature, aspirin has a low solubility in the stomach, and is only absorbed in the large intestine. Therefore, a longer time is required to achieve C_{max} . Protein binding of aspirin is estimated to be approximately $58.3\% \pm 9.6\%$ (Ghahramani, 1998). Furthermore, as much as 80% of the therapeutic dose of aspirin is metabolized by the liver via conjugation (Levy, 1972). Due to its poor availability of drug at the target site, it is more prudent to incorporate aspirin into this implant so that it may be released directly at the target site and at the desired moment.

3.3.2.6. Calibration curve of aspirin through serial dilution from a stock solution of aspirin

In order to plot a calibration curve for aspirin, the drug was initially dissolved in PBS to form a solution. An aspirin solution with a concentration of 0.5mg/mL has an absorbance of 1.3307. The wavelength of which aspirin absorbs the UV light was determined as 320nm (Li, 2009). The calibration curve was then plotted and depicted in Figure 3.10.

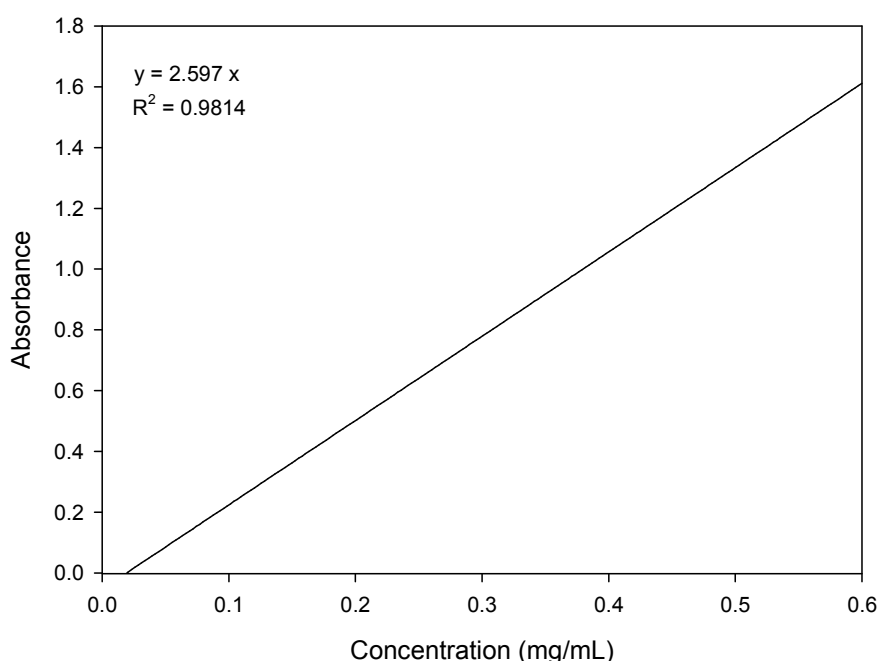


Figure 3.10. The calibration curve for the drug aspirin in pH7.4 PBS at 25°C.

3.3.2.7. Ibuprofen as a model drug in the Stimuli-Actuated Polymeric Device

The last drug which was considered for the incorporation of the SAPD was ibuprofen. Like many drugs mentioned in this section, it is a NSAID and acts through COX II inhibition and is mainly used for the treatment of arthritis, primary dysmenorrhoea, fever and other inflammatory conditions. It is derived from propionic acid (Adam, 1992). This therefore explains the poor solubility of ibuprofen in water and the increased solubility under basic conditions. The structure of ibuprofen is depicted in Figure 3.11.

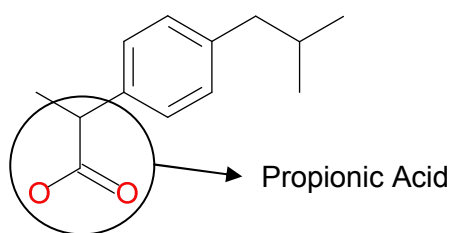


Figure 3.11. The chemical structure of ibuprofen.

The therapeutic dose of ibuprofen is 200-400mg three times daily, preferably after meals in order to prevent gastric ulceration. However, the pharmacokinetics of ibuprofen has indicated a bioavailability of approximately 75% and a protein binding of 99%. This indicates that ibuprofen is highly potent and a low dose is required at the target site in order to have anti-inflammatory effects. The half life is approximately 2 hours, which indicates a rapid

onset of action, and thus its suitability for use in the SAPD. Another important fact to note is that ibuprofen exists in both the (*R*) and the (*S*) enantiomers. In a human body, only (*S*)-enantiomers exhibits anti-inflammatory property, however, the body is capable of converting the inactive (*R*)-enantiomers into the active (*S*)-enantiomers (Avgerinos, 1991). The existence of the two isomers should not have interference on the use of this drug in the SAPD.

3.3.2.8. Calibration curve of ibuprofen through serial dilution from a stock solution of ibuprofen

Since ibuprofen exhibits poor solubility in the PBS, the PBS has to be heated to boiling point before the ibuprofen was added. An initial concentration of 1mg/mL was used, which was scanned under a UV wavelength of 273nm (Manzano, 2008). The calibration curve was then plotted as depicted in Figure 3.12.

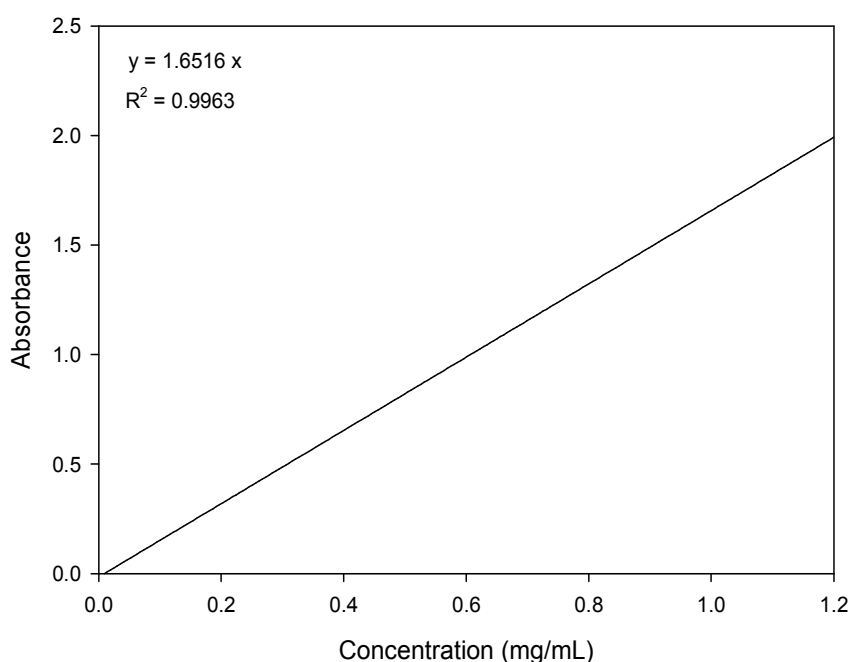


Figure 3.12. The calibration curve for the drug ibuprofen in pH7.4 PBS at 25°C.

3.3.3. Preparation of the crosslinked polyvinyl alcohol Stimuli-Actuated Polymeric Device with indomethacin as a model drug

3.3.3.1. Composition of the drug-loaded polyvinyl alcohol/polyaniline-based Stimuli-Actuated Polymeric Device

Four different devices were constructed and loaded with indomethacin in order to assess its electroactivity. The compositions of the four devices were depicted in Table 3.6. The method

of preparation for the first device was different than that of the other three devices and is discussed separately. In these devices, the PVA formed the hydrogel component, aniline and PANi acted as the EAP, Eudragit® formed the crosslinker and indomethacin was the drug intended for targeted delivery.

Table 3.1. The composition of all four devices synthesized. Indomethacin was loaded in all four devices, while varying grades of Eudragit® and PVA was used in order to assess difference in indomethacin released under the presence of electric current.

Reagents for the PVA/PANi -based SAPD	
Device 1	<ul style="list-style-type: none"> - PVA 8/88 (10g) - Aniline (5g) - Ammonium Persulfate (6.126g) - Indomethacin (100mg)
Device 2	<ul style="list-style-type: none"> - PVA 8/88 (5g) - PANi emeraldine doped (1.5g) - Eudragit® RL 100 (5g) - PEG 4000 (5g) - Indomethacin (100mg)
Device 3	<ul style="list-style-type: none"> - PVA 8/88 (5g) - PANi emeraldine doped (1.5g) - Eudragit® L100-55 (5g) - Indomethacin (100mg)
Device 4	<ul style="list-style-type: none"> - PVA 8/88 (5g) - Eudragit® L 100-55 (5g) - PEG 4000 (5g) - PANi emeraldine doped (1.5g) - Indomethacin (100mg)

3.3.4. The synthesis of drug-loaded Stimuli-Actuated Polymeric Device

Device 1 was prepared by dissolving PVA (10g) into 100mL of 1.0M HCl acid. Aniline (5g) was added into a 50mL of 3.0M HCl acid and stirred until fully dissolved and added into the polyvinyl alcohol solution. This mixture was left to cool in an ice bath. Ammonium persulfate (6.126g) was dissolved in another 50mL of 3.0M HCl acid separately and added drop-wise into the PVA/Aniline mixture for a time period of one hour whilst being stirred vigorously in an ice bath. This was to ensure that the polymerization of aniline was carried out under cold conditions. The ammonium persulfate acts as an oxidizing agent and an initiator to the polymerization of aniline. Following the addition of ammonium persulfate, the suspension was left to stir in an ice bath over a period of five hours before it was left in the fridge overnight for the polymerization to complete. The suspension was placed under a fume cupboard for 96 hours at room temperature in order to achieve maximum evaporation of the solvent. This method was adopted from a study by Mirmohseni and co-workers (Mirmohseni *et al.*, 2003). It was immersed in a 1:1 solution of acetone and 1.0M HCl solution for 12

hours to wash away all unreacted monomers. The hydrogel was dried for another 24 hours to ensure further evaporation of solvents. In order to load drugs into the system, 100mg indomethacin was dissolved in 100mL of heated PBS, the hydrogel was dissolved in 100mL heated distilled water and the two solutions were mixed together. Since PBS is miscible with water, it would ensure a homogenous mixture of the drug into the PVA hydrogel. The resulting drug-loaded PVA hydrogel was then left to stand in a mould until solidified.

The preparation for Device 2, 3 and 4 were identical, except for variation of the ingredients used (Table 3.6). PVA (5g) was dissolved in 20mL of boiling water followed by cooling to room temperature. Eudragit® (5g) and PEG 4000 (5g) were dissolved in two separate beakers with 20mL dichloromethane and mixed together once both were fully dissolved. Indomethacin (100mg) was added into the Eudragit®/PEG 4000 mixture and stirred until dissolved followed by addition into the cooled PVA solution. Due to the immiscibility between dichloromethane and water, the volume of water was kept to a minimum of 20mL. The resulting emulsion was blended with a pestle and mortar for ten minutes, followed by homogenizer for one minute. The emulsion was poured in a mould and left to dry in a fume cupboard for a period of 96 hours to ensure evaporation of the solvent. Once dried, the SAPD was rinsed with distilled water to ensure removal of any drug not incorporated into the hydrogel.

3.3.5. Gel compression measurement of the Stimuli-Actuated Polymeric Device

After the SAPD was synthesized, the hydrogels were tested for their strength to withstand forces. This was important as gel compression allowed us to assess the degree of crosslinking in the hydrogel. Gel strength was assessed with the use of a texture analyzer. The SAPDs were weighed and placed onto the TA.XT.plus Texture Analyzer (United Scientific, Gauteng, South Africa) where it was compressed by the rounded end probe. In this test, the rate of compression and time was set as a constant, while the force required for such compression was measured. The Texture Analyzer was set to move at a rate of 1.535mm/sec for a period of 2.890 seconds. The total compression into the hydrogel is depicted as Equation 3.1.

$$\text{Total Compression} = \text{Rate of movement} \times \text{Time} \quad \text{Equation 3.1}$$

According to Equation 3.1, the total compression into the hydrogel was 4.436mm. The force required for such compression was measured and the result is depicted in Table 3.7.

Table 3.2. The force required for compression of each device as measured by the texture analyzer.

Hydrogel Device	Force Measured During Compression
Device 1	0.9969 N
Device 2	1.3011 N
Device 3	0.9750 N
Device 4	0.0011 N

Based on the results obtained in Table 3.7, it was noted most force was required for the compression of Device 2. This may indicate an increased crosslinking between PVA and Eudragit® RL when compared to Device 1 and 3, while Device 4 required the least force for compression. This indicated that Device 4 may have to be handled with care due to its weak structural integrity and may not be favoured as a pharmaceutical formulation. All hydrogels were capable of returning to its original shape after compression which suggested that the yield value for these hydrogel may be much higher.

3.3.6. Surface morphology of the Stimuli-Actuated Polymeric Device

The next part was to assess the surface morphology of the SAPD. The surface morphology was closely linked to the texture and also gave an indication of the drug release profile of the SAPD. A porous hydrogel should release drug easier as opposed to a hydrogel which possessed a non-porous structure. The surface morphology of the SAPD was determined by using light microscopy. In addition, a porous hydrogel would probably be preferred due to its increased ability to absorb solvents and faster drug release profile as opposed to non-porous hydrogels. Surface morphology was captured under 40X magnification. Figure 3.13 a-d depicted the surface morphology of the 4 SAPDs.

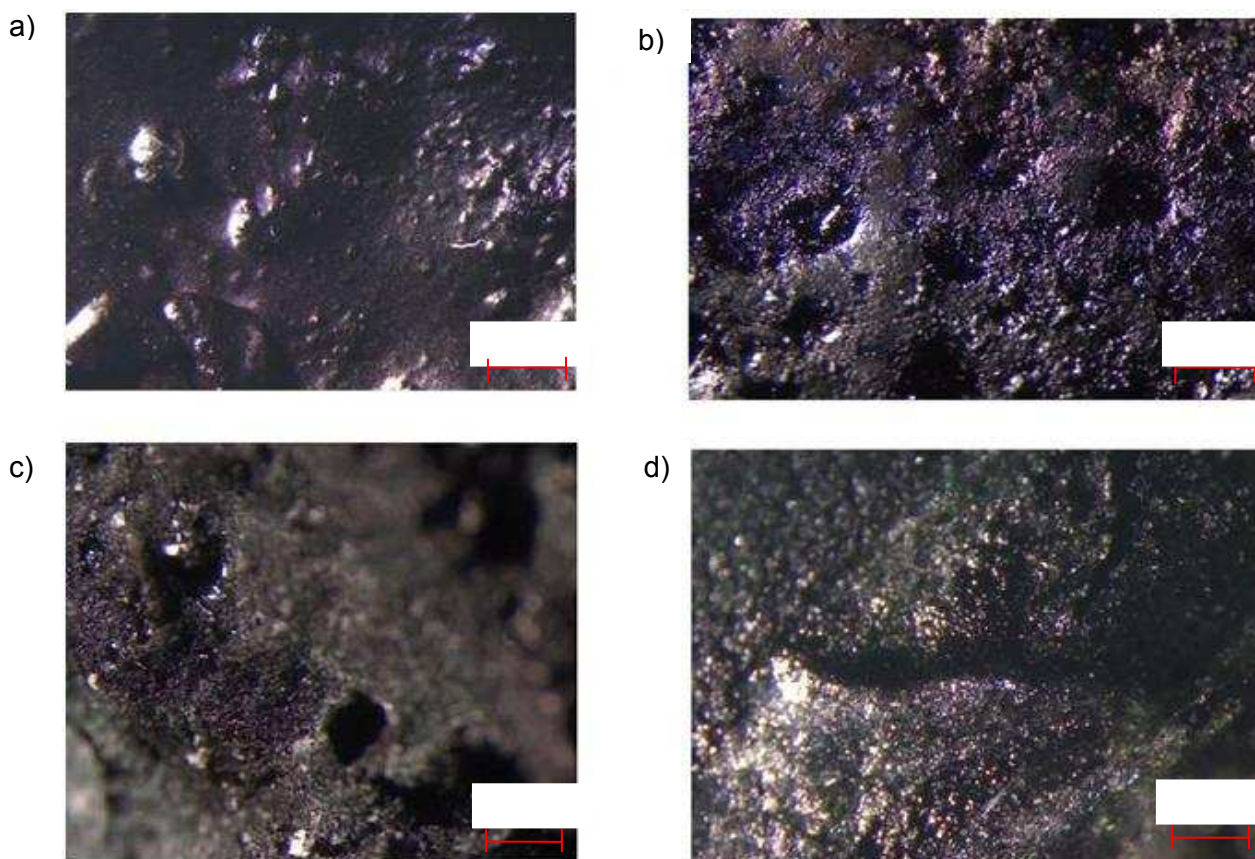


Figure 3.13. The surface morphology of Device 1-4 under 40X magnification, which showed a non-porous surface morphology.

Device 2, 3 and 4 have shown enhanced porosity in comparison to Device 1. This indicated that Device 2 may be the favoured Device, due to its porous structure and its ability to withstand high stress. Although Device 1 and Device 3 have both shown promising ability to withstand stress, Device 1 possessed a smooth surface morphology and therefore drug release from Device 1 may be hindered. Thus far, Device 2 and 3 seemed to be the most promising for the purpose of drug delivery.

3.3.7. Setup of the circuit for *in vitro* assessment of drug release from the Stimuli-Actuated Polymeric Device in the presence of an electric current

In order to determine the drug release profile of the drug-loaded SAPD, the devices were immersed into 100mL of PBS and electric currents were allowed to pass through it. The source of the current was obtained from a 9V battery cell. Copper wires 20cm in total length with a diameter of 2mm were used as the conductor and the electrodes used were iron electrodes. A multi-meter was connected in series in order to assess the amount of current passing through the circuit at any given time. The setup of the circuit was as depicted as in Figure 3.14

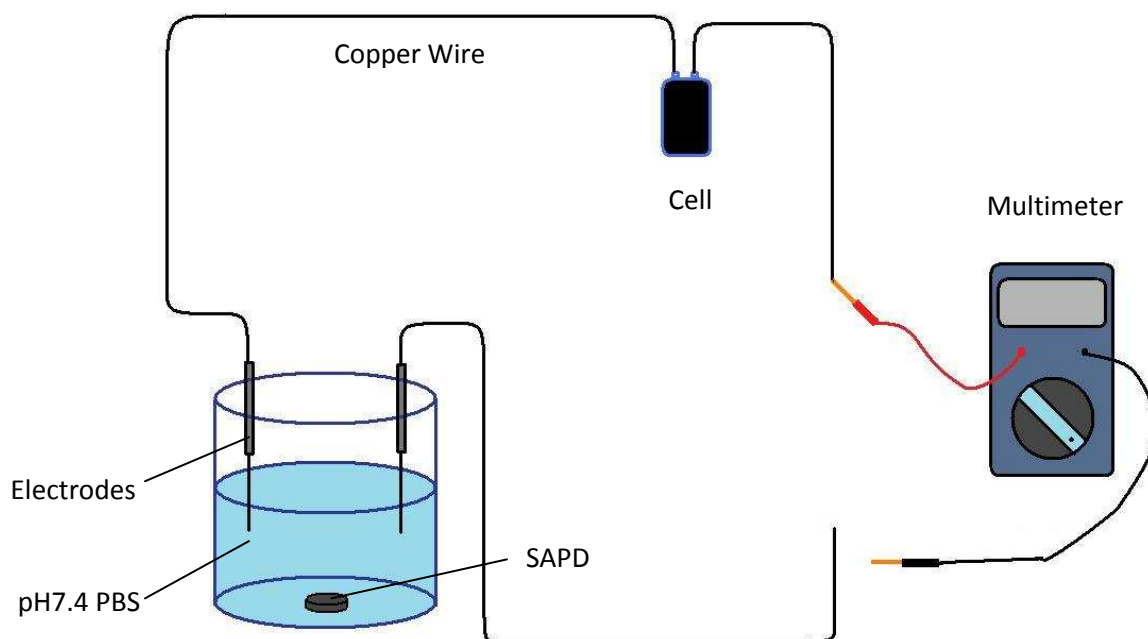


Figure 3.14. The setup of the circuit where drug release profile of the SAPD was conducted.

The devices were placed into 100mL of PBS and 9V of potential difference was applied to the circuit. The reading on the multi-meter indicated that 30mA of currents were passing through the circuit at the time of testing. PBS samples of 5mL were drawn via a syringe and replaced with 5mL of fresh PBS at various time intervals. The samples were analyzed for any presence of drugs in order to assess the behaviour of drug of the device. The time intervals for this study were 1, 2, 3, 4 and 5 minutes. These samples were tested for drug concentration via the use of an UV-visible spectroscopy. For comparison purpose, the device was divided into two pieces and one half was placed in 100mL of PBS in the absence of electric current to serve as control. Samples in the control group were collected at the same time intervals and assessed for any difference in drug concentration than that of the experiment.

3.3.8. The drug entrapment efficiency of the Stimuli-Actuated Polymeric Device

In order to test the drug entrapment of these devices, Device 4 was duplicated and loaded with 120mg of indomethacin. The Device weighed a total of 4.295g. This test was done in triplicate in order to ensure a consistent result. For the first test, a portion of the device with a mass of approximately 22mg was removed and dissolved in 80mL of heated PBS with the aid of a homogenizer. A sample of 1mL was taken from the 80mL and diluted with 4mL PBS. This diluted sample was scanned under UV-visible spectroscopy and the UV absorbance recorded was 0.01A.

$$0.01 = 9.7735 \times$$

Which gave us x equals 0.0010mg/mL in the 1:4 diluted samples. Working backwards, we multiplied by five to obtain the amount of drugs in 1mL of the sample, and finally multiplied by eighty to obtain the total amount of drug in the 22mg sample which was dissolved in 80mL PBS. Therefore, the total amount of drug present in the entire device equals $0.409 \times (4295/22) = 79.85\text{mg}$ and the total drug which was entrapped equals 66.54 %

For the second test, Device 4 was duplicated, with a total weight of 8.565g and loaded with 200mg indomethacin. 0.430g of sample was removed and dissolved in 100mL PBS, after which 1mL was diluted with 4mL of PBS again and scanned under the UV-visible spectroscopy. The reading obtained was 0.121A. We can therefore calculate the amount of drug entrapped in the device by using the same method for the first drug entrapment test. The total amount of drug present equated to 6.2 mg indomethacin in the 0.430g sample. Therefore, the drug entrapment efficiency was 61.74%

For the third test, Device 4 was duplicated and loaded with 200mg of indomethacin. The total weight of the device was 7.654g and a 0.385g sample was removed and assessed. The sample was dissolved in 100mL PBS, after which 1mL sample was extracted and diluted with 4mL PBS. The results obtained from the UV/visible spectroscopy indicated an absorbance of 0.145A. Therefore, the total amount of drug in the 0.385g sample was 7.418mg. This equated to 147.474g of indomethacin in the Device and a drug entrapment efficiency of 73.737%

From the above three tests, the drug entrapment efficiency of the device fell approximately in the range of 60-70% during synthesis.

3.3.9. The amount of drug release from Stimuli-Actuated Polymeric Device under the influence of electrical current

The samples were previously evaluated for any presence of drug by employing the UV-visible spectroscopy. The results obtained for both experimental and control Devices 1-4 is shown in Tables 3.8-3.11. The results are obtained in UV absorbance at a wavelength of 318nm. Study done on PANi has indicated that PANi has an absorbance peak at 365nm, 460nm and over 820nm (Nabid, 2008).

Table 3.3. The UV-absorbance of samples collected from Device 1.

Device 1	1 minute	2 minutes	3 minutes	4 minutes	5 minutes
Experiment (4.637g)	0.0001	0.0001	0.0002	0.0002	0.0002
Control (4.204g)	0.0001	0.0001	0.0001	0.0002	0.0002

As indicated in Table 3.8, there was no drug release from both the experiment and the control. There was negligible difference with regards to the amount of drug present in the sample and this device was not electroactive.

Table 3.4. The UV-absorbance of samples collected from Device 2.

Device 2	1 minute	2 minutes	3 minutes	4 minutes	5 minutes
Experiment	0.055mg	0.054mg	0.041mg	0.044mg	0.046mg
Control	0.015mg	0.016mg	0.019mg	0.015mg	0.020mg

The results obtained from Device 2 have indicated an enhanced release of indomethacin in the presence of electric current, as opposed to the control, which had a decreased rate of release. The slight decrease in drug concentration between various time intervals may be due to the dilution of the conducting medium when 5mL of PBS was used to replace the samples that were taken. These values were transformed into the quantity of drug present in the sample and would be discussed further on.

Table 3.5. The UV-absorbance of samples collected from Device 3.

Device 3	1 minute	2 minutes	3 minutes	4 minutes	5 minutes
Experiment	0.213mg	0.233mg	0.258mg	0.280mg	0.338mg
Control	0.106mg	0.100mg	0.102mg	0.129mg	0.219mg

Results from Device 3 have also indicated an enhanced release of indomethacin in the presence of electrical stimulation.

Table 3.6. The UV-absorbance of samples collected from Device 4.

Device 4	1 minute	2 minutes	3 minutes	4 minutes	5 minutes
Experiment	0.051mg	0.111mg	0.084mg	0.082mg	0.115mg
Control	0mg	0mg	0mg	0mg	0mg

Device 4 successfully released drug only in the presence of electrical current, while withholding the drug in the absence of electrical stimulation. Device 4 seemed the most promising following the assessment of the drug release profile in the presence of an

electrical field. However, the weak structural integrity meant that it should be handled with caution. It was also composed of a porous structure which indicated that it was capable of fluid absorption. The initial drug release study has shown that Device 4 may have the optimum drug release profile, however, further studies should be performed in order to assess the consistency and the mechanism of drug release of Device 4.

According to these results, indomethacin released from a Device 4 was too low to obtain therapeutic effects. This may be due to one of the three following reasons:

- The total amount of indomethacin used (100mg) was insufficient. Increased quantities of indomethacin could be used in future in order to assess for any possible increase in drug release from the SAPD.
- Electro-responsive behaviour from a hydrogel was mainly a surface phenomenon (de las Heras Alarcon, 2005) and initiating a response rapidly from the centre of a hydrogel is difficult. The surface area of the device could be increased in order to enhance its drug release.
- Even though 100mg of the drug was used for the synthesis of these devices, the drug entrapment was only approximately 60-70%. Furthermore, the device was divided into halves when tested for drug release. These devices were halved as the presence of excess polyaniline in the testing solution hindered the process of UV spectroscopy. Therefore, rendering only approximately 30-35mg of the indomethacin left in the device during the test. The SAPDs were only halved during this study only.

Although Device 3 has shown a release of a therapeutic dose of indomethacin, the drug leakage presented a problem and could not be used. This leakage should be addressed through better understanding of the physicochemical properties of the SAPD.

3.3.10. Chemical structure analysis of the Stimuli-Actuated Polymeric Device

In order to obtain better elucidation of the chemical structures of these four devices, FTIR was used in order to assess the IR peaks. By analyzing these peaks, it allowed us to observe any difference in chemical composition of the four devices, and therefore the cause of difference in drug release. Figure 3.15-3.18 depicts the FTIR results of the individual components of the devices, while Figure 3.19-3.22 depicts the FTIR results of Device 1-4 respectively. Peaks were labelled as (wavelength, % Transmittance).

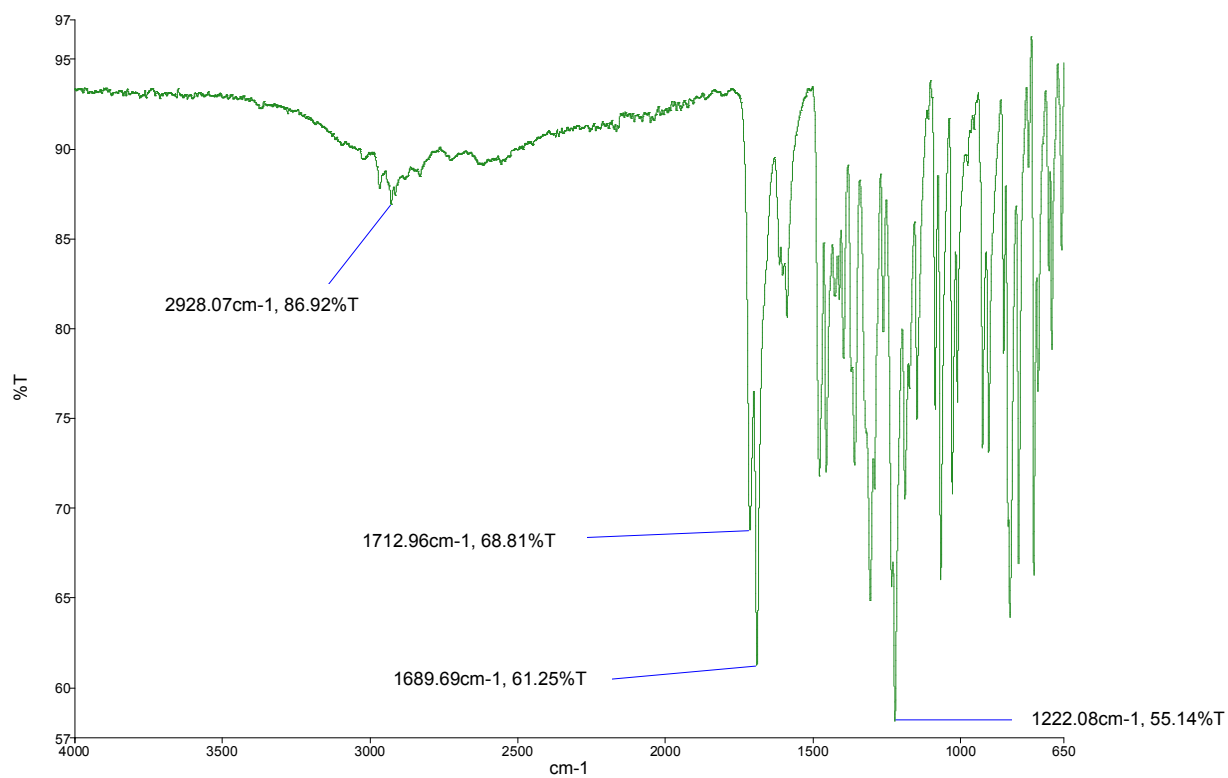


Figure 3.15. FTIR spectrum of Indomethacin.

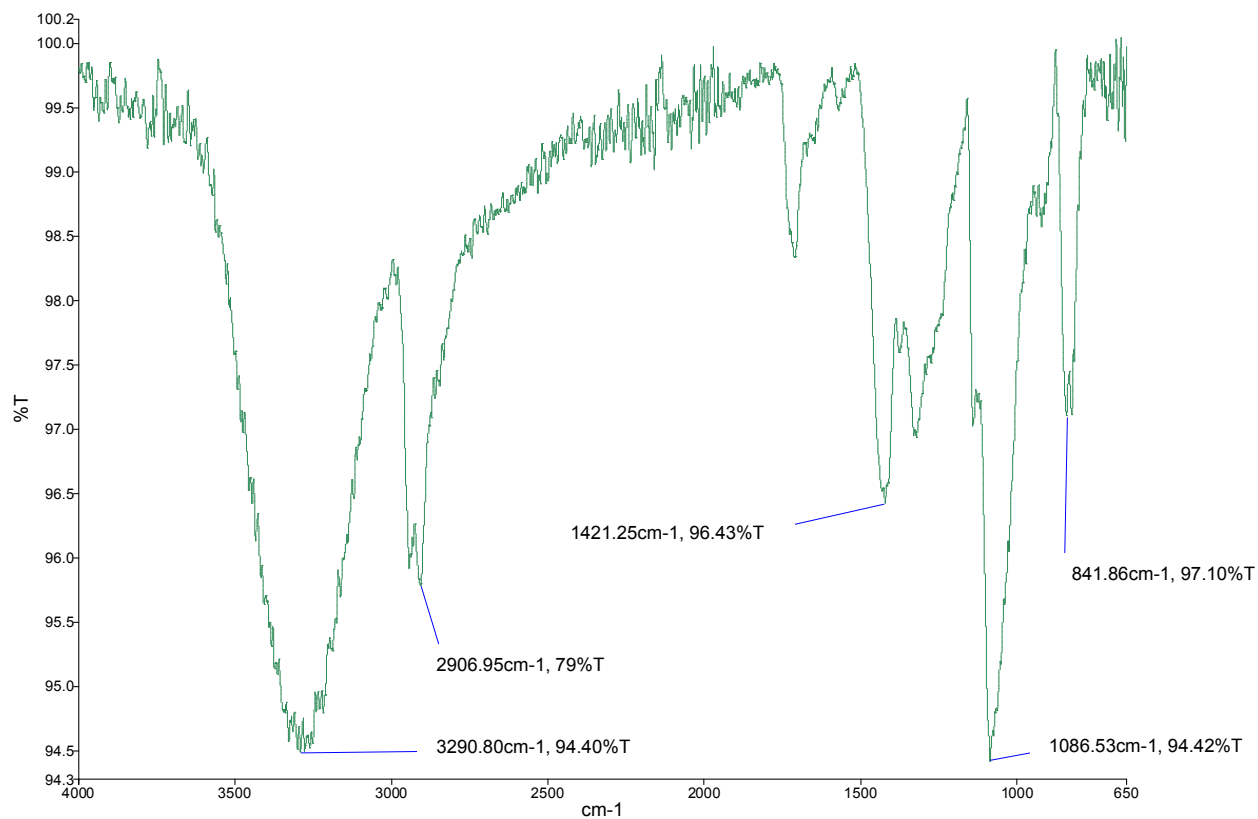


Figure 3.16. FTIR spectrum of polyvinyl alcohol.

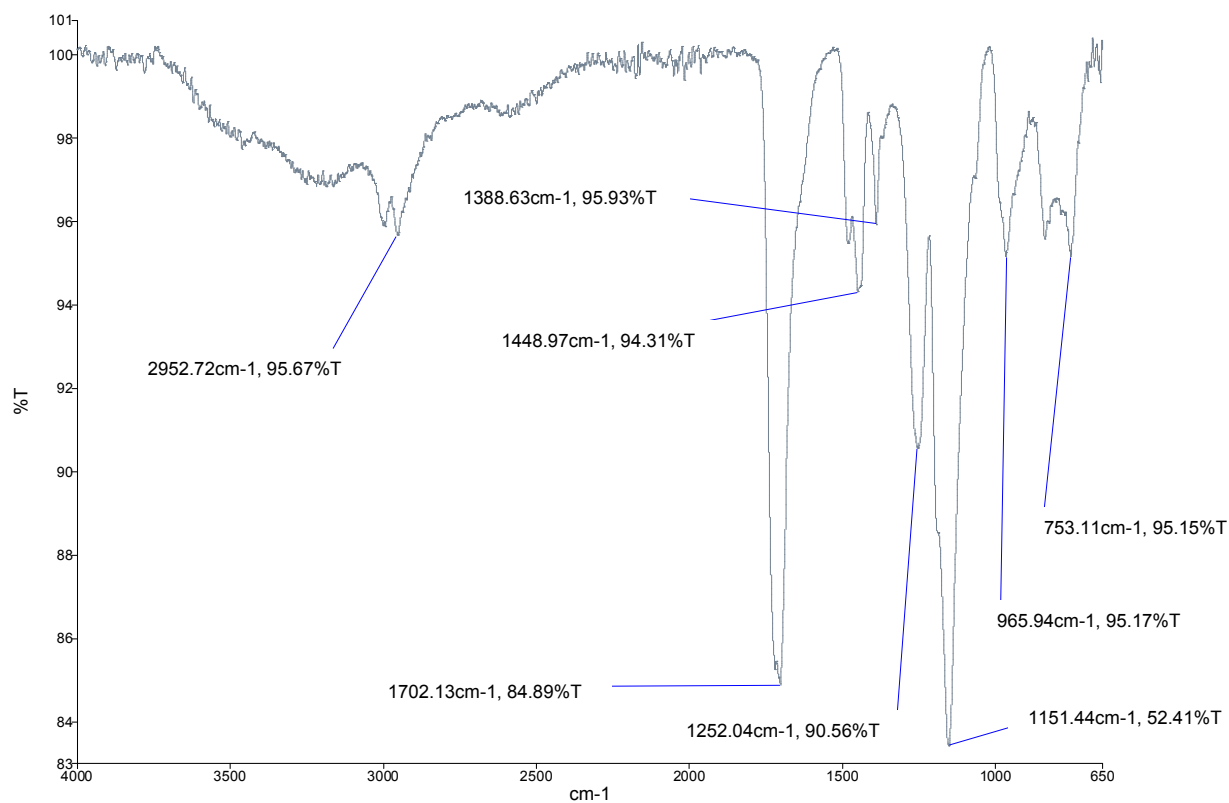


Figure 3.17. FTIR spectrum of Eudragit®.

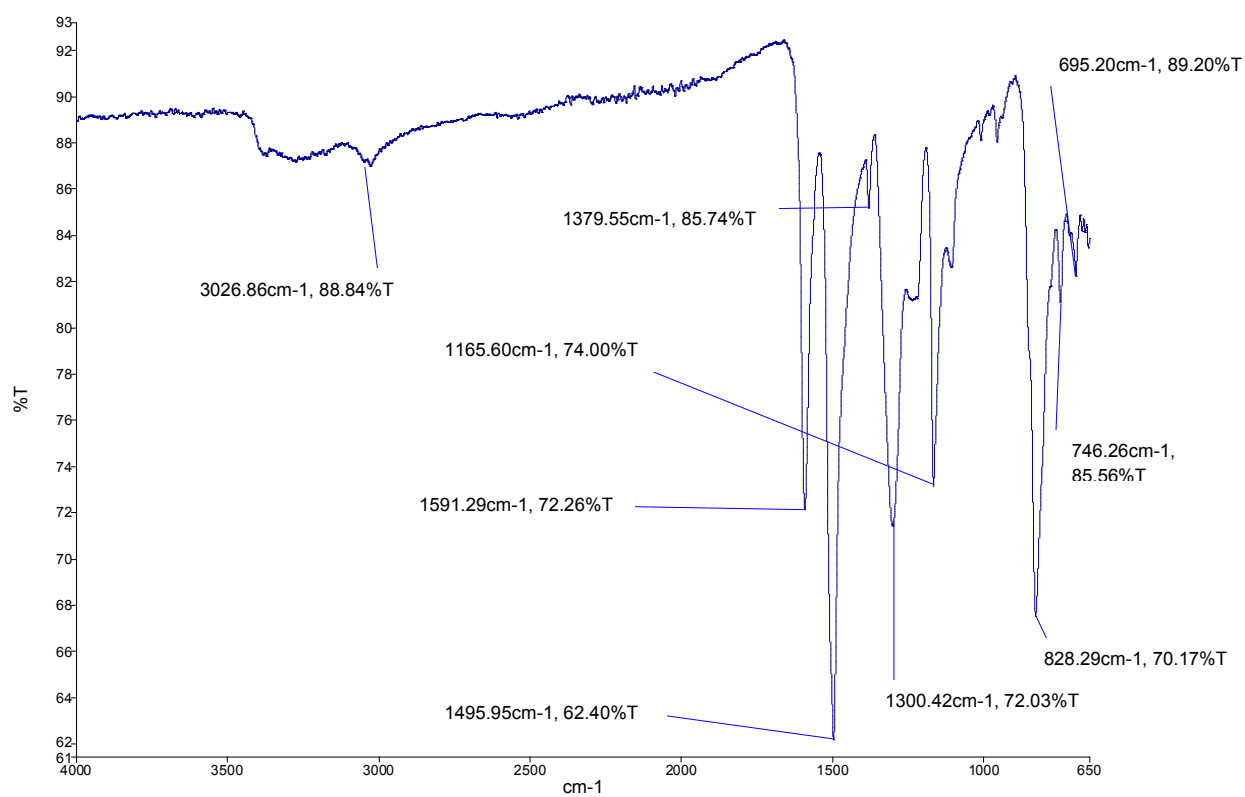


Figure 3.18. FTIR spectrum of polyaniline.

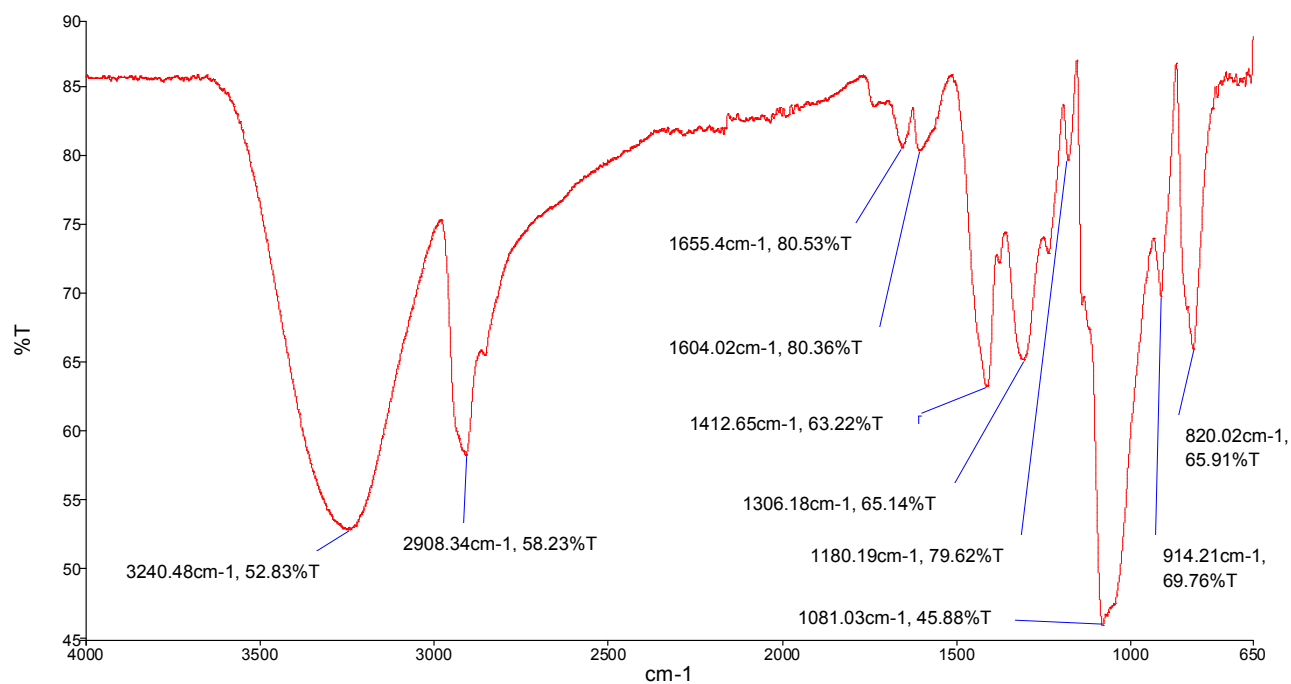


Figure 3.19. FTIR spectrum of Device1.

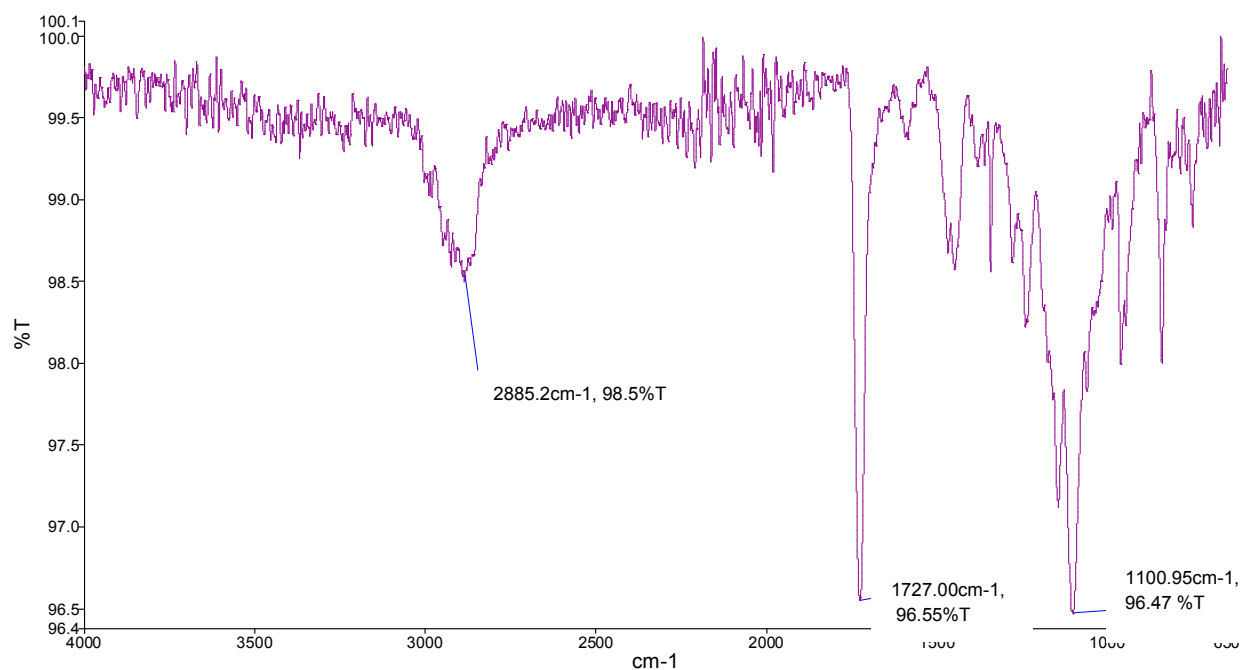


Figure 3.20. FTIR spectrum of Device 2.

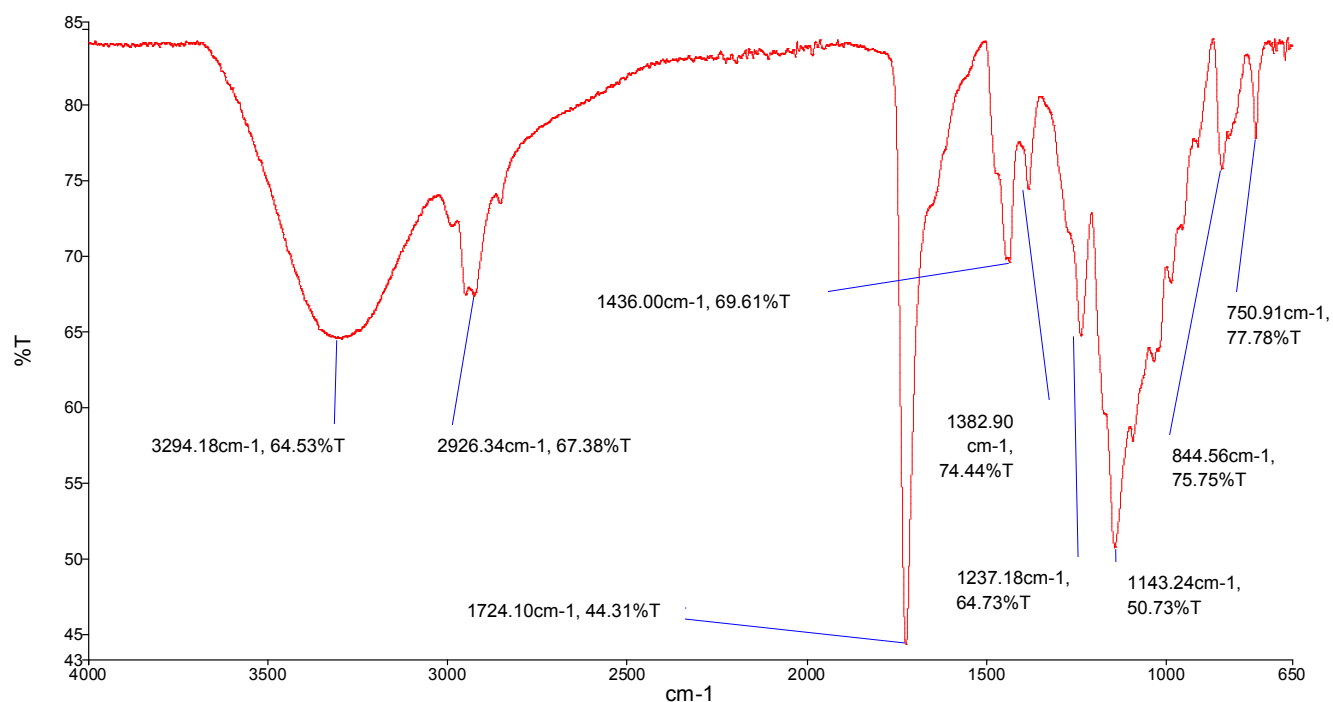


Figure 3.21. FTIR spectrum of Device 3.

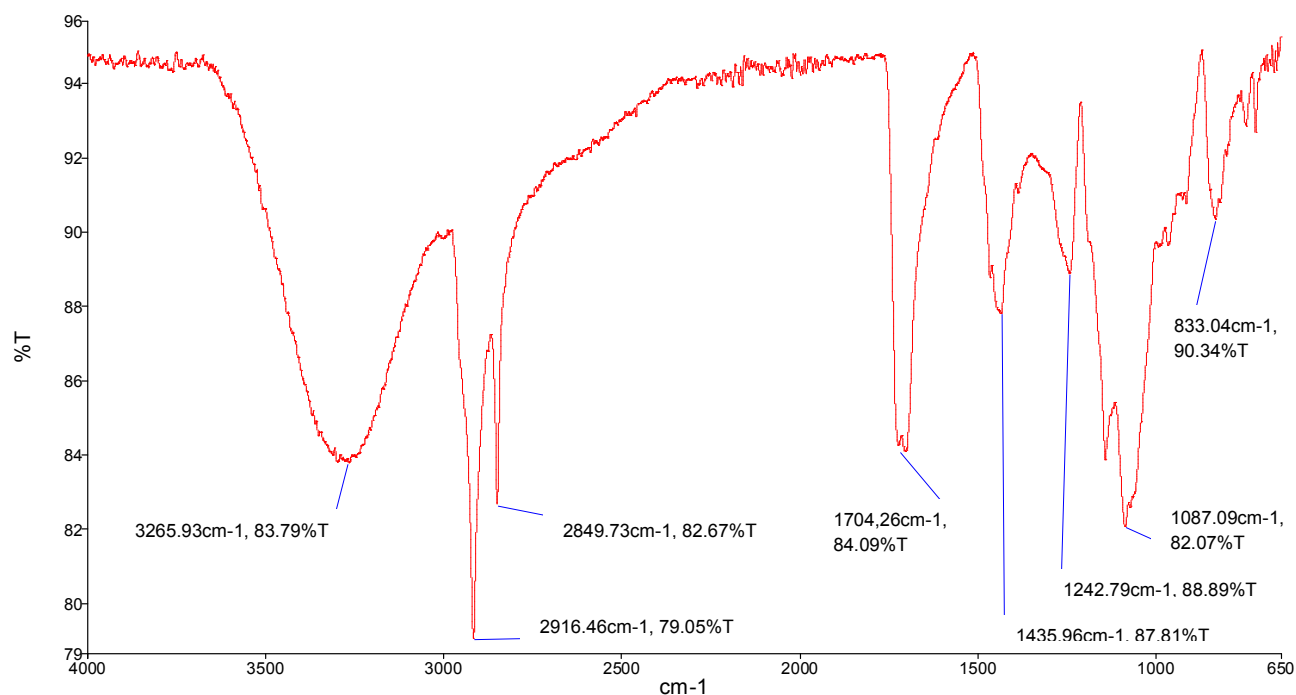


Figure 3.22. FTIR spectrum of Device 4.

The results obtained from the FTIR allowed us to conclude the following:

- Device 2 lacked the broad peak between $3200\text{--}3600\text{cm}^{-1}$ which indicated the lack of hydrogen-bonded alcohols, or phenolic groups.

- Weak bands at 3000cm^{-1} and 1600cm^{-1} followed by a moderate peak between $800\text{-}1000\text{cm}^{-1}$ indicated a para-substituted aromatic group as seen in PANi. These peaks were observed in all 4 Devices. Therefore PANi was confirmed as a component in all devices and this was further substantiated by an increased drug release when an electric current was applied across the device.
- In general one can observe that the FTIR spectra of the devices were a composite of the individual ingredients, with the exception of Device 2 which lacked the broad peak from $3200\text{-}3600\text{nm}$ of polyvinyl alcohol. Other variations may be due to the different ratios of the ingredients.
- The peaks exhibited by Device 1 and Device 4 were very similar, although it exhibited a very different drug release profile. This indicated that even though similar chemicals were used, the method of synthesis for the device also greatly alters the drug release profile. This may be attributed to the varying degree of crosslinking when using different methods for synthesis. This may be substantiated by the presence of bands at the same wavelength but with varying intensity between Device 1-4.

3.3.11. Proposed release mechanism of the Stimuli-Actuated Polymeric Device

The information that was obtained from this pre-formulation study has indeed shown that the use of PVA/ PANi in the SAPD does enhance the release of indomethacin upon the activation of an electric current. Although the crosslinking of the hydrogel enabled it to withhold more drug molecules, it also limited the rate of drug release from the hydrogel. Another important element which seemed to affect drug release was possibly the porosity of the hydrogel formed. As seen from the data obtained from Device 1, there was a lack of porosity as compared to Device 2, 3 and 4. This resulted in no drug release from Device 1, as compared to Device 2, 3 and 4. The drug entrapment of these devices also ranged from 60-70%.

A study done by Murdan and co-workers (2003) has suggested three possible mechanisms by which the movement of a drug out of the hydrogel may be controlled (Murdan *et al.*, 2003). These mechanisms include:

- Forced convection of drug as the hydrogel de-swells.
- Drug electrophoresis due to migration of drug toward charged electrodes.
- Drug liberation when the hydrogel was eroded upon electrical stimulation.

The mechanism of the effusion of drugs from the polymeric hydrogel device was thought to be that similar to that of iontophoresis. Under the presence of electric current, the anionic drug indomethacin (Fini, 2001) was drawn towards the positively charged cathode. It was this attractive force that enhanced the diffusion of the drug out of the SAPD. This mechanism was depicted in Figure 3.23. When a cross-linked Eudragit®-polyethylene glycol system was incorporated into the hydrogel, the drug was held in the hydrogel by a 3-dimensional network and movement out of the hydrogel toward the cathode may be hindered. This may have accounted for the decrease in drug release.

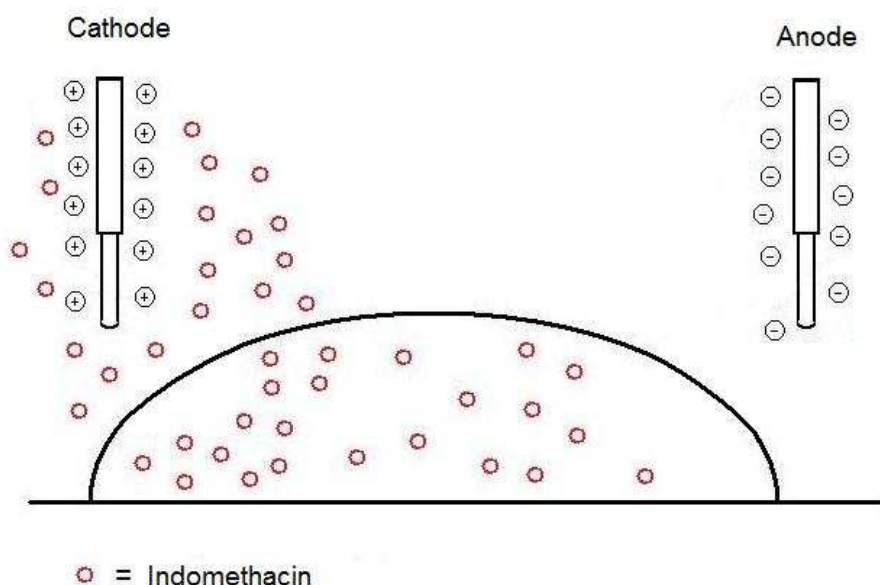


Figure 3.23. The possible mechanism for movement of the drug indomethacin out of the hydrogel

This mechanism was similar to that of iontophoresis which involves the migration of a charged drug towards an oppositely charged electrode. From the data obtained, a crosslinked hydrogel combined with PANi and indomethacin may prove to be useful for the purpose of the controlled release of indomethacin.

3.4. Concluding remarks

This study has shown that the use of PANi as an electro-responsive polymer in a crosslinked hydrogel may be used for the controlled release of indomethacin. The degree of response from these polymers may vary depending on the conditions of synthesis of these polymers. EAPs incorporated into a crosslinked hydrogel have shown electrical conductivity, and the

release of indomethacin was enhanced when indomethacin was blended into the hydrogel with an EAP in the presence of an electric current in the present study. Hydrogel systems which were undoped did show drug release even without the presence of an electrical current, although the degree of drug release was to a much smaller extent. The crosslinking of the hydrogel did successfully withhold the drug within the hydrogel, but such crosslinking also retarded the extent of drug release in the presence of electrical stimulation. This release may be due to the repulsive force caused by the like-charges of the negatively charged electrons from the electric current and the negatively charged (anionic) drug indomethacin, or it may be linked to processes such as iontophoresis. The use of PANi along with a crosslinked hydrogel may be a prospective drug delivery device for the controlled release of indomethacin by the means of an electrically-activated and controlled device in patients.

Aniline, which underwent polymerization in the solution of polyvinyl alcohol in 1.0M HCl acid showed no response when placed in electric current for the purpose of controlled release of indomethacin. However, PANi emeraldine which was incorporated into the polymeric hydrogel device did indeed demonstrated enhanced release of indomethacin. These release rates have shown to increase linearly as time progresses. In order for these devices to become practical, characteristics such as increased drug release should be investigated further. In addition, the response time should not exceed 1-2 minutes. This could be achieved by increasing the surface area of the hydrogel which would allow more drugs to move towards the charged electrodes. The enhanced effect of drug release may yet require further research before it could be used optimally, however, it does prove to be a potential and novel system for the controlled release of indomethacin via the stimulation of electrical currents.

CHAPTER 4

DESIGN AND FORMULATION OF A NON-SOLUBLE ELECTROACTIVE POLYMER- INCORPORATED HYDROGEL SYSTEM FOR THE CONTROLLED RELEASE OF A NON- STEROIDAL ANTI-INFLAMMATORY DRUGS

4.1 Introduction

Following the release of indomethacin from the SAPD, it was possible to construct an electroactive drug delivery system based on these preliminary designs. In order to achieve an improvement on the preliminary design, an understanding of chemistry was important. In this Chapter, we focused more on the chemical interactions which could possibly occur during the synthesis and release of the SAPD. Several factors were considered, such as drugs which carried negative charges which would be attracted to the positively charged cathode and vice-versa, while the degree of crosslinking would affect the amount of drugs entrapped in the system and its release profile. The degree of crosslinking may be determined by the amount of crosslinkers present, while the degree of polymerization was determined by the amount of initiators added with the monomer. Other factors such as methods which could be employed for incorporation of drugs and EAPs into the hydrogel system were also important, as the most efficient methods should yield the most stable system.

One of the problems encountered in Chapter 3 was the inability of the system to form a homogenous solution when dichloromethane was added with water. Therefore, when the SAPD was left to stand to enable solvent evaporation, separation of dichloromethane and water occurred. In order to rectify this problem, the first approach was to repeat the study but using different solvents. The solvent employed should be more polar when compared to dichloromethane, thereby allowing better miscibility with water. This should enhance the homogeneity of the system and yield a more precise release of drug dosage.

In the ensuing investigation, chloroform was used as a substitute for dichloromethane, since its chemical structure is similar to dichloromethane, although slightly more polar, which should exhibit better miscibility with water.

4.2. Materials and Methods

4.2.1. Materials

Chloroform (Unilab, Wadeville, Gauteng, South Africa) was used as a solvent. Polysodium styrene sulfonate (Sigma Aldrich, Steinheim, Germany) was tested as a polyelectrolyte, Glycerine (Merck, Wadeville, Gauteng, South Africa) and tri-ethyl citrate (Sigma Aldrich, Steinheim, Germany) was used as the plasticizer, Methylcellulose (Merck, Wadeville, Gauteng, South Africa) was assessed as a component of the hydrogel, Ethyl acetate, acetone, hexane, propylene glycol, liquid paraffin, chloroform, formic acid, sodium hydroxide, propionaldehyde, pyridine, formaldehyde and benzaldehyde were all obtained from Merck (Merck, Wadeville, Gauteng, South Africa) and used as solvents for the methylcellulose. Eudragit L100, S100, L100-55, E100, RS (Degussa, Darmstadt, Germany) was used as possible crosslinker with PEG 4000 (Merck, Wadeville, Gauteng, South Africa). Titanium dioxide, sodium benzoate, sodium thiosulfate, sodium chloride and potassium iodide (Merck, Wadeville, Gauteng, South Africa) were tested as salts for crosslinking. Diethyl acetamidomaleate (DAA) (Fluka Chemie, Buchs, Switzerland) was also tested as a crosslinker for the hydrogel system.

4.2.2. Determination of the physicochemical and physicomachanical properties of the Stimuli-Actuated Polymeric Device

The determination of the physicochemical and physicomachanical properties of the SAPD was important as we could use this data to assess the storage conditions of the SAPD, factors which affect its drug release profile and its stability in various environments. The physicochemical and physicomachanical properties would be analysed by using an array of techniques and equipments which would be essential for the understanding of the SAPD as a controlled release system.

4.2.3. Determination of chemical structures of the Stimuli-Actuated Polymeric Device

Various tests were performed in order to assess the physicochemical characters of the SAPD. Chemical structures of the SAPD were assessed by using the Fourier Transform Infra-Red (Perkin Elmer, Life & Analytical Science Inc., Shelton, CT, USA) to determine if there were any chemical reactions between the EAP, the excipients or the drugs.

4.2.4. Calorimetric analysis of the Stimuli-Actuated Polymeric Device

Differential Scanning Calorimetry (DSC1 Star^e, Mettler Toledo System, Uster, Zurich, Switerland) was used to assess the chemical structures of the polymer and drug when

exposed to various temperatures. Phases such as glass transition, crystallization and melting point allowed assessment of the transition temperature and enthalpy of the EAP. The transition temperature would play an important role in deciding the physical characteristics of the polymer such as brittleness and elasticity.

4.2.5. Determination of *in vitro* drug release from the Stimuli-Actuated Polymeric Device

The quantity of drug released into the PBS solution assessment was done using Ultra Violet (UV) spectroscopy (Cecil CE 3021, Cecil Instruments Ltd, Milton, Cambridge, UK). UV spectroscopy determines the quantity of drugs present by measuring the amount of light refraction. Therefore, drug concentration at various time intervals was measured by taking 5mL of the saline sample and running it under UV spectroscopy.

4.2.6. Surface morphology and textural analysis of Stimuli-Actuated Polymeric Device

Scanning electron microscopy (JSM 5600 Scanning Microscope, JEOL Ltd, Tokyo, Japan) will be used to determine the surface morphology of the SAPD. The SAPD would be viewed under high magnification and cross-linking or chain-shifting of the EAP may be visualised.

4.2.7. Assessment of possible erosion in the Stimuli-Actuated Polymeric Device

The erosion rate of the SAPD may be determined by weighing the difference in mass of the SAPD should any erosion occur. By using Equation 4.1, disk erosion under the absence of electrical stimulation was determined:

$$\% \text{ weight loss} = \frac{(\text{Initial weight}-\text{Remaining Weight})}{\text{Initial Weight}} \quad \text{Equation 4.1}$$

4.2.8. Electric conductivity test on the Stimuli-Actuated Polymeric Device

Electric conductivity of the SAPD may vary when doped with various counter ions. This would affect the behaviour and tensile strength of the SAP. The conductivity would be assessed by using the OAKTON[®] TDS Testr[™] (Model UD-35661-70, Solon, OH, USA). The electrode would be immersed in the saline solution and conductivity test would be performed on the SAPD. Conductivity was measured in μ Siemens

4.3. Results and Discussion

4.3.1. The use of chloroform for the formulation of a Stimuli-Actuated Polymeric Device and the assessment of drug release profile of chloroform-substituted device

The implantable system was synthesized in this experiment using different solvent, in order to assess for any difference in drug-release profile of the SAPD. Chloroform was used in the place of dichloromethane, due to the triple chlorine atoms bound to the carbon atom. This would theoretically increase the dipole movement when compared to dichloromethane, therefore an increased polar and miscibility with water. With regards to the chemical structure of dichloromethane, the dipole movement occurs on the two chlorine atoms which renders it only slight polar and immiscible with water. By replacing dichloromethane with chloroform, we should be able to increase the miscibility of the two liquids. Figure 4.1 depicts the dipole movements of the two compounds.

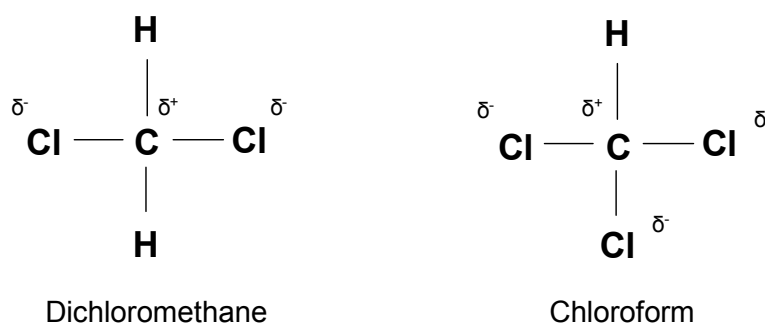


Figure 4.1. The dipole movements of dichloromethane and chloroform. In the case of dichloromethane, the dipole on both sides cancels each other out, while chloroform exhibits weak dipole movement from the third chlorine atom.

For this study, the methods and materials used were identical to that mentioned in Chapter 3 Section 3.3.5 for Device 2, with the exception that the dichloromethane which was used was replaced with chloroform. The resultant implant which was formed had a mass of 3.1835 ± 0.2436 g and did indeed show less signs of separation between the individual chemicals used. In order to test the drug release profile of the implant, the implant was immersed in 40mL of PBS and a potential difference of 0.5V was applied for 40 seconds. A sample of 5mL was taken and assessed for presence of drug. The control showed no release of drug even after 20 minutes. The results were tabulated in Table 4.1.

Table 4.1. The results obtained from the drug release assessment of the chloroform-substituted SAPD.

Time	40 seconds	80 seconds	120 seconds	160 seconds	200 seconds
Drug (%)	0.000261 ± 0.000032	0.000766 ± 0.000122	0.001214 ± 0.000256	0.001464 ± 0.000381	0.001507 ± 0.000212

The implant was left in the PBS for another 72 hours and samples were taken in order to assess if there was any leakage of drugs into the PBS in the absence of electric current. Two samples of 5mL were taken and the results shown in Table 4.2.

Table 4.2. The quantity of drugs present in the control sample after been immersed for 72 hours.

	Sample 1	Sample 2
Drug (%)	0.002576±0.000342	0.002489±0.000132

The results shown in Table 4.2 have indicated that drug leakage was still a problem, even in the chloroform-substituted SAPD. One possible alternative was to employ different drug, which might yield different drug release profile and behaviour.

4.3.2. The employment of diclofenac sodium as a model drug in the Stimuli-Actuated Polymeric Device

A SAPD which was identical to the one synthesized in Chapter 4 Section 4.3.1 was made except the indomethacin was substituted with diclofenac sodium. Diclofenac alone is only slightly soluble in water, while its sodium salt is readily soluble in water and therefore the sodium salt was preferred. By dissolving diclofenac sodium in water and adding it into the SAPD, it ensured homogenous dispersion of the drug. The preparation and the drug release profile were done identically as mentioned in Chapter 3 Section 3.3.10. The drug assessment result of this implant was shown as per Table 4.3.

Table 4.3. The drug release profile of the diclofenac-substituted implant after several time intervals.

Time	40 seconds	80 seconds	120 seconds	160 seconds	200 seconds
Drug (%)	0.000492 ±0.0000352	0.000673 ±0.0000532	0.000711 0.0000843	0.000847 ±0.000121	0.000794 ±0.000084

Firstly, the implant was assessed for any drug release in the absence of electric current. However, samples were taken every 5 minutes in order to determine the time when the drug leakage occurs, if any. The control implant was placed in 40mL PBS and 5mL samples were taken at 5 minutes interval to assess for any presence of drug. The results are tabulated in Table 4.4.

Table 4.4. The release of diclofenac sodium in the absence of the electrical current.

Control	5 minutes	10 minutes	15 minutes	20 minutes	25 minutes
Drug (%)	0	0.000873 ±0.000101	0.000294 ±0.000021	0.000361 ±0.000043	0.000384 ±0.0000418

This result has indicated that the drug leakage of the diclofenac-substituted system still occurred after 5-10 minutes. This indicated a problem which was not likely to be solved with substitution of drug since the molecular size of diclofenac sodium was relatively similar to other NSAID's such as indomethacin or ibuprofen. Therefore, another way in which to obtain controlled drug release from the SAPD would be to manipulate the hydrogel. One way to achieve this was to increase the degree of crosslinking, which would decrease the absorption of the hydrogel while increasing its structural integrity. This meant that the drug was more likely to be entrapped within the hydrogel which would in turn reduce or remove any possible drug leakage in the absence of an electrical stimulation.

The ensuing Sections focused on the possibility of using new materials for the synthesis of the SAPD in an attempt to resolve the drug leakage experienced.

4.4. The investigation of prospective materials which could be used as an electroactive polymer-incorporated hydrogel for the purpose of an electrically-controlled drug release system.

4.4.1. Incorporation of polysodium styrene sulfonate as a polyelectrolyte hydrogel for the purpose of controlled delivery of diclofenac sodium

In order to resolve the problem of drug leakage, polysodium styrene sulfonate (PSS) was chosen, due to its ability to dissociate completely in water which allows conduction of electrical current. In order to test the use of PSS as an electroactive hydrogel, 3 devices were synthesized, the first device with only PSS in order to test the efficacy of the electroactive hydrogel when PSS alone was used. The second and third had PANi and PPy respectively incorporated into the hydrogel as an EAP in order to enhance the electro-conductivity, which allowed us to compare the drug release profile with that of a PSS hydrogel. The PSS system was incorporated as indicated in Table 4.5.

Table 4.5. The compositions of the modified Devices 5-7.

Device	Constituents
Device 5	PSS (1g) Diclofenac sodium (500mg) Glycerine (5mL) PSS (1g)
Device 6	PANi (100mg) Diclofenac sodium (500mg) Glycerine (5mL)
Device 7	PSS (1g) PPy (100mg) Diclofenac sodium (500mg) Glycerine (5mL)

The implant was formulated by dissolving the PSS in 50mL of distilled water, followed by the diclofenac sodium and glycerine. Once all the components were dissolved, PANi and PPy were added into PSS Device 6 and PSS Device 7 respectively. These mixtures were homogenized for two minutes and left to stand for 72 hours until the water was evaporated from the system.

These devices were unsuitable as an implantable device due to their water solubility when they were submerged in the water. Since PVA exhibited insolubility in water at room temperature once it dries out from a solution it was decided to incorporate the PSS with PVA to prevent the dissolution of the PSS device in the water. This was done by adding 1g of dissolved PVA into each of the three devices as a last step during the synthesis. The solution was left to dry and the resultant hydrogel would again be tested. The results have indicated that the addition of PVA did not resolve the problem. This may be attributed to the lack of crosslinking between the PSS and PVA, or any of the components of the hydrogel. In addition, PSS itself exhibited plasticizing effects, which further lowered the structural integrity of the PVA. Therefore, the use of a PVA-PSS hydrogel system was inefficient and alternative materials should be investigated.

4.4.2. The use of methylcellulose as the hydrogel component of the Stimuli-Actuated Polymeric Device

One of the possible solutions to prevent drug leakage from the implant was to use different materials as a hydrogel. For this part of the study, methylcellulose was selected as a hydrogel into which an inter-penetrating network of PANi would be synthesized. Methylcellulose was selected to form the basis of the hydrogel because it has relatively low

cost, non-digestible, biocompatible and hypoallergenic. The chemical structure of methylcellulose resembles a polymer consisting of glucose molecules linked together and is shown in Figure 4.2. When placed in solvents, the hydroxyl group loses a hydrogen atom, which results in an O⁻ group and allows further chemical reactions. The CH₃ group does not offer any possible interactions and is therefore not part of the crosslinking process.

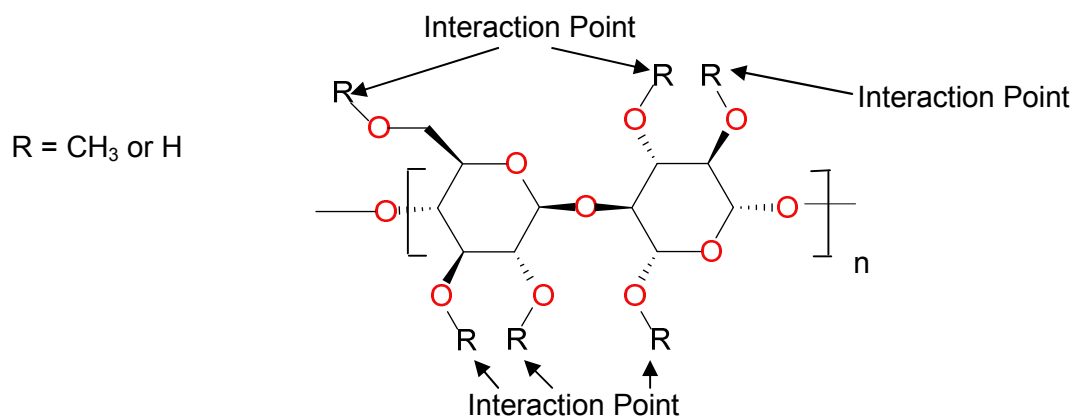


Figure 4.2. Chemical structure of methylcellulose. When dissolved in solvents, the OH group loses the hydrogen and allows chemical interactions.

In order for the methylcellulose to form a hydrogel, it has to be initially dissolved in a solvent followed by drying. The reason for this is that methylcellulose may undergo crosslinking when dissolved in certain solvents. Once the solvent evaporated from the system, the methylcellulose remains crosslinked. The aim was to form a three dimensional structure which allowed hydration while still remaining intact when placed in water or PBS. Various solvents were investigated in this study and the dissolved methylcellulose was allowed to dry for 48 hours in order to ensure total evaporation of the solvent. For this study, Methylcellulose with a mass of 2g was weighed out and dissolved in 30mL of various solvents. It was homogenized for one minute and left to stand under the fume hood in order to allow solvent evaporation. The solvents used and the hydrogels formed may be summarized as Table 4.6.

Table 4.6. The reactions of various materials with methylcellulose.

Reagents	Results
Acetone	No crosslinking of methylcellulose was observed when methylcellulose was mixed with acetone.
Ethyl acetate	No crosslinking of methylcellulose was observed when methylcellulose was mixed with ethyl acetate.
Hexane	No crosslinking of methylcellulose was observed when methylcellulose was mixed with hexane.
Propylene glycol	Methylcellulose was slightly soluble in propylene glycol. When the solvent was left to evaporate from the mixture, the resulted product was one which exhibited a greasy texture. This also indicated a lack of crosslinking between the methylcellulose and made it unsuitable for a hydrogel.
Liquid paraffin	There was minimal dissolution of methylcellulose in liquid paraffin. When this mixture was left to dry, a slurry mixture was obtained which was unsuitable for hydrogel formation.
Chloroform	Chloroform had successfully crosslinked with the methylcellulose mixture and when left to dry. It formed a hydrogel capable of hydration. However, the structural integrity also broke down in water and did not remain intact
Formic acid	Formic acid had successfully crosslinked with the methylcellulose. When left to dry, the resulting product was a thin, hard film of transparent methylcellulose. When this film layer was placed in PBS, degradation had started to occur after 72 hours.
Sodium hydroxide	A transparent hydrogel was formed when the compound was left to dry. When the hydrogel was left in water, swelling had occurred after 30 minutes, followed by degradation of the hydrogel, thus rendering it unsuitable for drug delivery.
Propionaldehyde	No chemical reaction was observed with this mixture and the result of this chemical combination was same as that of acetone combination.
Pyridine	Crosslinking of methylcellulose had occurred when pyridine was used as solvent and a hydrogel was obtained. Similar to the hydrogel obtained from sodium hydroxide, this hydrogel broke down under prolonged submersion in water
Formaldehyde	Crosslinking occurred rapidly when methylcellulose was mixed with

	formaldehyde. When left to dry, the resulting hydrogel had a white gelatinous texture and was resistant to water degradation when immersed for 4 hours. Peripheral degradation of the hydrogel occurred after 24 hours of immersion, which also rendered this combination unsuitable as subcutaneous implant.
Benzaldehyde	No chemical reaction was observed and resulted in a white flaky powder forming with a distinct almond smell.

After a series of tests conducted on methylcellulose as a component for the hydrogel, it was apparent that the reversible breakage of the crosslinked bonds rendered it unsuitable for the purpose of an implantable hydrogel. This reversible breakage of crosslinked bonds may be attributed to the high affinity of methylcellulose for any polar solvents. Crosslinking methylcellulose with various solvents was not capable of overcoming such affinity and crosslinked bonds broke down rapidly after the immersion of the hydrogel into a polar solvent. The concept of using methylcellulose was not feasible, as a sustained breakdown of this hydrogel would result in sustained release of indomethacin rather than a controlled release system. Alternative materials have to be investigated for the formation of an irreversible-crosslinked hydrogel.

4.5. Assessment of prospective crosslinkers and solvents for the synthesis of the Stimuli-Actuated Polymeric Device

4.5.1. Assessment of crosslinking behaviour between various grades of Eudragit® and polyethylene glycol 4000

In an attempt to resolve the drug leakage experienced from the SAPD, three possible solutions were deployed into the implantable system. One was to increase the degree of crosslinking within the hydrogel system, which would result in a hydrogel system with increased mechanical property, but also higher drug entrapment and therefore decreased drug leakage. The second option was to employ a different hydrogel. Different hydrogel offers different physicomachanical properties and therefore different drug release profile with the possibilities of holding more drugs. The third option was to use a different model drug, since different drugs exhibits different pKa, solubility and various chemical and physical properties. However, a study done on various drugs has indicated that substitution of different drugs in the system does not effectively prevent the leakage of the drug. Therefore, the first two options were still the ideal methods for drug entrapment. Methylcellulose did not

provide sufficient crosslinking in order to withhold the drug. Alternative materials and methods should be investigated.

This part of the test involved using different Eudragits[®] crosslinked with polyethylene glycol (PEG) in order to assess its crosslinking behaviour. PEG was selected as the crosslinker due to the two hydroxyl groups at the end of its chain which may be used to link the Eudragits[®]. Four different grades of Eudragit[®] were used, namely Eudragit[®] L100, Eudragit[®] S100, Eudragit[®] L100-55 and Eudragit[®] E100 in order to determine which grades exhibited the best crosslinking properties. All four of the Eudragit[®] has a functional group as to allow interactions with PEG. PEG with a high molecular weight should be used due to its intermediate hydrophobic property which would reduce the re-dissolution of the crosslinked hydrogel into any polar solvent and thus preventing any possible degradation of the hydrogel. The method of synthesis is depicted as follows: each of the above mentioned Eudragit[®] was weighed out into 2g and dissolved in 20mL of acetone. Similarly, 2g of PEG 4000 was dissolved in 20mL of water. The dissolved Eudragit[®] solution was added to the PEG 4000 solution while being stirred. The results were presented as Table 4.7.

Table 4.7. The reactions of various grades of Eudragit[®]

Grades of Eudragit[®]	Results
L100	A crosslinked hydrogel was formed which exhibited degradation in the presence of PBS.
S100	A slurry sticky solution was formed, which crosslinked instantly when PEG 4000 solution was added. When the resultant crosslinked product was left to dry, a brittle white mass was formed without any swelling or de-swelling properties, which made it unsuitable as a hydrogel.
L100-55	The product formed was a slurry white crosslinked solution when mixed with PEG 4000. The product was left to dry for 48 hours under a fume hood. The result was a soft, white crosslinked network which was capable of water absorption. This was one of the favourable results which indicated that Eudragit [®] L100-55 crosslinked with PEG may be used.
E100	Insoluble in acetone

The swellability of the SAPDs in this study was determined by any increase in size after submersion in the liquid until absorption was saturated.

4.5.2. The use of various solvents for the dissolution of Eudragit® and its effects on crosslinking

After Eudragit® L100-55 was selected as a favourable material for the purpose of crosslinking with PEG 4000, the effects of the solvents used were investigated. The crosslinking method was identical to that which was described in Chapter 4 Section 4.5.1. However, instead of acetone been the solvent of choice for the Eudragit®, it was replaced with methanol, ethanol and isopropyl alcohol. These three solvents were chosen as Eudragit® L100-55 exhibited high solubility in all three of these solvents. The resultant product was compared against each other in order to assess for any difference in texture or quantity. In all three cases, the texture of the product was constant, although the yield varied. By using the method described in Chapter 4 Section 4.5.1, methanol had the highest yield, with the dried product weighing $3.652 \pm 0.349\text{g}$, as compared to ethanol which was $1.745 \pm 0.153\text{g}$ and isopropyl alcohol which only yielded $0.843 \pm 0.122\text{g}$. This yield was also higher compared to acetone, which has a mass of $2.548 \pm 0.217\text{g}$. According to the results obtained from this experiment, the solubility of Eudragit® L100-55 seemed slightly higher in methanol, therefore resulting in a higher yield of crosslinked hydrogel and was the solvent of choice.

4.5.3. Assessment of drug entrapment efficiency of a crosslinked polyethylene glycol 4000/Eudragit® hydrogel system

From the four Eudragit® which was experimented with in Chapter 4 Section 4.5.1, the optimal materials which could be used for crosslinking was Eudragit® L100-55. A crosslinked PEG 4000 and Eudragit® system was made by initially dissolving 2g of PEG 4000 in 20mL water and 2g of Eudragit® dissolved in 20mL methanol in two separate beakers. In addition, 100mg of indomethacin was dissolved in the methanol solution containing the Eudragit®. Crosslinking occurred when the two solutions were mixed with each other whilst being stirred. With the indomethacin dissolved with the Eudragit®, the drug should be entrapped within the hydrogel system as the crosslinking occurs. In this way, drug entrapment was determined by assessing the amount of the drugs in methanol before and after crosslinking has occurred. This was done by collecting 1mL of the sample from the 20mL crosslinking solution followed by sample assessment under UV/visible spectroscopy. The result had indicated an absorbance of 1.8180. The quantity equated to 1.98mg in the 20mL sample. The original amount of indomethacin in the 20mL sample was 100mg, therefore, the drug entrapment efficiency would equate to $100 - 1.983 = 98.017\%$. This method of drug incorporation has proved to be very efficient and may be suitable for the further development of the implant.

4.5.4. The stability of the Eudragit[®] crosslinked system in the presence of water and phosphate buffer solution

Following the study done on the selection of a prospective crosslinker, Eudragit[®] L100-55 has shown the best properties and was selected for this stability study. A crosslinked system was synthesized as per Chapter 4 Section 4.5.1 and immersed in water in order to assess for any leakage of drug from the device. After 24 hours of immersion, the sample was scanned under UV/visible spectroscopy and had exhibited no signs of drug leakage. The device was immersed in PBS and drug leakage was assessed again. Degradation of the SAPD in the PBS was visible with the naked eye as quick as 15 minutes after immersion. The degradation commenced on the periphery and the crosslinked SAPD soon dissolved into the PBS. This may be attributed by the possible pH sensitive nature of certain Eudragit[®] towards alkaline pH. This was substantiated by the fact that drug was detected from the sample under UV/visible spectroscopy analysis. In order to prevent further degradation of the SAPD, Eudragit[®] which is pH-insensitive with a similar structure should be used. For this purpose, Eudragit[®] RS100 was selected as a substitute for the crosslinked hydrogel system.

4.5.5. The employment of Eudragit[®] RS100 for the purpose of crosslinking

Following the series of tests done on the crosslinked system formed by Eudragit[®] L100-55 and PEG 4000, it was essential that a different type of Eudragit[®] would have to be used in order to prevent the degradation of the crosslinked system. In this experiment, Eudragit RS100 was chosen because it is pH-insensitive, as opposed to Eudragit[®] L100, which is sensitive towards alkaline pH. The synthesis of the SAPD was carried out by dissolving 1g of PEG 4000 into 10mL of water and 1g of Eudragit[®] RS100 into 10mL of acetone in two separate beakers. The two solutions were added together and stirred with a glass rod. The result of this test had indicated that the two solutions did not form any crosslinking. This may be attributed to the functional group $-C_4H_9NCl$ found on the Eudragit[®] RS100 as opposed to the methyl group on the Eudragit[®] L100-55. The presence of the $-C_4H_9NCl$ functional group takes up a larger amount of space as compared to the methyl group and prevented the attachment of PEG4000 on this side of the polymer. Compared to the Eudragit[®] RS100, Eudragit[®] L100-55 only has a methyl side chain and allowed crosslinking to occur on both sides of the chain, ensuring a fully interlinked network of crosslinked hydrogel system. For this reason, it was crucial that a new material should be investigated so as to form a crosslinked system with desirable physicommechanical and physicochemical properties. Alternatively, a different class of crosslinkers may be used in the place of PEG 4000 in order to crosslink the Eudragit[®] RS100. The new crosslinker should be smaller in size so as not to be interfered by the $-C_4H_9NCl$ functional group. When Eudragit[®] was dissolved in acetone, it

became negatively charged and therefore reactive towards positively charged ions, allowing crosslinking to occur. The use of simple molecules as opposed to the bulky polymers as a crosslinker may be a better alternative for crosslinking. For this reason, several salts were dissolved in water followed by the mixing with Eudragit® solution in order to assess the crosslinking behaviour of these two chemicals. When a salt is immersed in water, it undergoes dissociation, thus forming both cations and anions. Crosslinking should occur with the cation and the Eudragit® when the two solutions were mixed. Five different salts were chosen for this experiment, which included titanium dioxide, sodium benzoate, sodium chloride, sodium thiosulfate and potassium iodide. All of these salts were relatively small in size when compared to polymers and yielded cations when dissolved. The dissociation of these salts may be depicted in Figure 4.3.

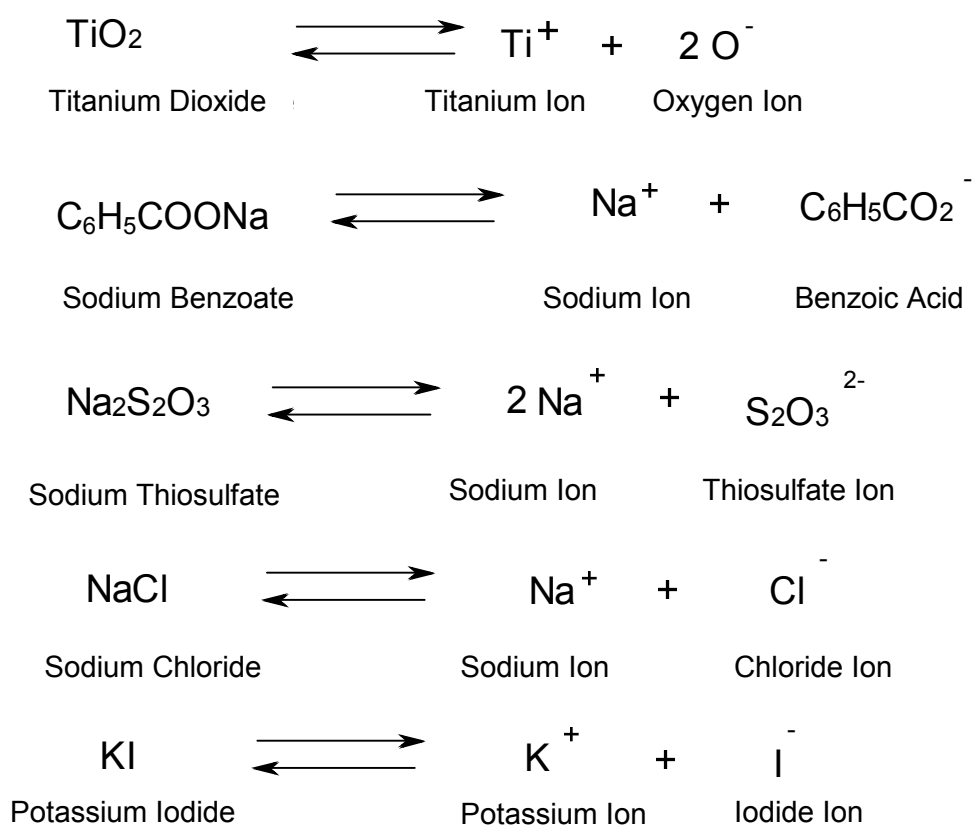


Figure 4.3. The various salts that were used in this experiment and the ions that they dissociate into when dissolved in water.

Eudragit® with a mass of 1g was weighed out and dissolved in 5mL of acetone, while 1g of the respective salts was dissolved in 5mL of water in two separate beakers. The two mixtures were added together and stirred with a glass rod. The resulting crosslinked product was rinsed with distilled water and left to dry overnight. It was assessed for its crosslinking

properties and the one with the highest yields was selected. The results may be summarized as per Table 4.6

Table 4.8. The quantity yielded by crosslinking with Eudragit® and the respective salts.

Crosslinker Salt	Titanium Dioxide	Sodium Benzoate	Sodium Thiosulfate	Sodium Chloride	Potassium Iodide
Weight	1.134g	1.235g	0.932g	1.691g	1.532g

As seen in Table 4.6, the most desirable salt to use for this crosslinking was the sodium chloride, as it produced the greatest yield of hydrogel with elastic properties. All crosslinked system was white in appearance, however, crosslinking with titanium dioxide and sodium benzoate had produced a hard and brittle white solid which deemed it unsuitable for this implant. Potassium iodide had also produced a similar yield as opposed to sodium chloride, but the crosslinked system produced was more brittle when compared to sodium chloride and was not preferred.

4.5.6. Crosslinking of Eudragit® RS100 and sodium chloride with indomethacin as a model drug for drug entrapment and drug release

Following the decision of combining sodium chloride and Eudragit® for the purpose of crosslinking, indomethacin was further incorporated into this system in order to determine its drug entrapment efficiency and drug release profile, both in the absence and presence of electrical current. This was done by dissolving both 1g of Eudragit® and 100mg of indomethacin in 5mL of acetone, while 1g of sodium chloride was dissolved in 5mL of water. The two solutions were mixed together and stirred with a glass rod. The crosslinked system was yellow in appearance, which was attributed to the indomethacin. The crosslinked system was left to dry for 24 hours and immersed in PBS for 12 hours in order to assess for any possible degradation in alkaline PBS. The result indicated that Eudragit® RS100 did not breakdown in an alkaline pH due to its pH-insensitivity. The implantable system was re-immersed in 20mL of PBS and 0.6 V of potential difference was applied for 40 seconds. Samples of 5mL were assessed under UV/visible spectroscopy. The result is presented in Table 4.7.

Table 4.9. The drug release of the SAPD gathered at the specified time intervals.

Time	40 seconds	80 seconds	120 seconds	160 seconds	200 seconds
Drug release (%)	0.000012 ±0.0000025	0.000012 ±0.0000031	0.000012 ±0.0000011	0.000014 ±0.0000012	0.000015 ±0.0000032

This result has indicated that drug was entrapped within the crosslinked SAPD and was not capable of moving outwards even in the presence of electrical current. This could be caused by the excessive crosslinking between the Eudragit® RS100 and the sodium chloride which prevented the drug from escaping the system. One possible solution to resolve this problem was the addition of a plasticizer into this system. A plasticizer improved the flexibility of this system while enhancing drug release and glycerine was chosen as the plasticizer for this part of the study as it has good biocompatibility and is readily available. In order to test this theory, five devices were made, each composed of varying amounts of plasticizer. It was loaded with drug and drug release was assessed. The composition of the three devices is summarized in Table 4.8.

Table 4.10. The composition of the modified Devices 8-12.

Devices	Composition
Device 8	- Eudragit® RS100 (1g) - Sodium Chloride (1g) -Indomethacin (100mg) -Glycerine (3mL)
Device 9	- Eudragit® RS100 (1g) - Sodium Chloride (1g) -Indomethacin (100mg) -Glycerine (5mL)
Device 10	- Eudragit® RS100 (1g) - Sodium Chloride (0.5g) -Indomethacin (100mg) -Glycerine (7mL)
Device 11	- Eudragit® RS100 (1g) - Sodium Chloride (0.5g) -Indomethacin (100mg) -Glycerine (2mL)
Device 12	- Eudragit® RS100 (1g) - Sodium Chloride (0.5g) -Indomethacin (100mg) -Glycerine (1mL)

The devices were made by dissolving the Eudragit® RS100 and indomethacin into 5mL of acetone, while sodium chloride was dissolved in water in two separate beakers. The amount of water used to dissolve the sodium chloride varies from 7mL in Device 10, 5mL in device 9 and 3mL in Device 8. Once the sodium chloride was dissolved, the glycerine was added into the sodium chloride solution and stirred until homogenously blended. The contents of the

two beakers were mixed together and stirred until crosslinking was completed. The crosslinked system was left to dry for 24 hours and placed in 40mL PBS for 12 hours in order to assess for any drug leakage. This was done by gathering 5mL of the PBS samples after 12 hours and scanned with UV/visible spectroscopy for any presence of drugs. As predicted, the texture of the crosslinked SAPD exhibited increased elasticity, but this relaxation of the chemical structure may have led to increased drug release from the crosslinked system. The results obtained from the UV/visible spectroscopy has indicated that drug leakage does occur in all three devices. The results were indicated in Table 4.9.

Table 4.11. The devices with varying amounts of plasticizer and its respective drug leakage.

Devices	Drug release (mg)
Device 8	0.3089
Device 9	0.5389
Device 10	0.7406
Device 11	0.2127
Device 12	0.1228

Plotting the above results into a graph of glycerine versus UV absorbance is an indication of the maximum amount of glycerine which may be used to improve the physicommechanical properties of the crosslinked system without the leakage of the drug into its surrounding. This was depicted in Figure 4.4, along with the Equation of the trend line. The Equation of the trend line may be depicted as Equation 4.2.

$$y=0.1319 x-0.012 \quad \text{Equation 4.2}$$

Therefore, in order to determine the maximum amount of glycerine which may be used as per Equation 4.2, we assume the absorbance, which was the y-value, was 0.

The extrapolated maximum amount of glycerine which may be used is 0.094mL. This approach was impractical because addition of 0.094mL of glycerine into 10mL of crosslinking solution did not yield any significant difference to the drug release profile. A different approach should be considered in terms of the crosslinked system and its drug entrapment.

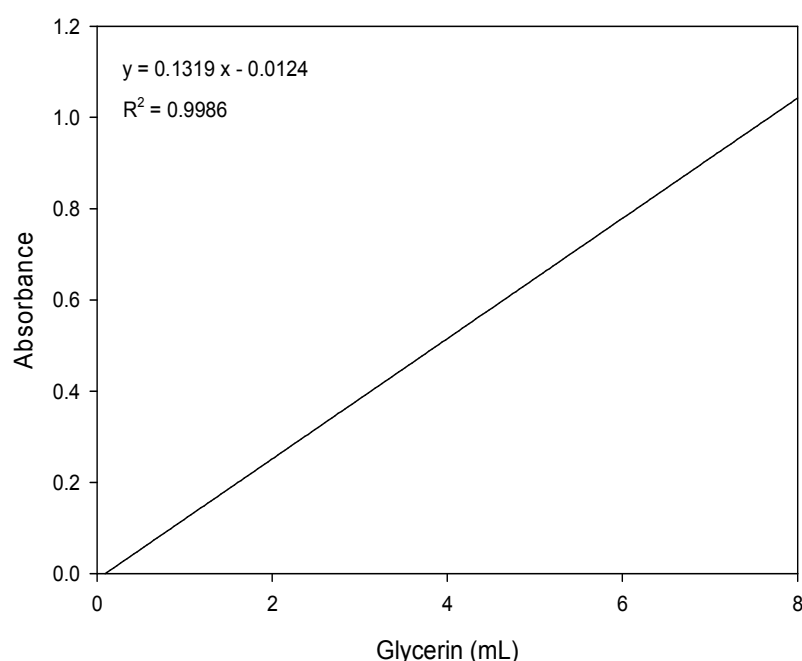


Figure 4.4. The relationship between the amount of glycerine used and the drug leakage from the stimuli-actuated polymeric device.

The use of an alternative plasticizer should be considered. The plasticizer used in the place of glycerine was tri-ethyl citrate, since it is a commonly used plasticizer with a good biocompatibility.

4.5.7. The employment of tri-ethyl citrate as a plasticizer

In this experiment, triethyl citrate (TEC) was used as an alternative substitute for glycerine in order to increase the elasticity of the crosslinked device while preventing the outward movement of the drug from the system to the surrounding fluids. In this study, 1g of Eudragit® RS100 was added into 10mL acetone and 1g of sodium chloride was added into 10mL of water along with 5mL of TEC. The problem with this design was the immiscibility of TEC with water. This may be attributed to the structure of the TEC which is depicted in Figure 4.5.

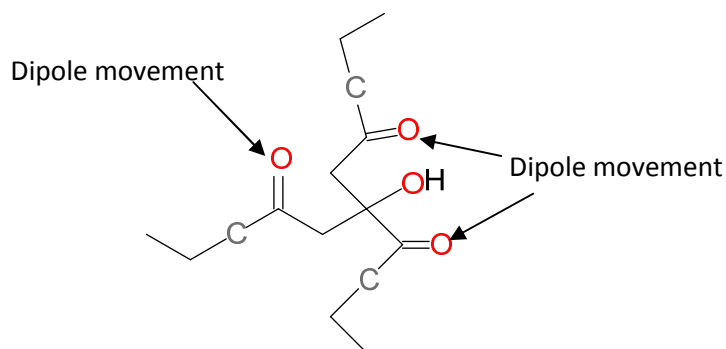


Figure 4.5. The chemical structure of tri-ethyl citrate.

Except for the few oxygen atoms which exhibited a weak dipole movement, the ethyl groups on the citrate structure were composed of hydrocarbons which would make this compound mainly non-polar in nature. Therefore, it exhibited immiscibility with polar solvents such as water. In order to improve the miscibility between water and TEC, 2.5mL Tween[®] 80 and 1.5mL Span[®] 80 was added into the water/TEC mixture. The Hydrophile-Lipophile Balance (HLB) value for this combination of Tween[®] and Span[®] is 10.98, which is appropriate for an oil-in-water emulsion. After the emulsion was formed, the Eudragit[®] RS100/acetone solution was mixed with the emulsion and stirred. The resulting product was left to stand until all solvents were evaporated. The resultant product, however, remained an emulsion which did not solidify. This may be attributed to the fact that TEC, which was organic by nature, was introduced into the system. Since oil is hydrocarbon in nature, it does not facilitate evaporation of the solvents and this system remained an emulsion. An alternative method besides the use of plasticizer should be considered due to the incompatibility of plasticizers with this system.

4.5.8. The employment of alternative materials as a component of the Stimuli-Actuated Polymeric Device

Following the assessment of the plasticizer in a crosslinked system, results have indicated that it was unsuitable due to excessive drug leakage. An alternate method which may be used to increase the elasticity of the crosslinked system was to apply heat. Application of heat to the system may facilitate a break between the bonds of various chemical structures, and therefore a weakening in structural integrity. Heat was applied during the crosslinking process rather than afterwards, because heating of the SAPD after its formation would mainly result in peripheral weakening of the SAPD. PVA was added into the hydrogel in order to act as a plasticizer, as water was absorbed into the PVA allowed it to have elastic properties. In addition, PVA has high tensile strength, flexibility and is biocompatible.

Therefore, the addition of PVA into a crosslinked Eudragit® system should provide adequate structural integrity while preventing excess crosslinking which hinders drug release. For this study, three separate devices were made, each made of different chemical compositions in order to assess any difference in its physicochemical properties after the completion of the device. The first was a standard hydrogel system, while the second had sodium chloride removed in order to determine if there was any interaction between the Eudragit® and the PVA. A device with ZnO₂ as the crosslinker was formulated so that comparison with the sodium chloride-loaded SAPD could be made. The devices were termed Device 13-15 and the materials used are summarized in Table 4.10.

Table 4.12. The composition of Devices 13–15.

	Composition
Device 13	PVA ₁₃₀₀₀ (1g) -Eudragit® RS100 (1g) -Sodium Chloride (1g) -PANi (0.2g) -Indomethacin (100mg)
Device 14	-PVA ₁₃₀₀₀ (2g) - Eudragit® RS100 (1g) -PANi (0.2g) -Indomethacin (100mg)
Device 15	-PVA ₁₃₀₀₀ (2g) -ZnO ₂ (0.5g) - Eudragit® RS100 (1g) -Indomethacin (100mg) -PANi (0.2g)

The devices were made by dissolving the PVA₁₃₀₀₀ in 10mL of water, followed by sodium chloride and the ZnO₂ in the case of Device 13 and Device 15 respectively. The Eudragit® RS100 was dissolved into 10mL of acetone, followed by PANi and indomethacin. The two solutions were added together and stirred with a glass rod. Crosslinking seemed to have occurred slightly as the viscosity thickened. This mixture was placed onto a flame to heat until the majority of the solvents have evaporated. The remaining mixture was left to stand for 48 hours to ensure further evaporation of the solvents.

These three systems were assessed for any drug leakage similar to the test done on Device 8. The result demonstrated these devices exhibited solubility in PBS and rapid degradation was observed when placed in the solvent. For further analysis, Device 13 was placed in several solvents to further determine its stability in various solvents and it has indeed

demonstrated solubility in solvents such as chloroform, aniline, ethanol, acetone, sulphuric acid, ethyl acetate, hydrochloric acid and acetic acid. This may be due to the high solubility of PVA₁₃₀₀₀ in polar solvents while Eudragit[®] is soluble in most organic solvents. Therefore, using PVA₁₃₀₀₀ and Eudragit[®] as the main body of the system may be the cause of this degradation, despite the fact the crosslinking of Eudragit[®] RS100 and its respective salts did occur. In fact, degradation also occurred in Device 14 and Device 15, which supported this assumption. In order to decrease this degradation, PVA₁₃₀₀₀ should be replaced with a less soluble polymer, which should be used to form the main frame of this crosslinked system.

4.5.9. The employment of high molecular weight polyvinyl alcohol in a crosslinked system

In order to prevent the degradation observed in the crosslinked PVA₁₃₀₀₀/Eudragit[®] RS100 system, PVAs with a higher molecular weight were chosen as a substitute as opposed to PVA with a lower molecular weights. High molecular weight PVA exhibits less water solubility and better crosslinking properties as opposed to the low molecular weight PVA. As part of this study, PVA with two different molecular weights were chosen, namely PVA₄₉₀₀₀ and PVA₈₈₀₀₀.

Since Eudragit[®] RS100 crosslinked with sodium chloride and not with the PVA, it was decided that Eudragit[®] RS100 and sodium chloride should be replaced with alternative chemicals which were capable of crosslinking with PVA. The aim was to replace the Eudragit[®] RS100 with PVA as the main body of the hydrogel. Since hydrogel is a three-dimensional crosslinked system, it would be prudent that the PVA itself be crosslinked instead of the Eudragit[®] RS100.

When PVA was dissolved in water, it presumably lost a hydrogen atom, which created a possible group for chemical reaction. This may create possible crosslinking between two PVA chains. This may be illustrated by Figure 4.6.

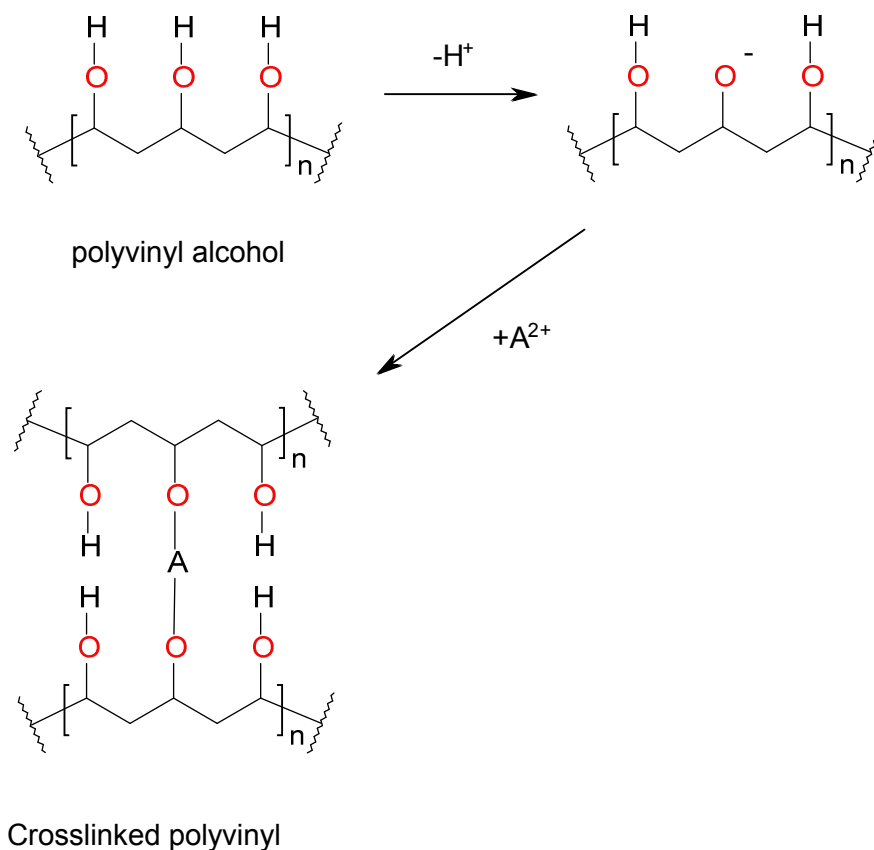


Figure 4.6. The crosslinking mechanism of polyvinyl alcohol which may be used for the synthesis of a polyvinyl alcohol crosslinked system. Here, the polyvinyl alcohol chains are crosslinked by a divalent compound A.

From the crosslinking mechanism seen in Figure 4.6, it was clear why a PVA with a longer chain would exhibit better crosslinking. It was for that reason a high molecular weight PVA was preferred over a low molecular PVA.

The two types of PVA used in this study were PVA₄₉₀₀₀ and PVA₈₈₀₀₀. Both have substantially higher molecular weight than the PVA₁₃₀₀₀ used. In order to assess the crosslinking behaviour of these two PVAs, 1g of the respective PVA were dissolved in 10mL of water. A crosslinker was dissolved in a solvent contained in a separate beaker. The two solutions were mixed together and stirred with a glass rod in order to facilitate the crosslinking. For this study, diethyl acetamidomalate (DAA) was chosen as a crosslinker, as it also demonstrates good biocompatibility. DAA with a mass of 2g was dissolved in 10mL of acetone. This was then mixed with the PVA solution. Crosslinking occurred spontaneously. This mechanism is similar to the one described in Figure 4.5 and is demonstrated in Figure 4.7. The crosslinked compound was then left to dry for 24 hours.

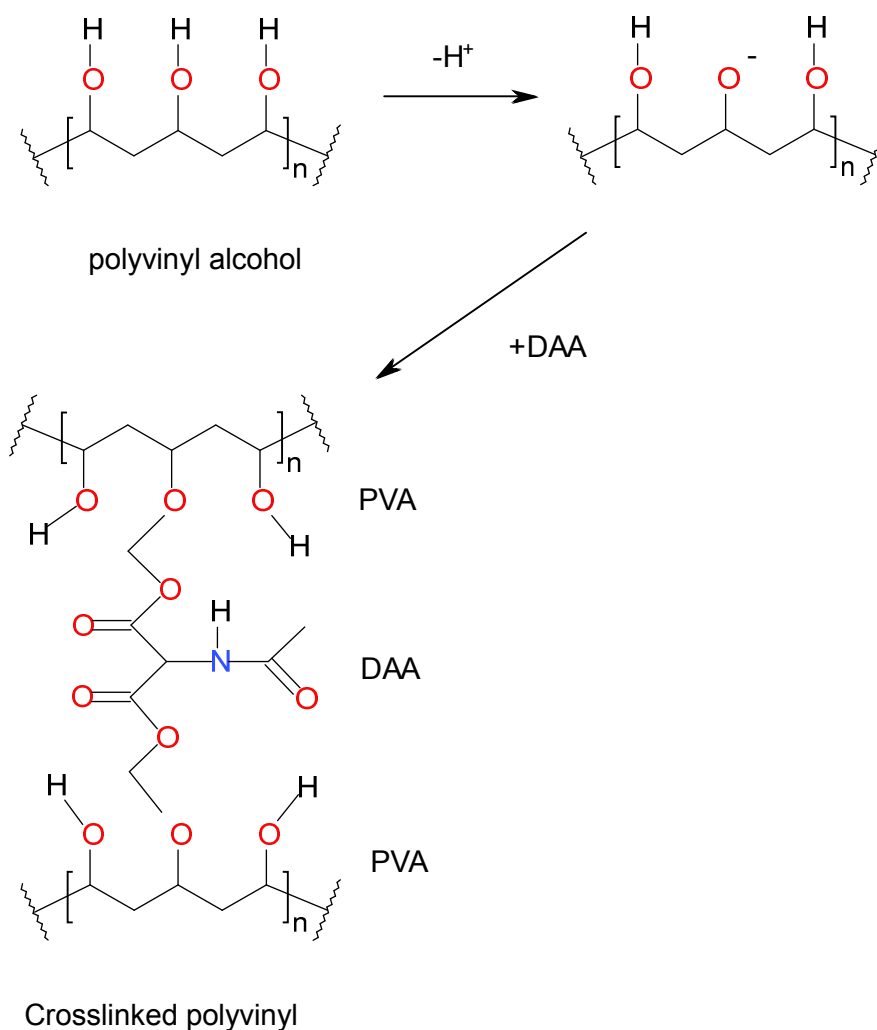


Figure 4.7. The crosslinking mechanism between polyvinyl alcohol and diethyl acetamidomalate.

The device formed with PVA₄₉₀₀₀ demonstrated slight degradation when placed in water under 24 hours. However, the device formed with PVA₈₈₀₀₀ demonstrated no degradation when placed under both water and PBS.

4.5.10. The employment of polyvinyl alcohol₈₈₀₀₀ and diethyl acetamidomalate in a crosslinked system and assessment of its drug release profile

Following the tests done on the higher molecular weight PVA, PVA₈₈₀₀₀, demonstrated the most favourable characteristic without any degradation when crosslinked with DAA. The next step was to incorporate a drug into the system which was capable of controlled release via an 'ON-OFF' mechanism. The drugs used included indomethacin, ibuprofen, diclofenac sodium and aspirin. Each of these drugs was dissolved in an appropriate solvent followed by

incorporation of these drug solutions into the crosslinked system. The drugs and its appropriate solvents may be described as follows:

- Indomethacin (100mg) – acetone (5mL)
- Ibuprofen (100mg) – acetone (5mL)
- Diclofenac sodium (100mg) – water (5mL)
- Aspirin (300mg) – acetone (5mL)

A quantity of 100mg was incorporated into each device as it was hoped that the device would release a controlled dose of a fraction of a milligram. This would ensure a prolonged release cycle could be achieved over a time period of 1-2 months. Aspirin dosage was increased as its potency is much lower when compared to drugs such as ibuprofen (Hersh, 2000). The crosslinked system was achieved by dissolving 0.5g of PVA₈₈₀₀₀ into 10mL of water while 2g of DAA was dissolved in 10mL of acetone in a separate beaker. The drug solutions were added into the acetone/DAA solution and stirred until homogenous. Lastly, the DAA/drug solution was poured into the PVA solution and stirred until crosslinking was completed. This crosslinked system was left to dry for 24 hours and a total of five devices were made, each identical in composition except for the model drugs. These devices were named as follow for the purpose of identification:

- Indomethacin-loaded Device – Device 16
- Ibuprofen-loaded Device – Device 17
- Diclofenac sodium-loaded Device – Device 18
- Aspirin-loaded Device – Device 19

One crucial assessment of these systems before any other assessments could be made would be its capability of withholding the drugs when placed in PBS without and activation from the stimulus. This was done by immersing the device into 30mL of the PBS for 24 hours. Samples of 1mL were then taken from the PBS and assessed for any presence of drug. The results are shown as in Table 4.11.

Table 4.13. The percentage of drugs which was present in the 30mL PBS sample. Device 14 and 16 has indicated drug leakage and unsuitable for SAPD.

Device	Drug present
16	0.00853±0.00143%
17	0.000%
18	0.00340±0.000412%
19	0.000%

The results obtained have indicated the two devices which were suitable for further study were Device 17 and Device 19. These two devices were capable of withholding the drugs when placed in PBS. However, it should be noted that the result was obtained from the

hydrogel without an EAP. With the addition of an EAP, the formation of an IPN could alter the characters of the drug release profile as compared to the plain hydrogel. Further analysis with EAP-incorporated hydrogel should be made in order to assess any differences in the drug release behaviour. These tests would be carried out further after Device 17 and 19 were assessed for its drug release profile.

4.5.11. Further assessment of drug release profile of the aspirin-loaded device and the ibuprofen-loaded device

As discussed in Chapter 4 Section 4.5.10, the ibuprofen-loaded device (Device 17) and aspirin-loaded device (Device 19) were further subjected to electric current under PBS in order to assess for any release in these drugs. This was done by placing the respective devices into 40mL of PBS and actuated by a potential difference of 1.2V and a current of 0.3A. The equipment used was a PGSTAT 302N potentiostat/galvanostat (Autolab, Utrecht, Netherlands) with platinum as the working electrode and gold as the counter electrode. The setup of the experiment may be depicted in Figure 4.8.

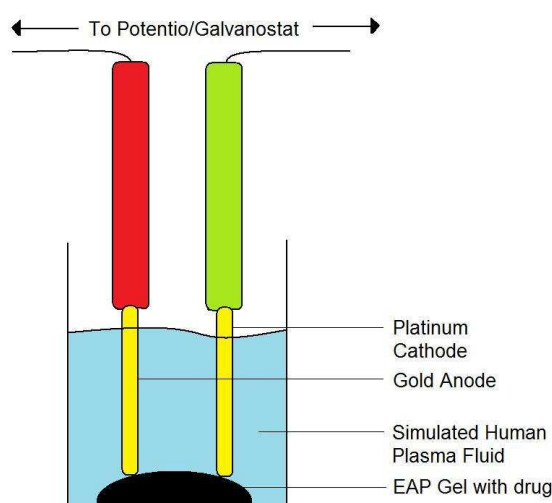


Figure 4.8. The setup which was used to determine drug release of the device under electric current.

Electric current was passed through the device for duration of 45 seconds before 1mL samples were taken. This was repeated three times, after which the sample was scanned via UV/visible spectroscopy for any presence in drug. The results obtained may be presented in Table 4.12.

Table 4.14. The results obtained from drug release (%) of the two Devices.

Device	45 seconds	90 seconds	135 seconds
Device 17	0.001889±0.0003%	0.002180±0.00021%	0.002446±0.00031%
Device 19	0.000%	0.000%	0.000%

The results in Table 4.12 have indicated that Device 19 did not respond to electric current, while Device 1 resulted in a drug release under electric current. Further assessment of Device 17 should be performed in order to evaluate its potential uses for an electrically activated crosslinked system.

4.5.12. Determination of a crosslinker ratio and its effect on the device

In order to establish the drug release profile of the system, further analysis of Device 15 was performed in order to evaluate its potential as a stimulus activated system. For this part of the experiment, three derivatives of Device 17 were made, each with varying amounts of DAA. All the devices were made identically to that of Device 15, except for the DAA used were 2g, 1g and 500mg. These devices were termed Device 20, Device 21 and Device 22 respectively. Each of these devices was exposed to electric current in order to assess its drug release profile. The results are summarized in Table 4.13.

Table 4.15. The quantity of drugs released by the system converted to percentage

Device	45 seconds	90 seconds	135 seconds	180 seconds
20	0.00170±0.0002%	0.00242±0.0003%	0.00823±0.0005%	0.02543±0.003%
21	0.02300±0.003%	0.02761±0.004%	0.04602±0.003%	0.05207±0.004%
22	0.00436±0.0003%	0.00484±0.0005%	0.00536±0.0004%	0.01259±0.002%

In order to achieve a therapeutic dose for ibuprofen, a minimum of 1.2mg must be present at the local site and the only device capable of achieving such dose was Device 21. The result has indicated that a crosslinker in the ratio of 1:1 DAA:PVA₈₈₀₀₀ would be preferred as opposed to other combination and was worth further evaluation. The optimum amount of each component to be used would be determined by the use of a Box-Behnken Design once appropriate variables were selected.

4.5.13. Addition of polyaniline as an electroactive polymer for the purpose of drug release enhancement from the crosslinked system

In order to enhance drug release from the crosslinked system, PANi as an EAP was blended into the crosslinked system in order to evaluate whether there was indeed an increase in drug release. For this study, Device 15 was made, with the addition of PANi which was

added into the acetone solution prior to the crosslinking. Five different devices were made, each with 10%, 5%, 2%, 1% and 0.5% of PANi incorporated into them. These devices were left to dry for 24 hours and immersed in distilled water for another 24 hours in order to rinse out any unreacted chemicals in the crosslinked system. The devices were assessed for its physical properties in order to determine its suitability to be used as a subcutaneous implant. It was discovered that the incorporation of PANi into the crosslinked system tends to decrease the integrity of the crosslinked system. The results have indicated that the higher the PANi that was incorporated, the lower the structural integrity. Crosslinked systems with 10% and 5% PANi were too weak and have exhibited deterioration when handled, therefore rendered it unsuitable for the purpose of a subcutaneous implant. Crosslinked systems with 2%, 1% and 0.5% PANi have shown good physical properties and could be handled without difficulty. For further study, the crosslinked device with the highest amount of PANi (i.e. 2%) and stability should be selected. During the formation of the crosslinked system, PANi was added in acetone and crosslinking were allowed to occur. PANi was only slightly soluble in acetone and much of it was unreacted. It could be possible that PANi may have been trapped between the 3-dimensional crosslinked networks of the crosslinked hydrogel system during its synthesis. The presence of the unreacted PANi between the crosslinked networks may have decreased the degree of crosslinking and a decrease in the structural integrity of the system as a whole.

With the presence of PANi now incorporated throughout the entire crosslinked hydrogel system, the drug release should be assessed in order to determine whether the use of PANi in this system would be beneficial. For the next study, drug-loaded SAPD would be assessed for its drug release behaviour. Aspirin-loaded device was excluded this study due to its lack of response towards electrical stimulation as observed in Chapter 4 Section 4.5.11.

4.5.14 Assessment of ibuprofen release from the Stimuli-Actuated Polymeric Device in the presence and absence of an electric current

Following the synthesis of an ibuprofen-loaded SAPD, the system was rinsed with distilled water three times, after which it was then immersed for a period of 12 hours in order to ensure complete removal of any unreacted chemical reagents or untrapped drugs. The SAPD was left to dry followed by immersion in the 50mL of PBS for 12 hours, after which 1mL sample was extracted and tested for any presence of drug. The UV absorbance of the 1mL sample has indicated that no leakage of drug had occurred in the absence of an electric current.

The next step was to assess the electroactivity of the SAPD when the system was in the presence of an electric current. For this part of the study, SAPD was placed in 20mL of PBS and PGSTAT was used with the same setup as in Figure 4.7. A potential difference of 1.2V was applied and 1mL samples were taken at a 45 second interval. After the 1mL sample was taken from the 20mL PBS, the stock solution was discarded and a fresh PBS was used for the next interval. A total of 6 samples were taken and assessed. The results may be summarized as per Table 4.15.

Table 4.16. The quantity of ibuprofen present in the samples extracted during the drug release assessment.

1 mL sampl e	45 seconds	90 seconds	135 seconds	180 seconds	225 seconds	270 seconds
Drug (%)	0.049±0.00 1	0.0446±0.0 02	0.045±0.00 3	0.0448±0.0 03	0.0454±0.0 02	0.0512±0.0 01

As seen from the results in Table 4.15, a therapeutic dose of ibuprofen was released into the PBS in the presence of an electric current. The extent of these release cycles would have to be analyzed in further studies.

Following the actuation of the SAPD, the crosslinked system may have experienced irreversible structural changes. These changes may affect future behaviour of the SAPD and therefore it was important that drug leakage test should be repeated again after the SAPD has been exposed to electric current. The SAPD was immersed in 10mL of PBS for 24 hours and a 1mL sample was assessed for any presence of ibuprofen. Contrary to the first result, drug was present in this sample, which indicated a possible change in structure of the SAPD or a change of ibuprofen characteristics after the application of electrical stimulation. The UV absorbance obtained from the sample was 0.0142, which equated to 0.226mg in the 1mL sample. The total amount of drug which leaked from the system was 2.26mg. If the ibuprofen-loaded SAPD was to be used, it would have to be further modified in order to ensure the proper functioning of the device.

4.5.15 Assessment of diclofenac sodium release from the Stimuli-Actuated Polymeric Device in the presence and absence of an electric current

The next study was performed on the diclofenac sodium-loaded SAPD. The first assessment was the test for any leakage of drugs in the absence of an electric current. The system was left in 50mL of PBS for 12 hours and the method used was identical to the one used in Chapter 4 Section 4.5.14. A sample of 1mL was taken and assessed under UV/visible

spectroscopy. The UV absorbance indicated a reading of 0.0800. Conversion of this reading to the quantity of drug equated to 0.59mg of diclofenac sodium which was in the 50mL sample. This indicated a leakage of a therapeutic dose of diclofenac sodium from the SAPD. The test was repeated twice more in order to confirm the leakage of diclofenac sodium and the UV reading indicated a presence of 1.87mg and 1.54mg of diclofenac sodium in the second and third test respectively. These results have confirmed that diclofenac sodium does continuously leak from the PANi-system and was unsuitable for an electro-active drug delivery approach.

This finding was contradictory to the first result obtained when diclofenac sodium was entrapped in the hydrogel without PANi. This leakage may have occurred due to the decreased crosslinking when PANi was incorporated into the hydrogel. This decrease of crosslinking may be the cause of drug leakage from the SAPD. For further development of the diclofenac sodium-loaded SAPD, a decreased amount of PANi should be used or an alternative method to increase the crosslinking should be investigated.

4.5.16 Assessment of indomethacin release from the Stimuli-Actuated Polymeric Device in the presence and absence of an electric current

The last system to be tested was the indomethacin-loaded SAPD. The indomethacin-loaded SAPD was initially left in 50mL PBS for 12 hours and 1mL sample was taken in order to assess for any drug. The results obtained from the UV/visible spectroscopy has indicated no drug leakage in the sample. This was followed by a drug-release profile of indomethacin-loaded SAPD in the presence of an electric current. The test method was done identically to Chapter 4 Section 4.5.14. and the results can be summarized in Table 4.16.

Table 4.17. Indomethacin released from the SAPD when exposed to electric current.

	45 seconds	90 seconds	135seconds	180 seconds	225 seconds
Drugs (%)	0.1200±0.02	0.1778±0.03	0.1022±0.01	0.1061±0.02	0.1108±0.01

The results indicated by Table 4.16 have shown that drug release was achieved when the SAPD was placed under electric current. As mentioned in Chapter 4 Section 4.5.14, it was important that the SAPD was assessed afterwards in order to ensure irreversible structural changes did not affect the SAPD once it was exposed to electric current. The system was left in 50mL of PBS again for 12 hours, and 1mL sample was taken and assessed for any presence of the drug. The results obtained from the UV/visible spectroscopy has indicated that no drug leakage was detected. This suggested that an indomethacin-loaded SAPD may possibly be used for the purpose of an electroactive drug delivery system.

The SAPD was assessed for further drug release consistency and capacity. The SAPD was immersed in PBS followed by actuation as mentioned in Section 4.5.14. This time, 35 samples were extracted and assessed by UV/visible spectroscopy for the quantity of drug released. The results were shown in Figure 4.9.

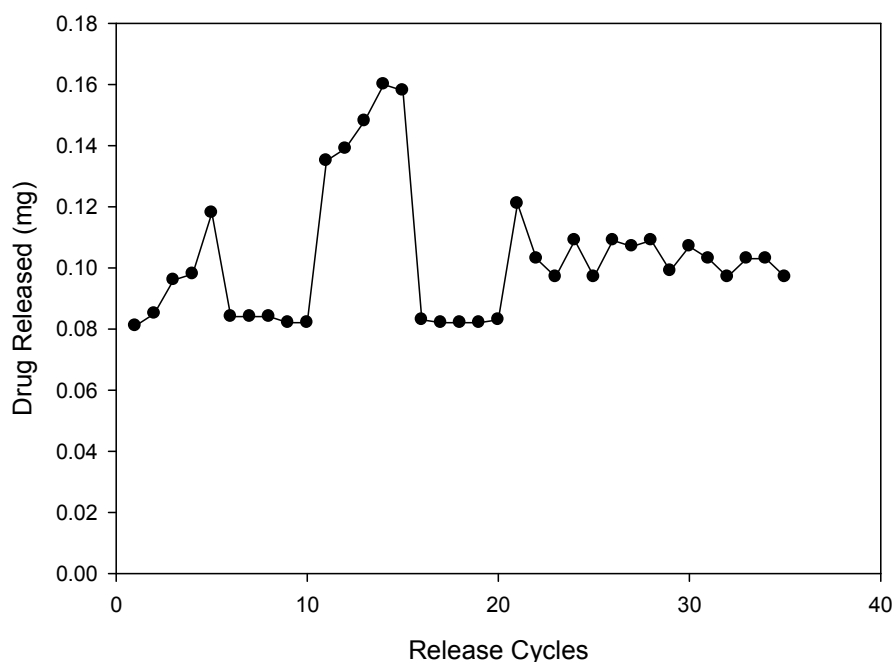


Figure 4.9. The amount of drug release from 35 release cycles.

As indicated by Table 4.17, the drug release ranged from 0.081mg to 0.160mg. The SAPD was assessed one last time for any leakage of drugs and was immersed in 50mL of PBS for 12 hours. A sample of 1mL was taken and the UV absorbance has indicated that there was no leakage of indomethacin when the SAPD was left immersed in the absence of electricity.

One challenge with an electroactive device such as this was that its response may slowly decrease with time. As one may see from Table 3.14, there was a slight difference in drug release from the first ten samples as compared to the last ten samples. This was probably due to the slightly lagged response from the SAPD when it was left immersed and unused in PBS. Such a phenomenon was possibly due to the ion exchange between the SAPD and the surrounding medium, which tends to diminish the electrochemical control of the drug release (Lira, 2005). The last step in this study was to determine how much of the drug could be released before the device was totally depleted of the drug. The SAPD was continuously actuated and samples were assessed for the drug until the drug release cycles ceased. The results are indicated in Table 4.18

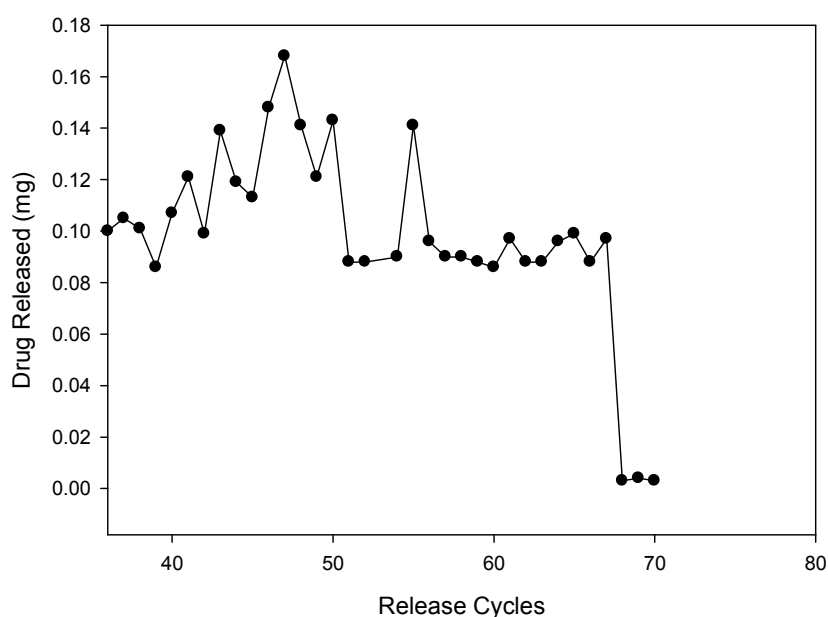


Figure 4.10. The drug release from release cycles 36-70

The results obtained have indicated the SAPD was capable of 67 release cycles. In this study, diclofenac sodium, ibuprofen and indomethacin were used and results have indicated that indomethacin was the only suitable drug for this implantable system, as no leakage has occurred when electric current was not applied to the SAPD. One possible explanation for this phenomenon could be the larger molecular size of indomethacin as compared to diclofenac sodium and ibuprofen. This larger molecular size meant that indomethacin were more likely to be entrapped within the three dimensional network of the hydrogel system. Although most diclofenac sodium and ibuprofen were well entrapped in the center of the hydrogel, drug leakage may still occur on the surface. As the drug was entrapped in the hydrogel system, it was possible to suggest a release mechanism of passive diffusion from the SAPD during actuation.

4.6. The synthesis of the Stimuli-Actuated Polymeric Device for the assessment of drug entrapment efficiency

Following the study done on the SAPD, three different types of drugs were incorporated and assessed for their drug release behaviours and physical properties. Although some of the drugs tested previously showed no signs of activity, it was decided to repeat the test again with the addition of PANi, in order to compare the results obtained with the addition of PANi as opposed to a plain hydrogel. The three drugs used were namely ibuprofen, indomethacin and diclofenac sodium. Following the formulation of the drug-loaded SAPD, it was assessed

for its drug release in the presence of an electric current. For this study, 100mg of the drug was dissolved into 10mL of acetone, along with 500mg of DAA and 20mg of PANi. 500mg of PVA was dissolved in 10mL of water in a separate beaker. The only exception was the diclofenac sodium, which was added into the 10mL PVA solution since diclofenac sodium was soluble in water and not acetone. The two solutions were added together and stirred with a glass rod until the crosslinking was completed. The hydrogel system was left to dry and the crosslinking solution was assessed under UV/visible spectroscopy for the amount of drug remaining. This would allow us to determine the amount of drug which was actually entrapped in the hydrogel system during the crosslinking process.

4.6.1 The drug entrapment efficiency of the Stimuli-Actuated Polymeric Device

Following the crosslinking of the aforementioned hydrogel, 20mL crosslinking solutions which were present after the hydrogel was removed. One mL sample was taken and assessed with UV/visible spectroscopy. The DEE assessment was first performed on the ibuprofen-loaded SAPD. The solvent in this case was a 1:1 water:acetone mixture. One problem encountered when assessing the amount of ibuprofen in the water/acetone mixture was that acetone and ibuprofen absorbs at similar wavelengths of UV light, which made it difficult to quantify the precise amount of ibuprofen present (Shin, 2001 and Kimura, 1997). It was for that purpose a SAPD identical to Device 15 was constructed, but the DEE shall be carried out with PBS as the surrounding medium, as ibuprofen exhibits solubility in PBS. This SAPD was placed in 50mL of PBS and homogenized for 5 minutes, followed by sonification for a further 2 minutes. Sample of 5mL was drawn from the 50mL PBS and assessed for any presence of drugs. The UV absorbance of the 5mL sample was 0.1394. The amount of drug presented in the 50mL sample equated to 4.22mg and therefore a DEE of only 4.22% since 100mg of ibuprofen was initially added into the device. This low amount of DEE rendered the ibuprofen an inappropriate drug for use in the hydrogel system.

For the second test, the indomethacin loaded SAPD device was tested. The UV absorbance in the 1mL sample obtained from the crosslinking solution was 0.138. The calibration curve may be presented as in Figure 4.9. The Equation for this graph was presented as Equation 4.3.

$$y=21.027 x$$

Equation 4.3

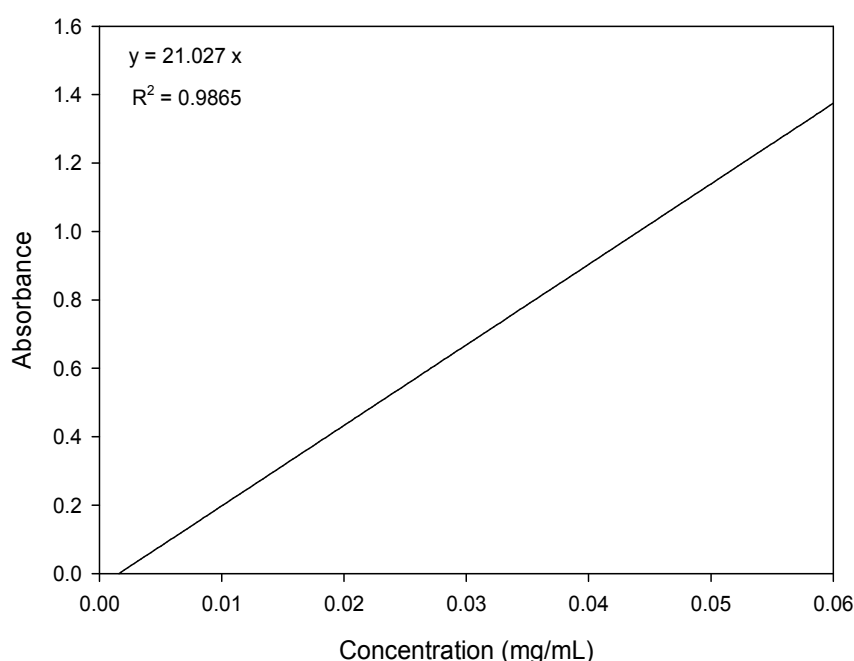


Figure 4.11. The calibration curve of indomethacin dissolved in 1:1 acetone:water solution under a wavelength of 318nm of UV light.

The amount of drugs present in the 1mL sample was assessed by using Equation 4.3. The amount of drugs present in the 20mL sample was 0.131mg and the amount of drug which was entrapped by the SAPD equated to $100 - 0.131 = 99.65\text{mg}$. The DEE recorded was 99.65%.

The last drug which was tested was diclofenac sodium. Similarly, a calibration curve was constructed with diclofenac sodium dissolved in 1:1 acetone:water and is presented as Figure 4.10. Due to the overlapping absorption wavelength between the diclofenac sodium and the acetone at 235nm (Shin, 2001 and Bravo, 2002), the wavelengths was shifted further to 320nm, where absorption of the UV light only occurs in the diclofenac sodium and not the acetone.

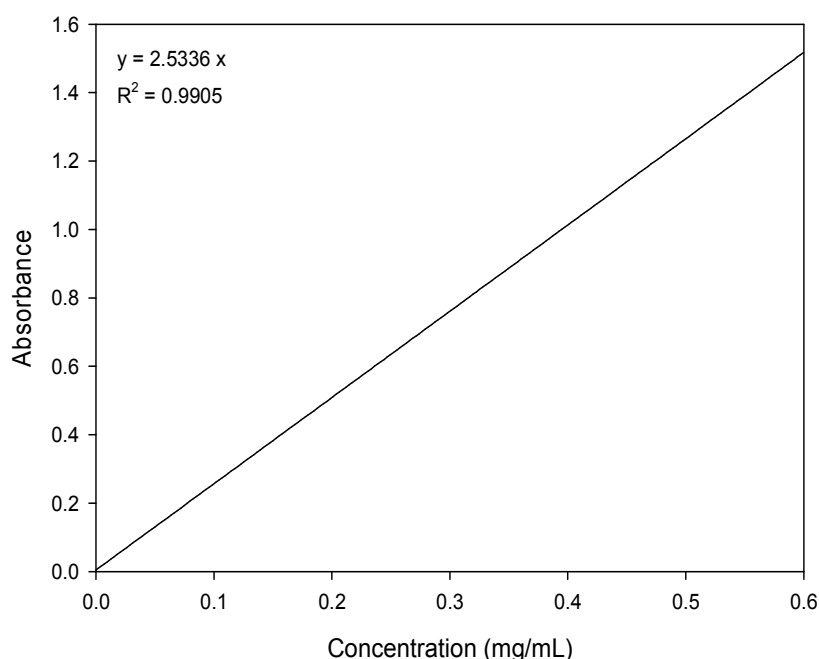


Figure 4.12. The calibration curve of diclofenac sodium dissolved in 1:1 acetone:water solution under a wavelength of 320 nm of UV light.

The Equation for this graph may be presented as Equation 4.4.

$$y = 2.5336 x$$

Equation 4.4

The DEE assessment was performed identically as mentioned in this Section and a UV absorbance of 1.37 was recorded. The amount of drug was calculated using Equation 4.4. The quantity of drug in the 20mL sample was 10.81mg. The DEE was $100 - 10.81 = 89.19\%$.

The indomethacin and the diclofenac sodium have exhibited good DEE when incorporated into the SAPD, with DEE higher than 85% in both cases. Ibuprofen has obtained DEE of less than 10% which rendered it unfeasible.

Based on the results obtained from Chapter 4 Section 4.5.16 and Chapter 4 Section 4.6.1, the most appropriate drug for further development would be the indomethacin. Indomethacin was the only drug which had shown electroactivity with a relatively high DEE. The incorporation of this drug into the SAPD may be appropriate and should be further investigated.

4.7. The drug release mechanism of the Stimuli-Actuated Polymeric Device

In this study, the drug release mechanism of the SAPD was explored. Murdan and co-workers (2003) have suggested a few methods in which a drug may be released via electro-responsive methods (Murda *et al.*, 2003). These methods were forced eviction of drug due to de-swelling, electrophoresis of drugs towards charged electrodes and erosion of hydrogel which led to liberation of drugs. The drug release mechanism from the SAPD may be one of these three possible mechanisms. During the evaluation of the SAPD, visible changes were observed which suggested the release mechanism was due to erosion. The SAPD before and after exposure to electric current was depicted in Figure 4.11 a and b respectively.

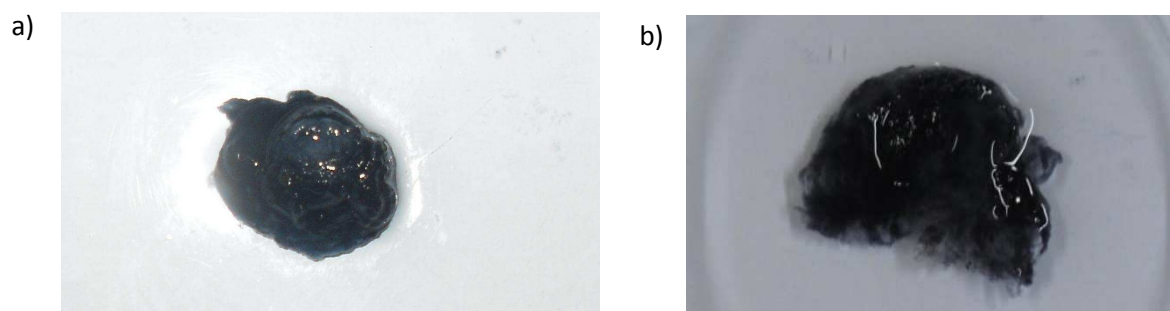


Figure 4.13. a) The SAPD before exposure to electric current. b) The SAPD after exposure to electric current

The SAPD in Figure 4.11 b) has shown erosions on the bottom side where the electrodes were placed. It was possible to assume that the release mechanism may be due to the erosion of the hydrogel, thus resulted in liberation of the drugs. When the same system was duplicated without the PANi, there were no signs of erosion, which suggested that PANi was linked to relate to the erosion of this hydrogel. Figure 4.13 depicts the SAPD after 60 release cycles. This figure clearly depicted the erosion which occurred on the SAPD when it was continuously exposed to electrical current. It was important to note that the erosion on the SAPD was a surface phenomenon only.



Figure 4.14. The erosion of the SAPD after 60 samples was taken.

Spherical erosions can be seen at the erosion sites where the electrodes were placed on the hydrogel. The colour of the SAPD has lightened in places where PANi was absent. They appear as translucent areas in the hydrogel in Figure 4.12. Drug release study done beyond 70 samples has shown that even though drug release no longer occurred, the SAPD was still undergoing erosion. This suggested that indomethacin did not contribute to the erosion of the SAPD.

Another important aspect which must be explored was any possible interactions which could have occurred between the SAPD and the indomethacin. This was important from a release mechanism point of view because if there was a possibility of any drug-hydrogel interaction, it may affect the structural integrity of the SAPD and therefore the erosion rate. This would ultimately affect the release rate of indomethacin from the SAPD. In order to determine if there was any reaction between the indomethacin and the SAPD, two experiments were conducted, namely FTIR and Differential Scanning Calorimetry (DSC).

4.7.1. Fourier Transform Infra-Red spectroscopy of the Stimuli-Actuated Polymeric Device with and without indomethacin

This experiment was conducted in order to assess for any structural changes between the SAPDs which was loaded with indomethacin and without it. The hydrogels compared was a placebo device of the SAPD and a drug-depleted SAPD. The results of SAPD with the drug and without the drug are indicated by Figure 4.15.

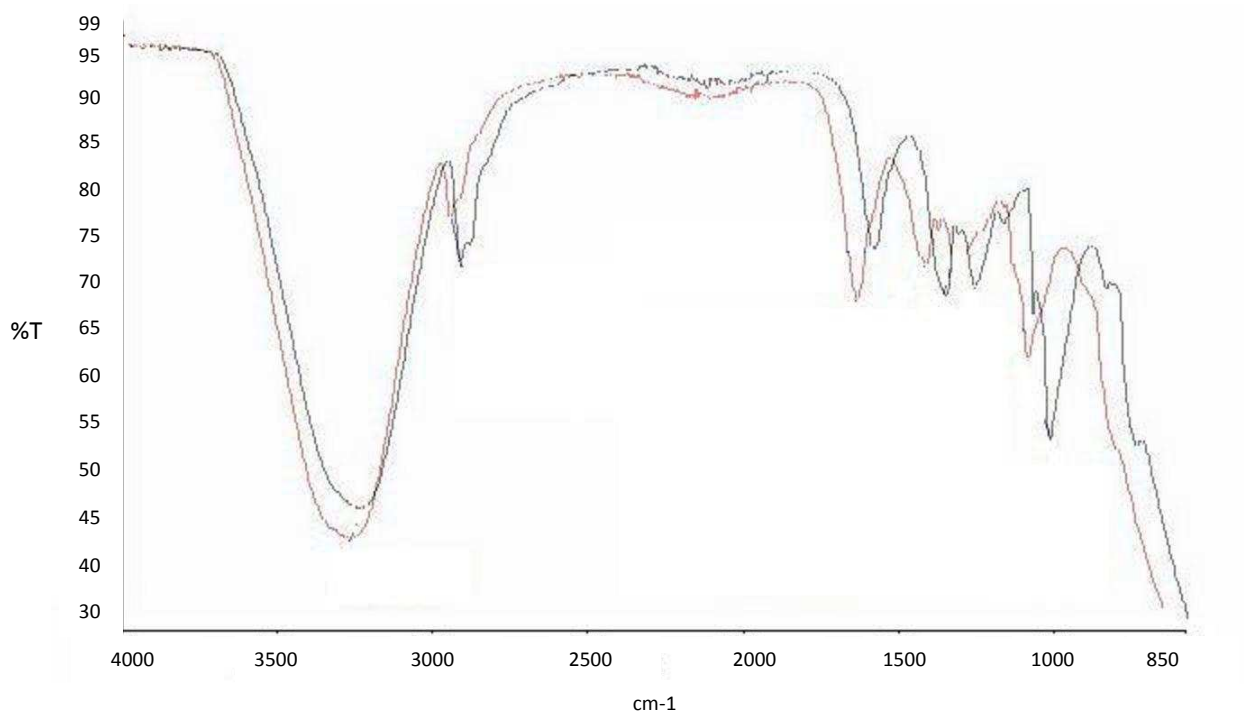


Figure 4.15. The FTIR of the eroded SAPD (blue) and SAPD without the indomethacin (pink)

As Figure 4.13 and 4.14 have indicated, there was no difference in the two structures and indomethacin did not have any direct interactions with the SAPD. This suggested that the drug was merely entrapped in the SAPD and was liberated when the SAPD underwent erosion. The drug was trapped in the SAPD during the crosslinking process and remained within the SAPD even during the swelled state until erosion occurred. There was no interaction between the drug and the SAPD.

4.7.2. Differential Scanning Calorimetry of the indomethacin-loaded Stimuli-Actuated Polymeric Device

Another method which was employed in order to determine whether there were any interaction between the drug indomethacin and the SAPD was DSC. The thermal reactions of the SAPD with and without the drug were compared, and any differences in the thermal reaction may suggest an interaction between the SAPD and the drug. The equipment used was the DSC1 Star[®] System (Mettler Toledo, Uster, Zurich, Switzerland). The DSC was first conducted on the indomethacin alone, followed by the SAPD without the indomethacin, and finally on the SAPD with the indomethacin. The results are shown in Figures 4.15-4.17.

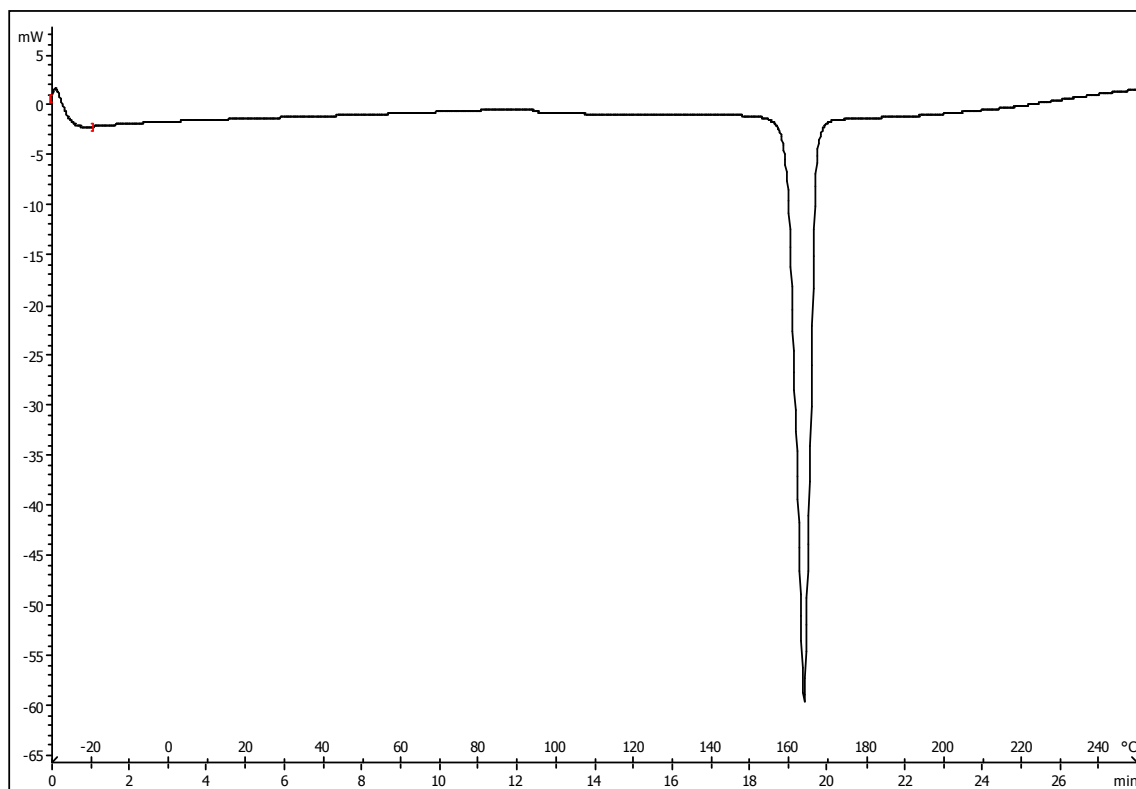


Figure 4.16. DSC thermogram obtained for indomethacin.

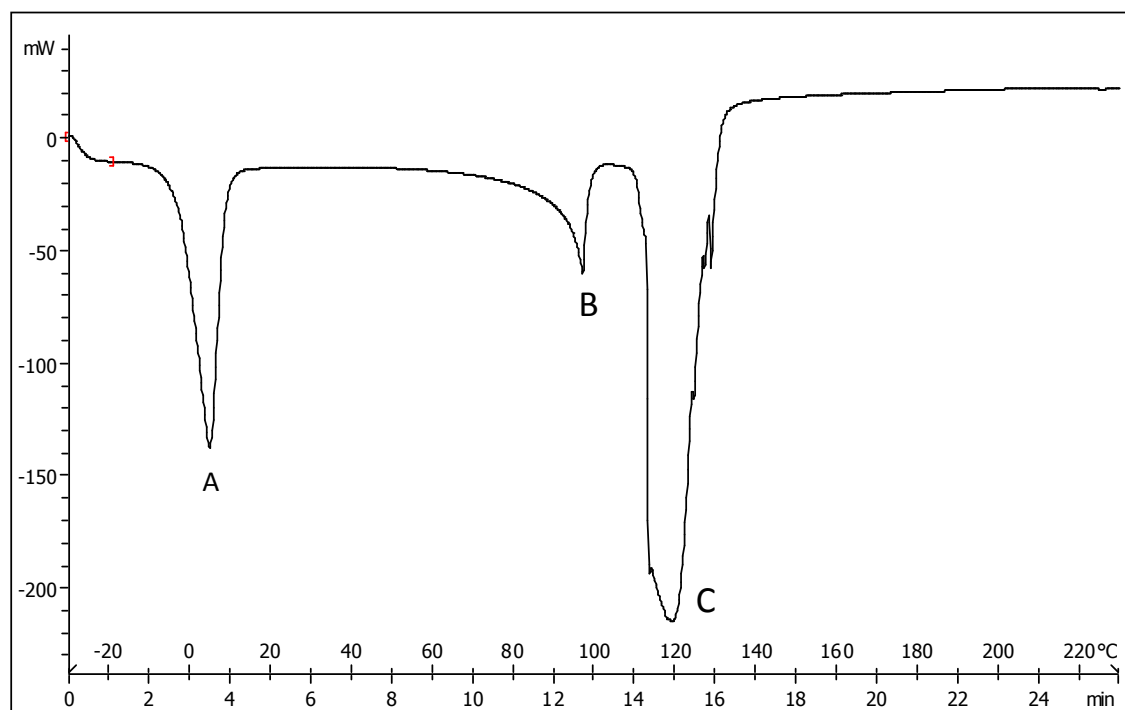


Figure 4.17. DSC thermogram of the stimuli-actuated polymeric device without the indomethacin.

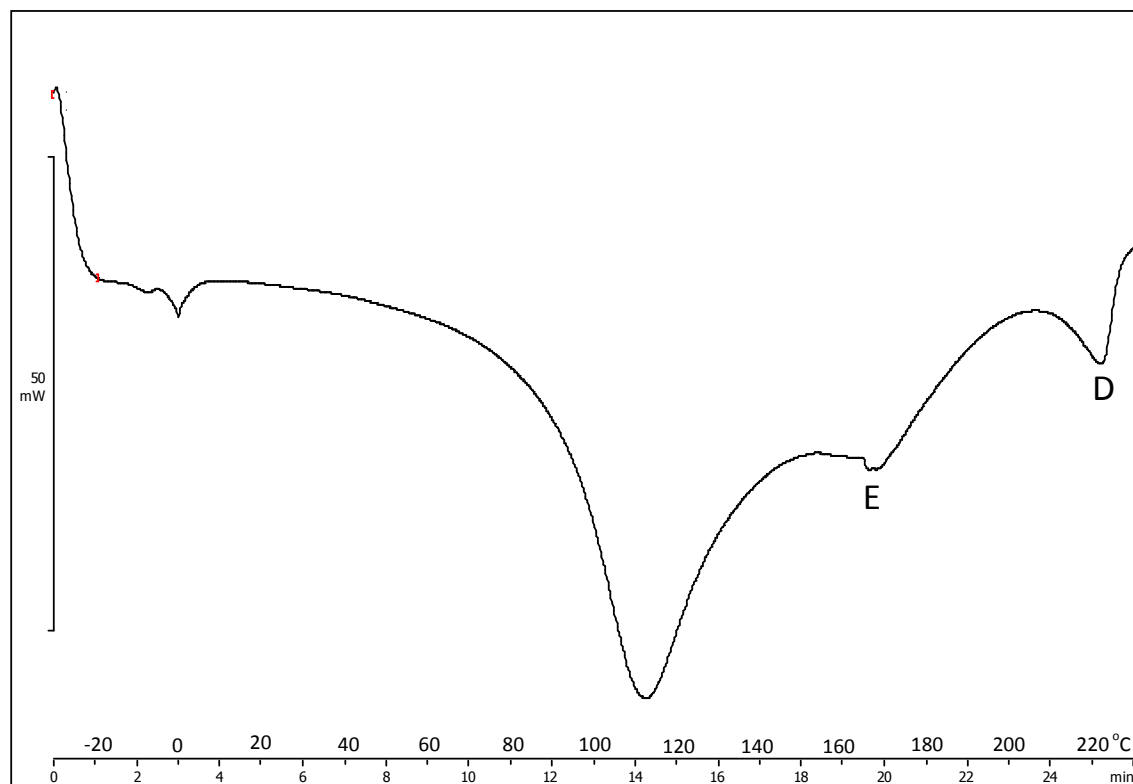


Figure 4.18. DSC thermogram of the stimuli-actuated polymeric device with the indomethacin.

Figure 4.15 and Figure 4.16 were the thermograms obtained from the indomethacin and the SAPD respectively. Figure 4.17 has shown an endothermic reaction at approximately 165°C. This endothermic reaction was most likely due to the melting of indomethacin, as previous studies have indicated that indomethacin has a melting point of 165°C (Chokshi, 2007). Figure 4.16 showed an endothermic reaction at approximately 5°C and a melting point of 120°C for the SAPD without the indomethacin. Figure 4.17 depicts the result of DSC obtained from the SAPD with the indomethacin loaded. In Figure 4.16, the endothermic reaction at peak A proposed represented glass transition of the SAPD due to the slight decrease in the baseline, as it returned slowly back to room temperature. Peak C might represent the melting point of the SAPD, which occurred at approximately 120°C. The small endothermic reaction represented by peak B has occurred due to a eutectic impurity and was not presented in Figure 4.17. Peak D in Figure 4.17 represented the thermal decomposition of the SAPD. This thermal decomposition was not seen in Figure 4.16 and may be attributed to the indomethacin which was entrapped in the SAPD. Similarly to the PANi, as the indomethacin was entrapped in the SAPD, it decreased the degree of crosslinking which occurred in the SAPD. This decrease in crosslinking may have decreased

the structural integrity and therefore a decrease in the decomposition temperature of the SAPD.

From Figure 4.16 and 4.17, one may see that the glass transition temperature and the melting point of the SAPD with and without the indomethacin were identical, which suggested identical chemical structure between the two. In Figure 4.17, peak E was present which was not seen in Figure 4.16, and may be due to the thermal degradation of the indomethacin. This may be verified by comparing it with Figure 4.15, which showed that the thermal degradation of the indomethacin was similar to the temperature range in peak E. In order to confirm the peaks D and E, modulated differential scanning calorimetry was performed. The use of modulated differential scanning calorimetry allowed more accurate assessment of these endothermic reactions and differentiates it from the artefacts which were commonly seen with differential scanning calorimetry. In this modulated differential scanning calorimetry, a sinusoidal heat increase was compared against that of a linear heat increase and provided a more distinctive understanding of the polymeric thermal behaviour. For this modulated differential scanning calorimetry, the temperature range was set between 160-180°C for peak E and 215-220°C for peak D, with an underlying heating rate of 1°C per minute. The temperature amplitude of modulation was 0.5°C with a loop segment of 1 and an increment of 0.8. Once the sinusoidal heat flow signals were obtained, these signals were averaged and a total heat flow could be obtained and allow for comparison against the standard DSC curve. The results obtained may be shown as Figure 4.18 a and b.

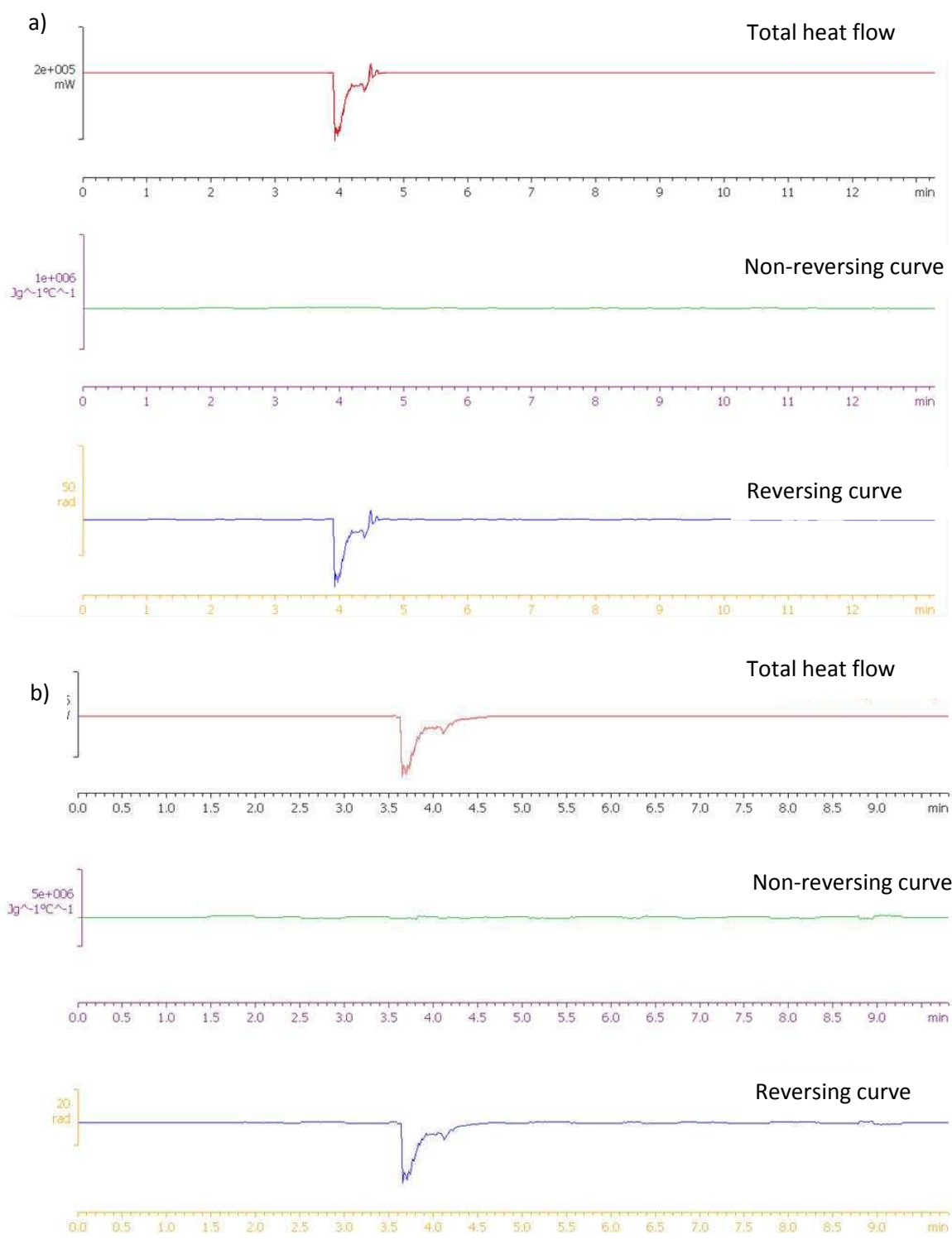


Figure 4.19. a) The MDSC thermogram obtained on peak E. b) The MDSC thermogram obtained on peak D.

The melting point of indomethacin in the SAPD and that of indomethacin alone were also identical and therefore indicated there was no interaction between the indomethacin and the SAPD. The presence of the endothermic peaks in the modulated differential scanning calorimetry has confirmed the existence of peak D and E.

4.7.3. Microscopy of the eroded Stimuli-Actuated Polymeric Device

4.7.3.1. Light microscopy of the eroded Stimuli-Actuated Polymeric Device

By analyzing the surface morphology, one was able to determine if there were any differences between the SAPD and the erosion sites and therefore the possible cause of the erosion. The surface morphology imaging was depicted in Figure 4.19 and 4.20. These two images were surface morphology of two different erosion sites captured on indomethacin-loaded SAPD.

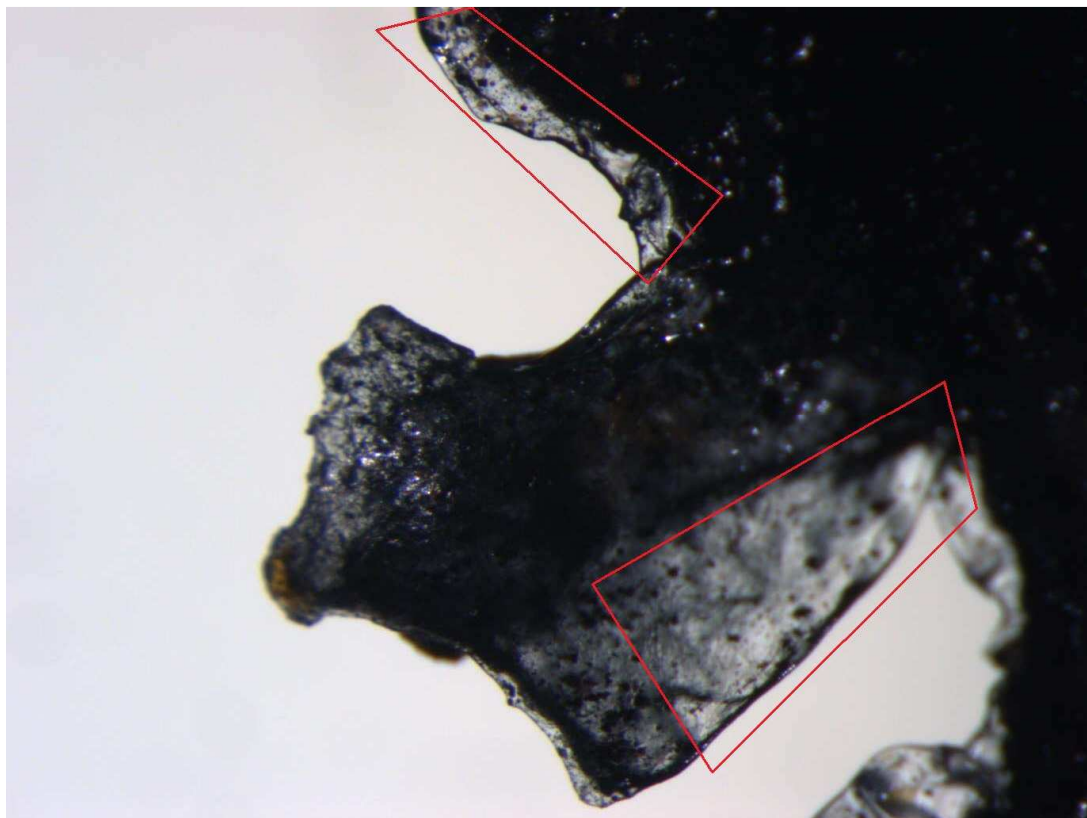


Figure 4.20. Microscopy of the first erosion site under 32X magnification.

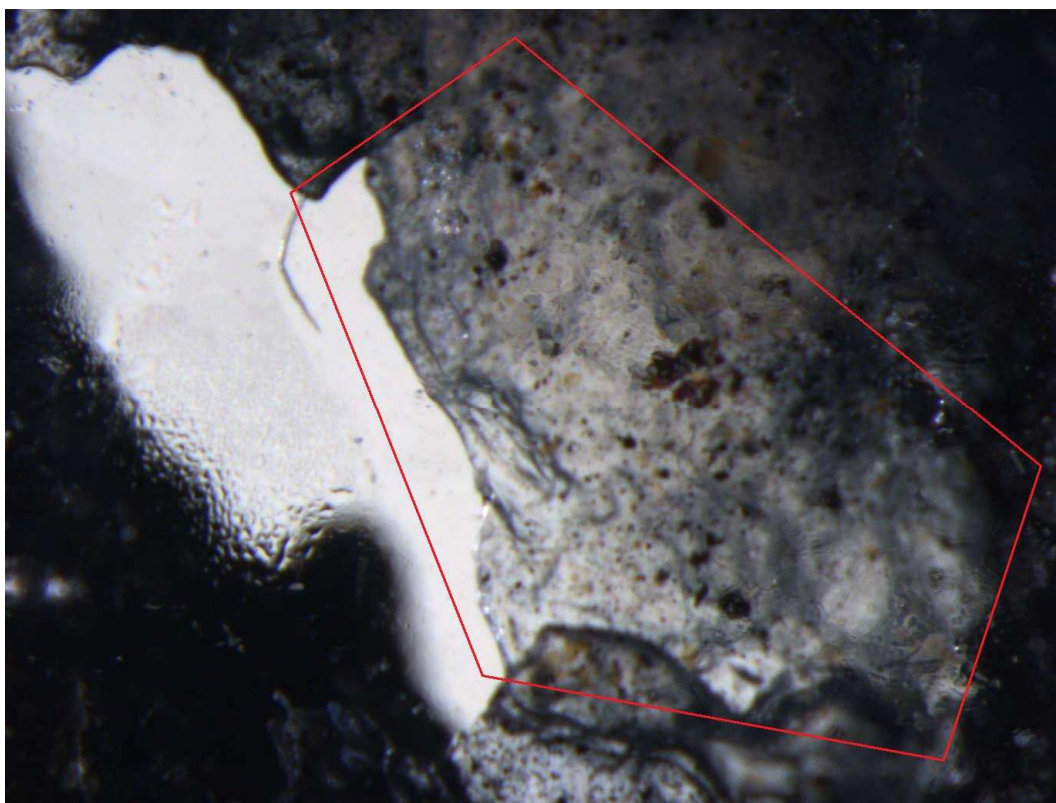


Figure 4.21. Microscopy of the second erosion site under 32X magnification.

As these two figures have shown, the colour of the SAPD at the erosion site was lighter. These areas are highlighted in red in the Figure 4.19 and 4.20. This may be attributed to the decrease in PANi as the erosion takes place, since it was the PANi that gives this hydrogel system the distinctive black colour. It was possible to link PANi to the erosions which occurred at these sites. As mentioned in Chapter 4 Section 4.7, the hydrogel system which was formed without PANi did not undergo any erosion when exposed to electric current, which strongly suggested that the interaction of PANi at the counter electrode played an important role towards the erosion of the SAPD.

4.7.3.2. Electron microscopy of the eroded Stimuli-Actuated Polymeric Device

Following the images obtained from the light microscopy on the erosion site of the SAPD, Scanning Electron Microscopy (SEM) was employed in order to obtain enhanced magnification of the erosion site. The model of the SEM used was the Phenom™ (FEI Company, Hillsboro, Oregon, USA). The application of the SEM allowed us to examine the surface morphology of the erosion site at 300-400 X magnification. The results are depicted in Figures 4.21 a) and b).

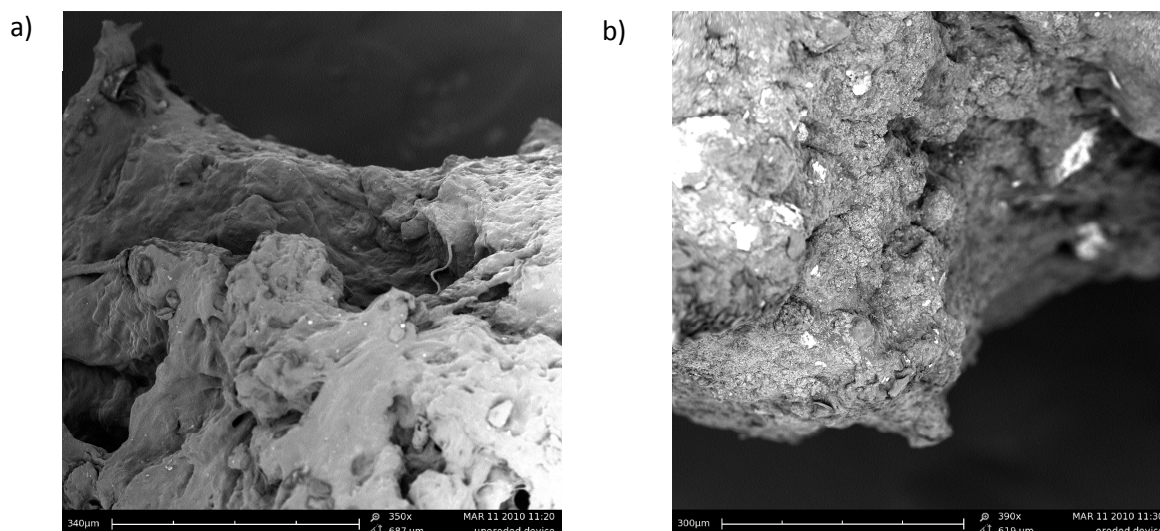


Figure 4.22. a) The surface morphology of an uneroded stimuli-actuated polymeric device at 350x magnification. b) The surface morphology of an eroded stimuli-actuated polymeric device at 390x magnification.

Figure 4.21 a and b depicts the difference in surface morphology of the two SAPDs. An uneroded SAPD exhibited a smooth surface morphology, which transformed to an uneven surface texture after the erosion has occurred. This may be due to the breaking of the crosslinked hydrogel structure, as pieces of the SAPD broke away from the main hydrogel, leaving the surface irregular and texturally rough. The use of this imaging has further confirmed that this erosion phenomenon occurred at a microscopic level. The study done thus far has indicated a possible mechanism of the erosion, however, further analysis using chemometric modelling would assist us further in determination of the erosion mechanism at an atomic level. This modelling is represented in Chapter 5 Section 5.4.3 and was undertaken once the SAPD was optimized.

4.7.4. The effect of polyvinyl alcohol and diethyl acetamidomalate on the rate of erosion in the Stimuli-Actuated Polymeric Device in the presence of electrical stimulation

In order to determine the affect of varying quantities of PVA and DAA on the erosion of the SAPD, five SAPDs with varying constituents were synthesized and exposed to electric current. Each system was synthesized with 20mg PANi, but the quantity of PVA and DAA were varied from 0.25-1.0g and 0.0-1.0g, respectively. This may be depicted as Table 4.19.

Table 4.19. Formulation template employed for preparing each SAPD system.

Formulation	DAA g (%)	PVA g (%)	PANi mg (%)	Erosion (% of original mass)
F1	0.0 (0.0)	0.5 (96.15)	20 (3.85)	14
F2	1.0 (65.79)	0.5 (32.89)	20 (1.32)	4
F3	0.5 (64.94)	0.25 (32.47)	20 (2.59)	6
F4	0.5 (32.89)	1.0 (65.79)	20 (1.32)	7
F5	0.25 (32.47)	0.5 (64.94)	20 (2.59)	11

Each system (F1-F5) was immersed in 25mL of PBS and exposed to 1.2V of potential difference for 10 minutes. The formulations were assessed for the extent of erosion and the effect of PVA and DAA on the hydrogel system was evaluated. Results revealed that F1 (14%) and F5 (11%) had higher rate of erosion compared to the minimal erosion rates of F2 (4%), F3 (6%) and F4 (7%), with F2 having the lowest erosion rate.

The rate of erosion was observed to be dependent on two factors: the extent of crosslinking determined by the hardness and the concentration of PANi in the hydrogel. Thus far, data has suggested that the lesser the degree of crosslinking and the higher the concentration of PANi, the higher the rate of erosion. Generally, crosslinking increases the structural integrity of the polymer matrix, thus decreasing the erosion rate (Emerson, 1993; Badenhorst, 2002 and Couppé, 2009). The water uptake also decreased and the swelling resulted in the formation of the rigid structure which ultimately affected the transport of ions across the hydrogel (Rokhade, 2007). With regards to the synthesis of the SAPD, the addition of PVA formed a loosely bound hydrogel network, the addition of DAA resulted in a rigid crosslinked network. In F1, there was no crosslinking between the polymeric chains of PVA due to the absence of the DAA, which resulted in a loose network and allowed the erosion of PANi in a concentration dependent manner. In addition, the higher mass % of PANi resulted in a higher rate of erosion. In the case of F2, the quantity of DAA was increased to twice that of PVA, which resulted in a highly dense rigid network structure as compared to F1. The mass % of the PANi in the hydrogel system was, furthermore, the lowest as compared to the other formulations resulting in the lowest percentage erosion. In the case of F3, having the same degree of crosslinking compared to F2, the lower quantity of PVA and DAA employed decreased the total hydrogel volume causing the PANi mass % to rise to 2.59%. The percentage erosion of F3 was thus similar to but slightly higher than that of F2. Formulation F4 was similar to F2 except that the quantity of the DAA and PVA used were switched. F2 was DAA dominant, which resulted in a rigid network, whereas F4 was PVA dominant thereby forming a loose network. Although it both possessed the identical PANi

concentration, F4 had a loosely crosslinked network and thus exhibited higher erosion when compared to F2. Formulation F5 demonstrated a higher erosion rate compared to F2, F3 and F4 because, similar to F4, the PVA was dominant over DAA, thus form a loosely crosslinked network. Furthermore, the quantity of PVA used was lower compared to F4 and resulted in a higher PANi mass %. The concentration of PANi was, however, not higher than that of F1. Although it exhibited higher erosion compared to F2, F3 and F4, it was still lower than that of F1.

In order to demonstrate the effect that volume had on the concentration of PANi, light microscopy was performed on SAPDs with various volumes. In this experiment, only the amount of PVA was varied, while the rest of the constituents were kept constant to the SAPD used in Chapter 4 Section 4.5.16. These pictures are demonstrated in Figure 4.22 a-c. Figure 4.22 a) depicted a device with 0.25g of PVA, which had the smallest volume and thus the highest concentration. Figure 4.22 b) showed a microscopy of the device with 0.5g of PVA, which had an intermediate volume while Figure 4.22 c) showed the microscopy of a device with 1g of PVA, which had the largest volume amongst all three devices.

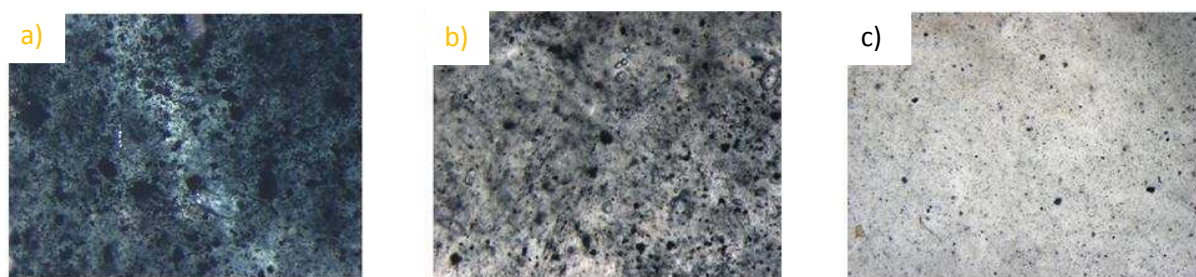


Figure 4.23. The concentration of PANi when PVA is a) 0.25g b) 0.5g and c) 1g

Figures 4.22 have shown that with an increase in volume of the SAPD, there was a decrease in concentration of the PANi, as indicated by a decrease in distribution of the black particles. As the volume increased, the more spread out the PANis become, and the less electro-responsive the SAPD became.

In order to further substantiate the effects that PANi concentration has on the erosion rate of the SAPD, two separate SAPDs were formulated, each with 0.5g PVA, 0.5g DAA and 100mg indomethacin. The only difference was that the first SAPD had only 1% w/w PANi while the second device had 3% w/w PANi incorporated into it. The two devices were immersed in 25mL PBS and a potential difference of 1.2V was applied for 400 seconds in order to assess the erosion rate. As speculated, the SAPD with the 3% w/w PANi has exhibited a significantly higher erosion rate than that of the 1% w/w SAPD. It was important to bear in mind the PANi concentration of the hydrogel system when formulating the drug delivery system.

Another important factor which determined the erosion rate was the amount of DAA added into the system. The more DAA that was added into the system, the less the rate of erosion, which suggested that DAA played a role in hindering erosion rate, possibly due to the increased crosslinking within the SAPD. In order to confirm this speculation, texture analysis was done on 3 different SAPDs. The test performed was a gel compression test. The hydrogel was compressed to a distance of 3mm, with a compression rate of 1mm/second. The force required to compress the hydrogel over a distance of 3mm was recorded. All three SAPDs used were identical to the one used in Chapter 4 Section 4.7, except the amount of DAA used was varied to 0g, 0.25g and 1g. The force required to compress the SAPD was presented in Figure 4.23 a-c.

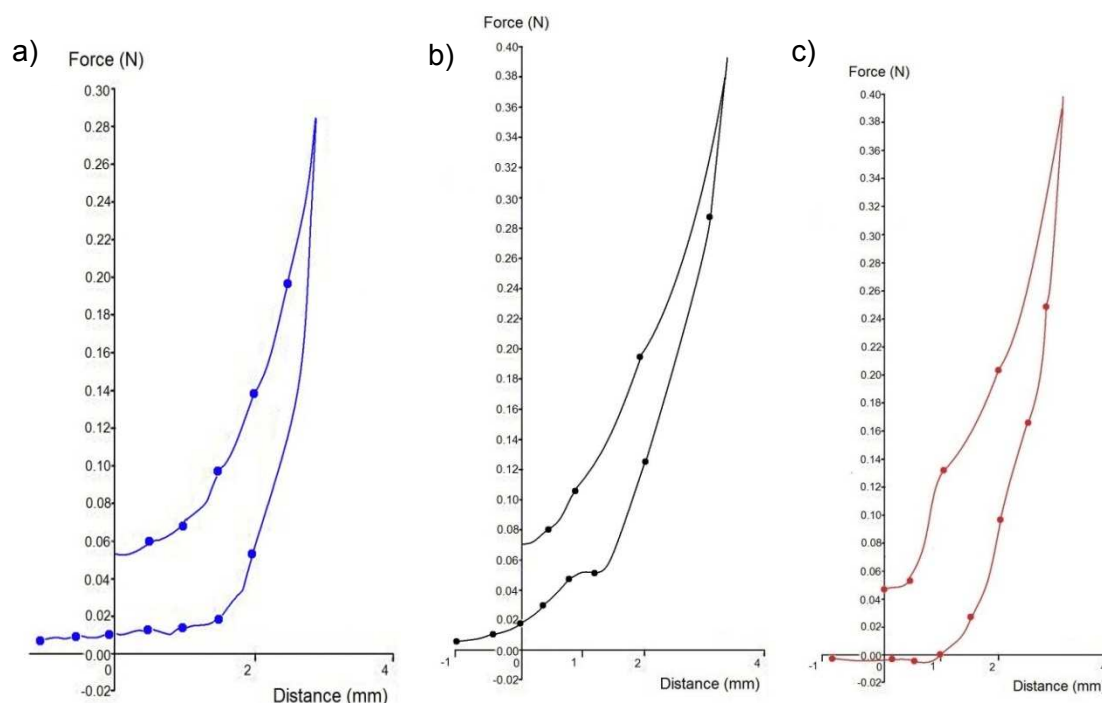


Figure 4.24. a) The force required for compression of the stimuli-actuated polymeric device with no DAA. b) The force required for compression of the stimuli-actuated polymeric device with 0.25g DAA. c) The force required for compression of the stimuli-actuated polymeric device with 1g DAA.

From the results obtained from Figure 4.23, there was an increase in the force required for compression of the SAPD by 3mm when DAA was incorporated into the SAPD. The required force for compression was the same for 0.25g DAA and 1g DAA, indicating there is an upper limit to the crosslink between PVA and DAA. This increase in force for compression when DAA was added may have indicated a crosslink between the DAA and the PVA as opposed to PVA alone.

This crosslinked system may also be tested by formulating two SAPDs, one with DAA and one without DAA. The two SAPDs were assessed for its drug release capability in the presence and absence of electric current. The two SAPDs were immersed in 20mL of PBS and a potential difference of 1.2V was applied for duration of 5 minutes. Samples of 4mL were taken afterwards and assessed for drug release. The PBS was discarded and the SAPD was immersed in a fresh batch of 20mL PBS. Samples were taken from 5 different SAPD. Figure 4.24 depicts the drug release from a SAPD with DAA and Figure 4.25 depicts the drug release from a SAPD without DAA.

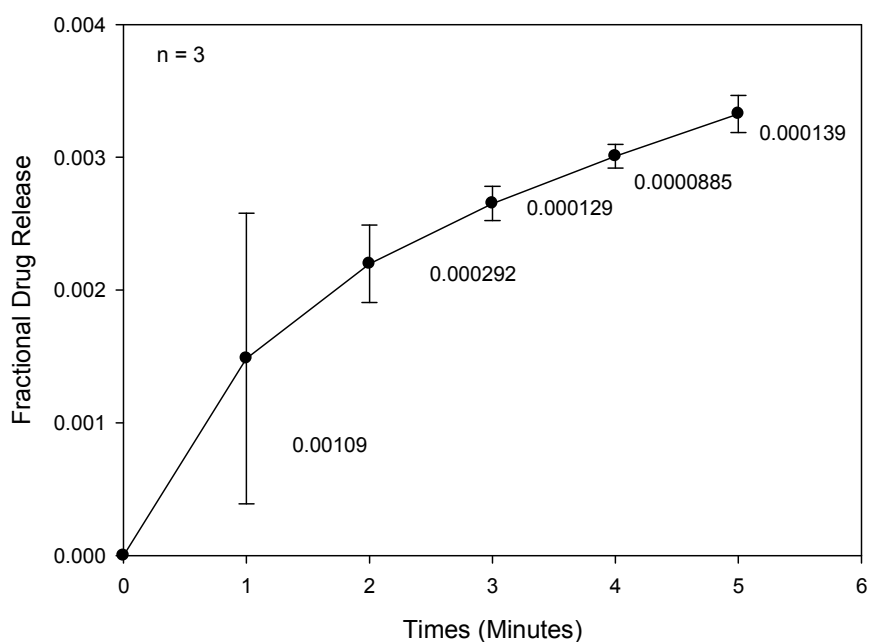


Figure 4.25. Drug release from the stimuli-actuated polymeric device with DAA.

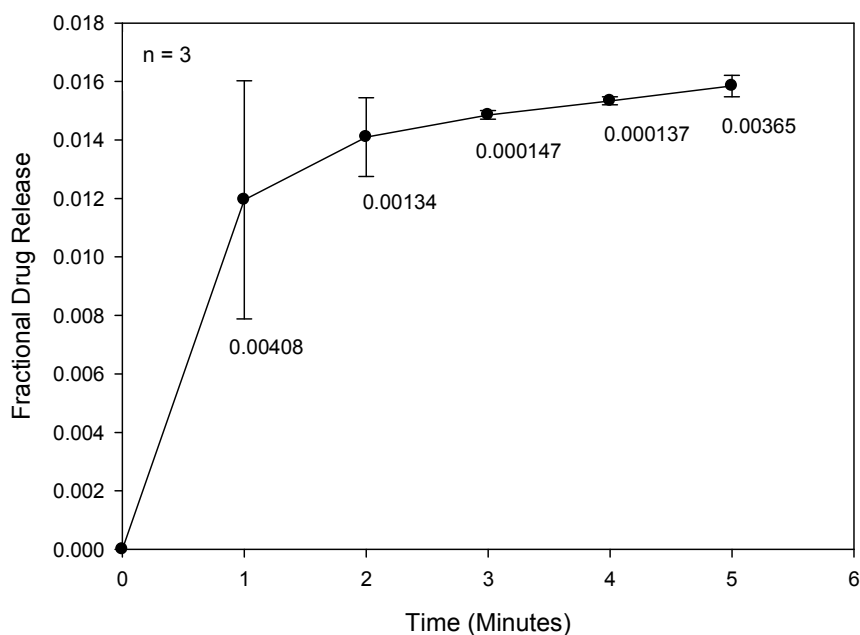


Figure 4.26. Drug release from the stimuli-actuated polymeric device without DAA.

From Figure 4.24 and Figure 4.25, one may see that drug release decreased significantly with the addition of DAA, suggesting the role of DAA in the SAPD as a crosslinker. Drug release was the highest initially and gradually dropped until a consistent drug release was reached. This may be due to the fact that this erosion was a surface phenomenon. As the SAPD erodes away, the surface-to-volume ration decreases, which rendered less and less surface to participate in the erosion until a consistency was reached.

Based on the data obtained in this Chapter, the preliminary mechanism of drug release may be interpreted as follows. When the SAPD was placed under the two electrodes during the drug release study, PANi coated around the counter electrode. It was assumed that the PANi was drawn towards the counter electrode. The experiment done in Chapter 4 Section 4.5.13 has shown that when PANi was incorporated into the crosslinked hydrogel system, it decreased the degree of crosslinking by becoming entrapped between the three dimensional network of the hydrogel system. When the counter electrode was placed onto the surface of the hydrogel, the PANi which was entrapped became drawn to the electrodes, and released itself from the SAPD. The PANi may have broken the crosslinked bond between the PVA and the DAA during this process, thus resulting in a weakening of structure and ultimately erosion. Since only the PANi which was close to the gold counter electrodes were drawn, only the structures around the electrodes will be weakened. This may explain the phenomenon of surface erosion. This schematic may be presented by Figure 4.26.

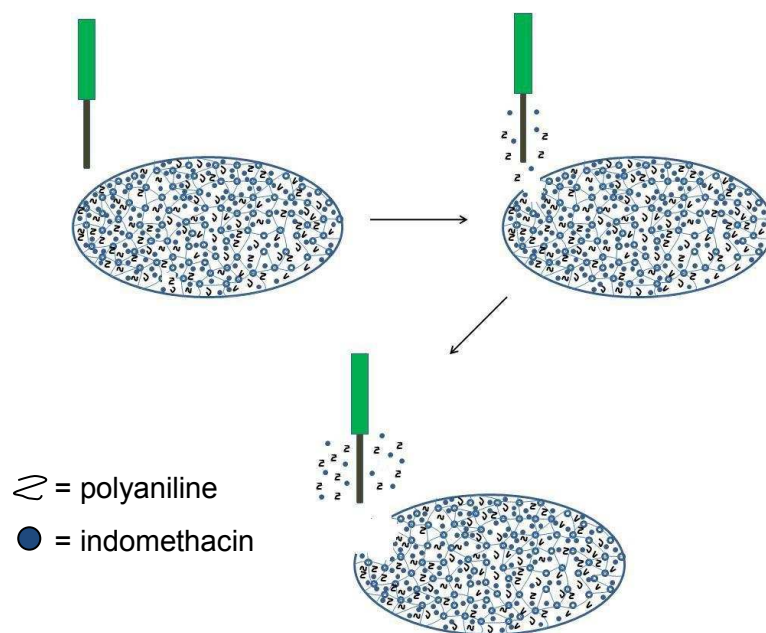


Figure 4.27. The proposed mechanism of the drug release from stimuli-actuated polymeric device.

This mechanism of erosion would require an even and adequate distribution of PANi throughout the hydrogel in order to achieve optimum drug release. As seen in Figure 4.17, the opaque areas where PANi was depleted have ceased to erode in the presence of the electric current. An increased amount of PANi should be considered for the optimization of the hydrogel system, however, the exact mechanism of the drug release and the erosion should be elucidated by further characterization of the SAPD.

4.8. Concluding remarks

In order to synthesize a SAPD which was electroactive, a hydrogel with adequate structural integrity and drug entrapment was synthesized. Hydrogel such as methylcellulose lost its structural integrity in water and was unsuitable. A crosslinked hydrogel between PVA and Eudragit® retained its structural integrity in water but exhibited a weakened structure when placed in basic pH, such as the PBS used with a pH of 7.4. This may have rendered the PVA/Eudragit® unsuitable due to its instability under physiological pH. PVA with a lower molecular weight was used, but was eventually replaced with a high molecular weight PVA because it exhibited no structural degradation when placed in solvents like water or PBS. Like other hydrogels, it exhibited swelling and the drug entrapment with indomethacin and diclofenac sodium was good. The compatibility between SAPD and various NSAIDs has also been investigated. NSAIDs were chosen because it could act locally and it has high potency.

The difference in this drug behaviour may be due to factors such as charge, molecular size and solubility of the drugs. It was important to ensure that the drug with the most appropriate characteristics was chosen. From this study, indomethacin has shown the best compatibility with the SAPD and was the drug of choice for this system. The major problem presented with several other NSAIDs was the leakage observed from the SAPD. In order to allow optimization and modification, it was important to assess the drug release mechanism and physicochemical behaviour of the SAPD. In this Chapter, the SAPD was constructed through a crosslinked hydrogel by employing various polymers. After the crosslinked hydrogel was synthesized, drugs were entrapped and DEE was used to assess the amount of the drug within the SAPD. Certain drugs were not retainable by the SAPD and drug leakage occurred, thereby rendering it unsuitable for the SAPD. Entrapped drugs were liberated when the SAPD underwent erosion. The erosion occurred may be attributed to the breakage of crosslinks between the PVA and DAA. Breaking a crosslink has been achieved by other researches and is a possible mechanism of release (Tezel, 2005; Susic, 2004; Conway, 1983). One reason for elucidation of the drug release mechanism of the SAPD was that it allowed the optimization of the SAPD. By understanding the factors such as the degree of polymerization, PANi distribution and drug entrapment, we could understand how these factors influenced drug release, which in turn allowed modifications to these factors as to allow optimum drug release profile.

CHAPTER 5

OPTIMIZATION AND ELUCIDATION OF THE RELEASE MECHANISM OF THE STIMULI-ACTUATED POLYMERIC DEVICE

5.1 Introduction

Once a design of the SAPD was achieved, the following step was the optimization of the various factors which affected the SAPD. These factors included internal factors such as the ratio of the constituents and external factors such electrical current. These factors may or may not affect the physicochemical and the physicomechanical properties of the SAPD, but the establishment of these parameters was important.

In order to determine the optimum working range of the SAPD, it was important to start with internal factors such as the ratio of constituents and the amount of drugs used. By varying the ration of constituents, the rate of drug release may be altered and the physicomechanical properties of the SAPD. The crosslinking should be adequate in order to provide good structural integrity but does not significantly hinder drug release. The amount of drug loaded should be maximized so that more drug release may be achieved and therefore prolonging the release cycle of the SAPD. In Chapter 4 Section 4.7.4, the erosion rate of various SAPDs under different ratio of constituents was investigated. In this Chapter, we have further tested the amount of drug release under various potential differences. Our current model suggested that the higher the erosion rate, the higher the drug release. A good starting point was to begin with a SAPD which contained a SAPD with high PANi concentration, high drug loading and intermediate volume. This should yield a high erosion rate while maintaining the structural integrity of the system. In order to ensure the SAPD synthesized was appropriate, computer simulation would be done to ensure that the optimum ratio was chosen.

Once the internal factors were established, the SAPD would be characterized for its drug release rate under different environmental factors. Environmental factors such as temperature and current strength was investigated in order to determine what affect these factors have on drug release. A change in temperature may affect the visco-elastic property of the SAPD. This change in physicomechanical property may determine the storage conditions and stability of the SAPD. Other characterization may have included properties

such as melting points, glass transition temperature and thermal degradation. Both characterization and optimization would be important in order to establish a foundation for *in vivo* experimentation.

5.2. Materials and Methods

5.2.1. Materials

The conductivity tester used was the TDSTest™ Kit Model WD-35661-70 (Oakton® instruments, Vernon Hills, IL, USA). The Box-Behnken quadratic design was performed by the use of a Minitab Statistical Software, Version 14 (Minitab Inc., State College, PA, USA). The potentiostat/galvanostat used for the cyclic voltammetry was the PGSTAT302N (Autolab, Utrecht, Netherland). Molecular Mechanics (MM) Computations in solvated system with water as solvent were performed using the HyperChem™ 8.0.8 Molecular Modeling System (Hypercube Inc., Gainesville, Florida, USA) and ChemBio3D Ultra 11.0 (CambridgeSoft Corporation, Cambridge, UK) on an HP Pavilion dv5 Pentium Dual CPU T3200 workstation. The rheometer used was the Haake Modular Advanced Rheometer System (Thermo Electron Corporation, Waltham, MA, USA). Arthrexin® 25mg capsule was used for comparative dissolution study. The dissolution machine used was Caley® Model 7ST (Techne, Cambridge, England). The software used for blood-drug concentration simulation was the Vensim PLE.

5.2.2. Optimization of external and internal factors of the Stimuli-Actuated Polymeric Device

5.2.2.1. The optimization of the constituent ratio in order to achieve rapid drug release upon activation.

The role that various polymers have contributed to the SAPD was previously assessed. Taking these factors into consideration, a SAPD with minimal crosslinking, intermediate volume and high PANi concentration should be a favourable starting point for further optimization of the SAPD. An experiment was conducted by immersing SAPD in 20mL of PBS followed by exposure to electric current for 45 seconds. The SAPD was left in the PBS for an hour prior to actuation with electrical stimulation. Samples were taken before and after actuation in order to assess the amount of drug released and if there was any drug leakage during the absence of electric current. This experiment was conducted over a three hour period. The SAPD was synthesized using 0.5g PVA, 0.5g, 2%^{w/w} PANi and 100mg

indomethacin. The DEE for this device was 70.25%. The results may be presented by Figure 5.1.

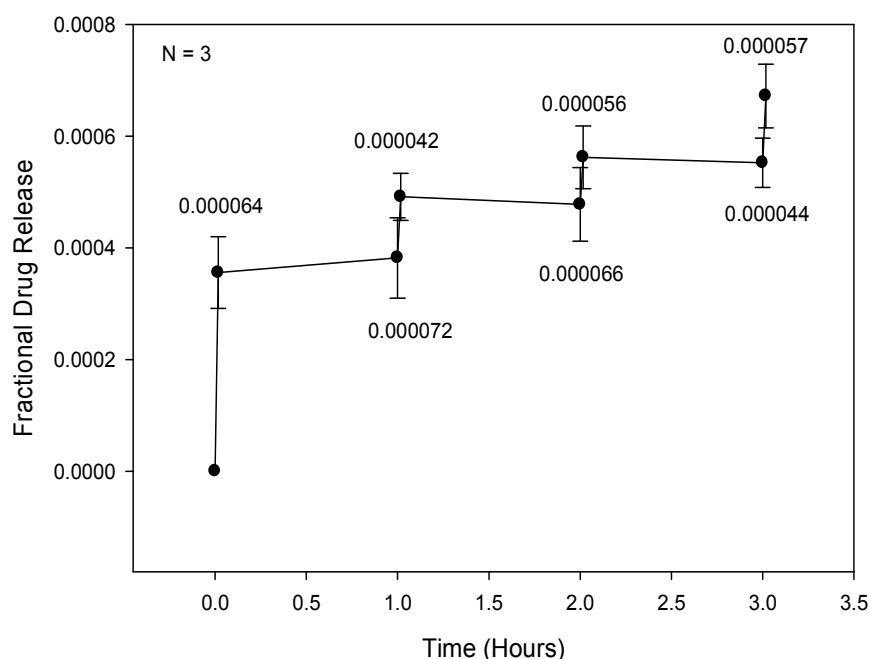


Figure 5.1. The fractional drug release profile of the stimuli-actuated polymeric device over a three hour period with 45 seconds of electric current at an hourly interval.

Based on results from Figure 5.1, the SAPD was capable of controlled release of drug in the presence of an electric current, although the initial release cycle was higher than the subsequent cycles. The stepwise increase in drug was an indication of a favourable drug release profile because it demonstrated significant increase in drug release when the SAPD was exposed to electric current for the short amount of time. It was important to determine the effects that various potential difference has on the SAPD. In order to standardize the potential difference applied, SAPDs were synthesized and exposed to varying potential differences of 0.3V, 1.2V, 2V, 3V, 4V and 5V. The drug release profiles were assessed and compared to the drug release profile of the SAPD under 1.2V. This would allow determination of any difference in terms of drug release behaviour and response caused by a difference in the voltage applied. The results may be summarized by Figure 5.2 which depicts fractional drug release against time when the SAPD was exposed to various potential differences.

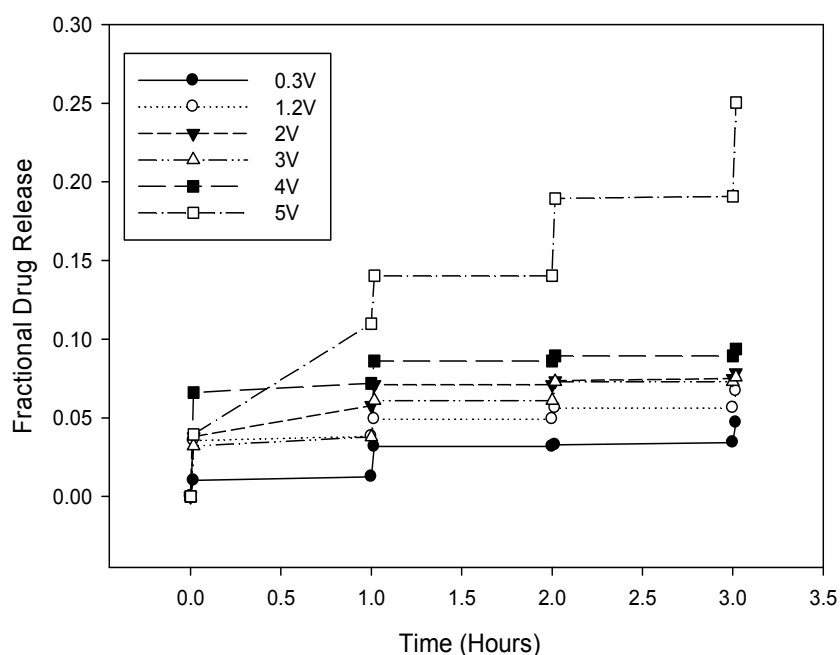


Figure 5.2. The fractional drug release from the stimuli-actuated polymeric device when exposed to various potential differences.

The results obtained from Figure 5.2 indicated that the drug release increased with an increase in the applied potential difference. By analyzing this result, it was possible to achieve a release of a therapeutic dose of indomethacin based on an 'ON-OFF' drug release profile. A high fractional drug release from the SAPD meant that the implant would have to be replaced frequently and is unfavourable.

By using the fractional drug release obtained after 4 release cycles, it enabled us to calculate the maximum amount of drug release possible under varying voltages. Figure 5.3 depicted the number release cycle possible when varying potential differences were used. The number of drug release achievable was constant between potential differences of 1.5V to 3.5V, as the fractional drug release did not differ significantly. However, the number of release cycle seemed to change drastically when the potential difference was shifted outside this range.

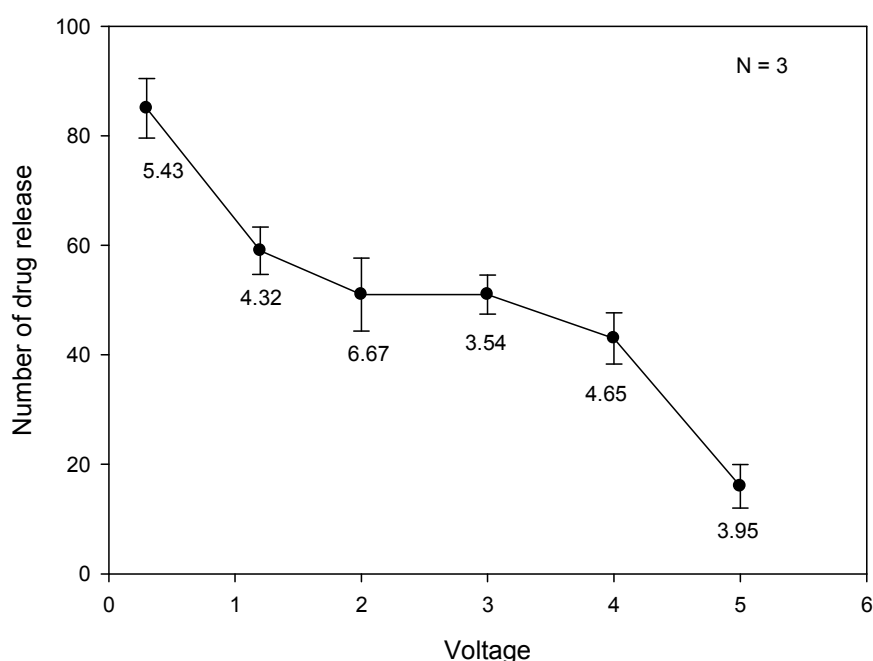


Figure 5.3. The quantity of drug release cycles achievable when various voltages were applied.

From Figure 5.3, we could determine the quantity of drug releases from the SAPD when various voltages were applied. Based on the results obtained from Figure 5.2 and Figure 5.3, it seemed feasible to use 1V as the optimum potential difference for the actuation of the SAPD. By using 1V as the standardized potential difference, it offered a release cycle of approximately 60 and provided adequate drug release of approximately 0.7mg into the surrounding area. This study was important as the optimization of the actuation voltage greatly affected the number of release cycles and the amount of drug released from the SAPD.

5.2.2.2. The optimization of the Stimuli-Actuated Polymeric Device with the use of a 3 Factor Box-Behnken Design

Once the actuation voltage was determined, the next step of optimization was to determine the ratio of the optimum constituents before further analysis can be performed. This study was guided through a three factor, three centre points Box-Behnken quadratic design. In order to form an optimized SAPD with high drug entrapment and minimum erosion, fifteen SAPDs with various combinations of the independent variables were synthesized and tested in accordance to their drug release profile, drug entrapment efficiency and rate of erosion. The three independent variables employed for the synthesis of SAPD included the hydrogel component formed by polyvinyl alcohol, the crosslinker DAA used to increase the structural integrity of the hydrogel and the EAP, namely PANi, to enhance the conductivity of the

SAPD. Table 5.1 represents the upper and lower limits for each of the variables. The limits for these variables were based on its ability to form a stable SAPD with optimal percentage drug release (maximum amount of drug release before depletion) with a minimal erosion rate and the 15 combinations for the SAPD.

Table 5.1. The upper and lower limit levels used for the Box-Behnken template.

Independent variables	Levels		Units
	Low	High	
PVA	0.5	0.8	Grams
DAA	0.0	0.3	Grams
PANi	1.0	4.0	% ^w / _w
Formulation	Composition		
	PANi (% ^w / _w)	PVA (g)	DAA (g)
1	1.00	0.80	0.15
2	4.00	0.65	0.30
3	1.00	0.65	0.30
4 ^a	2.50	0.65	0.15
5	2.50	0.80	0.00
6	4.00	0.80	0.15
7	1.00	0.65	0.00
8 ^a	2.50	0.65	0.15
9	2.50	0.50	0.00
10	4.00	0.50	0.15
11	2.50	0.50	0.30
12 ^a	2.50	0.65	0.15
13	2.50	0.80	0.30
14	1.00	0.50	0.15
15	4.00	0.65	0.00

Note: ^a The centre points for experimental design template

The 15 SAPDs were made as according to the combination depicted in Table 5.1. Each SAPD was given a constant dosing of 100mg indomethacin and the SAPDs were assessed for its drug release profile, drug entrapment efficiency (DEE) and the rate of erosion.

The preparation of the SAPD was based on the optimized values obtained from the Box-Behnken Design. The optimized value was obtained through a three factor, three centre point Box-Behnken quadratic design by measuring the drug release profile, the drug entrapment efficiency and the erosion rate of the SAPD. The aim of this design was to obtain a SAPD with drug release of approximately 1.7% of the total drug per release, with a maximum DEE and minimum erosion. The effects of the PVA, DAA and PANi on the SAPD was depicted in Figure 5.4 and the results of the optimization obtained from the Minitab[®] software are depicted in Table 5.2.

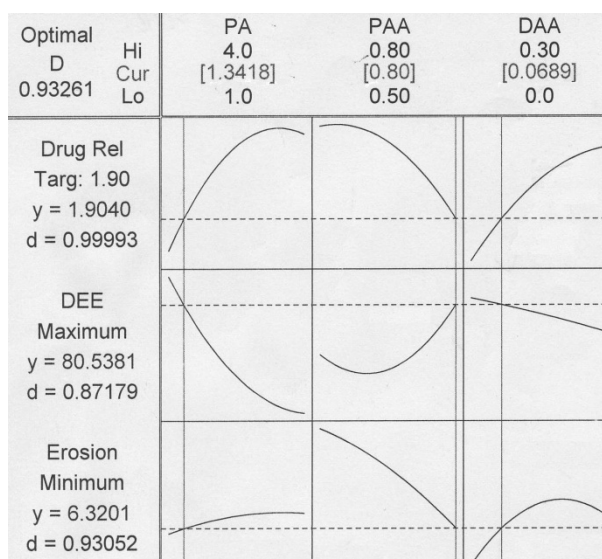


Figure 5.4. Optimization plots showing the effects of polyvinyl alcohol (PAA), polyaniline (PA) and DAA on the Drug release profile, DEE and the Erosion of the stimuli-actuated polymeric device.

Table 5.2. The results obtained from Minitab® for the optimization of the stimuli-actuated polymeric device.

Formulation	Drug Release after 8 cycles (%)	DEE (%)	Erosion (% of original weight)
1	1.90	89.44	5.50
2	12.00	37.89	17.32
3	18.00	43.18	10.43
4	24.00	36.62	14.16
5	16.00	39.74	8.97
6	11.00	59.22	7.36
7	5.90	73.67	5.67
8	57.00	23.87	4.28
9	12.00	82.02	15.91
10	7.70	82.43	23.39
11	15.80	41.95	8.77
12	24.40	36.07	24.36
13	42.00	34.25	9.05
14	41.00	25.07	15.31
15	34.00	26.63	10.16

Table 5.3 The probability of achieving each of the ideal characteristics when employing the yielded optimal value

Drug Release Target = 1.7% Yield = 1.9040 d = 0.99993	DEE Target = Maximum Yield = 80.5381 d = 0.87179	Erosion rate Target = Minimum Yield = 6.3201 d = 0.93052	D = 0.93261
--	---	---	-------------

Optimal = PANi (1.3418%^{w/w}), PVA (0.8g), DAA (0.0689g)

d = The probability of obtaining the yield value with the optimized values

D = The probability of the SAPD having the indicated yield value for drug release, DEE and erosion rate

The result depicted by Figure 5.4 demonstrated the effects of various components on the SAPD. An increase in PANi tended to increase drug release, due to the increase in erosion and interaction with the electrode. The DEE was, however, decreased with an increase in PANi. Both the PANi and indomethacin were incorporated into the SAPD via entrapment during the crosslinking of the hydrogel system. With the PANi and indomethacin competing with each other for entrapment, an increase of PANi in the hydrogel would mean a decrease in indomethacin. The erosion rate of the SAPD increased with an increase in the PANi concentration, although this increase reached a plateau with only a minute increase in PANi. The next constituent tested was the PVA. An increase in PVA decreased the erosion rate and ultimately the drug release rate. This decrease in erosion was attributed to the decrease in the PANi concentration caused by the increase in the volume of the hydrogel. The DEE was increased overall due to increased hydrogel volume which allowed more entrapment of the drug during the crosslinking. The last constituent used was the DAA. Results indicated by the Box-Behnken Design has indicated an overall increase in erosion and drug release rate, which was contradictory to our previous study done in Chapter 4 Section 4.7.4. An increase in DAA increased the crosslinking and thus the structural integrity of the SAPD. However, the results from this test indicated that DAA could have played a more significant role in the drug release mechanism of the PANi hydrogel system other than the crosslinker. These results may be depicted as Figure 5.5 which shows the effect of DAA, PANi and PVA on the drug release and the erosion of the SAPD.

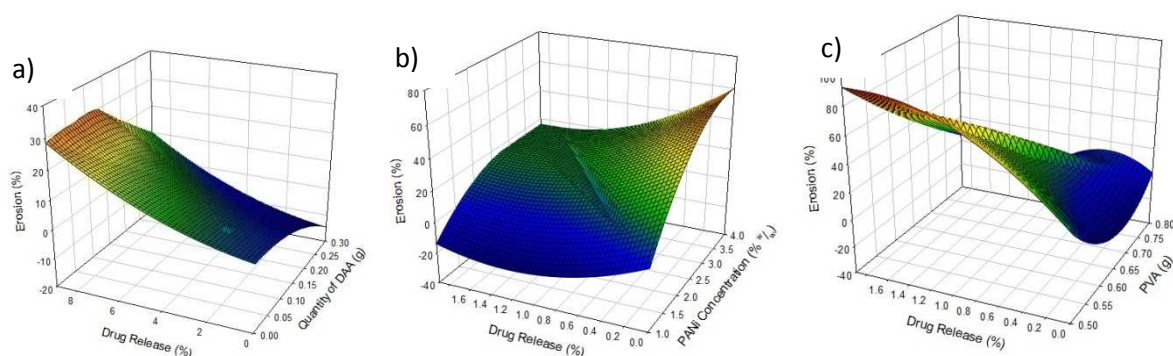


Figure 5.5. The surface area plot depicting the effect of a) DAA b) PANi and c) PVA on the SAPD

An optimized SAPD may be synthesized by employing 0.8g PVA crosslinked with 0.0689g of DAA with 1.3418%_{w/w} PANi incorporated within has a probability of 0.93261 of achieving the desired yield value as indicated by Table 5.2. The amount of indomethacin used for the formulation remained 100mg. The DEE should be approximately 80%, as indicated by the software, when used in these combinations.

5.3. Results and Discussion

5.3.1 The characterization and evaluation of the optimized Stimuli-Actuated Polymeric Device

Following the optimization of the SAPD with the use of the Minitab® software, the SAPD was synthesized according to the optimized value and evaluated in terms of its drug release profile, the DEE and the erosion rate. The quantity of the constituents used was the optimized value of 0.8g PVA crosslinked with 0.0689g DAA and a PANi concentration of 1.3418%^{w/w}. The amount of indomethacin used for this study remains 100mg. This optimized SAPD was tested for its drug release profile, DEE and erosion. The results obtained were compared against the target value obtained by the Box-Behnken Design. The results obtained for the drug release profile after 4 release cycles is depicted as Figure 5.6.

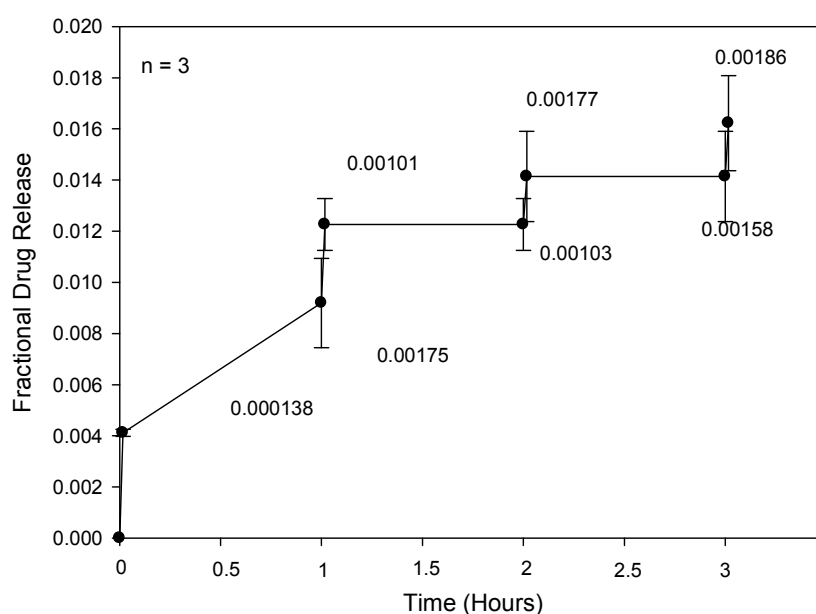


Figure 5.6. The drug release profile of the optimized stimuli-actuated polymeric device after 4 release cycles.

The results obtained were satisfactory when compared to the target values determined by the Box-Behnken design. The values for drug release profile, DEE and erosion rate were 1.622%±0.1857% (target 1.7%), 76.32±10.46% (target 80.5381%) and 5.73%±1.26% (target 6.3201%) respectively. Once these values were confirmed, the SAPD would be synthesized in accordance with these optimized values. The SAPD was further characterized in terms of its electroactivity and other properties.

5.3.2. Cyclic voltammetry of the the Stimuli-Actuated Polymeric Device

Cyclic voltammetry was performed on the SAPD in order to assess its electroactivity. The cyclic voltammetry was performed using PBS (pH 7.4) as the conducting solvent (Raoof, 2009; Zeng, 2002). The SAPD were homogenized into the PBS via a homogenizer for a period of 5 minutes followed by sonication at amplitude of 70% for a period of 3 minutes. The sonicator used was the Vibra-Cell™ (Sonics® Sonics & Material Inc., Newtown, CT, USA). The resultant solution was purged with nitrogen gas for 3 minutes prior to the cyclic voltammetry. The cyclic voltammetry was performed with the conventional three-electrode system with a saturate Ag/AgCl (3.0M KCl) as the reference electrode, a platinum wire as the auxiliary electrode and a 5mm glassy carbon electrode as the working electrode (Le, 2009). The scan rate of this cyclic voltammetry was 0.1V/second.

Cyclic voltammetry was performed in the SAPD in order to assess its electroactivity. The cyclic voltammetry showed the presence of two reduction wave and one oxidation wave. The range of the scan was from 2V to -2V with a scan rate of 100mV/second. The voltammogram was depicted in Figure 5.7.

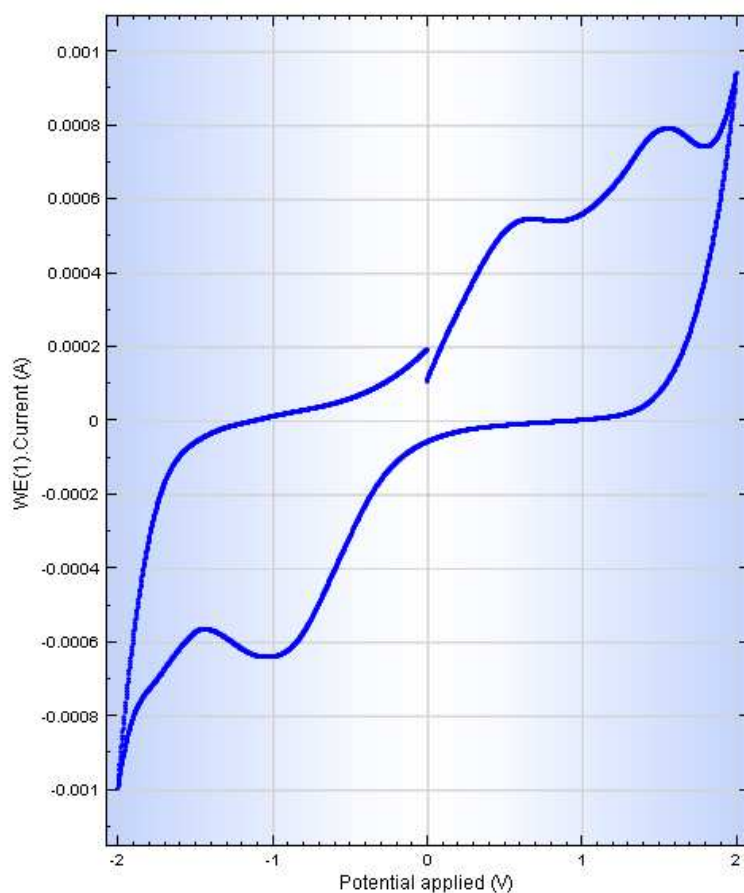


Figure 5.7. Cyclic voltammetry of the stimuli-actuated polymeric device in PBS.

The cyclic voltammetry of SAPD confirmed the presence of charge capacity (area under CV curve) for the SAPD. The curve indicated the presence of an intrinsic redox reaction between the electrode and the SAPD at the potential applied between 2V and -2V resulted from ion exchange between the electrodes and the electrolytes in the solvents carrying the mobile charge carrier to and from the SAPD. Under normal circumstances, PANi exhibited two pairs of redox peaks, one at 350mV and the other at 800mV (Wang, 1999). The voltammogram depicted in Figure 5.7 also exhibited two pairs of redox waves, however, these peaks have shifted to the right. These redox potentials shift may be due to more intricate reactions occur between the PANi, the hydrogel matrix, the electrolytes and the electrode. The result obtained from Figure 5.7 had indicated an oxidation peak occurring at approximately 0.6V and 1.4V and a reduction peak occurring around 1.5V and -1V. Since the PANi used for the synthesis of the SAPD was PANi emeraldine base, the first oxidation peak may be attributed to the transition of the first emeraldine oxidation state to the second emeraldine oxidation state. The second oxidation wave may be attributed to the transition of the second emeraldine oxidation state to the pernigraniline oxidation state (Chao, 2006). The change in the curve obtained in Figure 5.7 as compared to a standard voltammogram of PANi most likely resulted from ionic interactions occurring at the various interfaces between the PANi, hydrogel matrix, electrode and the electrolyte.

5.3.3. Conductivity measurement of the Stimuli-Actuated Polymeric Device

The SAPD was assessed for its conductivity in order to determine the role of the PANi in the SAPD. SAPDs with PANi concentrations of 1%, 2.5% and 4% w/w were synthesized. The results obtained are summarized in Table 5.3.

Table 5.4. The conductivity obtained from the SAPD containing various concentrations of PANi. Six readings were obtained for each concentration and an average was recorded as the result.

PANi concentration (% w/w)	Conductivity (μS)
1	97.45 \pm 7.00
2.5	108.20 \pm 4.52
4	130.30 \pm 11.99

The results from Table 5.3 indicated a linear increase in the conductivity of the SAPD with an increase in the PANi concentration. This increase may be contributed to the possibility that an increase in the PANi concentration within the hydrogel will result in a denser network structure of PANi and allowed more pathway for the electric current to travel between the two electrodes.

5.3.4. Molecular mechanics simulations of the Stimuli-Actuated Polymeric Device

The octamer of PANi and hexadecamer of polyvinyl alcohol was generated from standard bond lengths and angles employing polymer builder tools using ChemBio3D Ultra in its syndiotactic stereochemistry as 3D model. The individual polymer models were initially energy-minimized using MM+ force field and the resulting structures were again energy-minimized using the Amber 3 (Assisted Model Building and Energy Refinements) force field. The conformers having the lowest energy were used to create the polymer-polymer complexes (PVA-PANi). All MM simulations were performed under the influence of an external electric field ranging from 0.00a.u. to 0.05a.u. for cubic periodic boxes with dimensions of $25 \times 12 \times 25 \text{ \AA}^3$ containing one centred PVA-PANi complex with the centre of the cubic box and the remaining free space filled with water molecules and the same procedure of energy-minimization was repeated to generate the final models: PVA-PANi-0.01 to PVA-PANi-0.05. Full geometry optimizations were carried out in solvated system employing the Polak–Ribiere conjugate gradient method until an RMS gradient of 0.001kcal/mol was reached. Force field options in the AMBER (with explicit solvent) were extended to incorporate cut-offs to Inner and Outer options with the nearest-image periodic boundary conditions. The outer cut-off was set to 6.46Ångstroms and the inner cut-off was set to 2.46 Ångstroms to ensure that there were no discontinuities in the potential surface.

The environment surrounding the molecules of interest in molecular mechanics was defined in terms of a solvated system to prevent artefacts that arise from vacuum simulations and to reproduce bulk solvent properties well. Although the system could also be simulated in vacuum, but it may introduce artefacts in the molecular geometry due to surface charges of the charged molecules interacting with each other (as opposed to interaction with the solvent in a solvated system), producing molecular conformations that are unlikely to be present in any other environment. The system in present research was solvated by placing explicit water molecules in the simulation box with PVA-PANi complex and an external electric field in the direction of x-axis and of magnitude of 0.00a.u. to 0.05a.u. was applied to corroborate the electro-liberation of indomethacin from the SAPDs under the influence of applied potential. The calculated values for the various energies for the PVA-PANi MM simulations under the external electric field are illustrated separately as bond, angle (torsion) and van der Waals energies in Table 5.4. The total steric energy of the PVA-PANi complex increased with an increase in the electric field magnitude from 0.01au to 0.05au indicating the instability caused by the applied external electric field (Figure 5.8). This instability in majority was caused by bond torsion (82.93-335.47 kcal/mol) stretching followed by bond angle (44.67-141.34 kcal/mol) and minimally by van der Waals interactions (71.56-9857 kcal/mol).

Table 5.5. Calculated energy parameters (kcal/mol) of the PVA-PANi complex in a solvated system under the influence of electric field.

Structure	Energy (kcal/mol)				
	Total	$\Delta E_{\text{stimulation}}$	Bond	Angle	vdW
PVA-PANi-0.00	-3115.92	-	33.4948	56.3898	71.5598
PVA-PANi-0.01	-2826.36	+289.56	44.6791	82.9305	72.6148
PVA-PANi-0.02	-2643.41	+472.51	61.2286	129.845	76.1276
PVA-PANi-0.03	-2213.01	+902.91	86.1102	184.596	82.4647
PVA-PANi-0.04	-1982.23	+1133.69	111.422	255.45	91.9177
PVA-PANi-0.05	-1772.02	+1343.9	141.338	335.476	98.5723

vdW: van der Waals energy

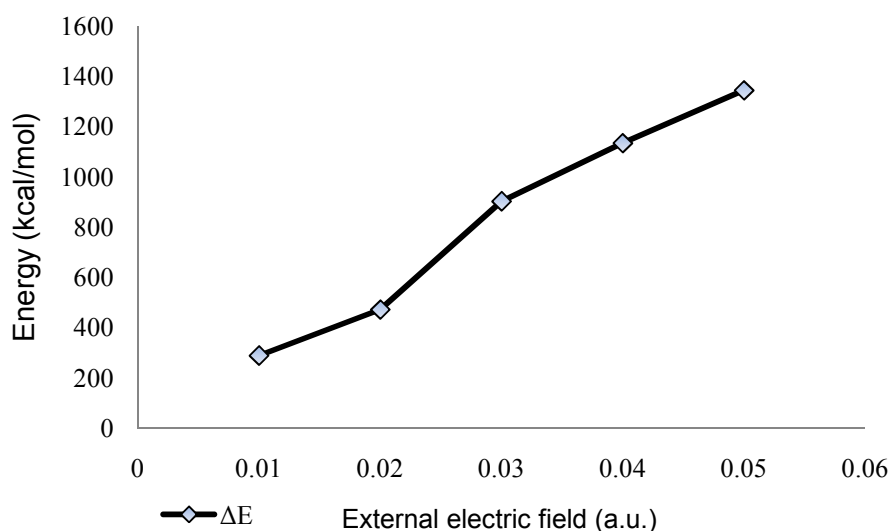


Figure 5.8. Variation in total steric energy as a function of applied external electric field.

The two strands of polymers were tightly bonded in a helical model, as shown by the plausible molecular model of the complex (Figure 5.9). This coiled coil state may be responsible for the non-decomposition, non-unwinding or non-eroding of the complex on its own in solvent. External electric fields may change the neutral arrangement of electrons on the surface of SAPDs and produce electrical forces that change the mechanical behaviour causing the adduct to form a coiled coil rather than an extended chain and resulted in the formation of globular aniline-vinyl complex. The MM simulations estimated the energy associated with vibration about the equilibrium bond length and the models tend to break down as a bond was stretched toward the point of dissociation. Further, the charge distribution affected the external electric field and made a new net field causing the outer shell of gel to reach the critical concentration for erosion and flake off. The increase in energy levels of harmonic oscillators, bond and angle terms, may have resulted in instability

which in turn caused complex dissociation followed by conversion of polymers into respective monomer units to stabilize the steric energy as electric field was increased in magnitude. These energy variations and subsequent erosion can be quantified in terms of amount of indomethacin released after the respective applied electric potential.

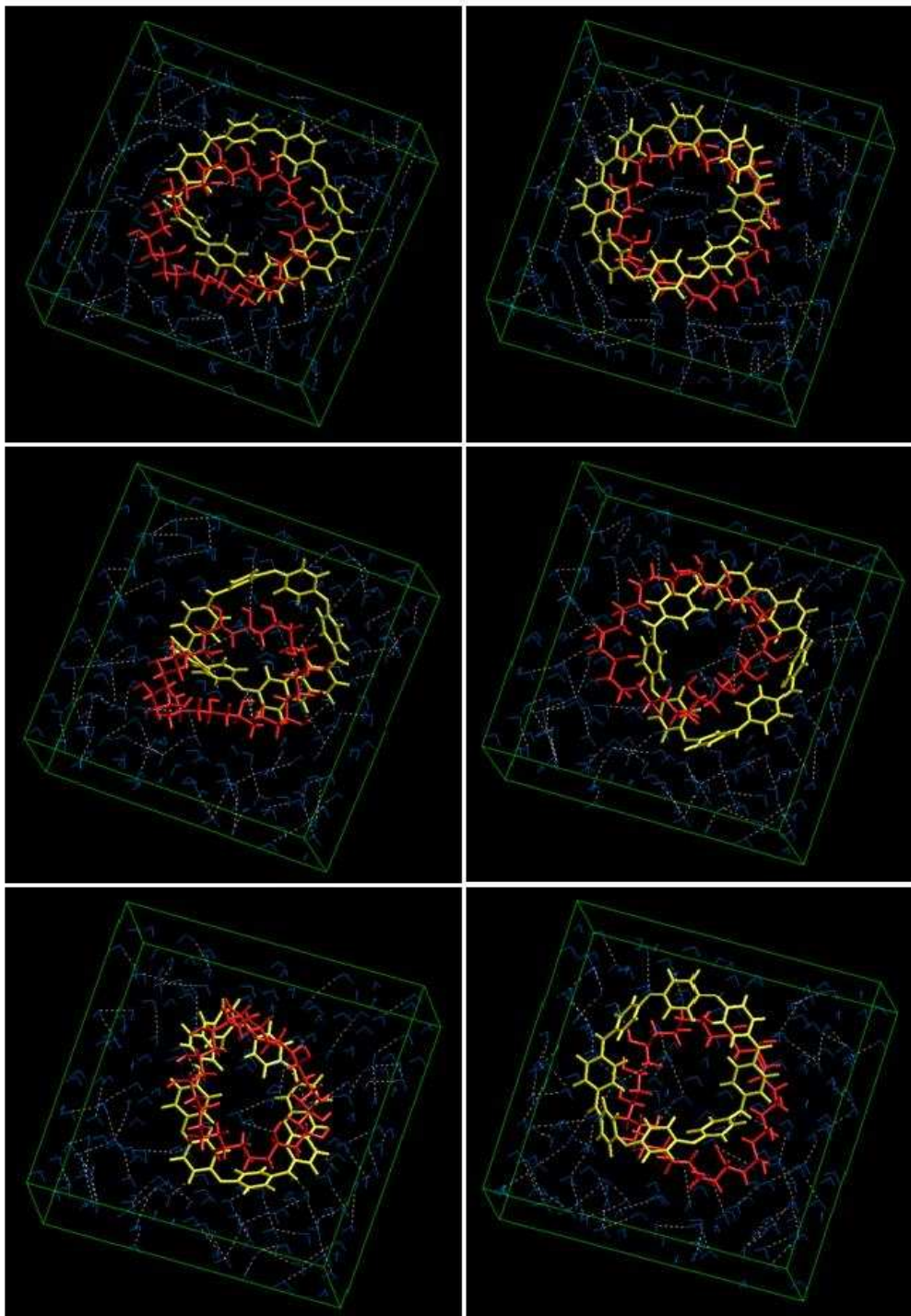


Figure 5.9. Visualization of geometrical preferences of PVA-PANi molecule after molecular simulation in a solvated system under external electric field. Colour codes- PANi (yellow), PVA (red) and water molecule (blue).

5.3.5. Rheological study of the Stimuli-Actuated Polymeric Device

The importance of rheological study in a hydrogel system is fundamental as the behaviour of the SAPD may vary between different temperatures (Carvalho, 2010). Rheology is the study of the flow of a matter. This study of flow is not particularly important in a solid as it did not exhibit much flow. In the case of a semi-solid and liquid, the stress and strain may affect the character of the substance, such as the case of a thixotropic flow. In this case, the system exhibited solid properties when left alone, but shifts to liquid properties when force was exerted onto the system (Donald, 1971). The study of rheology extends deeply into a wide variety of fields. Semi-solids which are mixed, sprayed, pumped, moulded, cooled, heated or rubbed have to undergo the rheological testing in order to test the stability of the system under various factors. Rheology has been mainly utilized in the pharmaceutical field as a polymer science. The characterization of the viscoelasticity behaviours of the polymers was an important factor, as it determined how the polymers behaved under mechanical stress. These properties may be affected by variables such as temperature, pressure, aging and the molecular weight of the polymer used. The testing of rheological properties is important in the field of pharmaceuticals in terms of tablet coating, spray coating, electrophoresis and roll coating (Honary, 2003). For the rheological study of the SAPD, the SAPD was initially dissolved into water by heating, upon which a gel was formed. This gel was tested by the use of a rheometer in order to assess the rheological property of the SAPD. The SAPD was dissolved by immersing 3.2g of SAPD into 10mL of water. The water was heated to boiling point and cooled to room temperature, which resulted in the gel formation. This gel was subjected to rheological study under specific test conditions. With the use of the rheometer, it was possible to determine the yield value and the storage and loss modulus of the SAPD in the semi-solid state. For a rheological study, there are several setups which may be utilized. These setups are shown in Figure 5.10.

Concentric
Cylinders – Very
low to medium
viscosity.

Cone and Plate –
Very low to high
viscosity.

Parallel Plates –
Low viscosity to
soft solids.

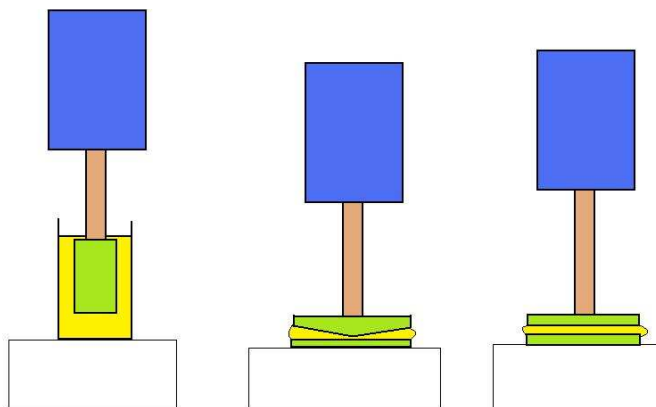


Figure 5.10. The possible setup of the rheometers which can be used. Each setup is suitable depending on the characteristic of the material being tested.

Since the SAPD formed a gel with an intermediate viscosity after it was dissolved, a parallel plate setup was chosen for this rheological assessment. The first test performed was the determination of yield value of the SAPD in the semi-solid form. This was done by plotting a stress-strain graph of the SAPD. The strain, which was the percentage displacement of the SAPD, was plotted against the stress, which was the pressure exerted upon the hydrogel. The determination of yield value was tested for the amount of force required before deformation occurred on the SAPD. The result may be depicted as Figure 5.11.

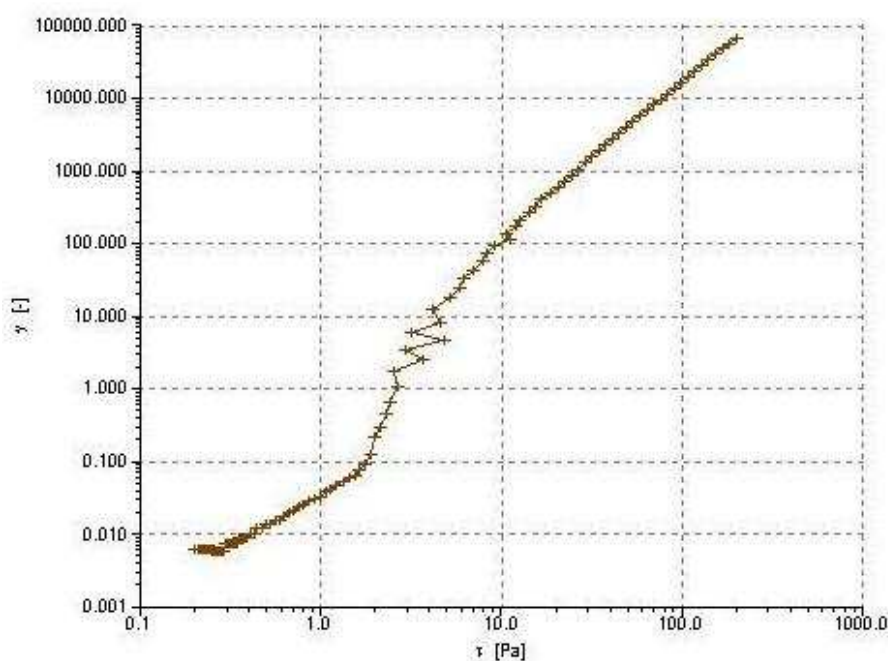


Figure 5.11. The yield value of the stimuli-actuated polymeric device.

The yield value indicated by the rheometer suggested that 1.295 Pa was required in order to deform the SAPD from its elastic state. This data demonstrated that the SAPD is capable of withstanding 1.295 Pa of force before permanent deformation occurs. The determination of the yield value was important as it allowed assessment of the pressure that the SAPD was able to withstand before it undergoes deformation. However, it did not assess the viscoelastic behaviour of the polymer system. For this purpose, the oscillatory rheology was used in order to assess the mechanical behaviours of the SAPD.

Oscillatory rheometry exerts a sinusoidal shear deformation to the specimen held between the two plates. The bottom plate exerts a strain on the sample via rotation, while the top plate remains stationary. A sinusoidal strain deformation was exerted to the sample, and the resultant torque exerted by the sample onto the upper plate was recorded as stress. The lag between these stress-strain relationships would demonstrate whether the sample exhibited predominantly plastic, viscous or viscoelastic properties. This relationship may be presented in Figure 5.12.

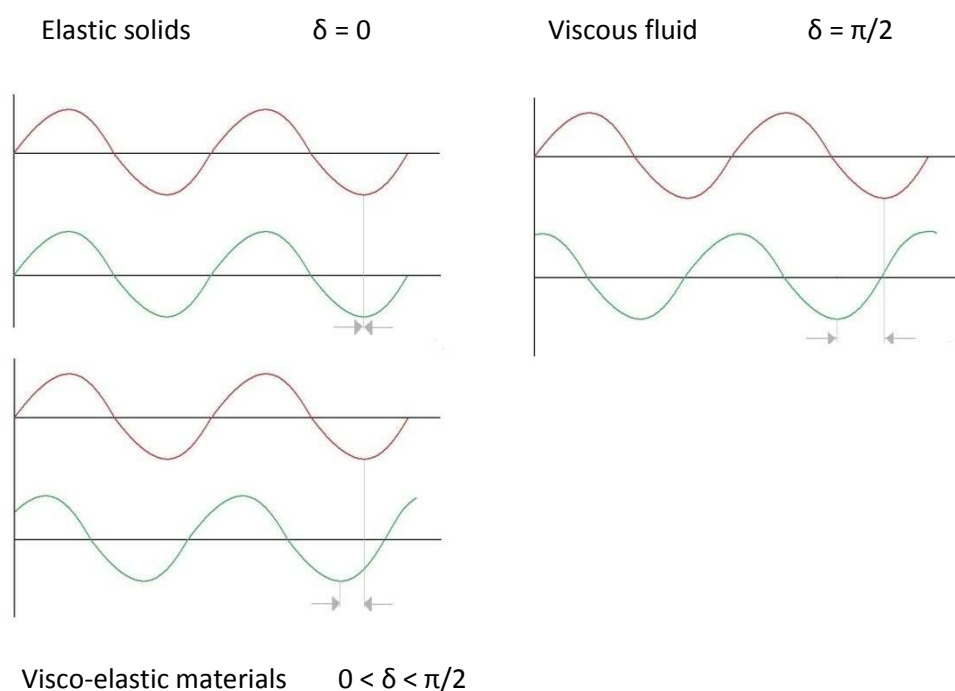


Figure 5.12. The lag between the stress-strain which may be used to determine whether the material under analysis exhibits predominantly liquid or solid properties (Weitz, 2007).

This information allowed us to determine the storage modulus (G'), loss modulus (G'') and the dynamic viscosity. The measurement of these factors assisted with evaluation in regards to solid or liquid behaviour of the SAPD at any time when the sinusoidal shear was exerted. In order to determine the modulus characteristic of the SAPD, oscillatory frequency sweep

was performed. The aim of this test was to start from a low frequency and end up with a high frequency while measuring the storage and loss modulus of the SAPD on the same set of axis. The result would be the crossover frequency and the modulus characteristic of the SAPD under different forces. This study started from a frequency of 0.5Hz and was continued until the loss modulus and the storage modulus crossover. The results obtained would allow determination of the shear when the liquid characteristics of the SAPD were equal to that of the solid characteristics. The result obtained was depicted as Figure 5.13.

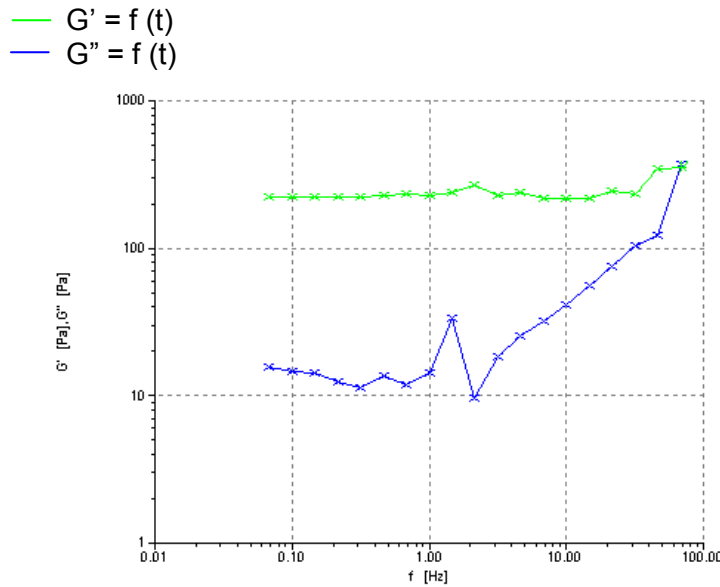


Figure 5.13. The results obtained by oscillatory frequency sweep showing both the storage modulus and the loss modulus of the stimuli-actuated polymeric device.

The results obtained from Figure 5.13 have shown that the crossover frequency occurred at approximately 70Hz. Equation 5.1 was used in order to convert the frequency into cycles per second.

$$\omega = 2\pi f \quad \text{Equation 5.1}$$

Where ω = angular speed measured in radians per second.

f = ordinary frequency measured in Hertz

Based on the crossover frequency of 70Hz, the angular frequency may be calculated as $2 \times \pi \times 70$ giving an angular speed of 439.6 radians per second. In order to convert the radians per second into cycles per second, we divided the 439.6 by 6.283, giving a value of 69.97 cycles per second. This indicated that the SAPD was able to withstand a high amount of stress before the solid property was lost under room temperature.

The next part of the study was to assess the temperature stability of the SAPD. In this study, the angular speed was kept at a constant of 10Hz, while the temperature was increased gradually from 20°C to 50°C. The storage and loss modulus was recorded and the temperature where the crossover occurred was recorded. The results may be depicted in Figure 5.14.

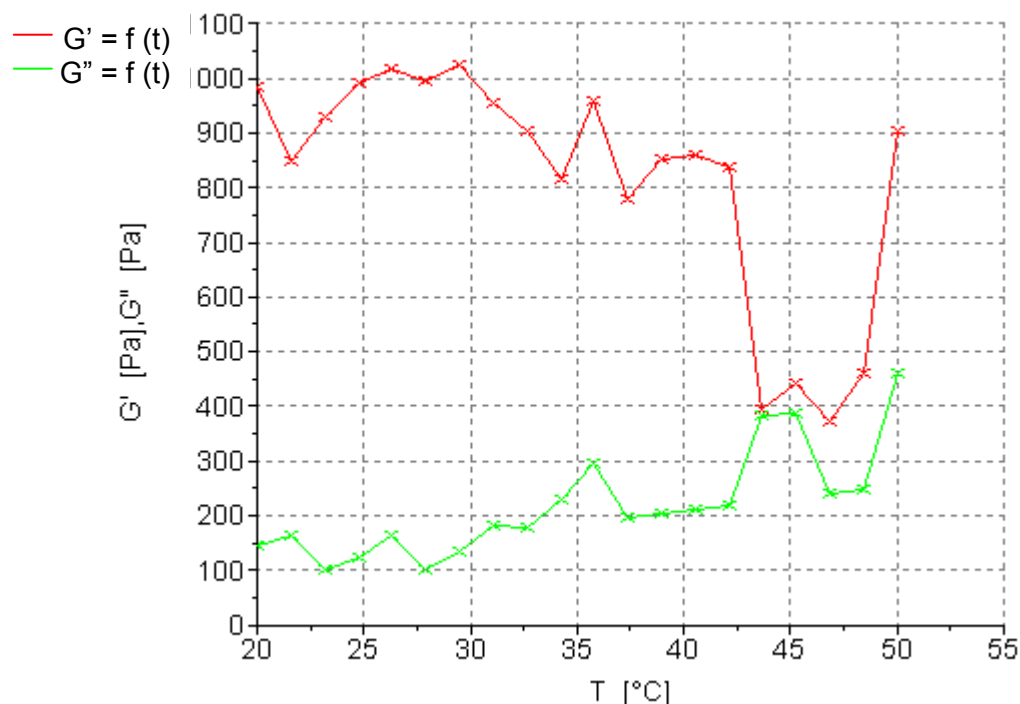


Figure 5.14. The effect of temperature on the storage and loss modulus of the stimuli-actuated polymeric device.

As with all semi-solids or viscous fluids, the higher the temperature, the more liquid properties it exhibits and the less viscous it becomes. Based on Figure 5.14, the SAPD exhibited primarily solid state behaviours until the crossover temperature was reached at approximately 43°C. At this point, the liquid state properties were almost equivalent to that of the solid state properties. Therefore, at a temperature of 43°C or higher, the SAPD would behave in a semi-solid manner, with liquid properties dominating at higher temperature. As indicated, the SAPD should be stable if stored below 40°C. By measuring these properties, it would allow the determination of the storage conditions of the SAPD in order to preserve its potency and efficacy. As indicated by the results obtained from this study, the SAPD offered good stability and handling under room temperature.

5.3.6. The comparison of the *in vitro* drug release profile between the Stimuli-Actuated Polymeric Device and the conventional oral system of indomethacin

This study aimed to compare the drug release profile of the SAPD as opposed to the conventional oral drug delivery system. The controlled release of SAPD should offer better targeted drug release with reduced side effects due to decreased systemic circulation of the indomethacin. The drug release profile of the optimized SAPD was compared against the drug release profile obtained from a 25mg indomethacin capsule. The capsules used for this study was the Arthrexin[®] 25mg capsule. The drug release profile was obtained by immersing the capsule in a buffer of pH1.2 and 6.4 respectively. The temperature of the buffer was kept at a constant of 37°C. The capsule was kept under a mesh positioned 2cm under the rotor in order to prevent the capsules from floating. The speed of the rotor was set to 50RPM as in accordance with the USP. Samples of 5mL were taken at an interval of 10 minutes and analyzed with the UV/visible spectroscopy. Five mL of fresh buffer was replaced after each sample was taken and the dilution factor was taken into account. The drug release from the indomethacin was expected to be higher in the pH 6.4 medium as it exhibited higher solubility in basic pH. The results obtained from the UV/visible spectroscopy may be depicted by Figure 5.15.

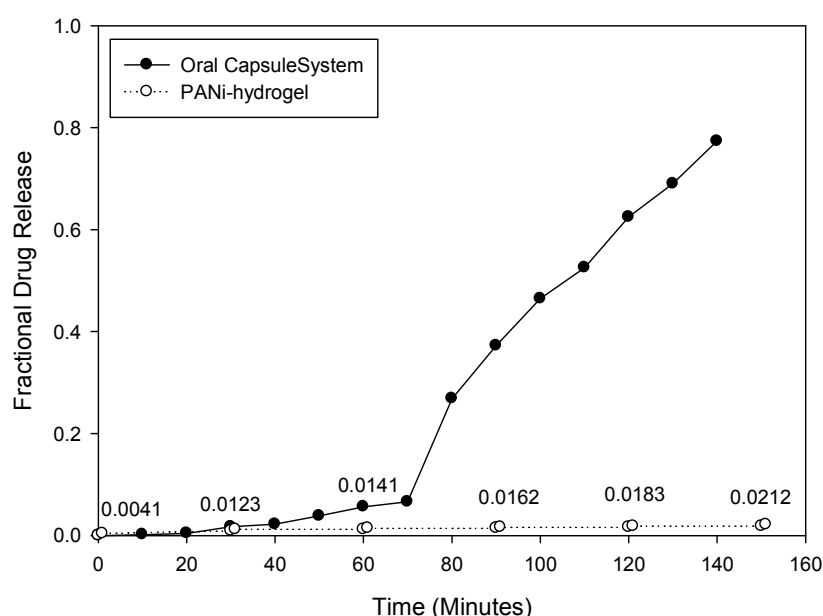


Figure 5.15. The drug release profile of the conventional oral system compared to the stimuli-actuated polymeric device.

The drug release profile from the oral indomethacin system was done with a gastric retention time of 70 minutes. The oral system was left in the pH1.2 buffer for 70 minutes, after which the system was transferred into the pH6.8 buffer. The drug release profile has indicated that drug release by the oral system in the stomach was minimal as compared to the intestinal

release. This may be attributed to the poor dissolution of indomethacin in the presence of an acidic environment as opposed to the basic environment of the intestine (Nokhodchi, 2005). The results obtained in Figure 5.15 showed that as opposed to the oral system, the SAPD was capable of controlled and prolonged release over a longer period of time with an “ON-OFF” mechanism. In addition, this would limit the amount of indomethacin in the systemic circulation and thus targeted release with minimal side effects. Another way to describe the advantage of this system over the conventional system may be shown by a computer generated simulation. This simulation depicted the conventional dose-related problem associated with oral system. The software simulation was performed with an eight hourly dosing of indomethacin. The results may be shown as Figure 5.16.

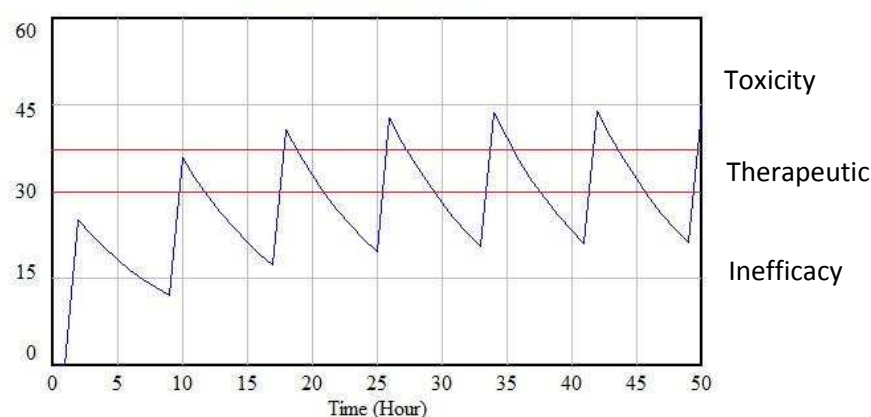


Figure 5.16. The computer generated simulation of an eight hourly dose of 25mg indomethacin.

Suppose the therapeutic window of indomethacin is between 30mg to 40mg of indomethacin, the drawback of a conventional oral dose becomes apparent. After the administration of the first dose, the patient would experience no effect since the drug had not reached the therapeutic windows. Following subsequent dosing, the patient did indeed reach therapeutic dose, but further dosing would result in peaks of toxicity whereby the patient would experience side-effects. The patient would also experience subsequent inefficacy where the drug diminishes below the therapeutic window some time before the next dose. This problem was commonly seen with oral dosing of drugs. With the use of targeted and controlled release of drug at the local site, it was possible to overcome these problems.

5.4. Concluding remarks

The use of HyperChem™ 8.0.8 Molecular Modeling System, ChemBio3D Ultra 11.0 and various other equipments allowed us to analyze and characterize the SAPD at a molecular

level. The use of these tools proved to be invaluable for the elucidation of the mechanism of drug release and erosion of the SAPD. The mechanism of erosion was indicated as the conversion of the polymer into the monomer and flaking of the outer crust of the gel due to charge distribution. The electroactivity of the SAPD was further assessed by the use of a cyclic voltammetry, which confirmed the presence of an oxidation-reduction reaction occurring when the SAPD was actuated. In addition, cyclic voltammetry has shown a shift of the redox peaks, thus suggesting an interaction of the PANi with one of the components of the SAPD. The optimization of the SAPD with the use of a 3 factor Box-Behnken Design allowed us to establish a relationship between the DAA, PANi and PVA with drug release, drug entrapment and erosion rate. The conductivity of the SAPD was further assessed and found to be directly proportional with the concentration of PANi in the hydrogel. This was further substantiated by the 3 factor Box-Behnken Design as an increase in the PANi has indicated an increase in erosion rate. This may be attributed to the increased conductivity of the PANi which resulted in an increased electrical flow through the SAPD and ultimately increased flaking and erosion. Lastly, the drug release profile of the optimized SAPD was compared against the conventional oral system. Results have indicated that indomethacin has a low dissolution rate in an acidic environment and drug release from the oral system was slow in the first few hours due to gastric retention. This may be attributed to the acidic nature of indomethacin which renders it insoluble in acidic environments. The dissolution rate did increase drastically when exposed to basic medium. This is also due to the increased solubility of indomethacin in a basic environment. The advantage of the SAPD would be the immediate availability of the drug at the target site whenever it was required by the patient. Factors effecting drug availability such as dissolution, first-pass metabolism and protein binding could be avoided. Since the drug release from the SAPD could be changed by varying the various components, it was also possible to synthesize SAPD ranging from slow release to fast release in order to treat different patients suffering from varying degrees of chronic pain.

CHAPTER 6

IN VIVO EVALUATION OF THE STIMULI-ACTUATED POLYMERIC DEVICE UPON SUBCUTANEOUS IMPLANTATION INTO A RAT MODEL

6.1 Introduction

The drug release profiles obtained from the SAPD has thus far been *in vitro*. Most of these *in vitro* studies have been, as much as possible, to simulate an *in vivo* environment. However, several factors such as extracellular fluids and skin conductivity were still difficult to replicate and the use of electric current through an *in vitro* approach may not provide an accurate drug release profile of the SAPD when implanted subcutaneously. The use of an animal model would provide a more accurate pharmacokinetic and pharmacodynamic profile of the SAPD.

The difference between *in vivo* and *in vitro* studies may be demonstrated by a simple example of bacterial exposure to an anti-biotic agent in an aqueous medium. Firstly, bacteria needed a surface onto which it adheres before it was capable of colonization and establishing an infection (Ethel, 2006; Soong, 2006 and Yah, 2008). The ultra-structure of the bacteria in an aqueous medium was also different to that of the bacteria found in human body. The rate of growth of bacteria *in vivo* was also slower than that compared to *in vitro* (Zak, 1982). The activity of certain anti-biotics such as beta-lactam was significantly affected by the rate of growth. Bearing the above factors in mind, it was clear that a pure *in vitro* study regarding the effects of anti-biotics was not sufficient and there was a need for further elucidation which required an *in vivo* study.

A study done on the *in vitro-in vivo* correlation for indomethacin has proven that blood samples and buffer samples did indeed show significant difference in drug concentration, T_{max} and C_{max} . This difference may range from approximately 9-74% for Area Under the Curve (AUC), 0-100% for T_{max} and 2-89% for the C_{max} based on the different apparatuses used (Lootvoet, 1992). Difference in data between *in vitro* and *in vivo* drug concentration was also observed in other drugs and correlation between the two sets of data was still necessary (Chen, 1995; Munday, 1955). The difference in blood concentration of drug between the two sets of data was not the only discrepancy. Another example was the potentiating effect that indomethacin has on the medullary cyclic AMP. Indomethacin was

thought to potentiate the hydro-osmotic action of vasopressin. This may be attributed to the ability of indomethacin to suppress the prostaglandins, especially that of prostaglandins E. However, the quantification of this effect was difficult to establish and *in vivo* study was necessary in order to obtain these results (Lum, 1977).

From an implantation point of view, drug release profile between *in vivo* and *in vitro* may differ greatly with just a small variant in thickness of skin, weight of animal model, drug concentration and particle size (Balasubramaniam, 2008). The site of implantation may also affect the drug release profile due to varying physiological factors present. Factors such as presence of inter-cellular protein would affect the interstitial colloidal pressure which would in turn affect drug release from the implant (Aukland, 1993). The degree of vascularisation was also important as the blood supply was responsible for carrying the drug away from the implantation site, and in certain cases, to the target site. Blood vessels also exhibited varying permeability in the human body, thus affecting the drug release profile further (Whang, 1989). Lastly, the rate of blood flow around the implantation area may vary and affect the drug release profile (Iyer, 2006). Blood flow may vary depending of the time of the day, exercising, blood pressure and various factors. These factors cannot all be accounted for by using *in vitro* study and hence an *in vivo* study for the SAPD was crucial in order to assess the pharmacokinetics and the pharmacokinetics of the SAPD as accurately as possible.

The drug release from the SAPD was activated by the presence of an electric current through the skin. The use of electric current through an *in vitro* approach (e.g. electrolyte solution) did not provide an accurate drug release profile of the SAPD when implanted subcutaneously. The use of an animal model would also provide a more accurate pharmacokinetic and pharmacodynamic profile of the SAPD.

Rats were a suitable model as it would be unethical to use human subjects as initial subjects. The use of animals larger than the rat would present problems as the number of animals required by the study was relatively large. One study conducted by Epping-Jordan *et al.* has subcutaneously implanted osmotic minipump containing nicotine using rat model (Epping-Jordan, 1998). Subcutaneous implant in rat model has been done on several studies in various fields of research (Tomilla, 2008; Russo, 2007; Macleod, 2005 and Arenaz, 2004). The blood samples obtained would be analysed with the use of High Performance Liquid Chromatography and Ultra Performance Liquid Chromatography.

6.2. Materials and Method

6.2.1. Materials

Mobile phase used was acetonitrile (Merck, Wadeville, Gauteng, South Africa), orthophosphoric acid (Merck, Wadeville, Gauteng, South Africa) and double deionised water obtained from the Milli-Q System. Control blank rat plasma was supplied from healthy donor. The drug used was indomethacin (Sigma Aldrich, Steinheim, Germany)). Healthy Sprague-Dawley rats were used for this *in vivo* release study. Blood samples were analyzed with the High Performance Liquid Chromatography (HPLC) model Waters 1525 Binary Pump with 2489 UV/visible detector. The column was a C₁₈ silica gel column (4.6×150mm, 5µm particle size, Waters) while the pre-filter used was a 0.44µm Millipore® filter. Further analysis was done with the Ultra Performance Liquid Chromatography model Waters Acquity Ultra Performance Liquid Chromatography System (Waters, Milford, MA, USA). The column used in the UPLC was a C₁₈ column (2.1×50mm, 1.7µm particle size, Waters). Tissue samples were sent to the IDEXX Laboratories for histological analysis.

6.2.2. Animal ethics clearance

This is to certify that this animal study has obtained clearance to use rats as an experimental model via the Animal Ethics Screening Committee (AESC) of the University of the Witwatersrand (As per Appendix).

6.2.3. *In vivo* studies to assess the biocompatibility and drug release kinetics from the Stimuli-Actuated Polymeric Device

Studies were conducted on Sprague-Dawley rats in order to assess the drug release profile of the SAPD. The SAPD was implanted subcutaneously, blood samples were taken at pre-determined time intervals and the results of the Control Group were compared to that of the Placebo Group. This would allow the quantification of the drug release from the SAPD *in vivo* in the rat. The blood samples were assessed for any presence of drug which would indicate drug release from the SAPD. In addition, tissue samples were harvested from the implantation site and histological examinations were performed in order to assess for any long-term inflammations or tumor formations.

6.2.4. Method and approach for the *in vivo* study of the Stimuli-Actuated Polymeric Device

All animal study procedures and surgeries were performed in collaboration with the Central Animal Service (CAS) of the University of Witwatersrand. The number and characteristics of animals required for this study was shown in Table 6.1

Table 6.1. The amount and species of animals required for this animal study.

Species	Strain	Sex	Age/Body Mass	Number required	Location
Rat	Sprague-Dawley	M/F	200-250g	18	Central Animal Service

This study was an interventional study. 18 rats with an initial weight of 200-250g were randomly assigned to 3 groups (n=6 in each group).

1. Test group 1 (n=6): SAPD was subcutaneously implanted into the flank (abdominal area) of each animal in this group. This group received a SAPD containing approximately 16mg/kg of indomethacin (van Kolfsooten, 1985).

2. Placebo group 2 (n=6): SAPD was subcutaneously implanted into the flank (abdominal area) of each animal in this group. This group received a drug-free SAPD.

3. Comparison group 3 (n=6): The rat in this group would receive intravenous administration of indomethacin (0.8mg/100g body weight) 15 minutes prior to their blood sample taken (Lacroix, 1996).

All the groups were provided with water and food *ad libitum*. The rats were caged in groups of fifteen and maintained on a 12hour light/12hour dark cycle. They were weighed daily so as to indicate their general state of well being. Cage activity by means of observation for 1 hour periods daily was in order to use to assess state of well being. At the final sampling point, rats from Group 1, 2 and 3 were sacrificed. The procedure of this animal study may be summarized by Figure 6.1.

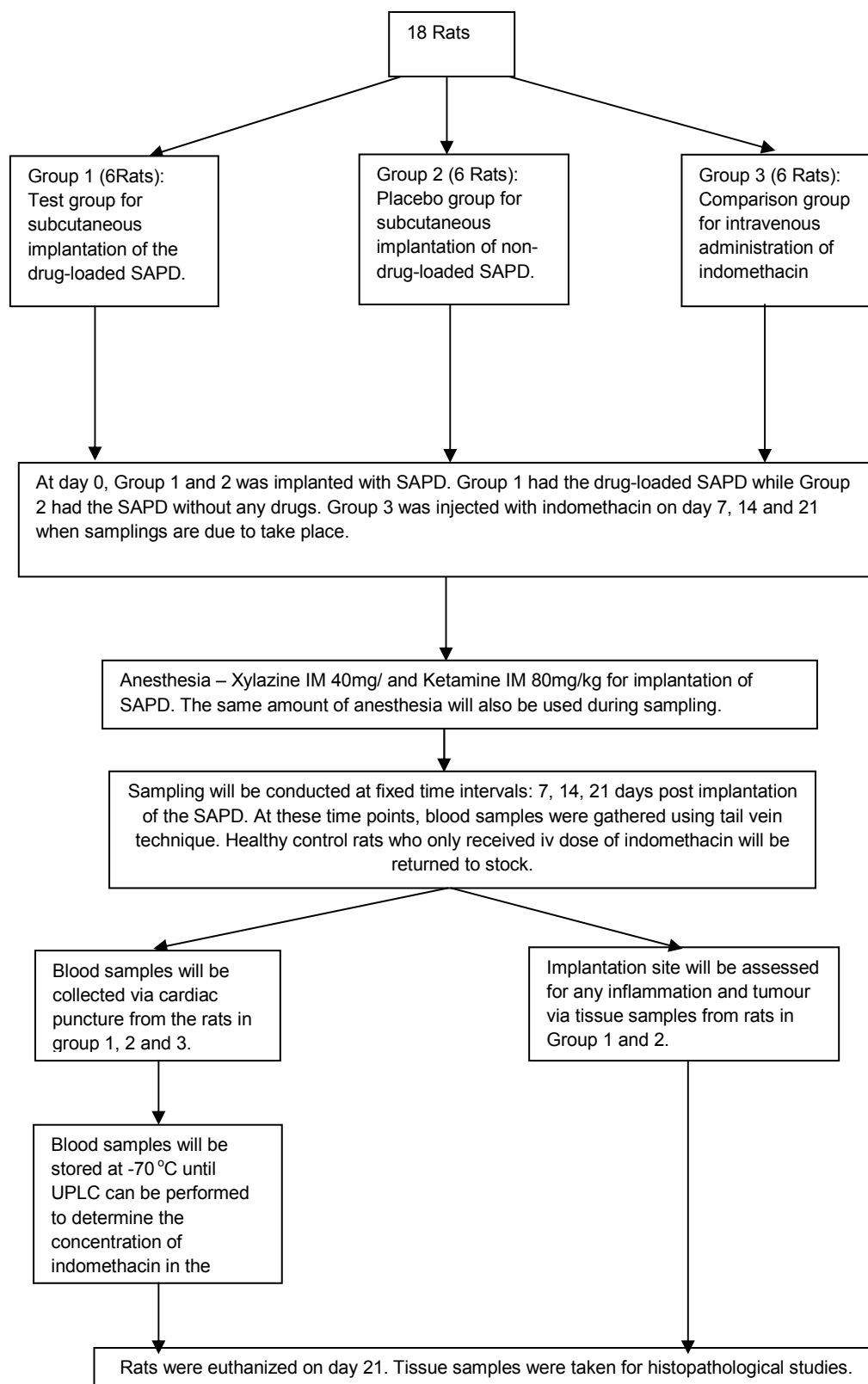


Figure 6.1. Schematic showing the design of the *in vivo* studies model for each time period.

6.2.5. Implantation of the Stimuli-Actuated Polymeric Device into the rat model

Six Experimental Group rats and the 6 Placebo Group rats were implanted subcutaneously in the flank (abdominal area), as shown in Figure 6.2, with the SAPD (1 x 1 x 0.3cm when fully hydrated). This was performed while the rats were under anaesthesia with xylazine (5mg/kg) and ketamine (100mg/kg). A 1.5 cm incision was made in the lower left flank for implantation and closed with a surgical wound clip. An injection of buprenorphine 0.1mg/kg subcutaneous injection was administered for 3 days after the surgery (Sweet, 2007).

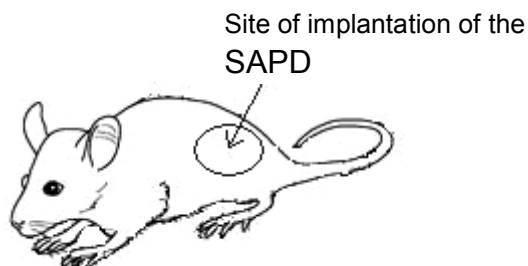


Figure 6.2. Sketch of the rat showing the site of implantation of the stimuli-actuated polymeric device into the flank abdominal area.

The SAPD was synthesized, loaded with indomethacin (16mg/kg) and sterilized (van Kolfshoten, 1985). The dimension of the SAPD for implantation was 1 x 1 x 0.3cm when fully hydrated. The SAPD was sterilized with Hibiscrub prior to implantation. Rats in Group 1 and 2 would receive the drug-loaded SAPD and the drug-free SAPD implanted subcutaneously respectively. Animals were first anaesthetised with xylazine (5mg/kg i.m.) and Ketamine (100mg/kg i.m.). The SAPD system was implanted on day 0 as a once off procedure.

The rat may develop an inflammatory response due to the presence of the implant. This would be treated with appropriate anti-inflammatory agents followed by a resting period in order to prevent any possible interference with the study. However, if the inflammation results in severe distress to the rats, those rats would be removed from the study. The experiment would also be terminated if the rats experience severe side effects such as gastrointestinal haemorrhage. Considering that the rats would be carrying the SAPD, indications of the animal being in distress such as a 15% reduction in weight or animals displaying sickness behaviour or showing deteriorating body condition would also result in the rats being removed from the experiment.

Once the SAPD was implanted, a potential difference of 1V would be applied to the SAPD implantation site. By applying the potential difference away from the heart, we aimed to prevent the current from flowing through the heart, thereby avoiding any possible fatality and

injury in the rats. Currently, no study has been done on the safety potential difference which could be applied to the rat. A potential difference of 1V was chosen because it was considered relatively safe. Commercial electronic rat traps such as Victor M240 Electronic Rat Trap[®] utilizes 8500V in order to kill a large rodent. Two electrodes was placed on the lower flank of the rat and a controlled voltage was applied by the use of a potentiostat (PGSTAT302N, Autolab, Utrecht, Netherland) in order to monitor the voltage going through the rat at any time. PGSTAT302N was utilized as it allowed the potential difference to be monitored at all time as well as safety termination of this study should a fluctuation occur. The experiment would be cut off at anytime should the voltage exceed 1.5V or the current exceed 200mA. The duration of the electric current during the sampling was 1.5 minutes. This sampling procedure would take place on day 7, 14 and 21.

6.2.6. Electrical actuation and safety procedures

The rat was placed on an insulating material and conductive gel was applied onto the two electrodes in order to enhance the current flow in order to ensure a conductive skin/electrode interface. The two electrodes were placed next to each other at the lower left flank. This setup was important as it directed the pathway of the current away from the heart and prevented any fatalities in the rat model. Under conventional circumstances in an electrical mat, the pathway of the current enters the rat from one of its legs and exits from another. This pathway would direct the current to pass through the heart of the rat and results in death. However, by placing the electrodes next to each other on the lower flank, the pathway of the current is cut short in order to prevent fatalities of the rats. This may be explained further in Figure 6.3 and 6.4.

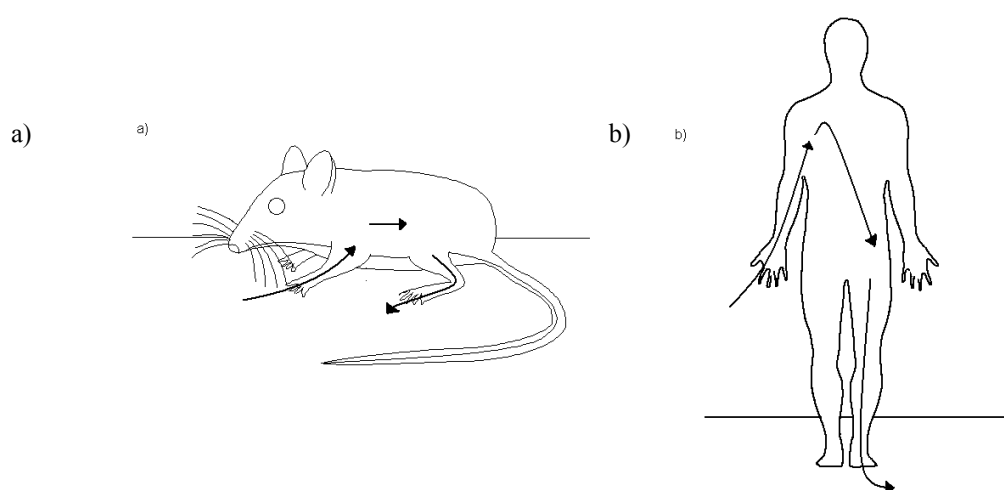


Figure 6.3. The pathway of a conventional electric shock.

From Figure 6.3, one can see that during an electrical shock, the current enters from the source and exits to the ground. In Figure 6.3 a), the electrical mat induced a current entering from the one leg of the rat and exits from the other, while in Figure 6.3 b), the man may have touched a bare wire with his right hand and as a result the current flowed through him to the ground. In both cases, there was a chance that the current would flow through the heart, leading to fatality. In Figure 6.4, we can demonstrate how this can be avoided.

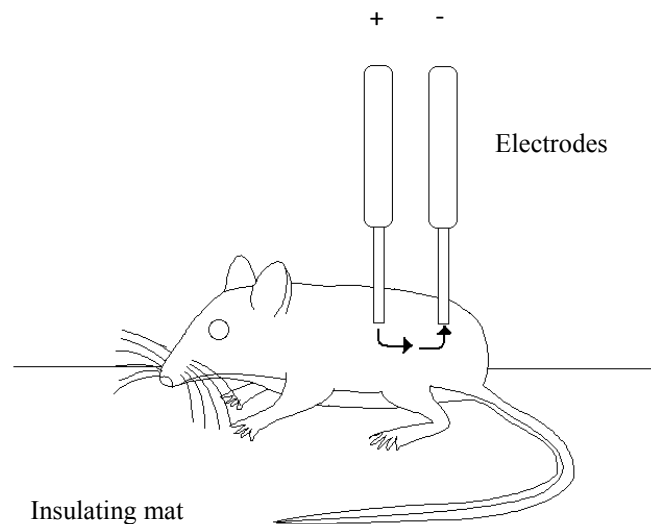


Figure 6.4. The setup to be used for the actuation of SAPD via electrical stimulation from the PGSTAT.

In Figure 6.4, the rat was placed on an insulating mat, thus preventing the electrical current from being grounded. The current entered the rat from the working electrode. Since there are no other pathways for the current to travel, the only option was to exit via the counter electrode placed adjacent to the working electrode. The electrode would be placed so that the SAPD was between the two electrodes and in the pathway of the electrical current, allowing actuation to occur. This setup would restrict the electric current locally and prevents the risk of injury or fatality to the rats.

Another safety measure may be attributed to the low voltage used with a DC setup for the testing of the SAPD. The threshold for rat muscle contraction to occur is measured to be approximately 0.03mA with maximum contraction occurring at approximately 0.2mA (Sobotka, 2010). In order to determine the quantity of current flowing between the two electrodes, Equation 6.1 was used.

$$I=V/R$$

Equation 6.1

Where I = current flowing in Amperes, V = the potential difference applied in Volts and R = the resistance of the conductor in Ohms. The electrical resistance of the rat skin is currently unknown, however, research done on human skin has indicated an electrical resistance of approximately 100000Ω on a dry skin (Fish, 1993). Therefore, application of 1V on a dry skin would yield $1/100000 = 0.01\text{mA}$ which is below the threshold for any form of muscle contraction to occur. A local application of 1V of potential difference should be, in this instance, adequate for the actuation of the SAPD without causing any injuries or fatalities to the rat model.

During the experimentation, the rat may experience discomfort such as stress, anxiety and fear. The use of electric current should not cause pain as electrical stimulation does not activate the nociceptors. Furthermore, the mammalian somatosensory system appears to lack receptors which are dedicated especially for electrical stimulation (Lindsay, 2005). The passing of electrical stimulation may induce involuntary muscle contraction (Bradford, 1985). Electrical stimulation therapy used to stimulate muscles generally used between 100-500V of potential difference, therefore the application of 1V should be sufficiently safe so as to avoid any discomfort caused from involuntary contraction of the muscle (Wong, 1986). The last possible discomfort may be the heat build-up when electric current is passed for a prolonged period. This heat build-up is dependent on the resistance of the conductor, the potential difference and the current. This may be calculated by Equation 6.2, where P = power in watt, I = current in ampere and R = resistance in Ohm.

$$P=I^2R \quad \text{Equation 6.2}$$

The current flowing through the skin was approximately 0.01mA and a resistance of 100000 Ohm. Therefore, the power generated by 1V would equate to 0.00001W. This meant that the energy delivered between the two electrodes equates to 0.00001J/second ($1\text{W} = 1\text{J/second}$). If the placement of the electrode was 90 seconds, the total energy delivered to the rat was 0.0009J. This may then be converted into 0.000215cal ($1\text{cal} = 4.184\text{J}$). In order to increase the temperature of 1 gram of water by 1°C , 1cal was required. Therefore, the use of the PGSTAT over a period of 90 seconds would only increase the surface temperature by a maximum of 0.000215°C . This amount of power is inadequate to produce any burn or discomfort onto the skin of the rats.

During this period, the animal may be restrained by either placing it in a modified conical plastic bottle, or it may be wrapped in a linen cloth (Preedy, 1988 and Omaye *et al.*, 1987).

The conical plastic bottles may be setup in accordance to the one setup by Omaye and co-workers (1987). This restraint device allowed minimal movements from the rat while inflicting no pain. This device may be depicted as in Figure 6.5. The device was mainly composed of two plastic bottles and a restraining clamp. A hole on the side of the flank allowed electrode placement for one and a half minutes, after which the rat may be returned and blood samples drawn. In order to decrease the anxiety of the rat, the rat should not be picked up by its tail at all time (Hurst, 2010). This sampling procedure would take place on day 7, 14 and 21.

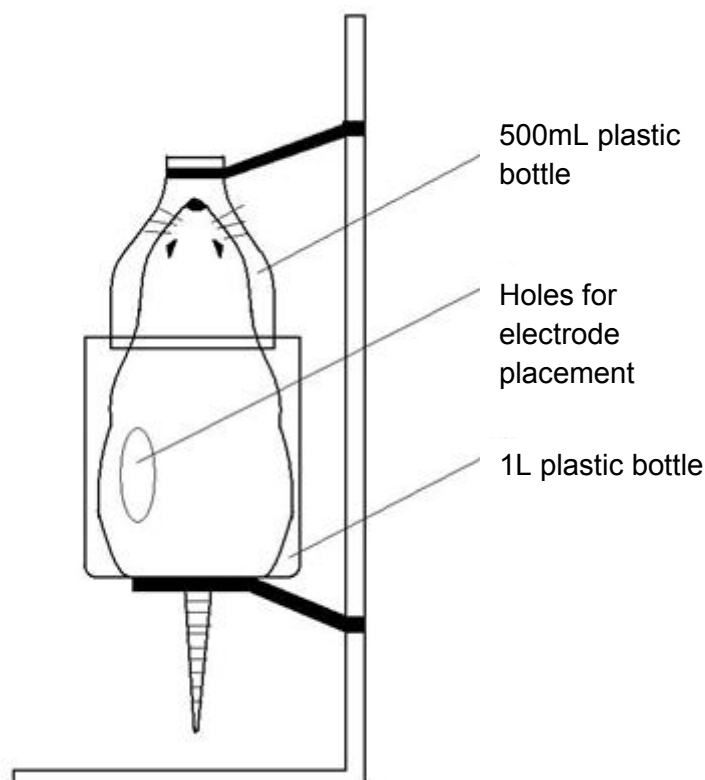


Figure 6.5. The setup of the rat restraint device during the drug release testing.

The animals were inspected around the implantation site for any signs of inflammation, infection on day 7, 14 and 21. This was also essential in determining the biocompatibility of the SAPD. Blood was drawn on day 7, 14 and 21 following the exposure of the SAPD to 1V. On average, the total blood volume of the rat is around 6-8% of total body weight. For non-terminal blood collection, 0.2-0.3mL of blood may be obtained from the tail vein, which was performed on day 7, 14 and 21 (Hoff, 2000).

The blood samples obtained from the rats were assessed for the presence of indomethacin by the use of HPLC. Initial blood samples obtained would be centrifuged at 3000G and the plasma was mixed with a solvent and injected into the HPLC in order to determine if there was any indomethacin present.

Anaesthesia was induced before the implantation and sampling of the SAPD. The anaesthesia was achieved with xylazine (5mg/kg) and ketamine (100mg/kg) prior to the procedure. This also ensured that the rat was in the correct position when the blood was drawn and prevented any possible injury which could be done to the rats (Hoff, 2000)

6.2.7. Drugs and medicinal substances to be used for this animal study

The drugs used for this study has to be dosed according to the amount required for therapeutic effects in a rat model. This included any drugs used for anaesthesia, the model drug used in the SAPD and the drug used for euthanasia. These drugs were administered by a veterinarian at the Central Animal Service (CAS) of the University of Witwatersrand. These drugs may be summarized in Table 6.2.

Table 6.2. The amount of drugs to be used for the animal study.

Drug/Substance	Route	Dose	Frequency
Indomethacin*	i.v.	0.8mg/100g	i.v. administration of the drug will be done weekly
	contained in the SAPD	16mg/kg	A once-off implantation of SAPD and weekly sampling
Xylazine**	Intramuscular injection	5mg/kg	Administered before implantation of SAPD and prior to euthanasia.
Ketamine***	Intramuscular injection	100mg/kg	Administered before implantation of SAPD and prior to euthanasia.
Sodium Pentobarbitone****	Intracardiac injection	200mg/kg	Administered once off for euthanasia.

* (van Kolfshoten, 1985)

** (Lacroix, 1996)

*** (Koshikawa, 1988)

**** (Kirschvink, 2005)

The i.v. administration of indomethacin would allow comparison between the i.v. dose, which was an instantaneous drug delivery form, against the SAPD and gave us an indication of the quantity of drugs entering the systemic circulation at any given time. Ideally, the drugs should be entrapped within the intercellular space at the site of inflammation as to permit entry of the drug into the cell membrane. Once into the cell membrane, the drug inhibits COX II enzyme, therefore preventing the conversion of arachidonic acid into prostaglandins

(Cheng, 2007). The amount of drug which entered the systemic circulation should be traceable in order to confirm the release of drug from the SAPD.

The drug was administered via the femoral vein of the rats (Wang 2010 and Mok, 1992). The dosage used is 0.8mg/100g (Lacroix, 1996) for this i.v. injection. An i.v. administration of 1.5mL has been done on rats weighing as little as 150g (Khong, 2000). For our purpose, 1.5mL injection will be sufficient. The rat in the comparison group should be weighed and the dosage calculated at 0.8mg/100g. The required amount should be dissolved in 1.5mL of sterile saline solution using aseptic technique following disinfection by UV light before it was given as an i.v. dose.

6.2.8. Plasma sampling from the rat model after the experimental procedure

Plasma levels of indomethacin were measured via blood samples obtained around the SAPD implantation site and would be analyzed using the High-Performance Liquid Chromatography (HPLC). The blood sample was obtained by the tail vein technique. This was performed by two people. One person restrained the rats by the use of a tightly-fitting, homemade bag of towelling while exposing the tail. The tail was held with one hand while an incision is made with the other hand. The tail was gently stroked and a blood drop formed at the site of incision. The blood drop may be collected for analysis (Fluttert, 2000). The tail vein technique was advantageous as the animal need not be anesthetized and it was not a terminal procedure (Oliveira, 2009; Beeton, 2007). The animal was returned to CAS until the next sampling was due to take place. The blood sample was stored in heparinised tube and centrifuge at 3000G for 15 minutes. The plasma sample was stored at -70°C until HPLC analysis (Sweet, 2007).

6.2.9. Liquid-liquid extraction technique for the separation of drug bound in plasma

Once the blood samples have been extracted from the rat model, the drug would have to be separated from the plasma sample before it was available for analysis via the HPLC. In order to achieve this, liquid-liquid extraction technique was used. The liquid-liquid extraction technique was used in cases where a solution contained two or more solutes. The solutes may be separated from each other by making use of the individual solubility of each solute. By placing the solution in the extraction fluid, the solutes would separate out from the solution into the extraction fluid based on its affinity for the extraction fluid. The extraction fluid typically contained an organic and inorganic phase and allowed the separation of non-polar solutes into the organic phase and the polar solutes into the inorganic phase. The two

solutes may be extracted following the evaporation of the respective solvents. This mechanism may be depicted in Figure 6.6.

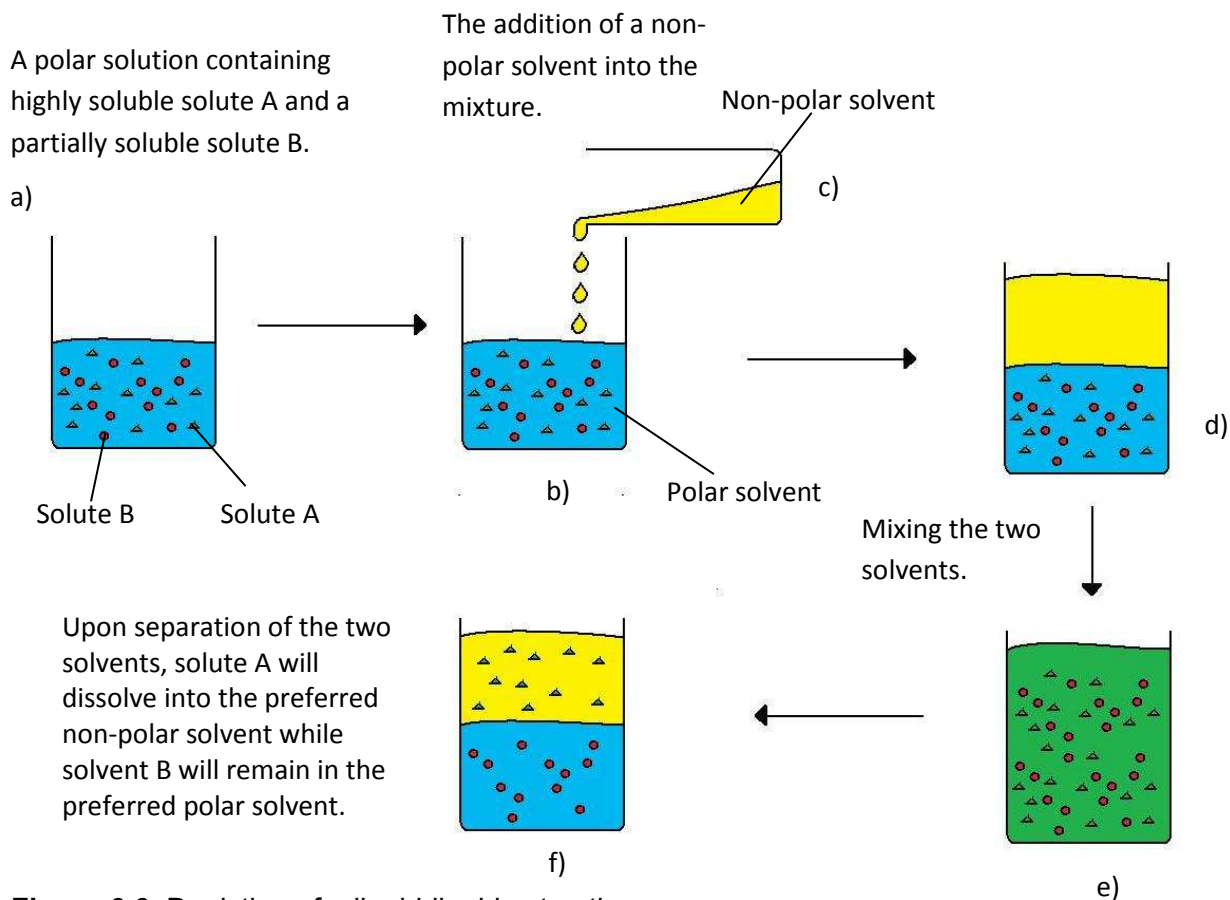


Figure 6.6. Depiction of a liquid-liquid extraction.

Based on Figure 6.6 above, the two different solvents may be separated when solutions were left to evaporate. By using this technique, it was possible to separate a drug from a blood sample collected from the rat model. The blood was centrifuged and the plasma was collected. The processed plasma sample may be mixed with another solvent in order to extract the drug out of the plasma. In the case of indomethacin, an organic solvent should be used since indomethacin exhibits high solubility in organic solvents as compared to other solvents (Yadav, 2009).

This method was initially tested by dissolving 100mg of indomethacin into a pH11.5 NaOH solution. After the indomethacin was dissolved, 350mg of sucrose was added into the indomethacin solution as a mixture. This mixture was poured into a liquid extraction phase consisted of 40mL water and 40mL chloroform. This mixture was vortexed at high speed for 1 minute before it was allowed to stand for solvent separation. The top layer consists of the polar solvent and was extracted with the use of a 5mL syringe. This polar solvent was left to dry overnight and the dried extract was analyzed with FTIR. The result obtained has

indicated a successful extraction of the sucrose from the indomethacin/sucrose solution. The FTIR spectra may be depicted as Figure 6.7.

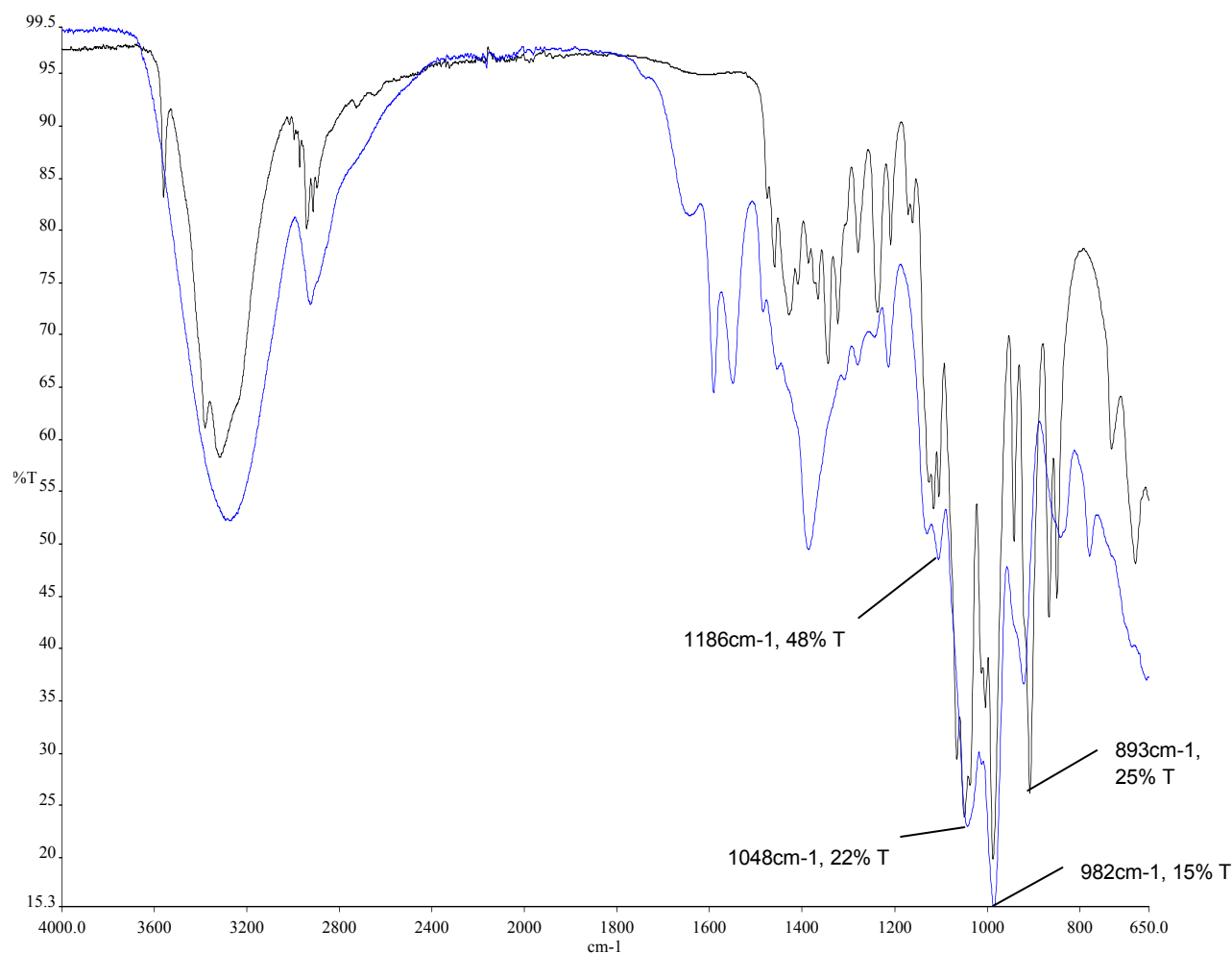


Figure 6.7. The FTIR spectrum obtained from the sucrose obtained via the liquid-liquid extraction technique is depicted as blue, while the FTIR spectrum of pure sucrose is depicted in black.

It was possible to determine that the dried extract obtained from the polar solvent was sucrose based on the comparison of the FTIR spectrum obtained against that of pure sucrose. This may be further confirmed by the corresponding spectra within the fingerprint region of this FTIR spectrum (1500-400 wave numbers). The dried extract from the non-polar phase also depicted a similar result for indomethacin. Therefore, by using the liquid-liquid separation technique, it was possible to separate the drug component from the plasma component, thus allowing analysis of the drug concentration in plasma via the use of the HPLC.

6.2.10. Subcutaneous implantation of the device into the rat

The first step of this *in vivo* study was the subcutaneous implantation of the device into the rats. Eighteen rats were used for this study, with 3 rats housed per cage. The rats were caged one week prior to implantation to allow time for acclimatization. They were also weighed and checked on a frequent basis to ensure their health was in good condition prior to the implantation. Rats 1-6 received an implant which contained the active drug indomethacin, while rats 7-12 received a placebo device which contained no drug. The rats were numbered by the use of a permanent marker on the tail and were labelled 1-18 numerically.

Following the acclimatization of the rats, the devices were implanted subcutaneously while under general anaesthesia. The pulse during this time was monitored by the senior veterinary nurse, while the implantation was performed by the veterinary surgeon. The entire procedure was simple and quick, with each implantation taking 5-10 minutes. The devices were disinfected with Hibiscrub prior to implantation. Figure 6.8-6.13 summarizes the entire subcutaneous implantation procedure.

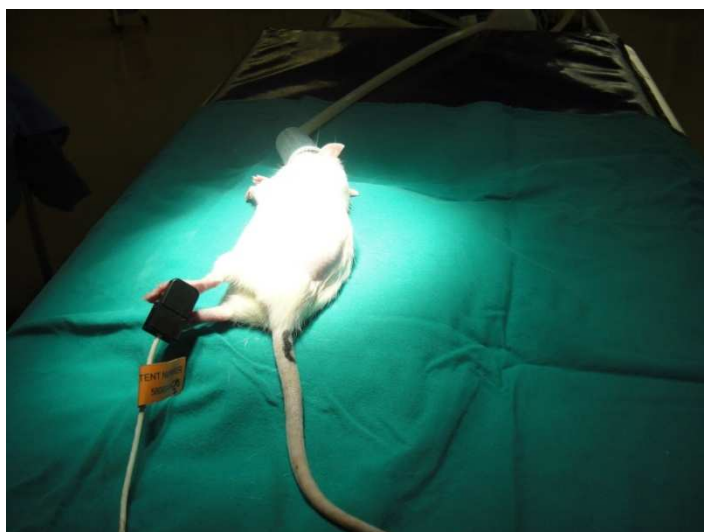


Figure 6.8. The rats were shaved on the left flank after general anaesthesia. Oxygen was given and pulse was monitored at all times.



Figure 6.9. The animals were draped and the surface was cleaned with Hibiscrub.

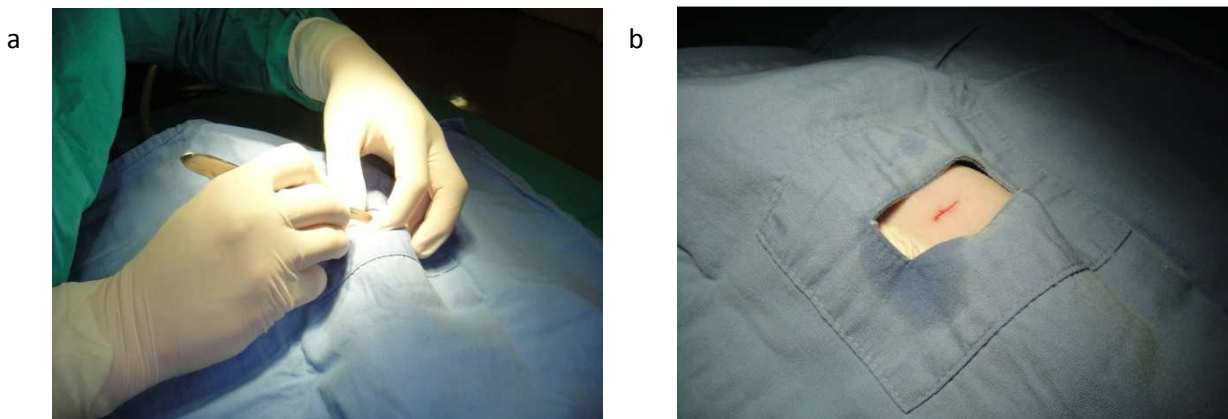


Figure 6.10. a) and b) A 1cm incision was made on the left flank of the rat.



Figure 6.11. The implantation of the device into a pocket made under the skin of the rat.



Figure 6.12. The incision was closed up by the use of suture.



Figure 6.13. Once the implantation was complete the rats were left in a cage where post-operative care was given until the animals had recovered.

Once the 6 active devices and the 6 placebo devices were implanted, the animals were given 10 days to recover and heal. Stitches were removed 5 days after the surgery. The rats were weighed again after ten days of recovery in order to determine their health condition. The implantation site was also checked for signs of swelling which indicated either inflammation or infection. The weight of the rats before and 10 days after the surgery are shown in Table 6.3.

Table 6.3. The difference in the weight of the rats 10 days after the implantation procedure was performed.

Rat	Initial Weight	Post-operation Weight (10 days)
1	230	250
2	222	232
3	238	251
4	233	252
5	228	241
6	224	247
7	224	223
8	219	236
9	228	237
10	215	222
11	214	218
12	218	235
13	235	246
14	222	236
15	234	245
16	211	224
17	238	242
18	218	225

The comparison of the weights before and after the operations has indicated that the rats were fit and healthy enough to proceed with the study. The rats did not show any signs of excessive weight loss. The post-operation weight also included the weight of the implantation.

6.3. Results and Discussion

6.3.1. High Performance Liquid Chromatographic analysis of plasma sample for the presence of indomethacin

Following the implantation of the SAPD into the rat model, blood samples were drawn on day 7, 14 and 21. The next step was the isolation of indomethacin from the plasma sample and analysis of drug release by utilizing the HPLC. The blood samples were taken from the rats which would indicate drug release from the device at the implantation site. Some of the drugs from the implantation site would be absorbed into the blood and presence of drug in the blood sample would indicate a release of drug at local site. Interstitial fluids cannot be used as sample since interstitial fluids in general does not yield enough quantity for analysis. Before the blood sample may be processed, it was collected in a heparinised tube. The recommended dosage for heparin is 70 units per 10mL. The blood samples gathered was 0.5mL, which required approximately 4 units of heparin. This equated to 4 μ L of the heparin

for the half mL blood samples. The collected blood samples were centrifuged and the plasma was extracted by the use of a 1mL syringe. The indomethacin was extracted from the plasma samples by the use of the liquid-liquid separation technique as mentioned. This was done by adding 100 μ L of phosphate buffer and 2mL of ethyl acetate into 400 μ L plasma sample. The mixture was vortexed vigorously for 10 minutes. The organic layer was separated and ethyl acetate was left to evaporate. The residue was re-dissolved in 200 μ L of the mobile phase and 50 μ L was injected for analysis by the HPLC. This method was adapted by a work done by Dawidowicz and co-worker (Dawidowicz *et al.*, 2009).

Before the samples could be analysed, a blank sample of indomethacin should be analysed for comparison purpose. This would assist us to ascertain whether the results obtained corresponded with that obtained by Dawidowicz and co-worker (2009). This method was tested by dissolving pure indomethacin into methanol at a concentration of 1mg/mL. Once the drug was dissolved, it was injected into the HPLC. The experiment was carried out under room temperature with a flow rate of 0.8mL per minute. The mobile phase consisted of 63% of acetonitrile and 37% of distilled water with the pH adjusted to 2 with 0.2% of orthophosphoric acid. The obtained result has indicated that the retention time did indeed correspond with previous study. This method seemed appropriate as the results had corresponded with that obtained from previous studies. The results may be presented as Figure 6.14 and 6.15.

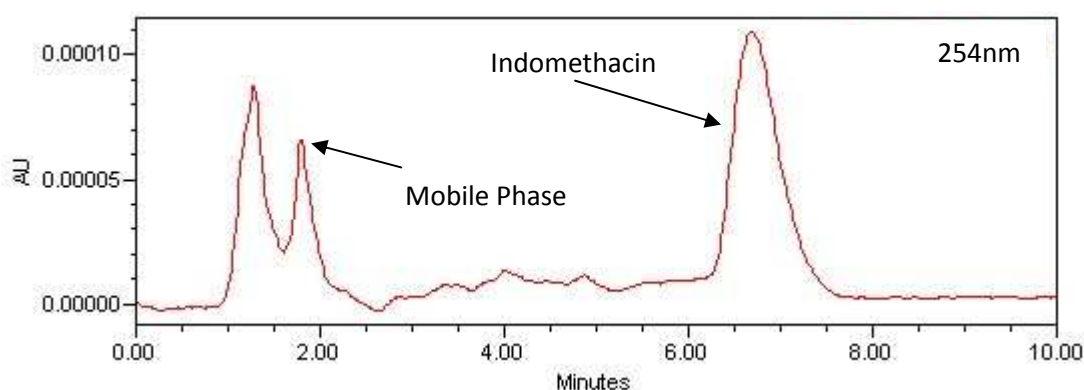


Figure 6.14. The HPLC chromatography obtained during the study.

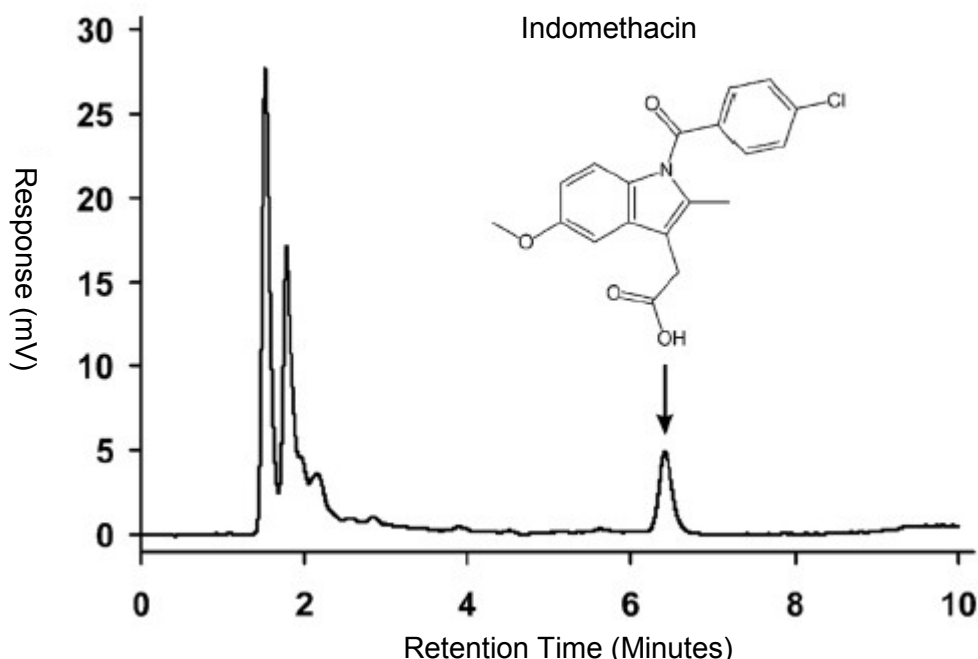


Figure 6.15. The HPLC chromatography obtained by Dawidowicz and co-workers (Dawidowicz *et al.*, 2009).

Based on the similarity of the two chromatography obtained, it was clear that this method was suitable for further analysis of the blood samples. The last part of the HPLC study was to assess whether heparin would be detected as a peak when injected into the HPLC under the same condition, since the blood samples would have contained heparin in order to prevent coagulation. The HPLC method was repeated identically, with the exception that the drug used was heparin. The results may be presented as Figure 6.16.

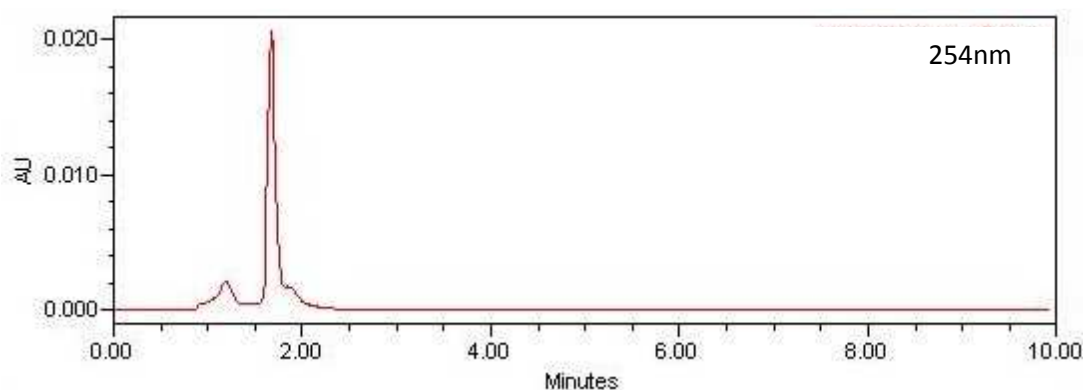


Figure 6.16. The chromatogram obtained from the HPLC when heparin was injected as sample.

As Figure 6.16 has depicted, the use of heparin did not interfere with the chromatogram at the wavelength of 254nm. The use of this method should prove to be appropriate for the sampling of blood sample for any presence of indomethacin. Once the method for HPLC was established, the blood samples may be further processed for injection into the HPLC to

allow further analysis for the concentration of drugs present. In order to determine the concentration of the drug in the blood sample, a calibration curve of indomethacin in the mobile phase was constructed. This graph may be presented as Figure 6.17 and was used to calculate the concentration of the total drugs present inside the blood sample obtained from the rat model.

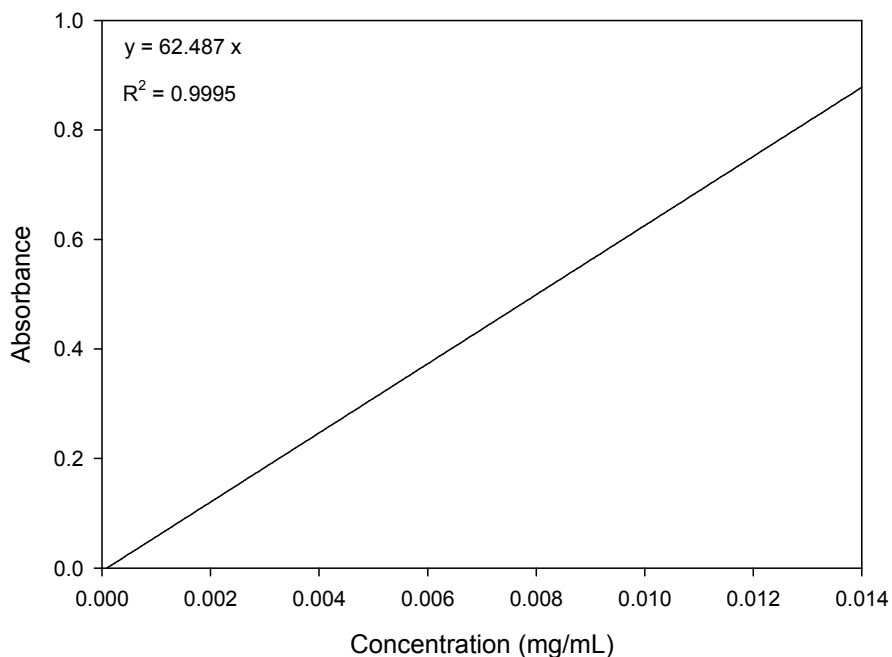


Figure 6.17. The calibration curve of the absorbance versus drug concentration in the mobile phase which may be used for determination of drug concentrations gathered from the rat model.

With the use of Figure 6.17, we would be able to work out the concentration of drugs in the blood sample based on the absorbance. The results obtained were depicted in Figure 6.18 a) to l) which depicted the blood sample obtained from rats in the Test Group and the Placebo Group.

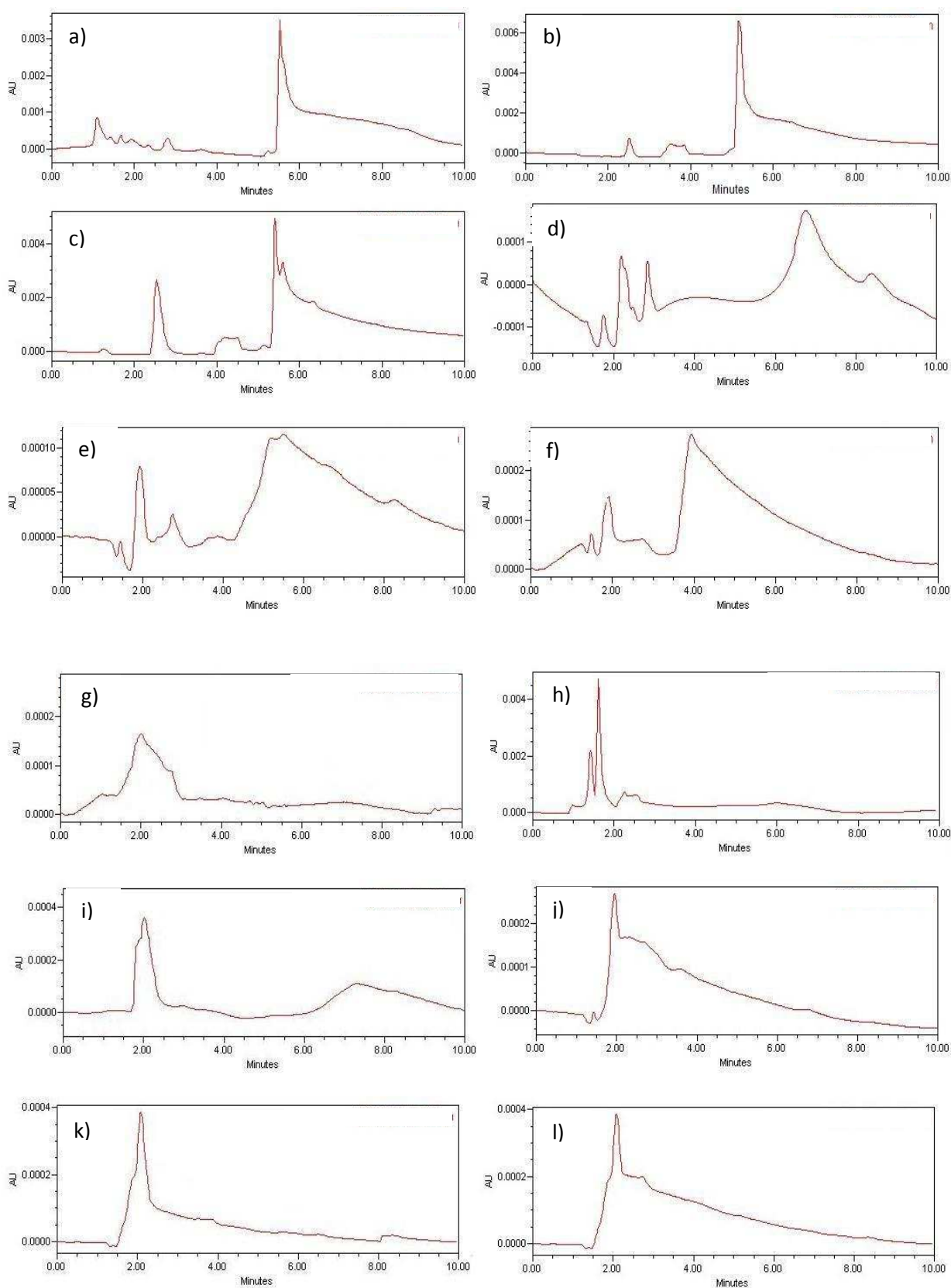


Figure 6.18. a) to f) indicated the blood samples obtained from rats in the test group, g) to l) indicates blood samples obtained from the placebo group.

As seen from the blood samples obtained from the test group, the presence of drug may be seen as a peak appearing around the 6th minute of the chromatogram. This peak was absent in the Placebo Group, which was used as a comparison for the Test Group. This absence of peak confirmed the release of drug in the test group. One set of blood sample taken between the 7 day release cycles has confirmed that, as indicated by the *in vitro* test, there was no drug leakage during each actuation. These results may be compared against the blood samples obtained from the comparison group in order to confirm that the degradation of the SAPD did not produce any possible untoward reaction during the release. The blood samples from the rats in comparison group may be presented as Figure 6.19.

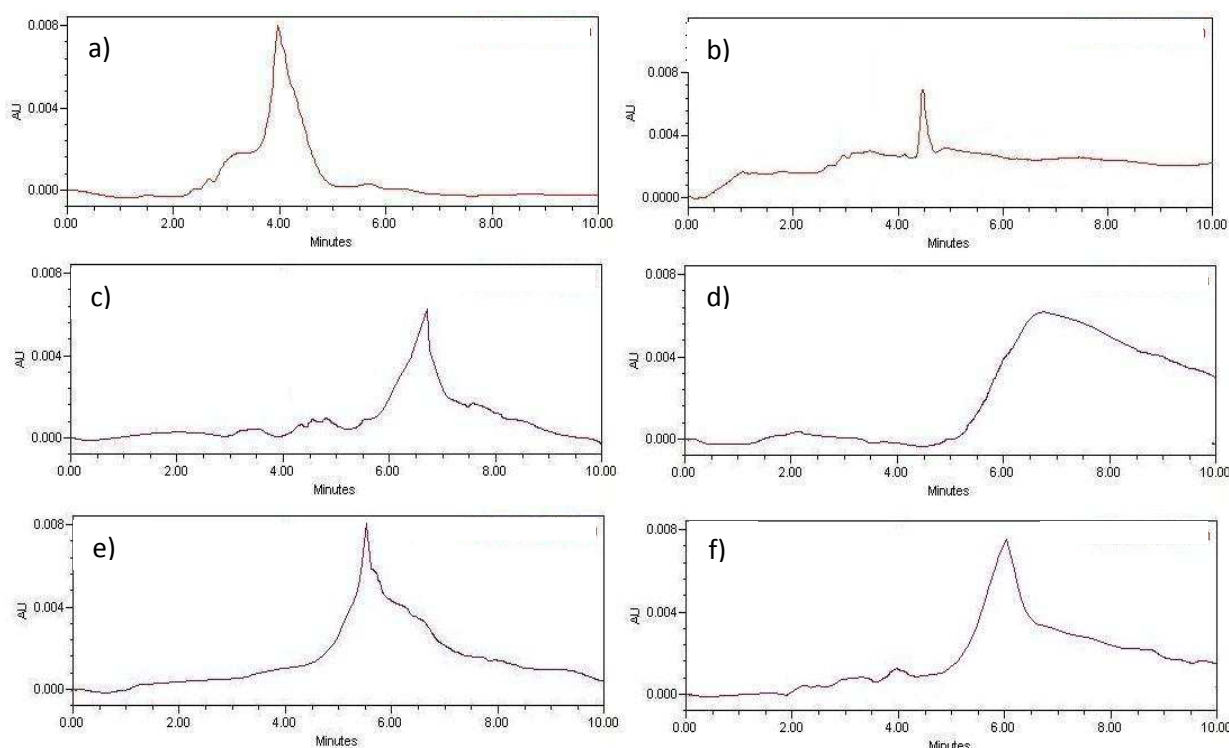


Figure 6.19. a)-f) The chromatogram of the 6 blood samples obtained when indomethacin were administered intravenously into the rats in the comparison group.

By using the data from Figure 6.17 and 6.18, one could see the chromatogram produced has indicated only the presence of indomethacin alone in the blood samples without any other possible metabolites which may occur during the release.

6.3.2. Further analysis of blood sample with the use of Ultra Performance Liquid Chromatography

The presence of drug in the rat plasma sample was further ascertained use the use of Ultra Performance Liquid Chromatography (UPLC). UPLC offered higher sensitivity and resolution with decreased retention time. Methods used on the HPLC may be incorporated onto the

UPLC, although several adjustments were required. The first adjustment required was the target injection volume. Since the column used in UPLC was much lower in dimension than the HPLC, volume adjustment was required in order to allow optimal analysis from the UPLC. The volume adjustment was done based on Equation 6.3.

$$\text{Target Injection Volume} = \text{Original Volume} \times \frac{\text{Target Column Volume}}{\text{Original Column Volume}} \quad \text{Equation 6.3}$$

By using Equation 6.3, the quantity of sample required for injection may be calculated as follows:

$$\text{Target Injection Volume} = 50\mu\text{L} \times \frac{3.14 \times 1.1^2 \times 50}{3.14 \times 2.3^2 \times 150} = 3.81\mu\text{L}$$

Besides from the quantity of the samples injected, the run time was also reduced due to the shorter column found in the UPLC. In order to determine the required run time for the UPLC, gradient duration from the original HPLC should be determined. The equation used for the calculation of gradient duration may be depicted as Equation 6.4.

$$\text{Gradient Duration} = \frac{\text{Gradient Volume}}{\text{Column Volume}} \quad \text{Equation 6.4}$$

$$\text{Gradient Volume} = \text{Flow Rate} \times \text{Time} = \frac{0.8\text{mL}}{\text{min}} \times 10\text{min} = 8\text{mL}$$

$$\text{Column Volume} = \pi \times r^2 \times \text{Length} = 3.14 \times 0.23^2 \times 15 = 2.49\text{mL}$$

$$\text{Therefore, Gradient Duration} = \frac{8\text{mL}}{2.49\text{mL}} = 3.21$$

The gradient duration of the HPLC column with a flow rate of 0.8mL/min for 15minutes was 3.21. The next part of the adjustment was the scaling of flow rate from the HPLC column to the UPLC column. This was done as using Equation 6.5.

$$\text{Target Flow Rate} = \text{Original Flow Rate} \times \frac{\pi \times r^2 \text{ of target}}{\pi \times r^2 \text{ of original}} = \text{Original Flow Rate} \times \frac{\pi \times r^2 \text{ of target}}{\pi \times r^2 \text{ of original}} \quad \text{Equation 6.5}$$

$$\text{Target Flow Rate} = 0.8\text{mL/min} \times \frac{2.1^2}{4.6^2} = 0.167\text{mL/min}$$

The last step was to calculate the gradient step time for the UPLC. This adjustment was necessary as the run time of the UPLC would be shorter than the HPLC and needed to be scaled down. This was calculated using Equation 6.6.

$$\text{Gradient Step Time} = \frac{\text{Gradient Step Volume}}{\text{Target Flow Rate}} \quad \text{Equation 6.6}$$

$$\text{UPLC Colum Volume} = \pi \times r^2 \times \text{Length} = 3.14 \times 0.105^2 \times 5 = 0.17\text{mL}$$

$$\begin{aligned} \text{Gradient Step Volume of HPLC} &= \text{Gradient Duration} \times \text{UPLC Colum Volume} = 3.21 \times 0.17 \\ &= 0.546\text{mL} \end{aligned}$$

$$\text{Gradient Step Time of HPLC} = \frac{0.546\text{mL}}{0.17\text{mL}} = 3.21 \text{ minutes}$$

Step 2 of the calculation required the calculation of gradient step time of the UPLC using Equation 6.7.

$$\text{Gradient Step Volume of UPLC} = \frac{\text{Gradient Step Volume of UPLC}}{\text{Target Flow Rate}} \quad \text{Equation 6.7}$$

$$\begin{aligned} \text{Gradient Step Volume of UPLC} &= \text{Gradient Duration} \times \text{Target Colum Volume} \\ &= 3.21 \times 0.17 = 0.5457\text{mL} \end{aligned}$$

$$\text{Gradient Step Volume of UPLC} = \frac{0.5457\text{mL}}{0.167\text{mL/min}} = 3.27 \text{ minutes}$$

Using the results obtained, we could then modify the HPLC method for the UPLC by keeping the same mobile phase, with an injection volume of 3.81 μ L, a flow rate of 0.167mL/min and a run time of 3.27 minutes. One set of blood sample from the placebo group and testing group were processed and injected into the UPLC. The results may be depicted as Figure 6.20 and Figure 6.21.

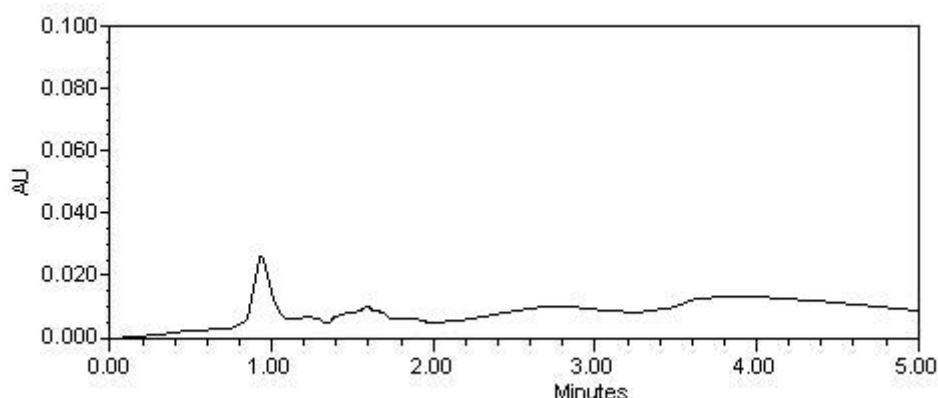


Figure 6.20. The UPLC chromatogram obtained for the rat blood sample in the placebo group.

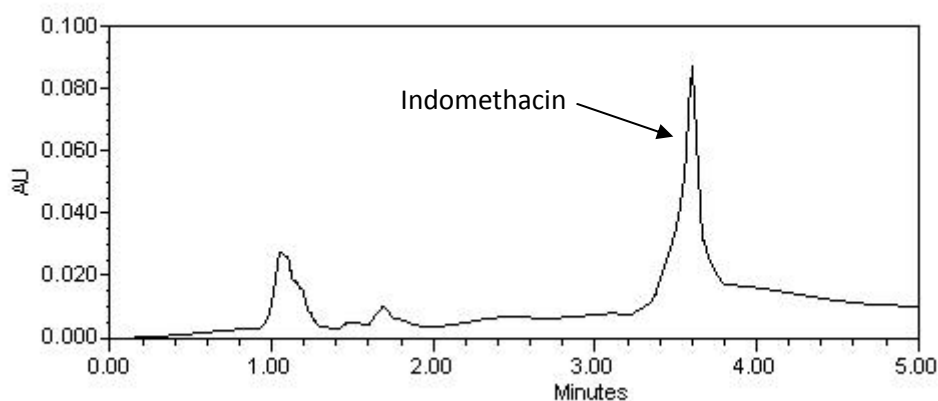


Figure 6.21. The UPLC chromatogram obtained for the rat blood sample in the test group.

Blood samples injected into the UPLC from the placebo group did not exhibit a peak at approximately 3.5 minutes of the run time. This peak was observed in the blood sample obtained from the Test Group and corresponded with the results obtained from the HPLC. The use of the UPLC has also confirmed the peak of indomethacin in the rat blood sample at a higher absorbance and a shorter run time. The retention time for the indomethacin in the UPLC was 3.62 minutes.

Blood samples were gathered for duration of 21 days with a release cycle every 7 days. The drug release over these 3 cycles was determined by the amount of drug present in the blood. Although the blood concentration of the drug did not necessarily represent that of the drugs present at the local site, it was an indication of the drug release which has occurred locally and entered the systemic circulation. This was due to the drawback that attempts to extract interstitial fluids from rat models do not yield sufficient quantities for analysis purposes. However, by looking at the drug concentrations in the blood samples, it would

demonstrate the consistency of drug release from each cycle. The drug-blood concentrations on the three release cycles may be presented as Figure 6.22.

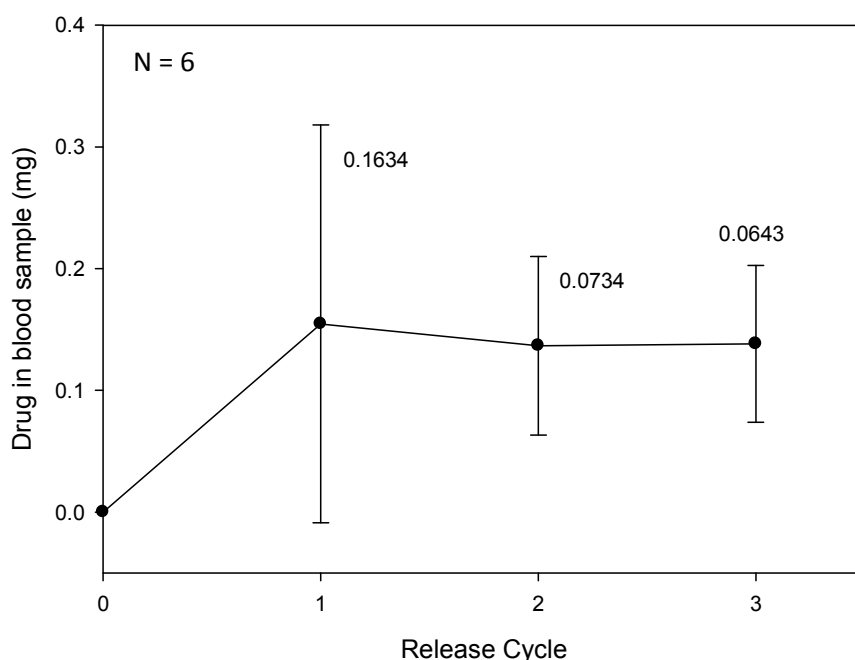


Figure 6.22. The drug release profile of the SAPD from the in vivo rat model.

The release cycle over the 21 day period has indicated a fairly consistent release and a favourable drug release profile. The large standard deviation exhibited in the first release cycle may be attributed to the increased drug release experienced with the first release cycle of the SAPD.

6.3.3. Histopathological sampling of the tissues obtained from the site of implantation

The final assessment for the biocompatibility of the SAPD was the histological examinations at the site of implant at the end of the *in vivo* study. This was done by taking samples from random rat models. These samples were compared against the samples taken from the rats in the Comparison Group in order to determine if there was any significant change in tissue morphology followed by the implantation of the SAPD. Six samples were taken for histological evaluation, with two samples from each group. The sample details were as follows:

Rat 1 & 2: Test Group (SAPD with indomethacin)

Rat 7 & 9: Placebo Group (SAPD without any drugs)

Rat 14 & 15: Control (healthy rats without any implantation)

The tissue samples around the SAPD implantation site underwent histological examination in order to determine the effect that SAPD has on the tissue morphology of the rat. The presence of any inflammatory infiltration, foreign body giant cells and hyalinization associated with tissue inflammation will be noted in order to determine the biocompatibility of the SAPD. These samples were sent off to the IDEXX Laboratories (IDEXX Laboratories, 19B Morris Street, East Woodmead, Willows Off Park, Johannesburg, Gauteng) in order to be assessed.

Once the tissue samples were submitted, these sections were processed overnight in an automated tissue processor according to the standard operating procedure of the IDEXX Laboratory. (PTA-his-SOP-27). Following the routine histological processing, wax blocks were produced in paraffin wax and sections of about 6µm cut according to IDEXX Laboratory SOP (PTA-his-SOP-30).

The slides were stained with Haematoxylin and Eosin according to the SOP. The results on the histological findings which show tissue morphology of rats in test group and placebo group may be presented as Figure 6.23-6.26.

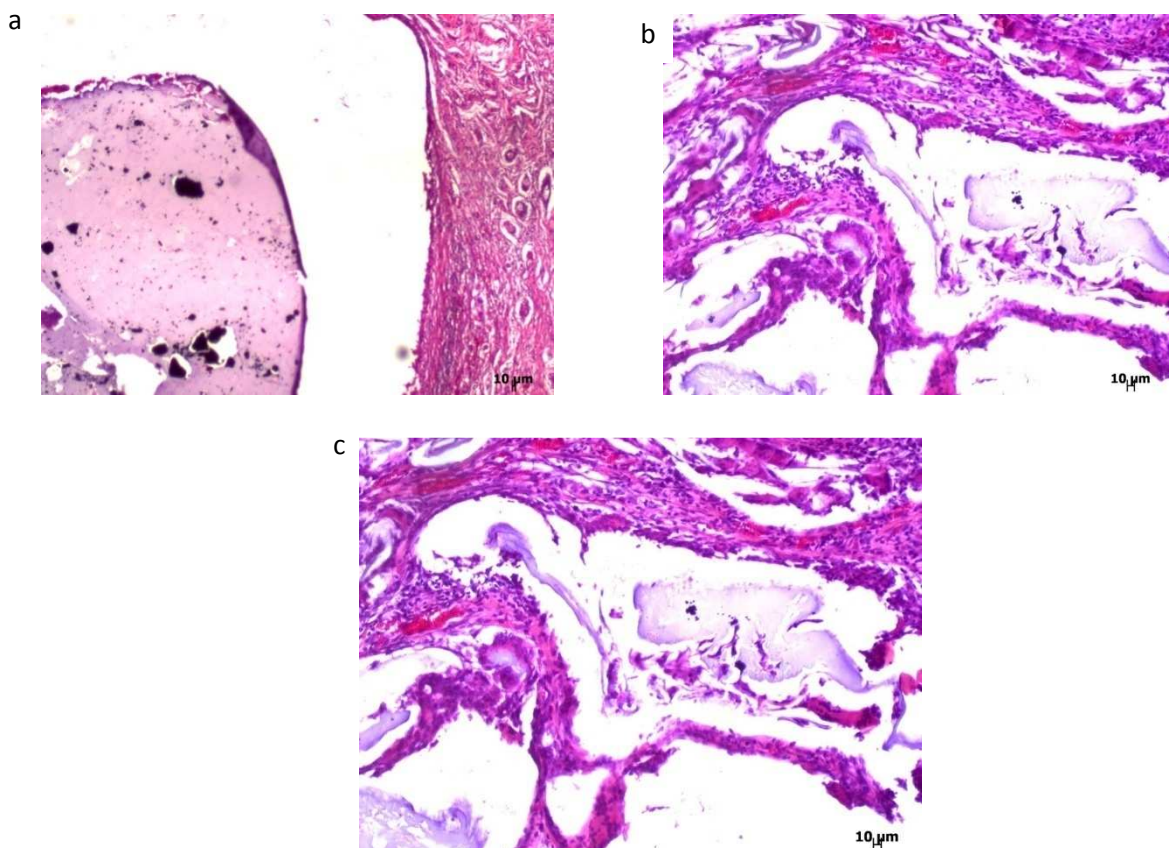


Figure 6.23. a), b) and c) The histological sample of rat 1 obtained from different areas of the implantation site.

The skin section revealed an implanted basophilic mass with black irregular granules embedded in the basophilic stained implant in the subcutaneous tissue. There were mild granulomatous inflammations observed surrounding the implant where macrophages and multinucleated giant cells are surrounding small fragments of the implant material in a foreign body granulomatous inflammatory process. Mild lymphocytic infiltrates and fibroplasia with encapsulation could be demonstrated.

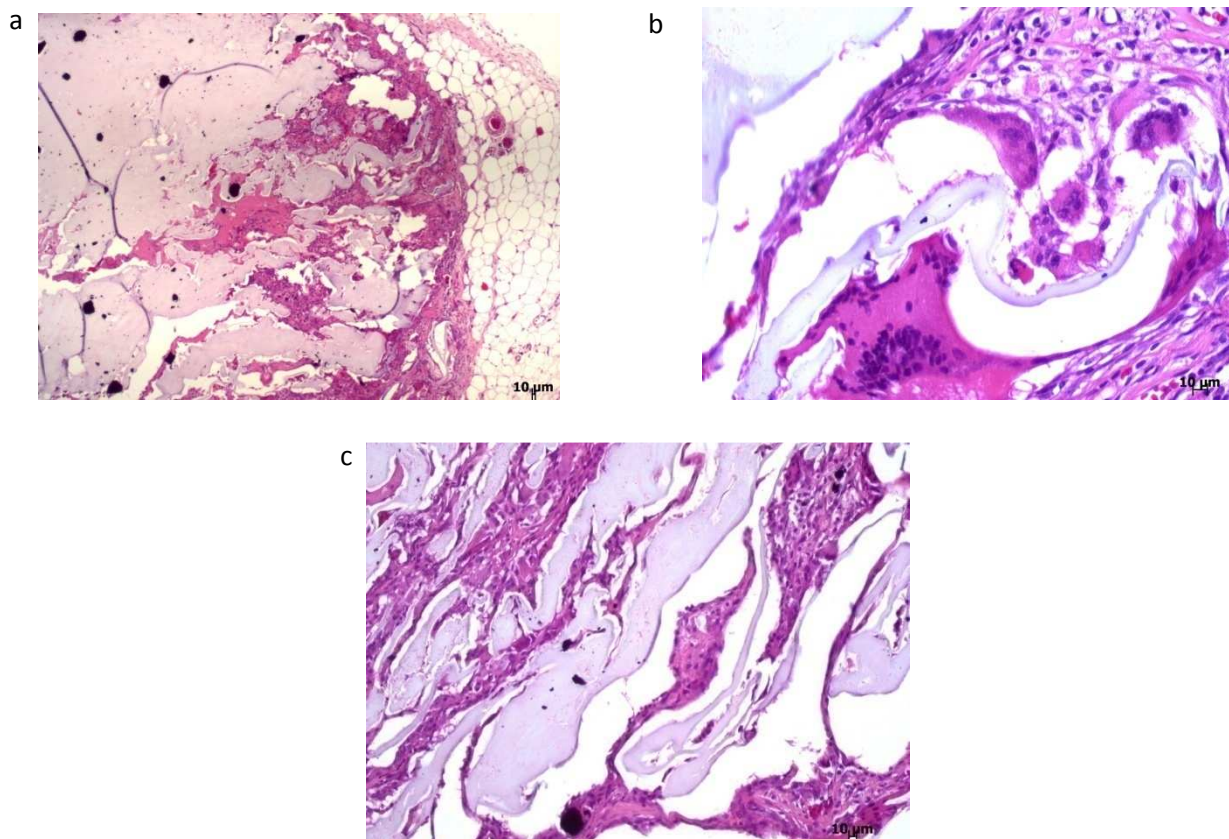


Figure 6.24. a), b) and c) The histological samples of rat 2 obtained from different areas of the implantation site.

The subcutaneous implant could be identified and was similar to that reported for rat 1, and again small areas of foreign body inflammation as well as fibrous capsule were observed encapsulating the SAPD.

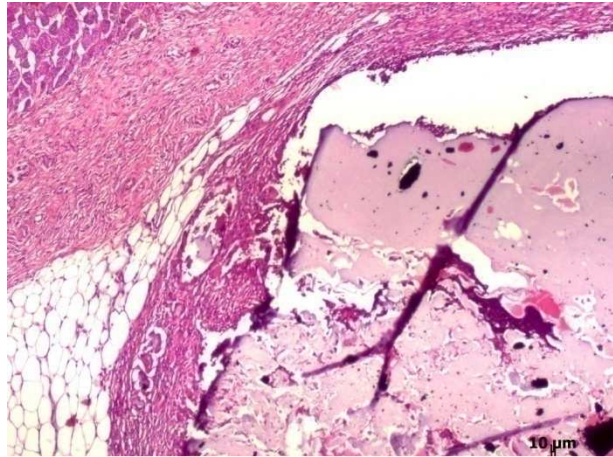


Figure 6.25. The histological sample of rat 7.

From the results obtained from rat 7, a mild foreign body granulomatous inflammation could be demonstrated with islands of fragment implant entrapped in the foreign body inflammation. Macrophages with epithelioid transformation as well as multinucleated giant cells are present. There was a well-developed fibrous capsule which was visible.

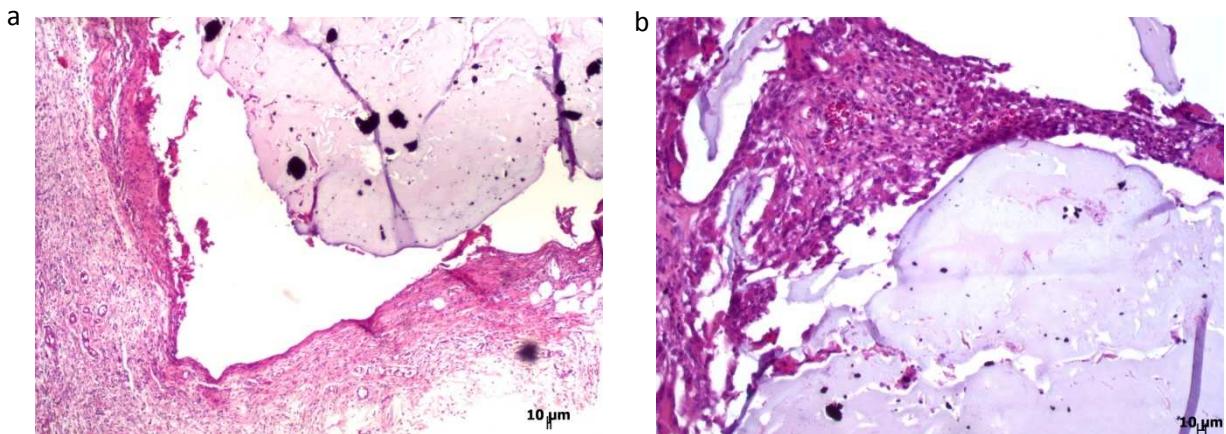


Figure 6.26. a) and b) The histological sample of rat 9 obtained from two different areas of the implantation site.

Lastly, the tissue samples obtained from rat 9 showed a basophilic implant can be identified in the subcutis with a mild peripheral foreign body granulomatous inflammation and fibroplasia to form a fibrous capsule on the periphery, encapsulating the transplant completely. The inflammatory reaction was mild. No morphological differences could be recorded and the transplant was surrounded by a mild foreign body inflammatory reaction, and was well-encapsulated in all of the abovementioned implantation sites. The control specimens were morphologically normal.

6.4. Concluding remarks

The use of an *in vivo* study has allowed us to determine the biocompatibility and the drug release profile when the SAPD was implanted subcutaneously. The SAPD was implanted subcutaneously into the rat model, and found to release drugs in the presence of electrical stimulation. This was done by sampling blood obtained from the rats at weekly interval. The results obtained from the HPLC and UPLC have indicated the presence of minute concentrations of drug in the blood, which ascertained the release of indomethacin from the SAPD into the surrounding tissue.

Results were also compared against the control group and interval blood samples obtained has shown that leakage of the drug has not occurred. This result also corresponds with that obtained from the *in vitro* study. The drug release from the SAPD over the 3 release cycles also seemed to be consistent.

The biocompatibility of the SAPD was determined accurately via histopathological analysis. The rats were checked daily after the implantation procedures were performed and showed no signs of illness. The site of implantation did not show any signs of swelling, which indicated the absence of inflammation or infection. The rats weighed during the implantation period have also shown a steady increase in body weight and growth. Histological results have shown that although mild inflammatory process was present, the overall biocompatibility of the SAPD remained fairly good. No tumor or signs of significant tissue changes were discovered. This was further substantiated by the general well-being of the rats during the duration of this study.

CHAPTER 7

CONCLUSIONS AND RECOMMENDATIONS

7.1 Conclusions

Worldwide, many patients suffering from chronic pain relied on chronic medication for their treatment. Those conventional treatments usually included oral drugs such as NSAIDs or opioids. However, long term use of these drugs may lead to side effects and, in the case of opioids, addiction and abuse which is great concern to the health care professionals (Carinci, 2010 and McCabe, 2008). Current researches into chronic pain have managed to produce COX II-selective NSAIDs which reduced the incident of gastric ulcer related with chronic NSAID use, but problems such as renal or hepatic toxicity still occurred with the use of the COX II-selective NSAIDs.

The development of SAPD allowed this device to be employed as an implantable controlled drug delivery system. By implanting the SAPD directly at the target site, it allowed the delivery of drug directly into its surrounding environment. SAPD observed during drug release study has indicated that erosion was primarily the mechanism of release and was confirmed with the use of a chemometric and molecular modelling approach. The erosion phenomenon would occur at the proximity of the electrode and happened at approximately 15 seconds of actuation. This was beneficial as it meant rapid drug delivery once the SAPD was actuated.

The SAPD should be implanted subcutaneously at the target site. Subcutaneous implantation is a simple and efficient procedure which is used frequently, as in the case of implantable contraceptives. The entire implantation procedure of the SAPD should take ± 10 minutes and was well tolerated in the rats during the *in vivo* study.

A stable HPLC method was adopted and further conversion of this method was done to allow more accurate assay of the blood sample on the UPLC. The use of these assays has demonstrated that drug release was achieved in the rat model and SAPD may be further developed for human implantation. The biocompatibility and potential toxicity has indicated no untoward effect and the SAPD have exhibited good biocompatibility.

7.2 Recommendations

Several controlled-release implantable devices were developed and tested with many more still underway. However, few of these systems were tested for their biocompatibility, and even fewer were tested for its drug release profile *in vivo*. This is due to the lack of animal studies in these stimuli-actuated implants. As mentioned, the use of the SAPD allowed direct drug release at the target site when required. This concept may be further developed so that in future other drugs may be incorporated. Extensive research needed to be conducted in order to develop alternative devices capable of controlled release of other drug substances using similar concepts. This may be useful for conditions which required a 'when necessary' drug dosing.

The results obtained from *in vivo* study using rat models have shown promising results. While the use of a rat model allowed assessment of the biocompatibility and drug release profile to a certain extent, further research using larger mammals such as apes may be beneficial as the results obtained may relate closer to that of humans. Extracellular fluid may be extracted with fewer difficulties and produced a more accurate result of the *in vivo* drug release of the SAPD.

Another importance of the primate study would be the further study on the erosion study of the SAPD in an *in vivo* setting. Current study suggested that eroded materials would be disintegrated by the macrophages in the body. Future study using *in vivo* models should also include erosion studies as to determine the fate of the eroded hydrogels.

External devices for the actuation of the SAPD should be developed. The actuation device should be portable, capable of varied electrical stimulation and affordable. Currently, a proposed method was to design the portable device as a watch which could then be actuated by the patient at the required time. The SAPD may also be stored as cartridges in the watch and implanted when required. The ease of implantation meant that it may be done at any clinic, hospital or pharmacy within 10-15 minutes. The ease of this process would offer great flexibility and convenience to the patients.

7.3. Future Outlook

The development of the novel SAPD would open up certain new opportunities in the field of stimuli-actuated controlled drug delivery device. This device may be modified to produce

SAPD with varying physicochemical properties and drug release profiles. The device may also be modified to incorporate various drugs which may be used for a wide range of health conditions over a period of one to two months. The patent of the SAPD was filed in South Africa, but further patent filing is in progress to ensure SAPD receives international patent. The development of such technology in South Africa would ensure that we compete with the pharmaceutical industries at an international level. Due to the flexibility of the SAPD, further development may include the incorporation of colchicine for gout, the release of ergotamine for patients suffering from frequent migraine, or any condition which requires infrequent dosing of drug.

REFERENCES

1. Adam S.S., The propionic acids: a personal perspective, **Journal of Clinical Pharmacology**, **32**(4), 1992, 317-323
2. Adnadjevic B., Jovanovic J., Novel approach in investigation of the poly (acrylic acid) hydrogel swelling kinetics in water, **Journal of Applied Polymer Science**, **107**(6), 2007, 3579-3587
3. Ali E., Mahmood K., Mansoor K., Electropolymerization of aniline on plastically deformed Pd surface: Structure at micro- and nano-scale, **Polymer Journal**, **38**, 2006, 329-334
4. Andersson M.R., Berggren M., Inganaes O., Gustafsson G., Gustafsson-Carlberg J.C., Selse D., Hjertberg T. Wennerstroem O., **Macromolecules**, **28**(22), 1995, 7525-7529
5. Anoopkumar-Dukie S., Lack B., Mcphail K., Nyokong T., Lambat Z., Maharaj D., Daya S., Indomethacin reduces lipid peroxidation in rat brain homogenate by binding Fe^{2+} , **Metabolic Brain Disease**, **18**(1), 2003, 1-9
6. Ansari R., Polypyrrole conducting electroactive polymers: synthesis and stability studies, **E-Journal of Chemistry**, **3**(4), 2006, 186-201
7. Arenaz B., Maestro M.M., Turnay J., Olmo N., Senén J., Gil Mur J., Lizarbe M.A., Jorge-Herrero E., Effects of periodate and chondroitin 4-sulfate on proteoglycan stabilization of ostrich pericardium. Inhibition of calcification in subcutaneous implant in rats, **Biomaterials**, **25**(17), 2004, 3359-3368
8. Asami R., Atobe M., Fuchigami T., Electropolymerization of an immiscible monomer in aqueous electrolytes using acoustic emulsification, **Journal of American Chemistry Society**, **127**(38), 2005, 13160-13161
9. Aukland K. and Reed R.K., Interstitial lymphatic mechanisms in the control of extra cellular fluid volume, **Physiology Review**, **73**, 1993, 1-78
10. Aurora-Prado M.S., Steppe M., Tavares M.F., Kedor-Hackmann E.R., Santoro M.I., Comparison between capillary electrophoresis and liquid chromatography for the determination of diclofenac sodium in a pharmaceutical tablet, **Journal of AOAC International**, **85**(2), 2002, 333-340
11. Avgerinos A., Noormohammadi A., Hutt A.J., Disposition of ibuprofen enantiomers following the oral administration of a novel controlled release formulation to healthy volunteers, **International Journal of Pharmaceutics**, **68**, 1993, 97-103

12. Badenhorst D., Maseko M., Tsotetsi O.J., Naidoo A., Brooksbank R., Norton, G.R. & Woodiwiss, A.J. Cross-linking influences the impact of quantitative changes in myocardial collagen on cardiac stiffness and remodeling in hypertension in rats. **Cardiovascular Research**, **57**(3), 2002, 632-641.
13. Bae W.J., Kim K.H., Jo W.H., A water-soluble and self-doping conducting polypyrrole graft copolymer, **Macromolecules**, **38**(4), 2005, 1044-1047
14. Balasubramaniam J., Srinatha A., Pandit J.K., Studies on indomethacin intraocular implants using different *in vitro* release method, **Indian Journal of Pharmaceutical Science**, **70**(2), 2008, 216-221
15. Barakzoy A.S., Moss A.H., Efficacy of the World Health Organisation Analgesic Ladder to treat pain in end-stage renal disease, **Journal of the American Society of Nephrology**, **17**, 2006, 3198-3203
16. Bar-Cohen Y., Electro-active polymers: Current capabilities and challenges, **Proceedings of the SPIE Smart Structures and Polymer Symposium, EAPAD symposium**, 2002, San Diego, CA
17. Bar-Cohen Y., Focus issues on biomimetics using electroactive polymers as artificial muscles, **Bioinspiration and Biomimetics**, **2**, 2007, Editorial
18. Bar-Cohen Y., Kim K.J., Choi H.R., Maddem J.D.W., Electroactive polymer materials, **Smart Material Structures**, **16**, 2007, 1-2
19. Bar-Cohen Y., Kim K.J., Choi H.R., Madden J.D.W., Electroactive Polymer Materials, **Smart Materials and Structures**, **16**, 2007
20. Bar-Cohen Y., Leary S., Shahinpoor M., Harrison J.O., Smith J., Electroactive polymers for planetary applications, **Smart structures and materials**, **3669**, 1999, 57-63
21. Bard A.J. and Faulkner L.R., **Electrochemical methods, Fundamentals and Applications**, 1980, John Wiley & Sons, New York.
22. Bator D.C., Clinical pharmacology of NSAIDs, **The Journal of Clinical Pharmacology**, **28**, 1988, 518-523
23. Bawa P., Pillay V., Du Toit L.C., Choonara Y.E., Stimulus responsive polymers and their applications in drug delivery, **Biomedical Materials**, **4** 2009, 1-15
24. Beeton C., Garcia A., Chandy K.G., Drawing blood from rats through the saphenous vein and by cardiac puncture, **Journal of Visualized Experiments**, **7**, 2007, 266
25. Bidez P.R., Li S., Macdiarmid A.G. *et al*, Polyaniline ,an electroactive polymer, supports adhesion and proliferation of cardiac myoblasts, **Journal of Biomaterial Science, Polymer edition**, **17**(1-2), 2006, 199-212

26. Bijur P.E., Kenny M.K., Gallagher E.J., Intravenous morphine at 0.1mg/kg is not effective for controlling severe acute pain in the majority of the patients, **Annals of Emergency Medicine**, **46**(4), 2005, 362-367
27. Bikram M., Gobin A.M., Whitmire R.E., West J.L., Temperature sensitive-hydrogel with SiO₂-Au nanoshells for controlled drug delivery, **Journal of Controlled Release**, **123**, 2007, 219-227
28. Borroughes J.H., Bradley D.D.C., Brown A.R., Marks R.N., Mackay K., Friend R.H., Burns P.L. Holmes A.B., Light-emitting diodes based on conjugated polymers, **Nature**, **347**, 1990, 539-541
29. Bott A.W., Electrochemical techniques for the characterization of redox polymers, **Current Separations**, **19**(3), 2001, 71-75
30. Bradford A. and O'Regan R.G., Acidaemia and hyperkalaemia following low voltage electric shock in the anesthetized cat, **Quarterly Journal of Experimental Physiology**, **70**, 1985, 101-113
31. Brahim S., Guiseppi-Elie A., Electroconductive hydrogels: electrical and electrochemical properties of polypyrrole-poly (HEMA) composite, **Electroanalysis**, **17**(7), 2004, 556-570
32. Brater DC., Renal effects of cyclo-oxygenase-2-selective inhibitors, **Journal of Pain Symptom Management**, **23**, 2002, 515-520
33. Braun D. and Heeger A.J., Visible light emission from semiconducting polymer diodes, **Applied Physics Letters**, **58**(18), 1991, 878-881
34. Braun D., Gustafsson G., McBranch D., Heeger A.J., Electroluminescence and electrical transport in poly(3-octylthiophene) diodes, **Journal of Applied Science**, **72**(2), 1992, 564-568
35. Bravo S.A., Lamas M.C., Salomón C.J., *In vitro* studies of diclofenac sodium controlled-release from biopolymeric hydrophilic matrices, **Journal of Pharmacy and Pharmaceutical Science**, **5**(3), 2002, 213-219
36. Brédas J.L., Scott J.C., Yakushi K., Street G.B., Polarons and bipolarons in polypyrrole: Evolution of the band structure and optical spectrum upon doping, **Physics Review B**, **30**(2), 1984, 1023-1025
37. Budtova T., Suleimenov I., Frenkel S., Electrokinetics of the contraction of a polyelectrolyte hydrogel under the influence of constant electric current, **Polymer Gels and Networks**, **3**, 1995, 387-393
38. Carinci A.J. and Mao J., Pain and opioid addiction: What is the Connection?, **Current Pain and Headache Reports**, **14**(1), 2010, 17-21

39. Carvalho J., Moreira S., Maia J., Gama F.M., Characterization of dextrin-based hydrogels: Rheology, biocompatibility and degradation, **Journal of Biomedical Materials Research**, **93A**, 2010, 389-399
40. Chambers J.Q. and Inzelt G., Temperature dependence of the voltammetric response of thin electroactive polymer films, **Analytical Chemistry**, **57**, 1985, 1117-1121
41. Chansai P., Sirivat A., Electrical field responsive polypyrrole in poly (acrylic acid) hydrogel for transdermal drug delivery, **Advances in Science and Technology**, **57**, 2008, 170-175
42. Chao D., Lu X., Chen J., Liu X., Zhang W., Wei Y., Synthesis and characterization of electroactive polyamide with amine-capped aniline pentamer and ferrocene in the main chain by oxidative coupling polymerization, **Polymer**, **47**, 2006, 2643-2648
43. Chen F., Metha P.G., Takiff L., McCullough R.D., Improved electroluminescence performance of poly(3-alkylthiophenes) having a high head-to-tail (HT) ratio, **Journal of Materials Chemistry**, **6**(11), 1996, 1763-1766
44. Chen J.I., Moody R.A., Huang J.C., Tripathy S.K., Synthesis and characterization of electroactive polymer based on pyrrole, **Molecular Crystals and Liquid Crystals**, **190**, 1990, 19-26
45. Chen S., Tsai Y. Chen S, Oxidation states and molecular motions in tosylate anion-doped polypyrroles, **Synthetic Materials**, **28**, 1989, C151-C156
46. Chen S.A. and Tsai C.C., Structure/properties of conjugated conductive polymers 2,3-ether-substituted polythiophenes and poly(4-methylthiophenes), **Macromolecules**, **26**(9), 1993, 2234-2239
47. Chen T.L., Wang M.J., Huang C.H., Liu C.C., Ueng T.H., Difference between *in vivo* and *in vitro* effects of propofol on deflorination and metabolic activities of hamster hepatic cytochrome P450-dependant mono-oxygenase, **British Journal of Anaesthesia**, **75**, 1995, 462-466
48. Cheng I., Liu X., Plummer S.J., Krumroy L.M., Casey G., Witte J.S., COX 2 genetic variation, NSAIDs, and advanced prostate cancer, **British Journal of Cancer**, **97**, 2007, 557-561
49. Chiba S., Kornbluh R., Pelrine R., Joseph J., Heydt R., Pei Q., High-field electrostriction of elastometric polymer dielectrics for actuation, **Smart Structures and Materials: Electro-active Polymers Actuators and Devices**, **3669**, 1999, 149-161

50. Chokshi R.J., Shah H.H., Sandhu H.K., Malick A.W., Zia H., Stabilization of low glass transition temperature indomethacin formulations: impact of polymer-type and its concentration, **Journal of Pharmaceutical Sciences**, **97**(6), 2007, 2286-2298
51. Cirić-Marjanović G., Dragičević L., Milojević M., Mojović M., Mentus S., Dojčinović B., Marjanović B., Stejskal J., Synthesis and characterization of self-assembled polyaniline nanotubes/silica nanocomposite, **Journal of Phys. Chem. B.**, **113**, 2009, 7116-7127
52. Conway M.W., Almond S.W., Briscoe J.E., Harris L.E., Chemical model for the rheological behaviour of crosslinked fluid system, **Journal of Petroleum Technology**, **35**(2), 1983, 315-320
53. Couppé, C., Hansen, P., Kongsgaard, M., Kovanen, V., Suetta, C., Aagaard, P., Kjær, M. & Magnusson, S.P. Mechanical properties and collagen cross-linking of the patellar tendon in old and young men. **Journal of Applied Physiology**, **107**, **2009**, 880-886.
54. Cox-Reijven L.M.P., Van Kreel B., Soeters P.B., Accuracy of bioelectrical impedance spectroscopy in measuring changes in body composition during severe weight loss, **Journal of Parenteral and Enteral Nutrition**, **26**(2), 2002, 120-127
55. Dawidowicz A.L., Kondziola K. Kobielski M., Determination of free indomethacin in human plasma using HPLC and UV detection, **Journal of Liquid Chromatography & Related Technologies**, **32**, 2009, 2686-2698
56. De Jong D., Jansen R., Hoefnagels W., Jellesma-Eggenkamp M., Verbee M., Borm G., Kremer B., No effect of one year treatment with indomethacin on Alzheimer's Disease Progression: A randomized controlled trial, **PLoS ONE**, **3**(1), 2008, e1475
57. De Koker S., Naessens T., De Geest B.G., Bogaert P., Demeester J., De Smedt S., Grooten J., Biodegradable polyelectrolyte microcapsules: Antigen delivery tools with Th17 skewing activity after pulmonary delivery, **The Journal of Immunology**, **184**, 2009, 203-211
58. De las Heras Alarcon C., Pennadam S., Alexander C., Stimuli responsive polymer for biomedical applications, **Chemical Society Review**, **34**, 2005, 276-285
59. de Oliveira D.T., Souza-Silva E., Rogerio Tonussi C., Gingival vein puncture: A new simple technique for drug administration or blood sampling in rats and mouse, **Scandinavian Journal of Laboratory Animal Science**, **36**(2), 2009, 109-113
60. De Rossi D., Kajiwara K., Osada Y., Yamauchi A., Eds A., **Polymers Gel Fundamental and Biomedical Applications**, Plenum Press: New York 1991

61. Deng K., Zhang P., Ren X., Zhong H., Gou Y., Dong L., Li Q., Synthesis and characterization of a pH/temperature responsive glycine-mediated hydrogel for drug release, **Frontiers of Material Science in China**, **3**(4), 2009, 374-379
62. Dimitriev O.P., Doping of polyaniline by transition metals: effect of metal cation on film morphology, **Synthetic Materials**, **142**(1-3), 2003, 299-303
63. Donald D.J. and Poehlein G.W., Characteristics of thixotropic behaviour, **Journal of Rheology**, **15**(1), 1971, 51-62
64. Dubois P., Rosset S., Koster S., Stauffer J., Mikhaïlov S., Dadras M., de Rooij N., Shea H., Microactuators based on ion implanted dielectric electroactive membranes, **Sensors and Actuators A**, **130-131**, 2006, 147-154
65. Ebbing D.D., **General Chemistry 5th edition**, Houghton Mifflin Company, 1996
66. Ehrick J.D., Deo S.K., Browning T.W., Bachas L.G., Madou M.J., Daunert S., Genetically engineered protein in hydrogels tailors stimuli-responsive characters, **Nature Materials**, **4**, 2005, 298-302
67. Emerson, D. & Ghiorse, W.C. Role of disulfide bonds in maintaining the structural integrity of the sheath of *Leptothrix discophora* SP-6. *J. Bacteriol.* **1993**, 175(24), 7819-7827.
68. Epping-Jordan M.P., Watkins S.S., Koob G.F., Markou A., Dramatic decrease in brain reward function during nicotine withdrawal, *Nature* **393** (1998), pp. 76-79
69. Ethel S., Bhat G.K., Hedge B.M., Bacterial adherence and humoral immune response in women with symptomatic and asymptomatic urinary tract infection, **Indian Journal of Medical Microbiology**, **24**(1), 2006, 30-33
70. Fichou D. and Ziegler C., Single crystals and thin films, **Handbook of Oligo- and Polythiophenes**; D. Fichou, Ed., Wiley-VCH: Weinheim, 1999, 185-282
71. Fini A., Feroci G., Fazio G., Interactions between indomethacin and heavy metal ions in aqueous solutions, **European Journal of Pharmaceutical Sciences**, **13**(2), 2001, 213-217
72. Fish R., Electric Shock, Part I: Physics and Pathophysiology, **The Journal of Emergency Medicine**, **11**, 1993, 309-312
73. Fluttert M., Dalm S., Oitzl M.S., A refined method for sequential blood sampling by tail incision in rats, **Laboratory Animals**, **34**, 2000, 372-378
74. Fortunato R., Branco L.C., Afonso C.A.M., Benavente J., Crespo J.G., electrical impedance spectroscopy characterization of supported ionic liquid membranes, **Journal of Membrane Science**, **270**, 2006, 42-49

75. Francis S., Kumar M., Varshney L., Radiation synthesis of superabsorbent poly (acrylic-acid)-carrageenan hydrogels, **Radiation Physics and Chemistry**, **69**, 2004, 481-486
76. Furstenberg C.T., Ahles T.A., Whedon M.B. *et al*, Knowledge and attitudes of health-care providers towards cancer pain managements: a comparison of physicians, nurses and pharmacists in the State of New Hampshire, **Journal of Pain Symptom Management**, **15**(6), 1998, 335-349
77. Gabrielli C., Keddam M., Nadi N., Perrot H., Ion and solvent transport across conducting polymers investigated by ac electrogravimetry. Application to Polyaniline, **Journal of Electroanalytical Chemistry**, **485**, 2000, 101-113
78. Gao F., Reitz F.B., Pollack G.H., Potentials in anionic polyelectrolyte hydrogel, **Journal of Applied Polymer Science**, **89**(5), 2003, 1319-1321
79. Geng Y., Jing X., Wang F., Solution properties of doped polyaniline, **Journal of Macromolecular Science and Physics**, **B36**(1), 1997, 125-135
80. Geng Y., Li J., Sun Z., Jing X., Wang F., Polymerization of aniline in an aqueous system containing organic solvent, **Synthetic Materials**, **96**, 1996, 1-6
81. Genoud F., Guglielmi M., Nechtschein M., Genies E., Salmon M., ESR study of electrochemical doping in the conducting polymer polypyrrole, **Physical Review Letters**, **55**(1), 1985, 118-121
82. Ghahramani P., Rowland-Yeo K., Yeo W.W., Jackson P.R., Ramsay L.E., Protein binding of aspirin and salicylate measures by *in vivo* ultrafiltration, **Clinical pharmacology and therapeutics**, **63**(3), 1998, 285-295
83. Glajchen M., Chronic pain: treatment barriers and strategies for clinical practice, **Journal of American Board Family Practice**, **14**(3), 2001, 211-218
84. Gnanakan S.R.P., Rajasekhar M., Subramania A., Synthesis of polythiophene nanoparticles by surfactant-assisted dilute polymerization method for high performance redox supercapacitors, **International Journal of Electrochemical Sciences**, **4**, 2009, 1289-1301
85. Goldstein J.L., Sostek M.B., Fort J.G., Riff D.S., Zhang Y., Plachetka J.R., 116 A single tablet multilayer formulation of enteric-coated naproxen coupled with non-enteric coated omeprazole is associated with a significantly reduced incidence of gastric ulcer vs. Enteric coated naproxen: a prospective, randomized double-blind study, **Gastroenterology**, **134**(4), 2008, A-19
86. Golembiewski J., Torrecer S., Katke J., The use of opioids in the postoperative settings: focus on morphine, hydromorphone and fentanyl, **Journal of Perianesthesia Nursing**, **20**(2), 2005, 141-143

87. Granstrom M., Harrison M.G., Friend R.H., Electrooptical polythiophene devices, *Handbook of Oligo- and Polythiophenes*; D. Fichou, Ed., Wiley-VCH: Weinheim, 1999, 405-458
88. Guimard N.K.E., Sessler J.L., Schmidt C.E., Toward a biocompatible and biodegradable copolymer incorporating electroactive oligothiophene units, *Macromolecules*, **42**(2), 2009, 502-511
89. Gupta S. and Sathyan G., Providing constant analgesia with OROS[®] hydromorphone, *Journal of Pain and Symptom and Management*, **33**(2), 2007, S19-S24
90. Han B., Du Y., Wang E., Simultaneous determination of pethidine and methadone by capillary electrophoresis with electrochemiluminescence detection of tris(2,2'-bipyridyl)ruthenium(II), *Microchemical Journal*, **89**(2), 2008, 137-141
91. Hasselström J., Eriksson S., Persson A., Rane A., Svensson J.O., J. Säwe J, The metabolism and bioavailability of morphine in patients with severe liver cirrhosis, *British Journal of Clinical pharmacology*, **29**(3), 1990, 289-297
92. Hatchett D.W., Josowicz M., Janata J., Acid doping of polyaniline: Spectroscopic and electrochemical studies, *Journal of Physical Chemistry B*, **103**(50), 1999, 10992-10998
93. Hawthorne A.B., Mahida Y.R., Cole A.T. Hawkey C.J., Aspirin-induced gastric mucosal damage: prevention by enteric-coating and relations to prostaglandin synthesis, *Journal of Clinical Pharmacology*, **32**(1), 1991, 77-83
94. He C., Kim S.W., Lee D.S., *In situ* gelling stimuli-sensitive block copolymer hydrogels for drug delivery, *Journal of Controlled Release*, **127**(3), 2008, 189-207
95. Heeger A.J., Semiconducting and Metallic Polymers: The Fourth Generation of Polymeric Materials, *Journal of Physical Chemistry B*, **105**, 2001, 8475-8491
96. Heinze J., Cyclic voltammetry – “Electrochemical Spectroscopy”. New analytical Method, *Angewandte Chemie International Edition in English*, **23**(11), 2003, 831-847
97. Henderson K.J., Zhou T.C., Otim K.J., Shull K.R., Ionically crosslinked tri-block copolymer hydrogels with high strength, *Macromolecules*, **43**, 2010, 6193-6201
98. Hersh E., Moore P., Ross G., Over-the-counter analgesics and anti-pyretics: A critical assessment, *Clinical Therapeutics*, **22**(5), 2000, 500-548
99. Hoff J., Methods of blood collection in the mouse, *Lab Animal*, **29**(10), 2000, 47-53
100. Hoffman A.S., Hydrogels for biomedical applications, *Advanced Drug Delivery Review*, **43**, 2002, 3-12

101. Honary S and Golkar M., Effect of polymer grade and plasticizer molecular weights on viscoelastic behaviour of coating solutions, **Iranian Journal of Pharmaceutical Research**, **2**(2), 2003, 125-127(2)
102. Hong D., Flood P., Diaz G., The side effects of morphine and hydromorphone patient-controlled analgesia, **Anesthesia and Analgesia**, **107**, 2008, 1384-138
103. Hong J., Yoon H., Jang J., Kinetic study of the formation of polypyrrole nanoparticles in water-soluble polymer/metal cation systems: A light-scattering analysis, **Small**, **6**(5), 2009, 679-686
104. Hotta S., Rughooputh S.D.D.V., Heeger A.J., Conducting polymer composites of soluble polythiophenes in polystyrene, **Synthetic Metals**, **22**, 1987, 79-87
105. Huang L., Hu J., Lang L., Wang X., Zhang P., Jing X. *et al*, Synthesis and characterization of electroactive and biodegradable ABA block copolymer of polylactide and aniline pentamer, **Biomaterials**, **28**, 2006, 1741-1751
106. Huang L., Hu J., Lang L., Wang X., Zhang P., Jing X., Wang W., Chen X., Lelkes P.I., MacDiarmid A.G., Wei Y., Synthesis and characterization of electroactive and biodegradable ABA block copolymer of polylactide and aniline pentamer, **Biomaterials**, **28**, 2007, 1741-1751
107. Huang L., Zhuang X., Hu J., Lang L., Zhang P., Wang Y., Chen X., Wei Y., Jing X., Synthesis of biodegradable and electroactive multiblock polylactide and aniline pentamer copolymer for tissue engineering applications, **Macromolecules**, **9**(3), 2008, 850-858
108. Huang Y., Yu H., Xiao C., pH-sensitive cationic guar gum/poly (acrylic acid) polyelectrolyte hydrogels: swelling and *in vitro* drug release, **Carbohydrate Polymers**, **69**(4), 2007, 774-783
109. Huang Y., Yu H., Xiao C., pH-sensitive cationic guar gum/poly (acrylic acid) polyelectrolyte hydrogels: Swelling and *in vitro* drug release, **Carbohydrate Polymers**, **69**(4), 2007, 774-783
110. Huang L., Chen C., Wen T., Development and characterization of flexible electrochromic devices based on polyaniline and poly(3,4-ethylenedioxythiophene)-poly(styrene sulphonic acid), **Electrochimica Acta**, **51**(26), 2006, 5858-5863
111. Hurst J.L. and West R.S., Taming anxiety in laboratory rats, **Nature Methods**, **7**, 2010, 825-826
112. Inoue T., Chen G., Nakamae K., Hoffman A.S., A hydrophobically-modified bioadhesive polyelectrolyte gel for drug delivery, **Journal of Controlled Release**, **49**(2-3), 1997, 167-176

113. Inzelt G. and Szabo L., The effect of the nature and the concentration of the counter-ions on the electrochemistry of poly (vinylferrocene) polymer film electrodes, **Electrochemical Acta**, **31**(11), 1986, 1381-1387
114. Iyer S.S., Barr W.H., Karnes H.T., Profiling *in vitro* drug release from subcutaneous implants: A review of current status and potential implications on drug product development, **Biopharmaceutics & Drug Disposition**, **27**, 2006, 157-170
115. Jabbari E., Tavakoli J., Sarvestani A.S., Swelling characteristics of acrylic acid polyelectrolyte hydrogel in DC current field, **Smart Material Structures**, **16**, 2007, 1614-1620
116. John R. and Wallace G.G., Doping-Dedoping of polypyrrole: A study using current measuring and resistance-measuring techniques, **Journal of Electroanalytical Chemistry** **145**, 1993, 145-160
117. Kamal A.H.M., Ahmed M., Wahed M.I.I., Amran S., Shaheen S., Rashid M., Anwar-UI-Islam M., Development of indomethacin sustained release microcapsule using ethyl cellulose and hydroxyl propyl methyl cellulose phthalate by o/w emulsification, **Dhaka University Journal of Pharmaceutical Science**, **7**(1), 2008, 83-88
118. Kamalaesh S., Tan P., Wang J. *et al*, Biocompatibility of electroactive polymers in tissue, **Journal of biomed Materials Res**, **52**, 2000, 467-478
119. Kamalesh S., Tang P., Wang J. *et al*, Biocompatibility of electroactive polymer in tissue, **Journal of Biomed Material Res**, **52**, 2000, 467-478
120. Kanokpom J., Sumonman N., Ratanaa R., Anuvat S., Electrically controlled release of sulfosalicylic acid from crosslinked poly (vinyl alcohol) hydrogel, **International Journal of Pharmaceutics**, **356**(1-2), 2008, 1-11
121. Karande P., Jain A., Mitragotri S., Relationship between skin's electrical impedance and permeability in the presence of chemical enhancers, **Journal of Controlled Release**, **110**, 2006, 307-313
122. Karyakin A.A., Karyakina E.E., Schmidt H., Electropolymerized Azines: A New group of electroactive polymers, **Electroanalysis**, **11**(3), 1998, 149-155
123. Katchalsky A., Polyelectrolytes and their biological interactions, **Biophysical Journals**, **4**(1), 1964, 9-41
124. Kearney P., Baigent C., Godwin J., Halls H., Emberson J., Patrono, Do selective cyclo-oxygenase-2 inhibitors and traditional non-steroidal anti-inflammatory drug increase the risk of atherothrombosis. Meta-analysis of randomized trials, **BMJ**, **332**(7553), 2006, 1302-1308

125. Kenji M., Shunzo S., Makoto U. Katsuhiko N., Synthesis of a novel soluble polyaniline using imide super-acid, **Nippon Kagakkai Koen Yokoshu**, **78**(1), 2000, 114
126. Khong T.F., Fraser S., Katerelos M., Paizis K., Hill P.A., Power D.A., Inhibition of heparin-binding epidermal growth factor-like growth increases albuminuria in puromycin aminonucleoside nephrosis, **Kidney International**, **58**, 2000, 1098-1107
127. Kim H.I., Park S.J., Kim S.I., Kim N.G., Kim S.G., Electroactive polymer hydrogels composed of polyacrylic acid and poly (vinyl sulfonic acid) copolymer for application of biomaterial, **Synthetic Metals**, **155**(3), 2005, 674-676
128. Kim J., Deshpande S.D., Yun S., Li Q., A comparative study of conductive polypyrrole and polyaniline coatings on electro-active papers, **Polymer Journal**, **38**, 2006, 659-668
129. Kim S.G., Lim J.Y., Sung J.H., Choi H.J., Seo Y., Emulsion polymerized polyaniline synthesized with dodecylbenzene-sulfonic acid and its electrorheological characteristics: temperature effect, **Polymer**, **48**(22), 2007, 6622-6631
130. Kim S.W., Bae Y.H., Okano T., Hydrogels: Swelling, drug loading and releases, **Pharmaceutical Research**, **9**(3), 1992, 283-290
131. Kim S.W., Temperature sensitive polymer for delivery of macromolecule drugs, **Advanced Materials in Biomaterial in Biomedical Engineering and Drug Delivery System**, 1996, 126-133
132. Kimura T., Shirota O., Ohtsu Y., Analysis of ibuprofen metabolites by semi-microcolumn liquid chromatography with ultraviolet absorption and pulsed amperometric detectors, **Journal of Pharmaceutical and Biomedical Analysis**, **15**, 1997, 1521-1526
133. Kincal D., Kumar A., Child A., Reynolds J., Conductivity switching in polypyrrole-coated textile fabric as gas sensors, **Synthetic Metals**, **92**(1), 1998, 53-56
134. Kinlen P.J., Frushour B.G., Ding Y., Menon V., Synthesis and characterization of organically soluble polyaniline and polyaniline block copolymers, **Synthetic Materials**, **101**, 1999, 758-761
135. Kinoshita Y., Kuzuhara T., Kobayashi M., Ikada Y., Reduction in tumor formation on polyethylene by collagen immobilization, **Journal of Long-term Effects of Medical Implants**, **5**, 1995, 275-284
136. Kirschvink N., Vincke G., Onclinx C., Peck M.J., Gustin P., Comparison between pulmonary resistance and Penh in anesthetised rats with tracheal diameter reduction and after carbachol inhalation, **Journal of Pharmacological and**

Toxicological Methods, **51**(2), 2005, 123-128

137. Kitani A., Yoshioka K., Maitani S. Ito S., Properties of elastic polyaniline, **Synthetic Materials**, **84**, 1997, 83-84
138. Kontturi K., Pentti P., Sundholm G., Polypyrrole as a model membrane for drug delivery, **Journal of Electroanalytical Chemistry**, **453**(1-2), 1998, 231-238
139. Koshikawa N., Tomiyama K., Omiya K., Kobayashi M., Ketamine anaesthesia has no effect on striatal dopamine metabolism in rats, **Brain Research**, **444**(2), 1988, 394-396
140. Kowalski D., Ueda M., Ohtsuka T., The effect of ultrasonic irradiation during electropolymerization of polypyrrole on corrosive prevention of the coated steel, **Corrosion Science**, **50**(1), 2008, 286-291
141. Ku C.C., Liepins R., **Electrical properties of Polymers-Chemical properties**, 1987, 4-5
142. Kulkarni R.V., Sa B., Electroresponsive polyacrylamide-grafted-xanthan hydrogels for drug delivery, **Journal of Bioactive and Compatible Polymers**, **24**, 2009, 368-384
143. Kumar D., Electrochemical and optical behavior of conducting polymer: poly (o-toluidine), **European Polymer Journal**, **35**(10), 1999, 1919-1923
144. Kurisawa M. and Yui N., Dual stimuli responsive drug release from interpenetrating polymer network structured hydrogel of gelatin and dextran, **Journal of Controlled Release**, **54**(2), 1998, 191-200
145. Kuwabata S., Okamoto K. Yoneyama H., Conductivity of polypyrrole films doped with aromatic sulphonate derivatives, **Journal of Chemical Society, Faraday Transactions 1**, **84**(7), 1988, 2317-2326
146. Lacroix S. and Rivest S., Role of cyclo-oxygenase pathways in the stimulatory influence of immune challenge on the transcription of a specific CRF receptor subtype in the rat brain, **Journal of Chemical Neuroanatomy**, **10**(1), 1996, 53-71
147. Le W., Liu Y., Hi G., Preparation of manganese dioxide modified glassy carbon electrode by anovel film plating/cyclic voltammetry method for H₂O₂. **Journal of Chilian Chemical Society**, **54**, 2009, 366-371.
148. Lederer M., Optical and electrochemical transducers based on functionalized conjugated polymers, **Advanced Materials**, **11**(18), 1999, 1491-1498
149. Lee J.Y. and Kim C.Y., Synthesis of soluble polypyrrole of the doped state in organic solvents, **Synthetic Metals**, **74**(2), 1995, 103-106
150. Lee J.Y., Song K.T., Kim S.Y., Kim Y.C., Kim D.Y., Kim C.Y., Synthesis and characterization of soluble polypyrrole, **Synthetic Materials**, **84**(1-3), 1997, 137-140

151. Lekpittaya P., Yanumet N., Grady B.P., O'Rear E.A., Resistivity of conductive polymer-coated fabric, **Journal of Applied Polymer Science**, **92**(4), 2004, 2629-2636
152. Levy G., Tsuchiya T., Salicylate accumulation kinetics in man, **New England Journal of Medicine**, **287**(9), 1972, 430-432
153. Li H., Luo R., Lam K.Y., Modeling of ionic transport in electric-stimulus-responsive hydrogel, **Journal of Membrane Science**, **289**, 2007, 284-296
154. Li L. and Hsieh Y., Ultra-fine polyelectrolyte hydrogel fibres from poly (acrylic acid)/poly (vinyl alcohol), **Nanotechnology**, **16**(12), 2005, 2852
155. Li L., Hsieh Y., Ultra-fine polyelectrolyte hydrogel fibres from poly (acrylic acid)/poly (vinyl alcohol), **Nanotechnology**, **16**(12), 2005, 2852-2860
156. Li N., Shan D., Xue H., Electrochemical synthesis and characterisation of poly(pyrrole-co-tetrahydrofuran) conducting co-polymer. **European Polymer Journal**, **43**(6), 2007, 2532-2539
157. Li Z., Chen P., Xu X., Ye X., Wang J., Preparation of chitosan-sodium alginate microcapsule containing ZnS nanoparticles and its effect on drug release, **Materials Science and Engineering: C**, **29**(7), 2009, 2250-2253
158. Lin J., Liu Y., Zhang Q.M., Change dynamics and bending actuation in Aquivion membrane swelled with ionic liquids, **Polymer**, **52**(2), 2011, 540-546
159. Lindsay S.E., **Handbook of Applied Dog Behaviour and Training, Vol.3: Procedures and Protocols**, 577
160. Lindström H., Holmberg A., Magnusson E., Lindquist S., Malmqvist L. Hagfeldt A., A new method for manufacturing nanostructured electrodes on plastic substrates, **Nano Letters**, **1**(2), 2001, 97-100
161. Lira L.M. and Cordoba de Torresi S.I., Conducting polymer-hydrogel composites for electrochemical release device: Synthesis and characterization of semi-interpenetrating polyaniline-polyacrylamide network, **Electrochemistry Communications**, **7**(7), 2005, 717-723
162. Lira L.M. and de Torresi S.I.C., Conducting polymer-hydrogel composite for electrochemical release devices: synthesis and characterization of semi-interpenetrating polyaniline-polyacrylamide networks, **Electrochemistry Communications**, **7**(7), 2005, 717-723
163. Lootvoet G., Beyssac E., Shiu G.K., Aiache J.-M., Ritschel W.A., Study on the release of indomethacin from suppositories: *in vitro-in vivo* correlations, **International Journal of Pharmaceutics**, **85**, 1992, 113-120

164. Lopes A., Martin S., Morão A., Magrinho M., Gonçalves I., Degradation of a textile dye, C I Direct Red 80 by electrochemical processes, **Portugaliae Electrochim Acta**, **22**(3), 2004, 279-94
165. LoVecchio F., Pizon A., Riley B., Sami A., D'Incognito C., Onset of symptoms after methadone overdose, **The American Journal of Emergency Medicine**, **25**(1), 2007, 57-59
166. Lu B., Wen R., Yang H., He Y., Sustained release tablet of indomethacin-loaded microcapsules: Preparation, in vitro and in vivo characterization, **International Journal of Pharmaceutics**, **333**(1-2), 2007, 87-94
167. Lum G.M., Aisenbrey G.A., Dunn M.J., Berl T., Schrier R.M., McDonald K.M., *In vivo* effect of indomethacin to potentiate the renal medullary cyclic AMP response to vasopressin, **Journal of Clinical Investigation** **59**(1), 1977, 8-13
168. Luo R., Li H., Birgersson E., Lam K.Y., Modelling of electric-stimulus-responsive hydrogels immersed in different bathing solutions, **Journal of Biomedical Materials Research Part A**, 2007, 248-257
169. Lyon M.E.G., Fay H.G., McCabe T. *et al*, Charge percolation in electroactive polymer films, **Journal of Chemical Society**, **86**(16), 1990, 2905-2910
170. Lyons M.E.G., Fay H.G., McCabe T., Corish J., Vos J.G., Kelly A.J., **Charge Percolation in Electroactive Polymer Films**, **86**, 1990, 2905-2910
171. Lü S., Liu M., Ni B., Gao C., A novel pH- and thermo-sensitive PVP/CMC semi-IPN hydrogel : Swelling, phase behavior, and drug release study, **Journal of Polymer Science: Part B: Polymer Physics**, **48**, 2010, 1749-1756
172. Aldissi M. and S.P. Armes S.P., Colloidal dispersions of conducting polymers, **Progress in Organic Coating** **19**, 1991, 21-58
173. Shabani-Nooshabadi M., S.M. Ghoreishi S.M. and M. Behpour M., Electropolymerized polyaniline coatings on aluminum alloy 3004 and their corrosion protection performance, **Electrochimica Acta**, **54**(27), 2009, 6989-6995
174. MacCall R.P., Ginder J.M., Leng J.M., Ye H.J., Manohar S.K., Masters J.G., Asturias G.E., MacDiarmid A.G., Epstein A.J., Spectroscopy and defect states in polyaniline, **Physics Review B**, **41**, 1990, 5202-5213
175. MacCall R.P., Ginder J.M., Roe M.G., Asturias G.E., Scherr E.M., MacDiarmid A.G., Epstein A.J., Massive polarons in large-energy-gap polymers, **Physics Review B**, **39**, 1989, 10174-10178
176. Macdonald S., Aspirin to be banned in under 16 year olds, **British Medical Journal**, **325**(7371), 2002, 988

177. Macleod T.M., Williams G., Sanders R., Green C.J., Histological evaluation of PermacolTM as a subcutaneous implant over a 20-week period in the rat model, **British Journal of Plastic Surgery**, **58**, 2005, 518-532
178. Mahomadnia Z., Zohuriaan-Mehr M.J., Kabiri K., Jamshidi A. Mobedi H., pH sensitive IPN hydrogel beads of Carrageenan-Alginate for controlled drug delivery, **Journal of Bioactive and Compatible Polymers**, **22**(3), 2007, 342-356
179. Manjunatha K.M., Ramana M.V., Satyanarayana D., Design and evaluation of diclofenac sodium controlled drug delivery system, **Indian Journal of Pharmaceutical Sciences**, **69**(3), 2007, 384-389
180. Manson J., Grobbee D., Stampfer M., Taylor J., Goldhaber S., Gaziano J., Ridker P., Burning J., Hennekens C., Aspirin in the primary prevention of angina pectoris in a randomized trial of United States physicians, **The American Journal of Medicine**, **89**(6), 1990, 772-776
181. Manzano M., Aina V., Areán C.O., Balas F., Cauda V., Colilla M., Delgado M.R., Vallet-Regí M., Studies on MCM-41 mesoporous silica for drug delivery: Effect of particle morphology and amine functionalization, **Chemical Engineering Journal**, **137**, 2008, 30-37
182. Masako I., Seiko Y., Kiyotake A., Toyo M., Countermeasure against morphine side effects, respiratory depression, itching and mouth dryness, **Clinic All-Round**, **52**(8), 2003, 2428-2432
183. McCabe S.E., Cranford J.A., West B.T., Trends in prescription drug abuse and dependence, co-occurrence with other substance use disorders, and treatment utilization: Results from two national surveys, **Addictive Behaviour**, **33**(10), 2008, 1297-1305
184. McCarthy P.A., Juang J., Yang S. Wang H., Synthesis and characterization of water-soluble chiral conducting polymer nanocomposites, **Langmuir**, **18**(1), 2002, 259-263
185. Mirmohseni A. and Wallace G.G., Preparation and characterization of processable electroactive polyaniline-poly vinyl alcohol composites, **Polymer**, **44**, 2003, 3523-3528
186. Mirmohseni A., Price WE. Wallace G.G., Electrichemically controlled transport of small charged organic molecules across conducting polymer membranes, **Journal of Membrane Science** **100**, 1995, 239-248
187. Miyata T., Asami N., Uragami T., A reversibly antigen-responsive hydrogel, **Nature**, **399**, 1999, 766-769

188. Mohanan A., Vishalakshi B., Charyulu R.N., Harish N.M. Ganesh S., Sustained release of metoprolol tartarate from radiation-grafted pH responsive hydrogels, **International Journal of Polymeric Materials**, **58**(1), 2009, 32-48
189. Moina Y.G., Andrade C., Molina E.M., Florit F.V., Rodríguez Presa M.I., Posada M.J., Conformational changes during the redox switching of electroactive polymers, **The Journal of the Argentine Chemical Society**, **91**, 2003, 119-134
190. Mok J.S.L., Chang P., Lee K.H., Kam T.S., Goh S.H., Cardiovascular responses in the normotensive rat produced by intravenous injection of gambirine isolated from the *Uncaria callophylla* Bl. ex Korth, **Journal of Ethnopharmacology**, **36**, 1992, 219-223
191. Moon D.K., Ezuka M., Maruyama T., Osakada K. Yamamoto T., Kinetic study on chemical oxidation of leucoemeraldine base polyaniline to emeraldine base, **Macromolecules** **26**(2), 1993, 364-369
192. Munday D.L. and Fassihi A.R., *In vitro-In vivo* correlation studies on a novel controlled release theophylline delivery system and on Theo-Dur tablets, **International Journal of Pharmaceutics**, **118**, 1995, 251-255
193. Murdan S., Electro-responsive drug delivery from hydrogel, **Journal of Controlled Release**, **93**, 2003, 1-17
194. Musiani M.M., Characterization of electroactive polymer layers by electrochemical impedance spectroscopy (EIS), **Electrochemical Acta**, **35**(10), 1990, 1665-1670
195. Nabid M.R., Golbabaee M., Moghaddam A.B., Dinarvand R., Sedghi R., Polyaniline/TiO₂ nanocomposite: enzymatic synthesis and electrochemical properties, **International Journal of Electrochemical Science**, **3**, 2008, 1117-1126
196. Naoi k., Oura Y., Maeda M., Nakamura S., Electrochemistry of surfactant-doped polypyrrole film (I): Formation of columnar structure by electropolymerization, **J. Electrochem. Soc.**, **142**(2), 1995, 417-422
197. Nguyen T.A., Kobot S., Ongarato D.M., Wallace G.G., The use of chronoamperometry and chemometrics for optimization of conducting polymer sensor arrays, **Electroanalysis**, **11**(18), 1999, 1327-1332
198. Nicholcon R.S. and Shain I., Theory of stationary electrode polarography, **Analytical Chemistry**, **36**(4), 1964, 706-723
199. Nokhodchi A., Javadzadeh Y., Siahi-Shadbad M.R., Barzegar-Jalali M., The effect of type and concentration of vehicles on the dissolution rate of a poorly soluble drug (indomethacin) from liquisolid compacts, **Journal of Pharmacy and Pharmaceutical Science**, **8**(1), 2005, 18-25

200. Omaye S.T., Skala J.H., Gretz M.D., Schaus E.E., Wade C.E., Simple methods for bleeding the unanesthetized rat by tail venipuncture, **Laboratory Animals**, **21**, 1987, 261-264
201. Otero T.F. and Padilla J., Anodic shrinking and compaction of polypyrrole blend: electrochemical reduction under conformational relaxation kinetic control, **Journal of electroanalytical Chemistry**, **561**, 2004, 167-171
202. Palaniappan S., Devi S.L., Thermal stability and structure of electroactive polyaniline-fluoroboric acid-dodecylhydrogensulfate salt, **Polymer Degradation and Stability**, **91**, 2006, 2415-2422
203. Palaniappan S., Saravanan C., John A., Emulsion polymerization for preparation of polyaniline-sulfate salt, using non ionic surfactant, **Journal of Macromolecular Science Part A**, **42**(7), 2005, 891-900
204. Palmre V., Lust E., Jänes A., Koel M., Peikolainen A-L., Torop J., Johanson U., Aabloo A., Electroactive polymer actuators with carbon aerogel electrodes, **Journal of Materials Chemistry**, **21**, 2011, 2577-2583
205. Palos G.R., Mendoza T.R., Cantor S.B., Aday L.A., Cleeland C.S., Perception of analgesic use and side effect – what the public values in pain management, **Journal of Pain and Symptom Management**, **28**(5), 2004, 460-473
206. Panero S., Prosperi P., Scrosati B., Properties of electrochemically synthesized polymer electrodes-IX. The effects of surfactants on polypyrrole films, **Electrochimica Acta**, **37**(3), 1992, 419-423
207. Park C., Orozco-Avila I., Concentrating cellulose from fermented broth using a temperature sensitive hydrogel, **Biotechnology Progress**, **8**(6), 2008, 521-526
208. Pathiratne K.A.S., Skandaraja S.S., Jayasena E.M.C.M., Linear sweep voltammetric determination of free chlorines in waters using graphite working electrodes, **Journal of National Science Foundation of Sri Lanka**, **36**(1), 2008, 25-31
209. Pawde S.M., Deshmukh K., Characterization of poly vinyl alcohol/gelatin blend hydrogel films for biomedical applications, **Journal of Applied Polymer Science**, **109**, 2008, 3431-3437
210. Peppas N.A., Bures C.D., Glucose-responsive hydrogels, **Encyclopedia of Biomaterials and Biomedical Engineering**, 2006
211. Pernaut J. and Reynold J.R., Use of conducting electroactive polymers for drug delivery and sensing of bioactive molecules. A redox approach, **Journal of Physical Chemistry**, **104**(17), 2000, 4080-4090

212. Pernaut J., Reynolds J.R., Uses of conducting electroactive polymers for drug delivery and sensing of bioactive molecules. A redox approach, **Journal of Physical Chemistry**, **104**(17), 2000, 4080-4090
213. Peteu S.F., Responsive materials configured for micro and nano-actuation, **Journal of Intelligent Material Systems and Structures**, **18**, 2007, 147-153
214. Philippova O.E., Hourdet D., Audebert R., Khokhlov A.R., Interaction of hydrophobically modified poly (acrylic acid) hydrogels with ionic surfactants, **Macromolecules**, **29**, 1996, 2822-2830
215. Pistoia G., Bagnarelli O., Maiocco M., Evaluation of factors affecting the radical electropolymerization of methylmethacrylate in the presence of HNO₃, **Journal of Applied Electrochemistry**, **9**(3), 1978, 343-349
216. Pleuvry B.J., Factors affecting drug absorption and distribution, **Anaesthesia and Intensive Care Medicine**, **6**(4), 2006, 135-138
217. Podczec F., The calculation of drug absorption rates of morphine sulphate from a sublingual aerosol preparation using quantified maximum entropy, **International Journal of Pharmaceutics**, **138**(2), 1996, 129-137
218. Posadas D. and Florit M.I., The redox switching of electroactive polymers, **Journal of Physical Chemistry**, **108**, 2004, 15470-15476
219. Prakash S.B., Urdaneta M., Christophersen M., Smela E., Abshire P., *In situ* electrochemical control of electroactive polymer film on a CMOS chip, **Sensors and Actuators B**, **129**, 2008, 699-704
220. Prasad S., Ewigman S., Hickner J., Acute gout: Oral steroid work as well as NSAIDs, **Journal of Family Practice**, **57**(10), 2008, 655-657
221. Prashantha K.V., IPNs based on polyol modified castor oil polyurethane and poly (HEMA): synthesis, chemical, mechanical and thermal properties. **Bull Mater Sci**, **24**, 2001, 535-538
222. Preedy V.R. and Garlick P.J., The influence and infusion on rates of muscle protein synthesis in the rat. Effects of altered respiratory function, **Biochemical Journal**, **251**(2), 1988, 577-580
223. Pyo M. and Reynolds J.R., Electrochemically stimulated adenosine 5'-triphosphate (ATP) release through redox switching of conducting polypyrrole films and bilayers, **Chemistry of Materials**, **8**(1), 1994, 128-133
224. Pyo M. and Reynolds J.R., Poly (pyrrole adenosine 5-triphosphate) (PP-ATP) and conducting polymer bilayers for transport of biologically active ions, **Synthetic Materials**, **71**, 1995, 2233-2236

225. Raghavan S., Harvey A.D., Humble S.R., New opioid side effects and implication for long term therapy, **Trends in Anaesthesia and Critical Care**, **1**(1), 2011, 18-21
226. Raoof J., Ojani R., Nematollahi D., Kiani A., Digital simulation of the cyclic voltammetry study of the catechols electrooxidation in the presence of some nitrogen and carbon nucleophiles. **International Journal of Electrochemical Science**, **4**, 2009, 810-819.
227. Reynold J.E.F., **Martindale: The Extra Pharmacopoeia 31st Edition**, 1996, 51-54
228. Rodrigues M.A. and De Paoli M., Electrochemical properties of chemically prepared polyaniline, **Synthetic Metals**, **41-43**, 1991, 2957-2962
229. Roeder J., Zucolotto V., Shishatskiy S., Bertolino J.R., Nunes S.P., Pires A.T.N., Mixed conductive membrane: aniline polymerization in an acid SPEEKmatrix, **Journal of Membrane Science**, **279**(1-2), 2006, 70-75
230. Rokhade A.P., Patil S.A., Aminabhavi T.M. Synthesis and characterization of semi-interpenetrating polymer network microsphere of acrylamide grafted dextran and chitosan for controlled release of acyclovir. **Carbohydrate Polymers**, **67**(4), 2007, 605-613
231. Rokhade, A.P., Patil, S.A., Aminabhavi T.M., Synthesis and characterization of semi-interpenetrating polymer network microsphere of acrylamide grafted dextran and chitosan for controlled release of acyclovir. **Carbohydrate Polymer**, **67**(4), 2007, 605-613
232. Roncali J., Conjugated poly(thiophenes): synthesis, functionalization and applications, **Chemical Reviews**, **92**(4), 1992, 711-738
233. Russo S.J., Bolanos C.A., Theobald D.E., DeCarolus N.A., Renthal W., Kumar A., Winstanley C.A., . Renthal N.E., Wiley M.D., Self D.W., Russell D.S., Neve R.L., Eisch A.J., Nestler E.J., IRS2-Akt pathway in midbrain dopamine neurons regulates behavioural and cellular responses to opiates, **Nature Neuroscience**, **10**(1), 2007, 93-99
234. Sadki S., Schottland P., Brodie N. Sabourand G., The mechanisms of polypyrrole electropolymerization, **Royal Society of Chemistry**, **29**, 2000, 283-293
235. Sadosky R., Methadon maintenance therapy, **American Family Physician**, July 15, 2000
236. Sakurai K., Tachibana H., Shiga N., Terakura C., Matsumoto M., Tokura Y., Experimental determination of excitonic structure in polythiophene, **Physical Review B**, **56**, 1997, 9552-9556

237. Samuelson L.A., Anagnostopoulos A., Alva K.S., Kumar J. Tripathy S.K., Biologically derived conducting and water soluble polyaniline, **Macromolecules** **31**(13), 1998, 4376-4378
238. Saovsky R., Public Health Issue: Methadone Maintenance Therapy, **Western Journal of Medicine**, **172**, 2000, 43-46
239. Scampicchio M., Lawrence N.S., Arecchi A., Mannino S., Determination of sulphite in wine by linear sweep voltammetry, **Electroanalysis**, **20**(4), 2007, 444-447
240. Schrof W., Rozouvan S., Hartmann T., Möhwald H., Belov V., van Keuren E., Nonlinear optical properties of novel low-bandgap polythiophenes, **Journal of the Optical Society of America B**, **15**(2), 1998, 889-894
241. Scott J.C., Pfluger P., Krounbi M.T. Street G.B., Electro-spin-resonance studies of polypyrrole polymers: Evidence for bipolarons, **Physics Review B**, **28**, 1983, 2140-2145
242. Semenchuk M.R., Sherman S., Effectiveness of Tizanidine in neuropathic pain- An open label study, **Journal of pain**, **1**(4), 2000, 285-292
243. Sengothi K., Tan P., Wang J., Lee T., Kang E.T., Wang H.C., Biocompatibility of polyaniline polymers in tissue: Biomaterial surface interactions, AIChE Annual Meetings, Dallas, Texas, 1999
244. Shang J., Shao Z., Chen X., Electrical behavior of a natural polyelectrolyte hydrogel: Chitosan/CArboxymethylcellulose hydrogel, **Biomacromolecules**, **9**, 2008, 1208-1213
245. Sheika C., Electroactive polymer artificial muscle for biomimetic robotics, **Journal of the Japan Society of Mechanical Engineers**, **107**(103), 2004, 928-929
246. Shin S.K., Kim S.K., Kim H.L., Park C.R., Two photon dissociation of acetone, acetaldehyde and acetic acid at 243nm: translational energy releases in the H atom channel, **Journal of Photochemistry and Photobiology A: Chemistry**, **143**(1), 2001, 11-16
247. Silk T. and Tamm J., Voltammetric study of the influence of cations on the redox switching process of halogenide-doped polypyrrole, **Electrochemical Acta**, **41**(11), 1996, 1883-1885
248. Singh D., Kuckling D., Koul V., Choudhary V., Adler H., Dinda A.K., Studies on copolymerization of *N*-isopropylacrylamide with poly (ethylene glycol) methacrylate, **European Polymer Journal**, **44**(9), 2008, 2962-2970

249. Sobotka S. and Mu L., Characteristics of tetanic force produced by the sternomastoid muscle of the rat, **Journal of Biomedicine and Biotechnology**, currently in press, Article ID 194984
250. Sohn K., Shih S.R., Park S.J., Kim S.J., Yi B., Han S.Y., Kim S.I., Hysteresis in a carbon nanotube based electroactive polymer microfiber actuator: Numerical modeling, **Journal of Nanoscience and Nanotechnology**, **7**(11), 2007, 3974-3979
251. Soong G., Muir A., Gomez M.I., Waks J., Reddy B., Planet P., Singh P.K., Kanetko Y., Wolfgang M.C., Hsiao Y., Tong L., Prince A., Bacterial neuraminidase facilitates mucosal infection by participating in biofilm production, **The Journal of Clinical Investigation**, **116**(8), 2006, 2297-2305
252. Sorenson M.H., Samoshina Y., Claesson P.M., Alberius P., Sustained release of ibuprofen from polyelectrolyte encapsulated mesoporous carrier, **Journal of Dispersion Science and Technology**, **30**(6), 2009, 892-902
253. Sui K., Gao S., Wu W., Xia Y., Injectable supermolecular hybrid hydrogels formed by MWNT-grafted-poly ethylene glycol and α -cyclodextrin, **Journal of Polymer Science**, **48**, 2010, 3145-3151
254. Sun Y.-M., Chen J.-P., Chu D.-H., Preparation and characterization of α -amylase-immobilized thermal-responsive composite hydrogel membrane, **Journal of Biomedical Materials Research**, **45**(2), 1999, 125-132
255. Susinc D., Varagic J., Ahn J., Frohlich E.D., Crosslink breaker s: a new approach to cardiovascular therapy, **Current Opinion in Cardiology**, **19**(4), 2004, 336-340
256. Sutani K., Kaetsu I., Uchida K., Matsubara Y., Stimulus responsive drug release from polymer gel: Controlled release of ionic drug from polyampholyte hydrogel, **Radiation Physics and Chemistry**, **64**(4), 2002, 331-336
257. Sutani K., Kaetsu I., Uchida K., the synthesis and the electric-responsiveness of hydrogel entrapping natural polyelectrolyte, **Radiation Physics and Chemistry**, **61**, 2001, 49-54
258. Sutar D., Aswal D.K., Gupta S.K. Yakhmi J.V., Electrochemical actuator from conductive electroactive polymer polypyrrole deposited on gold, **Indian Journal of Pure and Applied Physics**, **45**, 2007, 354-257
259. Sweet J.L., Choonara Y.E., Pillay V., Design and development of a novel controlled released PLGA alginate-pectinate polyspheric drug delivery system, **Drug Delivery**, **14**, 2007, 309-381
260. T. Budtova and P. Navard, Polyelectrolyte hydrogel swelling in a concentrated polymer solution, **Macromolecules**, **28**, 1995, 1714-1716

261. T.F. Otero T.F., H. Grande H., and J. Rodríguez J., Conformational relaxation during polypyrrole oxidation: From experiment to theory, **Electrochemical Acta**, **41**(11-12), 1994, 1863-1869
262. Taka T., Laakso J., Levon K., Conductivity and structure of DBSA-protonated polyaniline, **Solid State Communications**, **92**(5), 1994, 393-396
263. Tezel T.H., Sonmez K., Del Priore L.V., Kaplan H.J., Tissue reconstruction in AMD: breaking the collagen crosslink increases RPE reattachment rate onto aged inner Bruch's membrane, **Investigative Ophthalmology & Visual Science**, **46 E**, 2005, abstract 1212
264. Thornton P.D., McConnell G., Ulijn R.V., Enzyme responsive polymer hydrogel beads, **Chemical Communications**, 2005, 5913-5915
265. Tomilla M., Jokinen, J., Wilson T., Forsback A.-P., Saukko P., Penttinen R., Ekholm E., Bioactive glass-derived hydroxyapatite-coating promotes granulation tissue growth in subcutaneous cellulose implants in rats, **Acta Biomaterialia**, **4**(2), 2008, 354-361
266. van Kolfschoten A.A., Olling M., van Noordwijk J., Pharmacokinetic interactions between indomethacin and paracetamol in the rat, **Pharmaceutisch Weekblad Scientific Edition**, **7**, 1985, 15-19
267. van Kolfschoten A.A., Olling M., van Noordwijk J., Pharmacokinetic interactions between indomethacin and paracetamol in the rat, **Pharmaceutisch Weekblad Scientific Edition**, **7**, 1985, 15-19
268. Walter M.G., Wamser C.C., Synthesis and characterization of electropolymerized nanostructured aminophenylporphyrin films, **Journal of Physical Chemistry C.**, Article in press, 2010
269. Wang C., Fan Y., Lu H., Tsai T., Tsai M., Wang H., Evidence of *D*-phenylglycine as delivery tool for improving *L*-dopa absorption, **Journal of Biomedical Science**, **17**(71), 2010
270. Wang C.H., Dong Y.Q., Sengothi K., Tan K.L., Kang E.T. *In-vivo* tissue response to polyaniline. **Synthetic Metals**, **102**, 1999, 1313-1314
271. Wang L.X., Soczka-Guth T., Havinga E., Mullen K., Poly(phenylenesulfidephenylenamine)(PPSA) – the “Compound” of polyphenylenesulfide with polyaniline, **Angewandte Chemie International Edition in English**, **35**(13-14), 2003, 1495-1497
272. Wang Q., Mynar J.L., Yoshida M., Lee E., Lee M., Okuro K., Kinbara K., Aida T., High-water-content mouldable hydrogels by mixing clay and a dendritic molecular binder, **Nature**, **463**, 2010, 339-343

273. Wang X., Gu X., Yuan C. *et al*, Evaluation of biocompatibility of polypyrrole *in vitro* and *in vivo*, **Journal of biomed Materials Res**, **68A**, 2004, 411-422
274. Wang Y., Shen Y., Zhang Y., Yue B., Wu C., pH-sensitive poly acrylic acid (PAA) hydrogels trapped with polysodium-p-styrenesulfonate (PSS), **Journal of Macromolecular Science Part B**, **45**(4), 2006, 563-571
275. Wang Z., Kang J., Liu X., Ma Y., Capacitive detection of theophylline based on electropolymerized molecularly imprinted polymer, **International Journal of Polymer Analysis and Characterization**, **12**(2), 2007, 131-142
276. Weinstein S.M., Laux L.F., Thronby J.I. *et al*, Physician's attitude toward pain and the use of opioid analgesic: results of a survey from the Texas Cancer Pain Initiative, **Southern Medical Journal**, **93**(5), 2000, 479-487
277. Weitz P., Wyss H., Larsen R., Oscillatory Rheology: Measuring the viscoelastic behaviour of soft materials, **G.I.T. Laboratory Journal**, **3-4**, 2007, 68-70
278. Whang J.M., Quinn J.A., Graves D.J., Neufeld G.R., Permeation of inert gases through human skin: modelling the effect of skin blood flow, **Journal of Applied Physiology**, **67**, 1989, 1670-1686
279. Williams A.C., Yamane M.A., Barry B.W., Electrical conductivity through snake and human skin membranes, **European Journal of Pharmaceutical Sciences**, **4**(1), 1996, 146-146(1)
280. Wong R.A., High voltage versus low voltage electrical stimulation, **Physical Therapy**, **66**(8), 1986, 1209-1214
281. Yadav V.B. and Yadav A.V., Improvement of solubility and dissolution of indomethacin by liquisolid and compaction granulation technique, **Journal of Pharmaceutical Science & Research**, **1**(2), 2009, 44-51
282. Yah S.C., Harunal T., Enabulele I.O., Yusuf E.O., Bacterial adherence: the role of serum and wound fluid, **African Journal of Biotechnology**, **7**(21), 2008, 3821-3826
283. Yamada K., Tenshima K., Kobayashi N., Hirohashi R., Electropolymerization of aniline derivatives in non-aqueous solution without a proton donor, **Journal of Electroanalytical Chemistry**, **394**, 1997, 71-79
284. Yap W.T. and Durst R.A., Effects of resistance and capacitance on the chronoamperometry of polymer-coated electrodes as modeled by a finite elements digital simulation, **Journal of Electroanalytical Chemistry**, **216**, 1987, 11-19

285. Yap W.T., Durst R.A., Blubaugh E.A., Blubaugh D.D., Chronoamperometry of polymer-modified electrodes charge transport by diffusion and migration, **J. Electroanalytical Chemistry**, **144**, 1983, 69-75
286. Yin W. and Ruckenstein E., A water-soluble self-doped conducting polypyrrole-based copolymer, **Journal of Applied Science**, **79**(1), 2001, 86-89
287. You J., Auguste D.T., Conductive, physiologically responsive hydrogels, **Langmuir**, **26**(7), 2010, 4607-4612
288. Zak O. and Sande M.A., Correlation of *in vitro* antimicrobial activity of antibiotics with results of treatment in experimental animal models and human infections, **Action of Antibiotics in Patients**, L.D. Sabath (ed.) 1982, Hans Huber, Switzerland
289. Zeng Y.N., Zheng N., Osborne P.G., Li Y.Z., Chang W.B., Wang, Z.M., Preparation and cyclic voltammetry characterization of Cu-dipyridyl imprinted polymer. **Chinese Chemistry Letter**, **13**(4), 2002, 317-320.
290. Zhang H., Li H.X. Cheng H.M., Water-soluble multi-walled carbon nanotubes functionalized with sulphonated polyaniline, **Journal of Physical Chemistry B.**, **110**(18), 2006, 9095-9099
291. Zhang J., Yuan K., Wang Y., Zhang S., Zhang J., Preparation and pH responsive behaviour of poly(vinyl alcohol)-chitosan-Poly(acrylic acid) full IPN hydrogels, **Journal of Bioactive and Compatible Polymers**, **22**(2), 2007, 201-218
292. Zhao H., Price W.E. Wallace G.G., Synthesis, characterisation and transport properties of layered conducting electroactive polypyrrole membrane, **Journal of Membrane Science** **148**, 1998, 161-172
293. Zhao H., Price W.E., Too C.O., Wallace G.G. Zhou D., Parameter influencing transport across conducting electroactive polymer membranes, **Journal of Membrane Science** **119**, 1996, 199-212
294. Zhao H., Prince W.E., Wallace G.G., Effect of counter-ions employed during synthesis on the properties of polypyrrole membranes, **Journal of Membrane Science**, **87**, 1994, 47-56
295. Zhou Q., Miller L.L., Valentine J.R., Electrochemically controlled binding and release of protonated dimethyldopamine and other cations from poly(*N*-methylpyrrole)/polyanion composite redox polymer, **Journal Electroanalytical Chemistry**, **261**, 1989, 147-167
296. Zielińska E., Maślińska-Solich J., Lekawska E., Interaction of polyelectrolyte gels and surface active agents, **Polish Journal of Environmental Studies**, **8**(5), 1999, 327-330

297. Zinger B. and Miller L.L., Timed release of chemicals from polypyrrole films,
Journal of American Chemical Society, **106**(22), 1984, 6861-6863